TOPICS IN ORGANOMETALLIC CHEMISTRY

35

Volume Editor Allan J. Canty

Higher Oxidation State Organopalladium and Platinum Chemistry

Springer

35
Topics in Organometallic Chemistry

Topics in Organometallic Chemistry

Recently Published Volumes

Iridium Catalysis
Volume Editor: P. G. Andersson
Vol. 34, 2011

Iron Catalysis – Fundamentals and Applications
Volume Editor: B. Plietker
Vol. 33, 2011

Medicinal Organometallic Chemistry
Volume Editors: G. Jaouen, N. Metzler-Nolte
Vol. 32, 2010

C-X Bond Formation
Volume Editor: A. Vigalok
Vol. 31, 2010

Transition Metal Complexes of Neutral η^1-Carbon Ligands
Volume Editors: R. Chauvin, Y. Canac
Vol. 30, 2010

Photophysics of Organometallics
Volume Editor: A. J. Lees
Vol. 29, 2010

Molecular Organometallic Materials for Optics
Volume Editors: H. Le Bozec, V. Guerchais
Vol. 28, 2010

Conducting and Magnetic Organometallic Molecular Materials
Volume Editors: M. Fourmigué, L. Ouahab
Vol. 27, 2009

Metal Catalysts in Olefin Polymerization
Volume Editor: Z. Guan
Vol. 26, 2009

Bio-inspired Catalysts
Volume Editor: T. R. Ward
Vol. 25, 2009

Directed Metallation
Volume Editor: N. Chatani
Vol. 24, 2007

Regulated Systems for Multiphase Catalysis
Volume Editors: W. Leitner, M. Hölscher
Vol. 23, 2008

Organometallic Oxidation Catalysis
Volume Editors: F. Meyer, C. Limberg
Vol. 22, 2007

N-Heterocyclic Carbenes in Transition Metal Catalysis
Volume Editor: F. Glorius
Vol. 21, 2006

Dendrimer Catalysis
Volume Editor: L. H. Gade
Vol. 20, 2006

Metal Catalyzed Cascade Reactions
Volume Editor: T. J. J. Müller
Vol. 19, 2006

Catalytic Carbonylation Reactions
Volume Editor: M. Beller
Vol. 18, 2006

Bioorganometallic Chemistry
Volume Editor: G. Simonneaux
Vol. 17, 2006

Surface and Interfacial Organometallic Chemistry and Catalysis
Volume Editors: C. Copéret, B. Chaudret
Vol. 16, 2005

Chiral Diazaligands for Asymmetric Synthesis
Volume Editors: M. Lemaire, P. Mangeney
Vol. 15, 2005

Palladium in Organic Synthesis
Volume Editor: J. Tsuji
Vol. 14, 2005

Metal Carbenes in Organic Synthesis
Volume Editor: K. H. Dötz
Vol. 13, 2004

Higher Oxidation State Organopalladium and Platinum Chemistry

Volume Editor: Allan J. Canty

With Contributions by

John E. Bercaw · Allan J. Canty · Karen I. Goldberg · Kyle A. Grice · Jay A. Labinger · Helena C. Malinakova · Marc-Etienne Moret · David C. Powers · Joy M. Racowski · Tobias Ritter · Melanie S. Sanford · Margaret L. Scheuermann · Manab Sharma

Springer

Editor
Professor Allan J. Canty
UTAS Distinguished Professor
School of Chemistry
University of Tasmania
Private Bag 75, Hobart,
Tasmania
Australia 7001
allan.canty@utas.edu.au

ISBN 978-3-642-17428-5 e-ISBN 978-3-642-17429-2
DOI 10.1007/978-3-642-17429-2
Springer Heidelberg Dordrecht London New York

Library of Congress Control Number: 2011922659

Cover design: KünkelLopka GmbH

Printed on acid-free paper

Springer is part of Springer Science+Business Media (www.springer.com)

Volume Editor

Prof. Allan J. Canty

UTAS Distinguished Professor
School of Chemistry
University of Tasmania
Private Bag 75, Hobart,
Tasmania
Australia 7001
allan.canty@utas.edu.au

Editorial Board

Topics in Organometallic Chemistry Also Available Electronically

Topics in Organometallic Chemistry is included in Springer's eBook package *Chemistry and Materials Science*. If a library does not opt for the whole package the book series may be bought on a subscription basis. Also, all back volumes are available electronically.

For all customers who have a standing order to the print version of *Topics in Organometallic Chemistry*, we offer free access to the electronic volumes of the Series published in the current year via SpringerLink.

If you do not have access, you can still view the table of contents of each volume and the abstract of each article by going to the SpringerLink homepage, clicking on "Chemistry and Materials Science," under Subject Collection, then "Book Series," under Content Type and finally by selecting *Topics in Organometallic Chemistry*.

You will find information about the

- Editorial Board
- Aims and Scope
- Instructions for Authors
- Sample Contribution

at springer.com using the search function by typing in *Topics in Organometallic Chemistry*.
Color figures are published in full color in the electronic version on SpringerLink.

Aims and Scope

The series *Topics in Organometallic Chemistry* presents critical overviews of research results in organometallic chemistry. As our understanding of organometallic structures, properties and mechanisms grows, new paths are opened for the design of organometallic compounds and reactions tailored to the needs of such diverse areas as organic synthesis, medical research, biology and materials science. Thus the scope of coverage includes a broad range of topics of pure and applied organometallic chemistry, where new breakthroughs are being made that are of significance to a larger scientific audience.

The individual volumes of *Topics in Organometallic Chemistry* are thematic. Review articles are generally invited by the volume editors.

In references *Topics in Organometallic Chemistry* is abbreviated Top Organomet Chem and is cited as a journal. From volume 29 onwards this series is listed with ISI/Web of Knowledge and in coming years it will acquire an impact factor.

Preface

Palladium and platinum continue to play very significant roles in the development of fundamental organometallic chemistry and organic synthesis employing these metal centers in both stoichiometric and catalytic processes. The most common oxidation states exhibited by these elements cover the range 0 to +IV, and this volume has a central theme emphasizing the chemistry of oxidations states >+II, including metal–metal-bonded systems. At a broader level, there is significant emphasis on synthesis, structural chemistry of higher oxidation states, and mechanisms of stoichiometric and catalytic reactions involving the higher oxidation states. The synthetic and mechanistic chemistry of the higher oxidation states mandates a discussion of many aspects of lower oxidation states, in particular +II. In a formal electron book-keeping sense, some of the "higher oxidation state" complexes discussed here are closer to oxidation state +II, e.g., some metal–metal-bonded systems where Pd(II) and Pt(II) can be regarded as donors toward more electrophilic centers. The Editor has enlisted authors who are research active at the forefront of a selection of research areas of considerable current interest in the organometallic chemistry of palladium and platinum in higher oxidation states.

The Editor is very grateful indeed for the enthusiasm shown from the outset by authors for this venture and the manner in which they have adhered to the timeline for assembling their contributions: John Bercaw, Karen Goldberg, Kyle Grice, Jay Labinger, Helena Malinakova, Marc-Etienne Moret, David Powers, Joy Racowski, Tobias Ritter, Melanie Sanford, Margaret Scheuermann, and Manab Sharma. I am also appreciative of the timeliness of responses to my questions from the Springer staff, and the flexibility they have shown in accommodating requests.

Hobart, Tasmania, Australia — Allan J. Canty

Contents

Top Organomet Chem (2011) 35:1–28
DOI: 10.1007/978-3-642-17429-2_1

Five-Coordinate Platinum(IV) Complexes

Kyle A. Grice, Margaret L. Scheuermann, and Karen I. Goldberg

Abstract Octahedral organometallic platinum(IV) complexes have been known for more than a century. Mechanistic studies suggest that many reactions of these six-coordinate platinum(IV) complexes proceed through unobservable five-coordinate platinum(IV) intermediates. Only recently have five-coordinate platinum(IV) complexes been isolated and characterized. These novel complexes serve as models for unobserved intermediates in stoichiometric and catalytic reactions involving high oxidation state platinum. The isolation of five-coordinate complexes allows the unique reactivity of these unsaturated species to be investigated directly. This contribution describes the development of five-coordinate platinum(IV) from proposed intermediates to isolable complexes. The syntheses, characterization, and reactivity studies of complexes with this new coordination geometry of platinum(IV) are also presented.

Keyword Five-coordinate platinum(IV)

Contents

K.A. Grice, M.L. Scheuermann, and K.I. Goldberg (✉)
Department of Chemistry, University of Washington, Seattle, WA 98195, USA
e-mail: goldberg@chem.washington.edu

Abbreviations

acac	acetylacetonate
anim	*N*-(2,6-diisopropylphenyl)-2-[*N*-(2,6-diisopropylphenyl)imino-methyl]-benzenamide
Ar	aryl
Ar^F	3,5-bis(trifluoromethyl)phenyl
BAB	1,2-bis(*N*-7-azaindolyl)benzene
bpy	2,2′-bipyridine
BPICO	*N*-benzyl-*N*′,*N*′-dimethyl-*N*-(2-picolyl)ethylenediamine
BPMA	bis(2-pyridylmethyl)amine
Cp	cyclopentadienyl
dmdpb	dimethyldi(2-pyridyl)borate
dppbz	1,2-bis(diphenylphosphino)benzene
dppe	1,2-bis(diphenylphosphino)ethane
dpms	di(2-pyridyl)methanesulfonate
i-Pr	isopropyl
L	neutral ligand
Me-dpms	(6-methyl-2-pyridyl)(2-pyridyl)methanesulfonate
nacnac	*N*,*N*′-diaryl-β-diketiminate
NSiN	bis(8-quinolyl)methylsilyl
OTf	trifluoromethanesulfonate
PICO	*N*,*N*,*N*′-trimethyl-*N*′-(2-pyridylmethyl)ethylenediamine
Pyphane	[2.1.1]-(2,6)-pyridinophane
pz*	3,5-dimethylpyrazole
solv	solvent molecule
tacn	1,4,7-triazacyclononane
t-Bu	*tert*-butyl
t-Bubpy	4,4′-di-*tert*-butyl-2,2′-bipyridine
tmeda	*N*,*N*,*N*′,*N*′-tetramethylethylenediamine
Tp	hydridotris(pyrazolyl)borate
Tp′	hydridotris(3,5-dimethylpyrazolyl)borate
TPAB	1,2,4,5-tetrakis(5-(4-heptylphenyl)-7-azaindol-1-yl)benzene
TPMA	tris(2-pyridylmethyl)amine
X	anionic ligand

1 Introduction

Just as the octet rule is a key principle in main group chemistry, the 18-electron rule is a basic tenet taught in every class covering organometallic chemistry [1–23]. We learn that metal complexes with 18 valence electrons are stable, and that a metal with a d^n electron count will surround itself with dative ligands to supply 18–n electrons. For high-valent d^6 Pt(IV) and Pd(IV), the 18-electron rule is satisfied by

arranging six ligands around the metal center in an octahedral geometry. Organometallic complexes of Pt(IV) have been known for more than 100 years, and until recently, all of them rigorously obeyed the 18-electron rule. The first reported Pt(IV) alkyl compounds were the $[PtMe_3X]_4$ tetrameric complexes that satisfy the 18-electron rule through bridging halide interactions within a cubic structure (Fig. 1) [4, 5]. A very large number of six-coordinate octahedral Pt(IV) complexes with alkyl, silyl, and hydride ligands have since been reported and some representative examples are shown in Fig. 1 [6–12]. Note that the "three-legged piano stool" complex $CpPtMe_3$ is also considered octahedral, with the anionic Cp^- ring representing three 2-electron donors in a facial configuration, an arrangement similar to that of the Tp ligand.

Octahedral, 18-electron d^6 metal complexes of Pt(IV) are electronically and coordinatively saturated. These factors contribute to the high stability of the complexes as well as their limited reactivity with external reagents. Studies of the reactivity of Pt(IV) complexes have found that ligand loss to generate a five-coordinate intermediate is generally required as a preliminary step before a range of reactions including β-hydride elimination, insertion, and reductive elimination can occur.

Although five-coordinate complexes have been proposed intermediates for decades, until recently no examples of Pt(IV) complexes with this unique coordination environment had been reported. In fact, it was generally thought that five-coordinate Pt(IV) organometallic complexes would be too reactive to isolate or even observe. Proposed structures of these intermediates formed by ligand loss often had a solvent

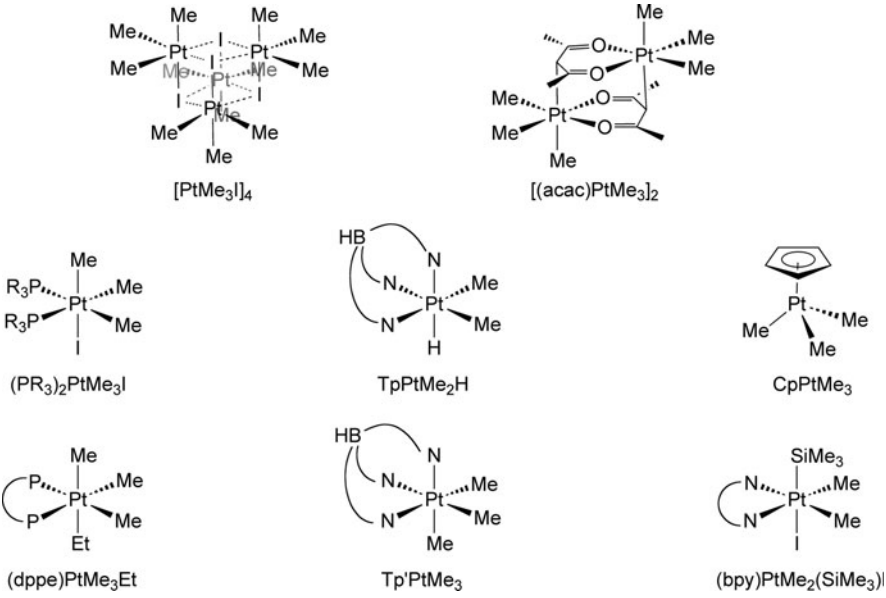

Fig. 1 Examples of octahedral Pt(IV) organometallic complexes [4–12]

molecule coordinated to adhere to the construct of the 18-electron rule [13, 14]. As we present in this chapter, unsaturated Pt(IV) species have now been prepared, isolated, and fully characterized. The synthesis of unsaturated Pt(IV) species validates the numerous mechanistic proposals put forth over the past several decades. Undeniably, a five-coordinate Pt(IV) species is a reasonable structure for a proposed reaction intermediate and it is not necessary to invoke the intermediacy of a six-coordinate solvento complex. Studies of the reactivity of these novel unsaturated Pt(IV) complexes are revealing unique and interesting chemistry relevant to fundamental transformations in organometallic chemistry.

2 Proposed Five-Coordinate Platinum(IV) Intermediates

2.1 Reductive Elimination from Pt(IV)

Reductive elimination from a six-coordinate octahedral Pt(IV) center results in the coupling of two formally anionic ligands and the formation of a four-coordinate square-planar Pt(II) species. It has been typically observed that coordinatively saturated six-coordinate Pt(IV) organometallic complexes are remarkably stable toward reductive elimination. It is generally only after loss of an ancillary ligand from the octahedral complex that reductive elimination takes place from Pt(IV).

The first suggestion that ligand loss was important in reductive elimination reactions from Pt(IV) complexes dates back more than 40 years. In 1969, Ettore observed that added iodide inhibited the reductive elimination of PhI from $L_2PtPh_2I_2$ in methanol and suggested iodide loss to form a six-coordinate solvento intermediate [13]. Several years later, a five-coordinate intermediate was proposed by Puddephatt in studies of C–C reductive eliminations from Pt(IV) complexes (see Sect. 2.1.1) [15]. Since then, the involvement of five-coordinate intermediates has been supported so consistently in both experimental (e.g., [10, 13–42]) and computational studies (e.g., [29, 30, 43–48]) of alkyl C–C, C–H, and C–X reductive elimination that it is now accepted as the norm in mechanistic schemes for reductive elimination from Pt(IV).

2.1.1 C–C Reductive Elimination

In 1974, Puddephatt and coworkers studied C–C reductive elimination reactions from the Pt(IV) complexes L_2PtMe_3X ($L_2 = (PR_3)_2$, dppe) in solution [15]. The pyrolyses of these compounds had been investigated several years earlier by Ruddick and Shaw [7]. Both groups saw high to quantitative yields of ethane and L_2PtMeX, the products of C–C reductive elimination from L_2PtMe_3X. Most interesting was Puddephatt's observation of a significant decrease in the C–C reductive

elimination rate in the presence of added phosphine ligand. This kinetic result suggests that an intermediate species is formed in the reaction by the loss of phosphine prior to C–C bond forming as shown in Scheme 1, **a**. Evidence of ligand exchange at the Pt(IV) complexes upon addition of ligand L′ to the reaction was also presented. The data are consistent with a mechanism involving the preliminary dissociation of a phosphine ligand to form a five-coordinate Pt(IV) intermediate prior to rate-determining C–C reductive coupling. Concerted C–C coupling occurs from the five-coordinate intermediate and the resulting unsaturated Pt(II) species is trapped by exogenous ligand to form the stable square-planar product. In virtually every subsequent study investigating $sp^3C–sp^3C$ reductive elimination reactions from Pt(IV) or Pd(IV), the mechanistic evidence has supported the formation of a five-coordinate intermediate on the reaction pathway [10, 16–30, 49–52].

Five-coordinate intermediates in C–C reductive elimination from L_2PtMe_3X can be generated in a variety of ways depending on the nature of L and X (Scheme 1). If L is a monodentate neutral ligand (e.g., a phosphine), the intermediate is generated by dissociation of L as described earlier (Scheme 1, **a**) [15, 16]. The use of a bidentate phosphine ligand would make phosphine dissociation less favorable and so a decrease in the rate of reductive elimination is expected. Indeed, C–C reductive elimination of ethane from $(dppe)PtMe_3I$ was found to require much higher temperatures than C–C reductive elimination from $(PMePh_2)_2PtMe_3I$ [15].

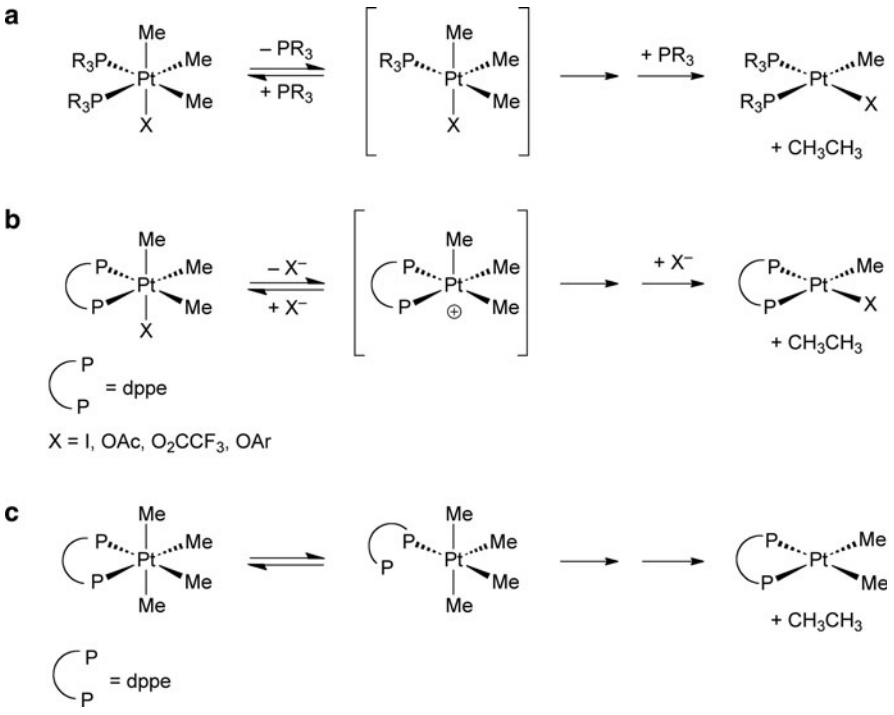

Scheme 1 Five-Coordinate intermediates in C–C reductive elimination reactions [10, 15–23, 27, 28]

Later mechanistic studies determined that the reductive elimination reactions of the bidentate phosphine complexes do proceed via a ligand loss pathway but involve a different type of five-coordinate intermediate [17, 18]. When L_2 is a chelating ligand, dissociation of the X^- anion takes place to generate a five-coordinate cationic intermediate (Scheme 1, **b**) [17–22, 27, 28]. When L_2 is a chelating phosphine and X is a group that cannot readily dissociate (e.g., an alkyl), reaction rates are very slow and very high temperatures (e.g., 165 °C) are required to induce reductive elimination [10]. The mechanism for reductive elimination of ethane from these complexes was determined to involve reversible dissociation of one arm of the chelating phosphine to generate a five-coordinate intermediate prior to C–C coupling (Scheme 1, **c**) [10, 23, 24].

2.1.2 C–X Reductive Elimination

Five-coordinate Pt(IV) intermediates have also been proposed as key intermediates in carbon–heteroatom (C–X) reductive elimination reactions from Pt(IV) [17, 18, 21, 22, 27, 28, 40–42]. For example, upon thermolysis of L_2PtMe_3X (L_2 = chelating phosphine; X = I, OAc, O_2CCF_3, OAr, $NHSO_2R$, OH), the kinetic evidence supports dissociation of X^- anion from the Pt center to generate a five-coordinate Pt(IV) cation. Nucleophilic attack of the X^- on a Pt–Me group of the cationic intermediate generates the MeX product as shown in Scheme 2 [17, 18, 21, 22, 27, 28]. This mechanism is the microscopic reverse of MeX oxidative addition to a square planar d^8 metal complex [1–3] and also models the product release step in catalytic alkane functionalization by platinum [40, 41, 53, 54]. C–C reductive elimination, which takes place by concerted C–C coupling from the cationic five-coordinate intermediate, was also observed as a competitive reaction in the thermolyses of these L_2PtMe_3X complexes. With an understanding of the mechanisms of the alkyl C–C and C–X reductive elimination reactions from Pt(IV) (Scheme 2), it was possible to change the reaction conditions to favor either C–C or C–X coupling [17, 18, 21, 22, 27, 28]. For example, addition of excess X^- inhibits C–C reductive elimination while not affecting C–X reductive elimination. This occurs because the first step of both reactions, formation of the five-coordinate intermediate, is inhibited by added X^- as shown in Scheme 2. The rate of the second step in the C–X reductive elimination reaction, nucleophilic attack on the intermediate by X^-, increases with added X^-. The opposite dependences of the two reaction steps on the X^- concentration cancel one another. Increasing the solvent polarity or adding Lewis acid additives accelerates the formation of the five-coordinate intermediate, but these conditions also reduce the nucleophilicity of X^- resulting in a preference for C–C coupling over C–X coupling.

Nucleophilic attack on a Pt(IV) alkyl has been proposed as the product forming step in Shilov catalysis wherein alkanes are converted to alcohols and alkyl chlorides using Pt salts in aqueous solution [40, 41, 53, 54]. Kinetic studies of the proposed product-forming step using the model platinum complex $[MePtCl_5]^{2-}$ found that the loss of a chloride ligand occurs prior to nucleophilic attack [40, 41]. As these investigations were carried out in aqueous solution, it was not possible to

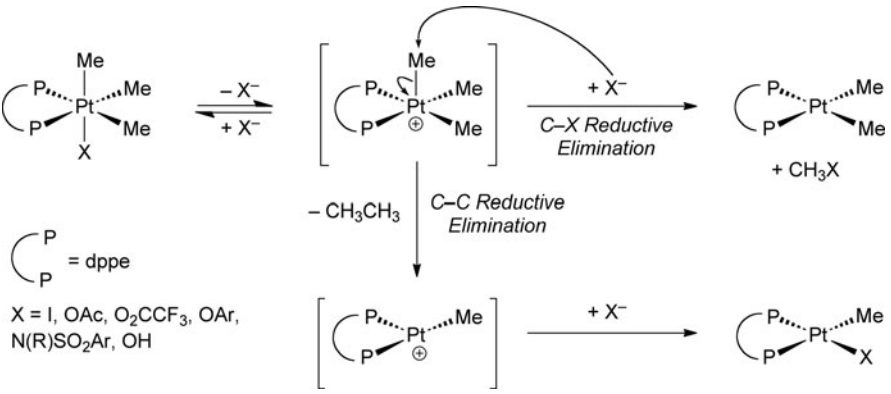

Scheme 2 Five-coordinate intermediates in C–X reductive elimination reactions [17, 18, 21, 22, 27, 28]

distinguish between attack at a five-coordinate Pt(IV) intermediate or at a solvento (aquo) six-coordinate complex. Similarly, the formation of C–O bonds via nucleophilic attack on Pt(IV) alkyl complexes has been proposed in reductive elimination reactions from (dpms)Pt(IV) complexes [55, 56]. The dpms ligand bears a hemilabile sulfonyl group, which is coordinated to the platinum in the Pt(IV) complexes but not in the Pt(II) products. While a five-coordinate intermediate has not been formally proposed, it is notable that the Pt(IV) complex isomerizes to place the alkyl group trans to the sulfonyl prior to the C–O coupling step. It is difficult to assess experimentally whether the sulfonyl group in these systems dissociates prior to or concurrently with the nucleophilic attack. The former would involve a true five-coordinate intermediate.

A mechanism of concerted C–O coupling (not a nucleophilic attack pathway) from a (dpms)Pt(IV) system to produce substituted epoxides has also been reported [57]. In these examples, whether the reaction procceds via a concerted C–O coupling directly from the six-coordinate Pt(IV) complex or after dissociation of the sulfonyl group to generate a five-coordinate intermediate is difficult to distinguish experimentally. It is notable that isomerization resulting in placement of the strong trans influence alkyl portion of the oxetane ring trans to the sulfonyl was observed prior to the reductive elimination. Such isomerizations generally proceed through five-coordinate intermediates, suggesting that the formation of a fluxional five-coordinate intermediate prior to C–O coupling would be a kinetically viable pathway for this reductive elimination.

2.1.3 C–H Reductive Elimination

Five-coordinate Pt(IV) intermediates are also proposed in C–H reductive elimination from Pt(IV) alkyl hydrides. Protonation of Pt(II) alkyls at low temperature (−78 °C) with HX resulted in the first spectroscopic observations of Pt(IV) alkyl hydride

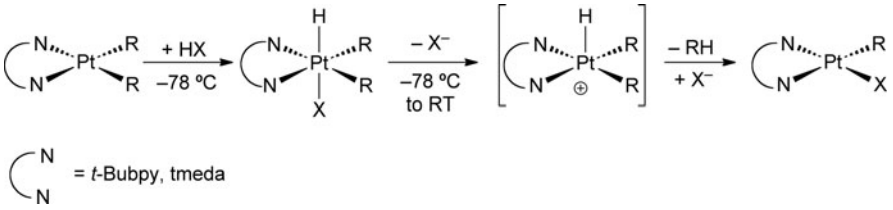

Scheme 3 Five-coordinate intermediates in C–H reductive elimination reactions [58, 59]

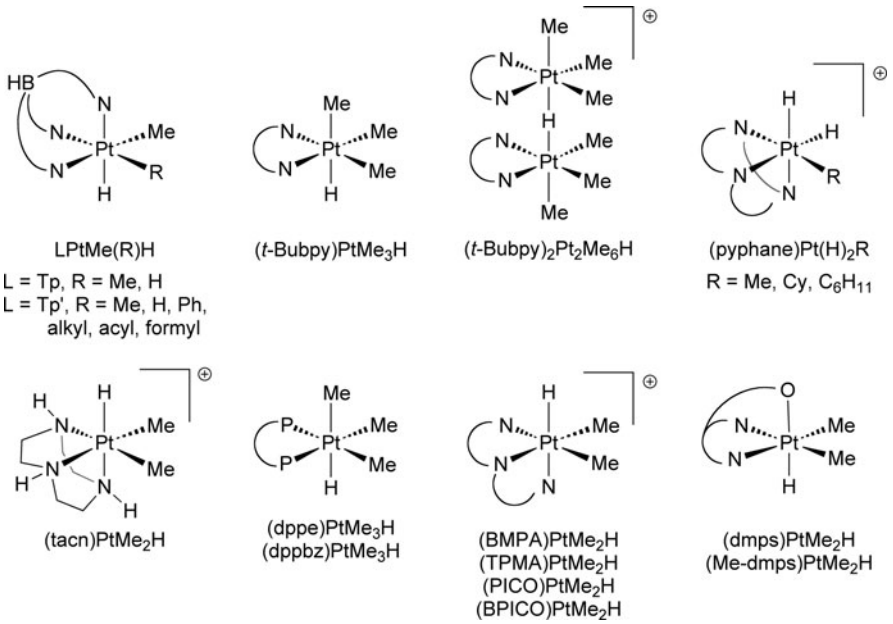

Fig. 2 Stable platinum(IV) alkyl hydride complexes [8, 10, 23, 35, 60–69]

complexes (Scheme 3) [58, 59]. As the solutions were allowed to stand or were warmed to room temperature, the products of C–H reductive elimination were observed. Kinetic evidence supported the dissociation of halide to generate a cationic five-coordinate Pt(IV) center prior to the C–H coupling reaction. In 1996, the first examples of isolable Pt(IV) alkyl hydride species, which are stable at room temperature, were reported [8, 60]. The complexes, $TpPtMe_2H$ and $Tp'PtMe_2H$, do not contain any labile ancillary ligands. This lack of labile ligands has been recognized as a key factor in the unusual thermal stability of these complexes. All subsequently reported isolable Pt(IV) alkyl hydride complexes share this characteristic of nonlabile ancillary ligands as illustrated by the examples in Figure 2 [10, 23, 35, 61–69].

In most studies of C–H reductive elimination from Pt(IV) alkyl hydride complexes, a mechanism involving dissociation of a ligand and formation of a five-coordinate Pt(IV) intermediate prior to concerted C–H coupling has been proposed

[31–39, 44, 47, 70, 71]. There have been only a few exceptions where C–H reductive elimination has been reported to proceed by a concerted C–H coupling from the six-coordinate Pt(IV) complex. Calculations have shown that such a direct C–H reductive elimination can be favored if the entropy gained by ligand dissociation is minimized with a chelating ligand [45, 46, 48]. This suggestion was confirmed by experimental work in which the reductive elimination of methane from L_2PtMe_3H (L_2 = dppe, dppbz) was studied [23]. However, the reactivity of these two Pt(IV) alkyl hydride complexes are notable exceptions to the more general observation of preliminary ligand dissociation occurring prior to C–H reductive elimination from Pt(IV). The vast majority of the studies of C–H reductive elimination from Pt(IV) suggests the involvement of a five-coordinate intermediate. Notably, the principle of microscopic reversibility then implies that the same five-coordinate intermediates are also involved in most C–H oxidative addition reactions to Pt(II) [70–73].

2.2 β-Hydrogen Elimination from Pt(IV)

β-Hydride elimination reactions are ubiquitous transformations in organometallic chemistry. It is well known that in order for β-hydride elimination to occur from a metal alkyl, an open site cis to the alkyl is needed [1–3]. It is not surprising then that without facile ligand loss octahedral Pt(IV) alkyls are stable with respect to β-hydride elimination. However, once ligand loss occurs, the five-coordinate Pt(IV) intermediates are susceptible to β-hydride elimination [23, 74]. For example, the β-hydride elimination product ethylene was produced competitively with the C–C reductive elimination products, ethane and propane, upon thermolysis of $(dppe)PtMe_3Et$ at 165 °C [23]. Methane was also observed as a product in this reaction. In this system, the results of mechanistic experiments were consistent with chelate opening to generate a five-coordinate intermediate from which both concerted C–C coupling and β-hydride elimination occur (Scheme 4). The $(dppe)PtMe_3H$ product expected after the release of ethylene in the β-hydride elimination process was not observed under the reaction

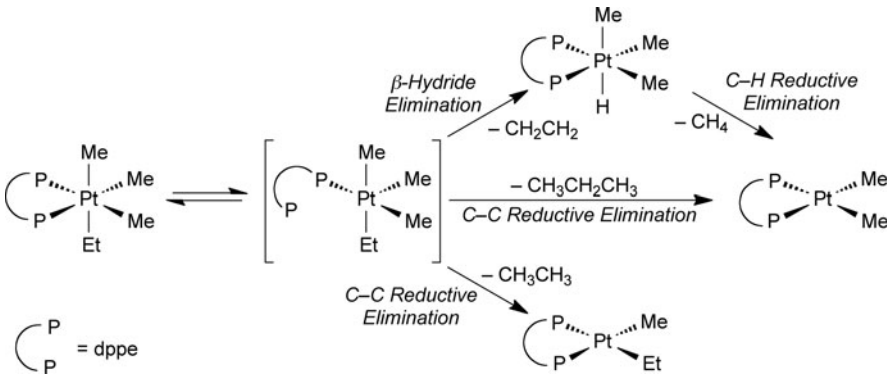

Scheme 4 Five-coordinate intermediates in β-hydride elimination reactions from Pt(IV) [23]

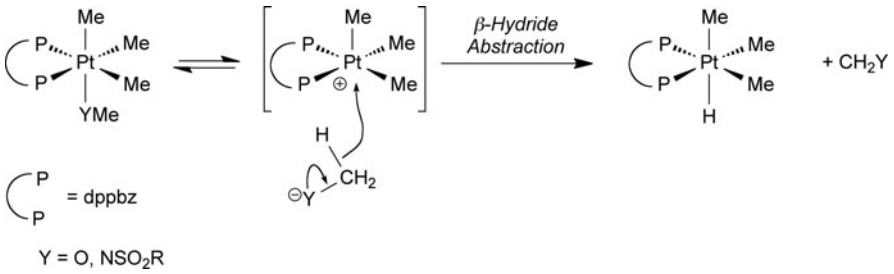

Scheme 5 Five-coordinate intermediates in β-hydride abstraction reactions from Pt(IV) [27, 28]

conditions. However, this is not surprising as (dppe)$PtMe_3H$ is known to undergo reductive elimination of methane at much lower temperatures than those at which the thermolysis reaction of (dppe)$PtMe_3Et$ was studied [23]. C–H reductive elimination from (dppe)$PtMe_3H$ yields methane and the Pt(II)Me_2 product, (dppe)$PtMe_2$.

The products of formal β-hydride elimination were also observed upon thermolysis of (dppbz)$PtMe_3$(YMe) (Y = O, NSO_2R) [27, 28]. This reactivity is interesting because the dppbz ligand is more rigid than the dppe ligand and is significantly more resistant to chelate opening. Despite the strongly chelated dppbz phosphine ligand, the products expected from β-hydride elimination of the YMe group were clearly observed to form competitively with the products of C–C and C–X reductive elimination. Detailed studies of these reactions indicate that the mechanism of β-hydride elimination for these heteroatom groups on Pt(IV) differs from the accepted mechanism for metal alkyl groups. However, a five-coordinate Pt(IV) species is still involved. Evidence supports the dissociation of the anionic heteroatom group to generate a five-coordinate cationic Pt(IV) intermediate. The five-coordinate Pt(IV) center then abstracts a hydride from the dissociated anion to yield the observed products (Scheme 5). Thus, the same five-coordinate Pt(IV) intermediate is involved in β-hydride abstraction and in C–C and C–X reductive elimination from these complexes.

2.3 Five-Coordinate Rh(III) and Ir(III) Complexes

Although five-coordinate Pt(IV) species have long been proposed as intermediates in the fundamental organometallic transformations described earlier, until recently, isolable five-coordinate Pt(IV) complexes were unknown. This is somewhat surprising since isoelectronic five-coordinate Rh(III) and Ir(III) complexes have been known since the 1960s and 1970s, respectively [75, 76]. A range of five-coordinate Ir(III) organometallic complexes have been reported including bis-hydrocarbyl, hydrido aryl, and even hydrido alkyl species [77, 78]. The results of mechanistic studies of reductive elimination reactions to form C–C and C–H bonds from these complexes are consistent with direct, concerted couplings from the five-coordinate species [78, 79]. Five-coordinate Ir(III) alkyl hydride species

are particularly important because they are proposed as intermediates in iridium catalyzed alkane dehydrogenation and alkane metathesis reactions [80–82].

3 First Isolable Five-Coordinate Pt(IV) Complexes

In 2001, the first examples of isolable five-coordinate Pt(IV) complexes were reported (Fig. 3) [83, 84]. The neutral complex ($^{i\text{-Pr}}$nacnac)$PtMe_3$ (**1a**) was prepared from K$^{i\text{-Pr}}$nacnac and $[PtMe_3(OTf)]_4$ in pentane solvent [83] and silyl hydride complexes $[\kappa^2\text{-}((Hpz^*)BHpz^*_2)Pt(H)_2SiR_3][BAr_4^F]$ ($R_3 = Et_3$ (**2a**), Ph_3 (**2b**), Ph_2H (**2c**)) were prepared by the addition of $[H(Et_2O)_2][BAr_4^F]$ to $Tp'Pt(H)_2SiR_3$ or by the reaction of $[\kappa^2\text{-}((Hpz^*)Bhpz^*_2)PtH(solv)][BAr_4^F]$ with R_3SiH [84]. These unprecedented five-coordinate Pt(IV) complexes are stable in solution at room temperature and were characterized by NMR spectroscopy. Compounds **1a** and **2a** were also characterized in the solid state by X-ray crystallography. An almost perfect square pyramidal geometry about the Pt center was observed for ($^{i\text{-Pr}}$nacnac)$PtMe_3$, with close to 90 ° angles between the ligands around the metal [83]. In contrast, the structure of the cationic Pt(IV) species $[\kappa^2\text{-}((Hpz^*)Bhpz^*_2)Pt(H)_2SiEt_3][BAr_4^F]$ (**2a**) has N–Pt–Si angles that are close to 120 °, suggesting a distorted square pyramid in which the metal is not in the plane of the base of the pyramid, but more toward the center [84]. The Pt-hydrides were not located crystallographically.

The ^{1}H NMR spectrum of ($^{i\text{-Pr}}$nacnac)$PtMe_3$ (**1a**) at room temperature contains only one resonance for the three Pt–Me groups, a sharp singlet with ^{195}Pt satellites ($^2J_{Pt-H} = 74$ Hz) [83]. If the complex existed in solution as a static square pyramid, separate signals would be expected for the basal and the axial Pt–Me groups. If it existed as a static trigonal bipyramid in solution, separate signals would also be expected as Me groups would be located in both the axial and the equatorial positions. The observation of a single resonance suggests a fluxional molecule that exchanges the three Pt–Me groups on the NMR timescale. The $^2J_{Pt-H}$ is consistent with the average value expected based on two equatorial Pt–Me groups trans to N and an axial Pt–Me group trans to an open site. For comparison, in the complexes (NN)$PtMe_3OTf$ (NN = bpy, tmeda, diimine), the Me groups trans to the nitrogen donor ligands have $^2J_{Pt-H}$ values of *ca.* 66 Hz, whereas the $^2J_{Pt-H}$ trans to

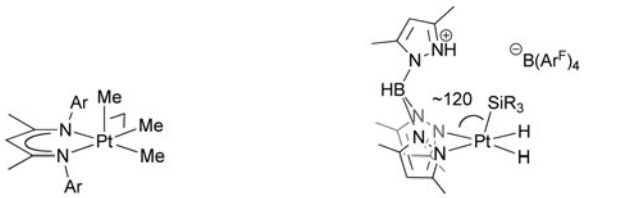

($^{i\text{-Pr}}$nacnac)$PtMe_3$
1a, Ar = 2,6-diisopropylphenyl

$[(\kappa^2\text{-}((Hpz^*)BHpz^*_2))Pt(H)_2SiR_3][BAr^F_4]$
2a, $R_3 = Et_3$
2b, $R_3 = Ph_3$
2c, $R_3 = Ph_2H$

Fig. 3 First reported five-coordinate Pt(IV) complexes [83, 84]

the weak donor OTf is *ca.* 80 Hz [20]. Thus, a Pt–Me group trans to an open site could be expected to have a $^2J_{Pt-H}$ value of *ca.* 80 Hz or higher. Such a high value was later confirmed in studies of [(BAB)$PtMe_3$][OTf] (see Section 4). Fluxionality is common for five-coordinate d^6 metal species [85–88]. The observed scrambling of the Pt–Me groups in L_2PtMe_3X prior to C–C reductive coupling [15, 23, 37] has been explained by the expected fluxionality of the five-coordinate Pt(IV) intermediates that form prior to reductive elimination. No change in the NMR spectrum of **1a** was observed when the sample was cooled to −50 °C, indicating that the fluxional process is still rapid at low temperatures [83]. In comparison, evidence of positional exchange between the silyl ligand and the hydrides was not observed in the solution NMR spectra of [κ^2-((Hpz*)$BHpz^*_2$)$Pt(H)_2SiR_3$][BAr_4^F] (**2a–c**) [84].

4 Survey of Known Five-Coordinate Pt(IV) Complexes

Following the first reports of isolable five-coordinate Pt(IV) species, several other stable five-coordinate Pt(IV) species have been prepared and characterized. These complexes are illustrated in Fig. 4 [89–99].

A variety of methods have been used to prepare five-coordinate platinum(IV) complexes. The five-coordinate Pt(IV) species with trimethyl substitution at platinum have been synthesized by reaction of bidentate ligands with $[PtMe_3OTf]_4$ (**1a–d**, **3**, **4a–c**, **9**), or by reaction of MeOTf with a Pt(II)Me_2 species (**9** and **10**) [83, 89, 90, 92–95, 99]. The first examples of five-coordinate Pt(IV) species with silyl ligands (**2a–c**) were obtained by reaction of six-coordinate Tp′PtH_2Me species with acid in the presence of silanes. These conditions resulted in C–H reductive elimination followed by Si–H oxidative addition [84]. Later, five-coordinate Pt(IV) species were synthesized directly from the reaction of silane with a Pt(II) precursor (**5a–c**, **7a**) [97, 98]. Complex **6** was obtained by reaction of an anionic Pt(II) dialkyl species with Me_3SiOTf [91]. Complexes **8a** and **8b**, which each have a silyl group incorporated into the chelating ligand backbone, were synthesized from six-coordinate Pt(IV)OTf precursors via salt metathesis with the noncoordinating anion $B(C_6F_5)_4$ [96].

Most of the reported five-coordinate Pt(IV)Me_3 complexes are fluxional and the Pt–Me groups exchange on the NMR time scale, as described earlier for **1a**. Complexes **1b–d**, **3**, and **4a–c** are reported to exhibit such fluxionality and only a single Pt–Me ^{1}H NMR signal is observed for these complexes at room temperature [89, 90, 92–94]. Complex **9** exhibits two broad Pt–Me ^{1}H NMR signals in a 2:1 ratio at room temperature [95]. The broadness of the signals indicates a slow exchange of the Pt–Me groups and warming to 45 °C resulted in coalescence of the signals. Cooling the solution to –53 °C results in sharp Pt–Me signals in the ^{1}H NMR spectrum, with $^2J_{Pt-H} = 67.2$ and 84.4 Hz for the basal and axial positions, respectively [95]. The limited fluxionality of **9** compared to the other fluxional $PtMe_3$ complexes is likely due to a higher rigidity of the BAB ligand and/or increased steric interference by the benzene ring that inhibits efficient isomerization. The dinuclear complex **10** shows no fluxionality of the Pt–Me groups at room temperature by

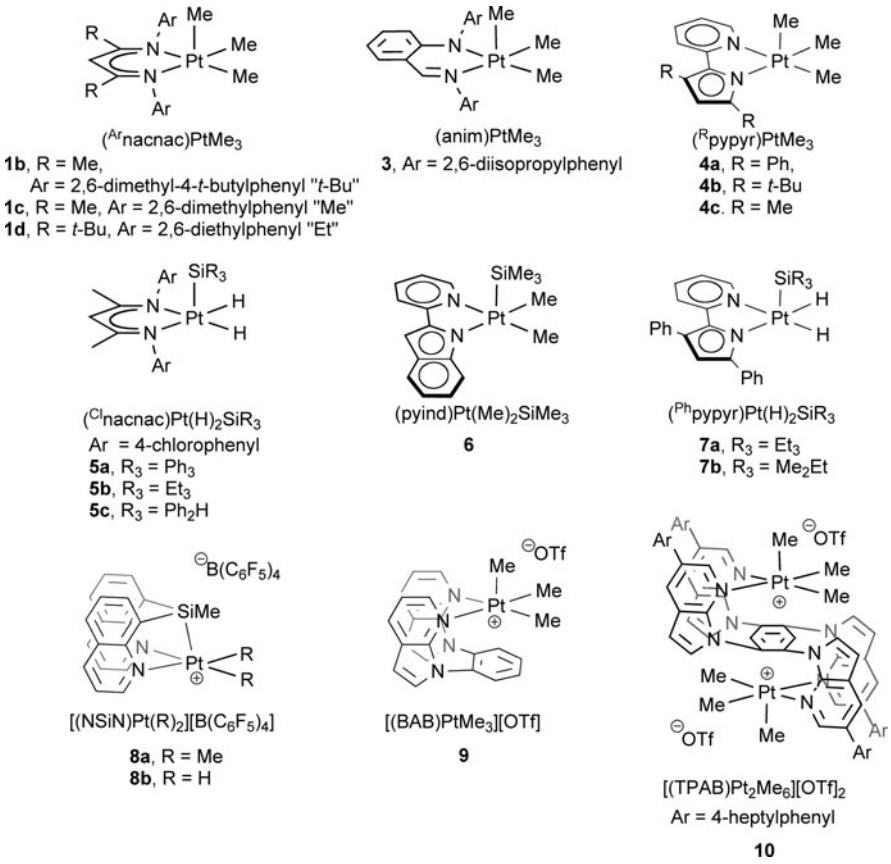

Fig. 4 Other reported five-coordinate Pt(IV) species [89–99]

NMR ($^2J_{Pt–H}$ = 68.0 and 78.8 Hz for the basal and axial positions, respectively) [99]. The $^2J_{Pt–H}$ for the axial Pt–Me group measured in solution is relatively low for a Me group trans to an open site. The binuclear structure might simply be too rigid or an interaction of the Pt open site with the central benzene ring of the ligand may be inhibiting the fluxionality of the Pt–Me groups. Notably, in the crystal structure of **10,** each platinum center is only 2.51 Å away from the nearest carbon on the central benzene ring of the ligand backbone. This situation may be somewhat similar to that of the (dmdpb)$PtMe_3$ complex (**11**) where the potential "open site" was instead shown to be occupied by a C–H agostic interaction. A short distance (2.02 Å) was observed between the Pt center and a proton on the B–CH_3 group (Fig. 5) [100]. No fluxionality of this complex was observed in solution with two separate signals for the basal and axial Pt–Me groups ($^2J_{Pt–H}$ = 64.9 and 84.9 Hz, respectively). Coupling from ^{195}Pt to the B–CH_3 group observed in the ^{1}H NMR spectrum of **11** ($J_{Pt–H}$ = 58.1 Hz) provides strong evidence for the existence of an interaction between the Pt and the B–CH_3 group in solution. NMR spectra at elevated temperature were not reported for **10** or **11**.

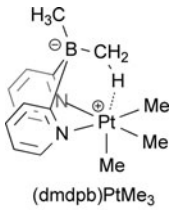

Fig. 5 Agostic interaction between Pt(IV) and a ligand C–H [100]

The Pt(IV) silyl complexes **2a–c**, **5a–c**, **6**, and **7a–b** are not fluxional on the NMR time scale, and exist solely as the isomers with the silyl group trans to the open site [84, 91, 96–98]. This rigidity could be attributable to steric factors and/or the high trans-influence of the silyl group.

The stability of five-coordinate Pt(IV) complexes is striking considering their unsaturated coordination environments. We can note some similarities among this small group of isolable complexes (Fig. 4) and can begin to speculate on factors that may help stabilize these unusual complexes against coordination of a sixth ligand or decomposition, possibly through β-hydride elimination or reductive elimination. First, β-hydride elimination cannot occur because the alkyl groups in the known five-coordinate Pt(IV) complexes do not contain any β-hydrogens. Second, all the complexes have chelating nitrogen donor ligands, which are known to stabilize Pt(IV) (and Pd(IV)) with respect to reductive elimination [19, 43, 101, 102]. Third, all the complexes bear anionic strong σ-donating monodentate groups (alkyls, hydrides, and silyls) and one of these strong trans influence ligands is always trans to the open site, which may inhibit coordination to the open site. Finally, the open site in many of the reported complexes is sterically protected, which likely plays a role in stabilizing some of the complexes by preventing coordination of a sixth ligand. This is particularly evident for **9** where an arene ring appears to completely block the approach of any incoming ligand [95]. Complexes similar to **9** such as (*t*-Bubpy)$PtMe_3OTf$, which do not have steric protection to prevent coordination of triflate, solvent, or adventitious ligands, are reported to exist as six-coordinate Pt(IV) complexes at room temperature [20]. It is notable as well that in the examples of cationic five-coordinate Pt(IV) complexes, which do not have steric congestion around the open site, a noncoordinating counterion such as BAr_4^F or $B(C_6F_5)_4$ is employed (complexes **2a–c** and **8a–b**) [84, 96]. For the neutral ($^{i\text{-Pr}}$nacnac)$PtMe_3$ complex **1a**, steric protection of the open site is significant as can be seen in the space filling model shown in Fig. 6 [83]. When **1a** was reported as the first five-coordinate Pt(IV) alkyl complex, it was thought that this steric protection was a key element in its stability. However, as can be seen in Fig. 4, a variety of complexes with considerably less steric congestion about the open site such as the (^{R}pypyr)Pt and (pyind)Pt complexes **4**, **6**, and **7** are also isolable. The open site of the ($^{t\text{-Bu}}$pypyr)$PtMe_3$ complex, **4b**, is clearly accesible as shown in Fig. 6 [93].

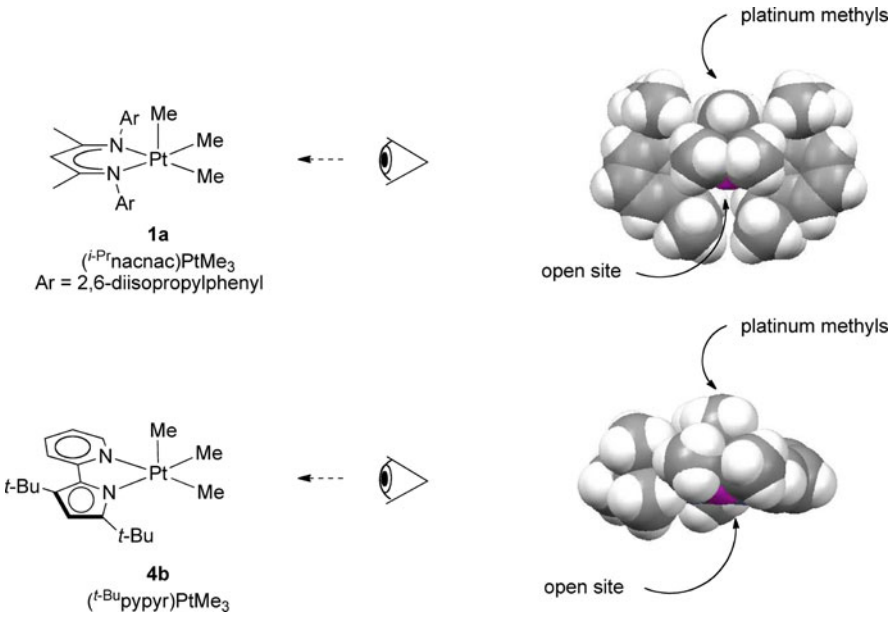

Fig. 6 Space filling models of ($^{i\text{-Pr}}$nacnac)$PtMe_3$ (**1a**) and ($^{t\text{-Bu}}$pypyr)$PtMe_3$ (**4b**)

Although (nacnac)Pt(IV) complexes are five-coordinate, the related acac-ligated Pt(IV) complex is not [6]. $[(acac)PtMe_3]_2$ is a dimer of two potentially five-coordinate (acac)$PtMe_3$ species in which the central carbon on the acac backbone coordinates to another Pt center, giving each Pt an electron count of 18 (Fig. 1) [6]. A similar dimerization could occur in the (nacnac)$PtMe_3$ species **1a–d**, but the steric hindrance provided by the aryl substituents likely prevents such dimerization. Steric bulk on the ligand, even if distant from the open site, can also limit the propensity for dimerization. While ($^{t\text{-Bu}}$pypyr)$PtMe_3$ complex **4b** was characterized as a mononuclear five-coordinate Pt(IV) complex by X-ray crystallography [93], the closely related but the less sterically encumbered methyl-substituted (^{Me}pypyr)$PtMe_3$ complex **4c** forms a noncentrosymmetric dimer in the solid state with a weak interaction (2.52 Å) between the metal center and the 2-pyrrolide carbon of an adjacent molecule [94]. This interaction may also be important in solution at low temperature as the ^{1}H NMR NOESY spectrum of **4c** at –53 °C in CD_2Cl_2 was consistent with such dimer formation. However, the interaction is relatively weak and all NMR spectra recorded at room temperature are consistent with a description of **4c** as a mononuclear fluxional five-coordinate Pt(IV) complex.

5 Reactivity of Five-Coordinate Platinum(IV) Complexes

As discussed earlier, five-coordinate species have been identified as key intermediates in the reactions of six-coordinate Pt(IV) and four-coordinate Pt(II) metal complexes. The recent isolation of model five-coordinate platinum(IV) complexes

has offered the first opportunity to probe the reactivity of such species directly. Reductive elimination reactions have been observed from several of the isolable five-coordinate complexes and the reactivity of the open site with various ligands and reagents has been examined. A survey of the investigations of the reactivity of these unusual complexes is presented in this section.

5.1 Coordination of Monodentate Ligands

In early syntheses of five-coordinate species, it was thought that potential ligands could readily occupy the empty coordination site and needed to be avoided. Thus, coordinating solvents were deliberately not used. Yet some of the first five-coordinate complexes, **2a**–**c**, and later the five-coordinate complexes, (NSiN)PtR_2 (**8a**–**b**), were prepared using reagents with coordinated ether molecules (i.e., $[H(Et_2O)_2][BAr_4^F]$ and $[Li(Et_2O)_3][B(C_6F_5)_4]$). Despite the presence of potentially coordinating ether in the reaction mixture, no evidence of ether coordination was observed in the solid state structures [84, 96]. Indeed, subsequent studies of stable five-coordinate species have shown them to be considerably more discerning in their reactivity with nucleophiles than had been initially anticipated. For example, (^{Cl}nacnac)PtH_2SiPh_3 **5a** showed no interaction with nitriles, even neat acetonitrile [104]. The (NSiN)PtR_2 complex **8a**, which has an unobstructed open site, was exposed to an atmosphere of ethylene with no observable reaction [96].

Some five-coordinate Pt(IV) complexes have been observed to react with L-type ligands to generate the expected six-coordinate complexes, although the strengths of these interactions are variable. For example, (^{Ph}pypyr)PtH_2SiEt_3 (**7a**) reacts with 4-dimethylaminopyridine to give an isolable six-coordinate Pt(IV) complex [97]. In contrast, the typically strongly coordinating PMe_3 was found to bind only weakly to (^{Cl}nacnac)PtH_2SiPh_3 (**5a**) at room temperature, as evidenced by the unusually low Pt–P coupling constant of 745 Hz in the six-coordinate adduct [104]. The (^{Ph}pypyr)$PtMe_3$ complex (**4a**) was shown to coordinate ethylene at low temperature to form a six-coordinate complex, as demonstrated by three inequivalent Pt–Me signals in the ^{1}H NMR of **4a** in the presence of ethylene at −69 °C [93]. Coelescence of the signals was observed upon warming, indicative of reversible binding of the ethylene to **4a**. The reactivity of ($^{t\text{-Bu}}$nacnac)$PtMe_3$ (**1b**) with CO and *tert*-butylisocyanide (*t*-BuNC) has also been investigated [103]. Carbon monoxide was found to bind reversibly to form a six-coordinate species. In the absence of CO, the Pt–Me groups of ($^{t\text{-Bu}}$nacnac)$PtMe_3$ undergo rapid exchange at temperatures as low as –80 °C as evidenced by a single Pt–Me resonance in the ^{1}H NMR spectrum. In the presence of CO, distinct resonances for the axial and equatorial methyl groups were evident at –40 °C. Upon warming to room temperature, a very broad Pt–Me resonance, shifted upfield from that of the five-coordinate species, was observed suggesting reversible CO binding on the NMR time scale. In contrast, the isolable six-coordinate complex ($^{t\text{-Bu}}$nacnac)$PtMe_3$(CN*t*-Bu) was formed with *t*-BuNC

[103]. The isocyanide *t*-BuNC is generally considered a better σ-donor and poorer π-acceptor than CO [3]. Thus, these five-coordinate complexes, though unsaturated, appear to be somewhat discriminating in their coordination of ligands.

5.2 Reductive Elimination

Mechanistic studies of C–C reductive elimination from six-coordinate platinum(IV) complexes have consistently indicated the involvement of five-coordinate species on the reaction pathway (see Sect. 2.1.1). If the novel five-coordinate Pt(IV) complexes that have been isolated over the last decade are to serve as functional models for these intermediates, then direct C–C coupling, without preliminary ligand association or dissociation, should be observable from the alkyl complexes. Studies of the thermolyses of several five-coordinate Pt(IV)Me_3 complexes have provided convincing evidence for direct, concerted C–C reductive elimination from the five-coordinate species.

Ethane, the expected product of C–C reductive elimination was observed upon thermolysis of the five-coordinate complexes (^{Ph}pypyr)$PtMe_3$ (**4a**) and ($^{t\text{-Bu}}$pypyr)$PtMe_3$ (**4b**) in benzene [93]. The production of methane was also observed in these reactions. In the case of (^{Ph}pypyr)$PtMe_3$ (**4a**), no stable platinum product could be identified. However, upon thermolysis of the *t*-Bu substituted **4b**, a bimetallic complex (**12**) was isolated in good yield (Scheme 6). If the thermolysis of **4b** was carried out in benzene-d_6, CH_3D was observed in addition to CH_4 and the cyclometalated alkyl group in the bimetallic complex was completely deuterated. The mechanism shown in Scheme 6 accounts for these results. Reductive elimination from ($^{t\text{-Bu}}$pypyr)$PtMe_3$ (**4b**) yields the three-coordinate Pt(II) intermediate, **A**, which may be stabilized by an interaction with solvent or by an agostic C–H interaction. Such unsaturated or weakly ligated Pt(II) species are known to be involved in the activation of C–H bonds [31, 70, 71]. Two options are available to this reactive Pt(II) species: C–D activation of solvent (path a) or intramolecular C–H bond activation leading to cyclometalation of a *t*-Bu substituent (path b). Both options lead to Pt(IV) species that would reductively eliminate methane (or methane-d_1) to yield intermediate **B**. The observation of both CH_3D and CH_4 indicates that intermolecular arene activation and intramolecular cyclometalation are competitive. The full deuteration of the alkyl arm in the product indicates that arene activation and cyclometalation are both reversible. Formation of the final binuclear product, **12**, was proposed to result from trapping of the unsaturated intermediate **B** by starting material, ($^{t\text{-Bu}}$pypyr)$PtMe_3$ (**4b**).

Thermolysis of either **4a** or **4b** in the presence of ethylene led to isolable products **13a** and **13b** in which efficient trapping of **B′** (the orthometalated analog of **B**) or **B**, respectively, with ethylene occurs as shown in Scheme 7. Analysis of the rates of reaction of **4a** with respect to ethylene concentration showed that ethylene can bind to the five-coordinate Pt(IV) species and inhibit C–C reductive elimination. These results support direct C–C coupling from the five-coordinate complexes and establish the validity of these species as functional models for the intermediates

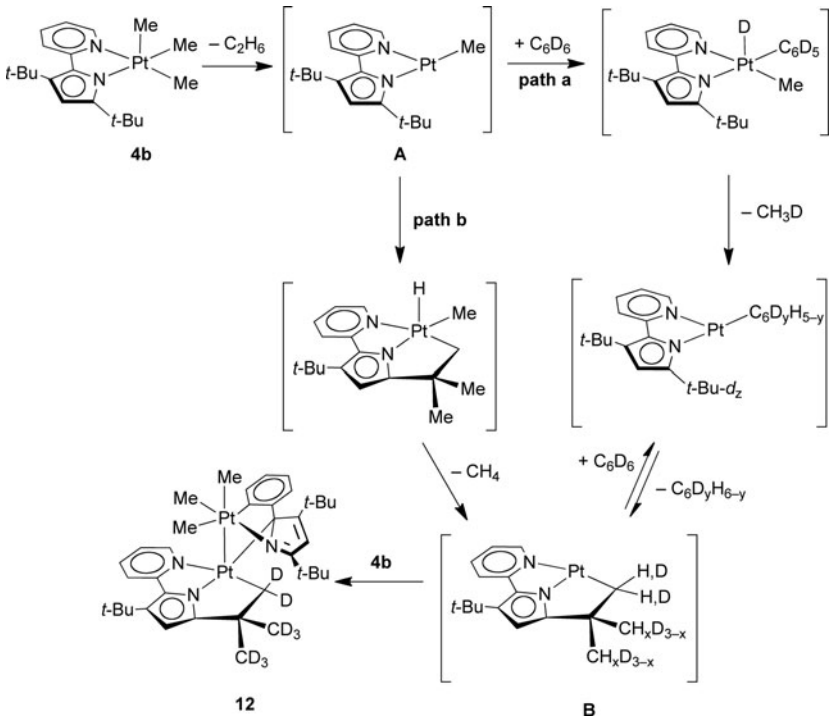

Scheme 6 Reductive elimination from **4b** to yield **12** [93]

previously proposed in C–C reductive elimination reactions from six-coordinate Pt(IV) complexes. The rates of reductive elimination from **4a** were measured in the presence of varying amounts of ethylene, and the rate constant for the concerted C–C reductive elimination, k_2, was determined ($k_2 = 6.3(4) \times 10^{-4}$ s^{-1}). Previous determinations of rate constants for alkyl C–C reductive elimination were from six-coordinate Pt(IV) and therefore included a contribution from a preliminary ligand dissociation step [10, 15–18, 21–25, 27, 28].

C–C reductive elimination was also observed upon thermolysis of ($^{i\text{-Pr}}$nacnac)$PtMe_3$ (**1a**) and (anim)$PtMe_3$ (**3**) [83, 92]. The rate of ethane elimination from these complexes was slower than from (^{Ph}pypyr)$PtMe_3$ **4a** with rate constants of $3.0(2) \times 10^{-6}$ s^{-1} and $2.1(2) \times 10^{-5}$ s^{-1} measured for **1a** and **3**, respectively. Although the ($^{i\text{-Pr}}$nacnac)$PtMe_3$ and (anim)$PtMe_3$ complexes appear quite similar in their structures, the change in the electronics of the ligand backbone with the incorporation of an arene ring in the anim ligand results in almost an order of magnitude difference in their rate constants for reductive elimination. It had previously been difficult to make such direct comparisons concerning the key C–C bond-forming step as prior measurements of rate constants of reductive elimination from Pt(IV) involved contributions from the preliminary ligand dissociation step.

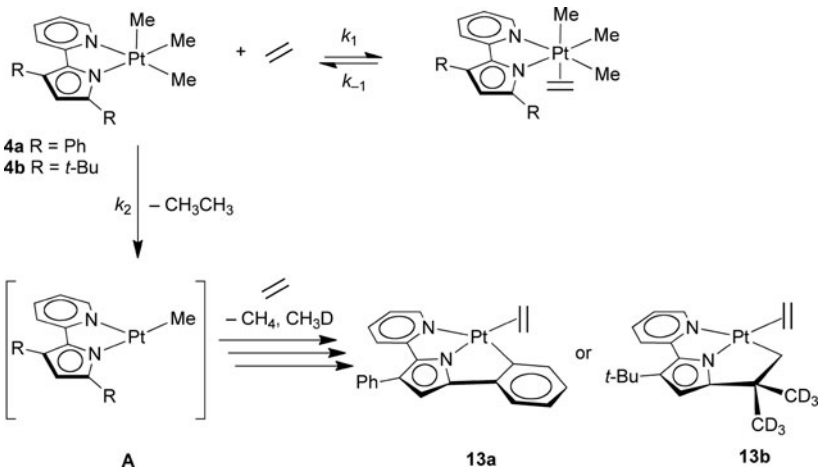

Scheme 7 Reductive elimination from **4a** and **4b** in the presence of ethylene [93]

In addition to the C–C coupling product ethane, methane was also detected in the thermolysis of ($^{i\text{-Pr}}$nacnac)$PtMe_3$ (**1a**) and (anim)$PtMe_3$ (**3**). The platinum products of the thermolysis reactions are the Pt(II) hydride complexes **14** and **15** in which the isopropyl substituent on the aryl group of the ligand has undergone dehydrogenation and coordination to the metal center [89, 92]. When the reaction was carried out in deuterated benzene solvent, complete deuteration of the isopropyl groups of the product (including the dehydrogenated group) was observed. This result is explained by the mechanism shown in Scheme 8. Reductive elimination of ethane from either five-coordinate complex generates a three-coordinate Pt(II) species. Intramolecular oxidative addition of a C–H bond of one of the isopropyl groups generates a five-coordinate Pt(IV) methyl hydride complex. Rapid reductive elimination of methane produces the unsaturated cyclometalated Pt(II) complex. This cyclometalated Pt(II) intermediate can undergo either intermolecular oxidative addition of a solvent C–D bond or intramolecular β-hydride elimination to generate the Pt(II) olefin hydride product. Reversible C–H/C–D oxidative addition/reductive elimination prior to the β-hydride elimination step results in the deuteration of the isopropyl groups [92].

An important element of the reductive elimination of ethane from these five-coordinate Pt(IV) complexes is that three-coordinate Pt(II) species capable of C–H activation are generated. As described above, a three-coordinate Pt(II) species can participate in an intramolecular activation of a ligand C–H bond or an intermolecular activation of a solvent C–H bond. When the cyclometalated group formed by intramolecular activation can undergo β-hydride elimination, dehydrogenation of the ligand has been observed. Notably, intermolecular dehydrogenation of solvent was observed when intramolecular dehydrogenation was not possible. Thus, thermolysis of the ($^{t\text{-Bu}}$nacnac)$PtMe_3$, **1b**, wherein the isopropyl groups of **1a** have been replaced by methyl groups, in neohexane or cyclohexane solvent, led to efficient intermolecular alkane activation followed by β-hydride elimination to yield a Pt(II)

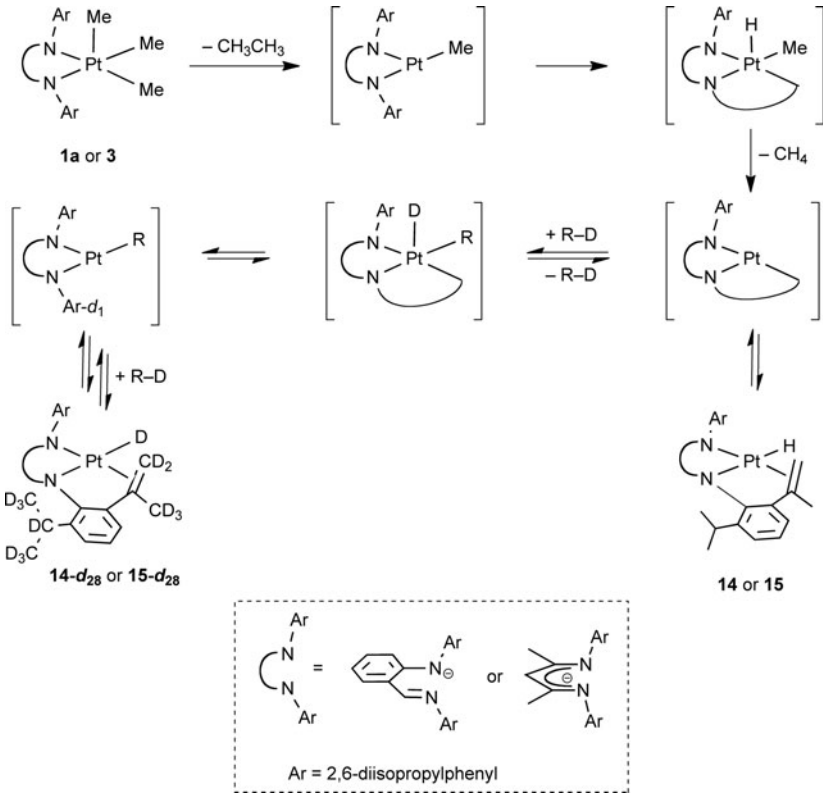

Scheme 8 C–C Reductive elimination from **1a** and **3** and H–D exchange [92]

olefin hydride complex [90]. The Pt(II) neohexene hydride was capable of performing stoichiometric transfer dehydrogenation in cyclohexane solvent to form the Pt(II) cyclohexene hydride and free neohexane. However, no catalytic transfer dehydrogenation of cyclohexane was observed with excess neohexene. Catalytic transfer dehydrogenation of diethyl ether (1.3 turnovers) was achieved with the related unsubstituted nacnac ligand complex, (nacnac)Pt(neohexene) hydride, in the presence of excess neohexene in diethyl ether solvent [104].

Reductive elimination of ethane from five-coordinate Pt(IV) alkyl complexes has also led to the generation of three-coordinate complexes that have shown catalytic activity in the hydroarylation of olefins. In contrast to the *t*-Bu or Ph substituted pypyr ligands which underwent facile cyclometalation and trapping with ethylene (Scheme 7), when the Me-substituted (^{Me}pypyr)PtMe$_3$ (**4c**) was heated in benzene solvent under a pressure of ethylene, ethyl benzene product was produced with a TON of 26 [94]. Other combinations of arenes and olefins were also observed to yield hydroarylation products when (^{Me}pypyr)PtMe$_3$ complex **4c** was used as a catalyst precursor. Presumably C–C reductive elimination of ethane is followed by C–H activation of the arene, reductive elimination of methane, and then

coordination and insertion of the olefin. Mechanistic studies were consistent with olefin insertion into the Pt–Ph bond followed by *intra*molecular arene C–H oxidative addition, alkyl C–H reductive elimination, *inter*molecular arene C–H oxidative addition, and C–H reductive elimination of the product. Five-coordinate intermediates are implied in this mechanism immediately after each C–H bond oxidative addition to Pt(II) and immediately prior to each C–H reductive elimination from Pt(IV).

Five-coordinate Pt(IV) species with silyl ligands are poised to perform Si–C or Si–H reductive elimination from Pt(IV). Note that the microscopic reverse of the latter reaction, Si–H oxidative addition, was used to synthesize the first five-coordinate Pt(IV) complexes with silyl ligands (**2a**–**c**) [84]. Complex **6**, which has Pt–Me groups and a Pt–$SiMe_3$ group, was observed to react over time at room temperature to form tetramethylsilane, the product of Si–C reductive elimination, and intractable Pt products [91]. The five-coordinate complex (^{Ph}pypyr)Pt$(H)_2SiEt_3$, **7a**, was found to react with $HSiMe_2Et$ to form product **7b**. Study of this reaction showed that Si–H reductive elimination from **7a** was rate-determining and it occurred directly from the five-coordinate complex [97]. Reaction of **7a** with phosphines at room temperature led to the formation of a Pt(II)H(PR_3) complex and free silane, the product of Si–H reductive elimination. Complex **7a** was observed to be an active catalyst for the hydrosilylation of ethylene, *tert*-butylethylene, and alkynes [97].

The syntheses of isolable five-coordinate Pt(IV) complexes have allowed the direct study of C–C and Si–H reductive elimination processes. Rate constants can now be determined for these bond-forming reactions that do not include contributions from preliminary dissociation of ligands as is generally the case when the reactions occur from octahedral complexes. In addition, reductive elimination from five-coordinate Pt(IV) complexes allows access to highly reactive Pt(II) species, which have been shown to perform intra- and intermolecular C–H activation and to provide entry points into catalytic hydroarylation and hydrosilylation reactions.

5.3 *Metal–Ligand Cooperativity*

Recently, it was found that ($^{t\text{-Bu}}$nacnac)$PtMe_3$, **1b**, reacts with ethylene (reversibly) and 3,3-dimethylbutyne to form cycloaddition products **16** and **17** wherein both the open site at the metal center and the ligand backbone are involved in reaction with the exogenous substrate (Scheme 9) [103]. This type of reactivity to form bicyclic complexes has also been observed with another five-coordinate Pt(IV) nacnac complex. (^{Cl}nacnac)PtH_2SiPh_3, **5a**, reacts with acetylene, phenylacetylene, and phosphaalkynes to form the coordinatively saturated six-coordinate products shown in Scheme 9 [104]. Both the open site and the reactive site on the ligand are important in these reactions. Other coordinatively unsaturated, typically trigonal planar, (nacnac)M complexes have been observed to undergo analogous cycloaddition reactions of alkenes, alkynes, ketones, ketenes, and diazo compounds to form bicyclic products [105–110].

A closely related bicyclic product was also recently observed in the activation of molecular oxygen by a five-coordinate Pt(IV) complex [103]. The five-coordinate ($^{t\text{-Bu}}$nacnac)$PtMe_3$, **1b**, was found to react with dioxygen in toluene-d_8 to form a

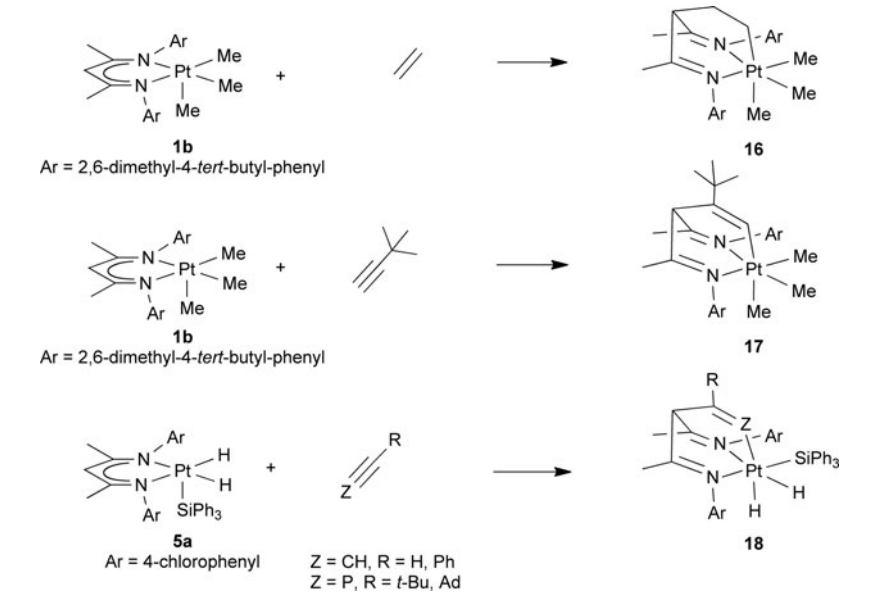

Scheme 9 Cycloaddition reactions involving five-coordinate Pt(IV) nacnac complexes [103, 104]

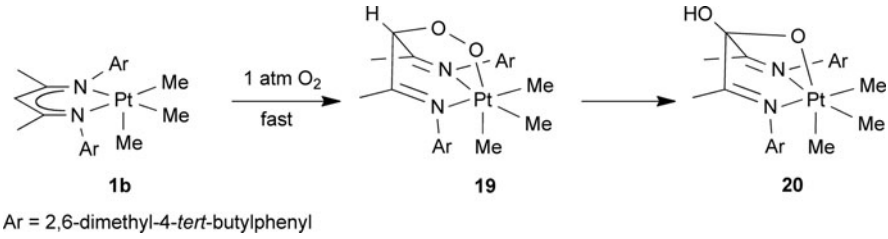

Scheme 10 Cycloaddition of dioxygen with ($^{t\text{-Bu}}$nacnac)PtMe$_3$ **1b** [103]

six-coordinate peroxo species, (**19**), in which one oxygen atom is bound to the metal center and the other to the central carbon of the ligand backbone (Scheme 10). The peroxo species, **19**, was characterized in solution by ^{1}H and ^{13}C NMR spectroscopies. Over time, the peroxo species generates a more stable complex in which the O–O bond has been cleaved (**20**, Scheme 10). This latter complex was characterized by X-ray crystallography. Pt(IV) complexes bearing a similar chelate structure to this final product have been formed from the reaction of (DPK)PtMe$_2$ (DPK = di-2-pyridyl ketone) with H_2O_2 [111].

The observation of the peroxo intermediate in the reaction of ($^{t\text{-Bu}}$nacnac)PtMe$_3$, **1b**, with oxygen is significant. There was one previous report of a (nacnac)Cu complex being oxidized by molecular oxygen at the central carbon of the ligand backbone [112]. In this (nacnac)Cu case, a peroxo species analogous to **19** was proposed, but not observed, as an intermediate in the reaction. A formal cycloaddition of molecular

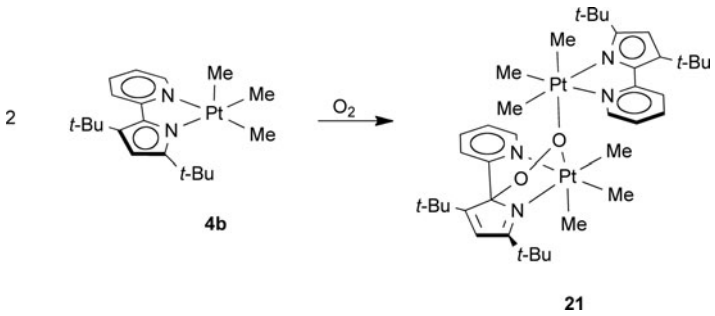

Scheme 11 Reaction of dioxygen with ($^{t\text{-Bu}}$pypyr)$PtMe_3$ (**4b**) [113]

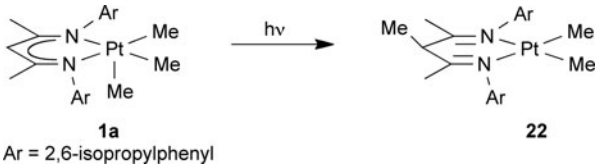

Scheme 12 Methyl migration from Pt(IV) to a ligand carbon [83]

oxygen to form a peroxo species has also been found with ($^{t\text{-Bu}}$pypyr)$PtMe_3$ complex **4b**. The crystallographically observed product was a bimetallic peroxo species, in which the peroxo moiety binds to both the metal centers and the carbon in the ligand backbone of one of the metals (**21**, Scheme 11). This bimetallic structure could be viewed as a monomeric peroxo complex, wherein the oxygen is bound to the metal and the ligand backbone (somewhat analogous to **19**) acting as a ligand to a second five-coordinate Pt(IV) center. Under an oxygen atmosphere, the spectroscopic data support a monomeric peroxo complex in solution [113].

It appears that the presence of a site where a negative charge can be localized on the ligand may play a significant role in promoting the observed reactions of oxygen, olefins, and alkynes with the five-coordinate ($^{t\text{-Bu}}$pypyr)$PtMe_3$, ($^{t\text{-Bu}}$nacnac)$PtMe_3$, and (^{Cl}nacnac)$Pt(H)_2SiPh_3$ complexes. In the pypyr ligand, electron density can potentially be localized on the 2-position of the pyrrolide ring and, in the nacnac ligands, on the central carbon of the ligand backbone. The reactivity of this site in nacnac is also seen when ($^{i\text{-Pr}}$nacnac)$PtMe_3$ (**1a**) is exposed to light. Formal methyl cation migration from Pt to the central carbon of the ligand backbone is observed resulting in a diimine Pt(II) dimethyl complex **22** (Scheme 12) [83]. The examples of metal–ligand cooperativity in the reactions of five-coordinate complexes ligated by nacnac and pypyr ligands (above) are significant because they suggest that the involvement of reactive sites on the ligand may prove critical in the transformations of five-coordinate complexes and unobserved five-coordinate intermediates. Further investigations of five-coordinate complexes beyond those ligated by nacnac or pypyr ligands are needed to more fully understand the importance of this ligand involvement.

6 Conclusions and Future Directions

Five-coordinate intermediates are important in many fundamental reaction steps at Pt(IV) including C–C, C–X, and C–H bond formation. Once thought to be too reactive to isolate or observe, 16 electron, five-coordinate platinum(IV) complexes have now been synthesized, isolated, and fully characterized. The existence and reactivity of these complexes validate the many proposals of five-coordinate intermediates in the reactions of octahedral six-coordinate platinum(IV) complexes. In addition, we can now study their structures and reactivity with a wide range of substrates to better guide the development of catalytic reactions. Interesting reactivity has been observed with exogenous reagents such as olefins and molecular oxygen. The direct, thermally promoted C–C or Si–H reductive elimination from five-coordinate Pt(IV) complexes has allowed access to reactive Pt(II) species, which can perform catalytic bond activation and functionalization reactions such as hydroarylation and hydrosilylation. As more examples of complexes sharing the five-coordinate Pt(IV) structure become available, we will further our understanding of the factors that govern the stability and reactivity of these novel species. The insight gained from studying these five-coordinate Pt(IV) complexes is also likely to be applicable to reactions of Pd(IV), where five-coordinate intermediates have also been proposed but not yet observed.

Acknowledgments We gratefully acknowledge the support of the US National Science Foundation (NSF), which has funded research in our laboratory in this area over the last decade (CHE-0137394, CHE-0719372, and CHE-1012045).

References

1. Crabtree RH (2009) The organometallic chemistry of the transition metals, 5th edn. Wiley, Hoboken
2. Spessard GO, Miessler GL (2009) Organometallic chemistry, 2nd edn. Oxford University Press, New York
3. Hartwig J (2010) Organotransition metal chemistry: from bonding to catalysis. University Science Books, Sausalito, CA
4. Pope WJ, Peachey SJ (1907) Proc Chem Soc London 23:86–87
5. Pope WJ, Peachey SJ (1909) J Chem Soc Trans 95:571–576
6. Menzies RC (1928) J Chem Soc 565–566
7. Ruddick JD, Shaw BL (1969) J Chem Soc A 2969–2970
8. Canty AJ, Dedieu A, Jin H, Milet A, Richmond MK (1996) Organometallics 15:2845–2847
9. Robinson SD, Shaw BL (1963) Zeitschrift fuer Naturforschung 18b:507
10. Crumpton DM, Goldberg KI (2000) J Am Chem Soc 122:962–963
11. Roth S, Ramamoorthy V, Sharp PR (1990) Inorg Chem 29:3345–3349
12. Levy CJ, Puddephatt RJ, Vittal JJ (1994) Organometallics 13:1559–1560
13. Ettore R (1969) Inorg Nucl Chem Lett 5:45–59
14. Levy CJ, Vittal JJ, Puddephatt RJ (1996) Organometallics 15:35–42
15. Brown MP, Puddephatt RJ, Upton CEE (1974) J Chem Soc Dalton Trans 2457–2465
16. Roy S, Puddephatt RJ, Scott JD (1989) J Chem Soc Dalton Trans 2121–2125

17. Goldberg KI, Yan JY, Winter EL (1994) J Am Chem Soc 116:1573–1574
18. Goldberg KI, Yan JY, Breitung EM (1995) J Am Chem Soc 117:6889–6896
19. Hill GS, Puddephatt RJ (1997) Organometallics 16:4522–4524
20. Hill GS, Yap GPA, Puddephatt RJ (1999) Organometallics 18:1408–1418
21. Williams BS, Holland AW, Goldberg KI (1999) J Am Chem Soc 121:252–253
22. Williams BS, Goldberg KI (2001) J Am Chem Soc 123:2576–2587
23. Crumpton-Bregel DM, Goldberg KI (2003) J Am Chem Soc 125:9442–9456
24. Arthur KL, Wang QL, Bregel DM, Smythe NA, O'Neill BA, Goldberg KI, Moloy KG (2005) Organometallics 24:4624–4628
25. Procelewska J, Zahl A, Liehr G, van Eldik R, Smythe NA, Williams BS, Goldberg KI (2005) Inorg Chem 44:7732–7742
26. Madison BL, Thyme SB, Keene S, Williams BS (2007) J Am Chem Soc 129:9538–9539
27. Pawlikowski AV, Getty AD, Goldberg KI (2007) J Am Chem Soc 129:10382–10393
28. Smythe NA, Grice KA, Willams BS, Goldberg KI (2009) Organometallics 28:277–288
29. Shahsavari HR, Rashidi M, Nabavizadeh SM, Habibzadeh S, Heinemann FW (2009) Eur J Inorg Chem 2009:3814–3820
30. Lindner R, Wagner C, Steinborn D (2009) J Am Chem Soc 131:8861–8874
31. Wick DD, Goldberg KI (1997) J Am Chem Soc 119:10235–10236
32. Fekl U, Zahl A, van Eldik R (1999) Organometallics 18:4156–4164
33. Reinartz S, White PS, Brookhart M, Templeton JL (2000) Organometallics 19:3854–3866
34. Puddephatt RJ (2001) Coord Chem Rev 219–221:157–185
35. Jensen MP, Wick DD, Reinartz S, White PS, Templeton JL, Goldberg KI (2003) J Am Chem Soc 125:8614–8624
36. Zhang F, Jennings MC, Puddephatt RJ (2004) Organometallics 23:1396–1404
37. Zhang F, Prokopchuk EM, Broczkowski ME, Jennings MC, Puddephatt RJ (2006) Organometallics 25:1583–1591
38. Feducia JA, Campbell AN, Anthis JW, Gagné MR (2006) Organometallics 25:3114–3117
39. Wik BJ, Ivanovic-Burmazovic I, Tilset M, van Eldik R (2006) Inorg Chem 45:3613–3621
40. Luinstra GA, Labinger JA, Bercaw JE (1993) J Am Chem Soc 115:3004–3005
41. Luinstra GA, Wang L, Stahl SS, Labinger JA, Bercaw JE (1995) J Organomet Chem 504:75–91
42. Canty AJ, Denney MC, van Koten G, Skelton BW, White AH (2004) Organometallics 23: 5432–5439
43. Hill GS, Puddephatt RJ (1998) Organometallics 17:1478–1486
44. Bartlett KL, Goldberg KI, Borden WT (2000) J Am Chem Soc 122:1456–1465
45. Bartlett KL, Goldberg KI, Borden WT (2001) Organometallics 20:2669–2678
46. Michel C, Laio A, Mohamed F, Krack M, Parrinello M, Milet A (2007) Organometallics 26:1241–1249
47. Vastine BA, Webster CE, Hall MB (2007) J Chem Theory Comput 3:2268–2281
48. Michel C, Milet A (2008) J Mol Struc-Theochem 852:54–61
49. Byers PK, Canty AJ, Crespo M, Puddephatt RJ, Scott JD (1988) Organometallics 7: 1363–1367
50. Canty AJ (1992) Acc Chem Res 25:83–90
51. Dücker-Benfer C, van Eldik R, Canty AJ (1994) Organometallics 13:2412–2414
52. Lanci MP, Remy MS, Kaminsky W, Mayer JM, Sanford MS (2009) J Am Chem Soc 131:15618–15620
53. Hutson AC, Lin M, Basickes N, Sen A (1995) J Organomet Chem 504:69–74
54. Stahl SS, Labinger JA, Bercaw JE (1998) Angew Chem Int Ed 37:2180–2192
55. Vedernikov AN, Binfield SA, Zavalij PY, Khusnutdinova JR (2006) J Am Chem Soc 128:82–83
56. Khusnutdinova JR, Zavalij PY, Vedernikov AN (2007) Organometallics 26:2402–2413
57. Khusnutdinova JR, Newman LL, Zavalij PY, Lam Y-F, Vedernikov AN (2008) J Am Chem Soc 130:2174–2175

58. Hill GS, Rendina LM, Puddephatt RJ (1995) Organometallics 14:4966–4968
59. Stahl SS, Labinger JA, Bercaw JE (1995) J Am Chem Soc 117:9371–9372
60. O'Reilly SA, White PS, Templeton JL (1996) J Am Chem Soc 118:5684–5689
61. Hill GS, Puddephatt RJ (1996) J Am Chem Soc 118:8745–8746
62. Hill GS, Vittal JJ, Puddephatt RJ (1997) Organometallics 16:1209–1217
63. Jenkins HA, Yap GPA, Puddephatt RJ (1997) Organometallics 16:1946–1955
64. Prokopchuk EM, Jenkins HA, Puddephatt RJ (1999) Organometallics 18:2861–2866
65. Haskel A, Keinan E (1999) Organometallics 18:4677–4680
66. Reinartz S, Brookhart M, Templeton JL (2002) Organometallics 21:247–249
67. Vedernikov AN, Caulton KG (2002) Angew Chem Int Ed 41:4102–4104
68. Jenkins HA, Klempner MJ, Prokopchuk EM, Puddephatt RJ (2003) Inorg Chim Acta 352:72–78
69. Vedernikov AN, Fettinger JC, Mohr F (2004) J Am Chem Soc 126:11160–11161
70. Fekl U, Goldberg KI (2003) Adv Inorg Chem 54:259–320
71. Lersch M, Tilset M (2005) Chem Rev 105:2471–2526
72. Norris CM, Templeton JL (2004) Organometallics 23:3101–3104
73. Labinger JA, Bercaw JE (2011) The role of higher oxidation state species in platinum-mediated C-H bond activation and functionalization. Top Organomet Chem 35:29–60
74. Brown MP, Puddephatt RJ, Upton CEE, Lavington SW (1974) J Chem Soc Dalton Trans 1613–1618
75. Baird MC, Lawson DN, Mague JT, Osborn JA, Wilkinson G (1966) Chem Commun (London) 129–130
76. Kubota M, Blake DM, Smith SA (1971) Inorg Chem 10:1430–1433
77. Ghosh R, Emge TJ, Krogh-Jespersen K, Goldman AS (2008) J Am Chem Soc 130: 11317–11327
78. Bernskoetter WH, Hanson SK, Buzak SK, Davis Z, White PS, Swartz R, Goldberg KI, Brookhart M (2009) J Am Chem Soc 131:8603–8613
79. Bernskoetter WH, Schauer CK, Goldberg KI, Brookhart M (2009) Science 326:553–556
80. Krogh-Jespersen K, Czerw M, Kanzelberger M, Goldman AS (2001) J Chem Inf Comput Sci 41:56–63
81. Krogh-Jespersen K, Czerw M, Summa N, Renkema KB, Achord PD, Goldman AS (2002) J Am Chem Soc 124:11404–11416
82. Goldman AS, Roy AH, Huang Z, Ahuja R, Schinski W, Brookhart M (2006) Science 312:257–261
83. Fekl U, Kaminsky W, Goldberg KI (2001) J Am Chem Soc 123:6423–6424
84. Reinartz S, White PS, Brookhart M, Templeton JL (2001) J Am Chem Soc 123:6425–6426
85. Hoffman PR, Caulton KG (1975) J Am Chem Soc 97:4221–4228
86. Ashworth TV, Chalmers AA, Singleton E (1985) Inorg Chem 24:2125–2126
87. Heyn RH, Macgregor SA, Nadasdi TT, Ogasawara M, Eisenstein O, Caulton KG (1997) Inorg Chim Acta 259:5–26
88. Huang D, Streib WE, Bollinger JC, Caulton KG, Winter RF, Scheiring T (1999) J Am Chem Soc 121:8087–8097
89. Fekl U, Goldberg KI (2002) J Am Chem Soc 124:6804–6805
90. Fekl U, Kaminsky W, Goldberg KI (2003) J Am Chem Soc 125:15286–15287
91. Karshtedt D, McBee JL, Bell AT, Tilley TD (2006) Organometallics 25:1801–1811
92. Kloek SM, Golberg KI (2007) J Am Chem Soc 129:3460–3461
93. Luedtke AT, Goldberg KI (2007) Inorg Chem 46:8496–8498
94. Luedtke AT, Goldberg KI (2008) Angew Chem Int Ed 47:7694–7696
95. Zhao S-B, Wu G, Wang S (2008) Organometallics 27:1030–1033
96. Sangtrirutnugul P, Tilley TD (2008) Organometallics 27:2223–2230
97. McBee JL, Tilley TD (2009) Organometallics 28:3947–3952
98. West NM, White PS, Templeton JL, Nixon JF (2009) Organometallics 28:1425–1434
99. Zhao S-B, Cui Q, Wang S (2010) Organometallics 29:998–1003

100. Khaskin E, Zavalij PY, Vedernikov AN (2007) Angew Chem Int Ed 46:6309–6312
101. van Asselt R, Rijnberg E, Elsevier CJ (1994) Organometallics 13:706–720
102. Rendina LM, Puddephatt RJ (1997) Chem Rev 97:1735–1754
103. Scheuermann ML, Fekl U, Kaminsky W, Goldberg KI (2010) Organometallics 29: 4749–4751
104. West NM, White PS, Templeton JL (2007) J Am Chem Soc 129:12372–12373
105. Radzewich CE, Coles MP, Jordan RF (1998) J Am Chem Soc 120:9384–9385
106. Phillips AD, Laurenczy G, Scopelliti R, Dyson PJ (2007) Organometallics 26:1120–1122
107. Yao S, van Wüllen C, Driess M (2008) Chem Commun 5393–5395
108. Gregory EA, Lachicotte RJ, Holland PL (2005) Organometallics 24:1803–1805
109. Basuli F, Huffman JC, Mindiola DJ (2003) Inorg Chem 42:8003–8010
110. Carey DT, Cope-Eatough EK, Vilaplana-Mafé E, Mair FS, Pritchard RG, Warren JE, Woods RJ (2003) Dalton Trans 1083–1093
111. Zhang F, Broczkowski ME, Jennings MC, Puddephatt RJ (2005) Can J Chem 83:595–605
112. Yokota S, Tachi Y, Itoh S (2002) Inorg Chem 41:1342–1344
113. Luedtke AT (2007) Synthesis, structure, and reactivity of five-coordinate platinum(IV) complexes. PhD Thesis, University of Washington, Seattle, WA

Top Organomet Chem (2011) 35:29–60
DOI: 10.1007/978-3-642-17429-2_2

The Role of Higher Oxidation State Species in Platinum-Mediated C–H Bond Activation and Functionalization

Jay A. Labinger and John E. Bercaw

Abstract The Shilov system, a mixture of di- and tetravalent chloroplatinate salts in aqueous solution, provided the first indication of the potential of organotransition metal complexes for activating and functionalizing alkanes under mild conditions; the participation of higher-valent species plays a crucial role. In this chapter, we discuss the experimental and computational studies that have led to detailed mechanistic understanding of C–H activation and functionalization by both the original Shilov system and the many subsequent modifications that have been developed, and assess the prospects for practical, selective catalytic oxidation of alkanes using this chemistry.

Keywords Alkane functionalization · Hydrocarbon oxidation · Platinum

Contents

J.A. Labinger and J.E. Bercaw
Arnold and Mabel Beckman Laboratories of Chemical Synthesis, California Institute of Technology, Pasadena, CA 91125, USA
e-mail: jal@its.caltech.edu, bercaw@caltech.edu

1 Introduction

Today, there are well-established examples of facile C–H bond activation by just about every transition metal in the periodic table, but the historical pride of precedence goes to platinum. The conversion of alkanes to alcohols by chloroplatinate salts, under what appeared at the time to be remarkably mild conditions, was first reported by Alexander Shilov and his coworkers around 1970. The initial triggering discovery was actually made by Garnett and Hodges [1], who examined H/D exchange in arenes catalyzed by acidic solutions of $[Pt^{II}Cl_4]^{2-}$. In itself this reaction may have seemed unremarkable, perhaps just an analog of the well-known mercuration of arenes; but the paper also mentioned (with no details) that aliphatic C–H bonds of methyl substituents on arenes, and even in cyclohexane, also exhibited some exchange. Following up on this observation, Shilov demonstrated that alkane C–H bonds undergo the exchange reaction [2] and subsequently decided (for reasons that are not completely obvious [3]) to add $[Pt^{IV}Cl_6]^{2-}$ to the system, thus obtaining a much more interesting reaction: moderately selective oxidation of alkanes to alcohols and chloroalkanes (Scheme 1) [4].

This paper and subsequent studies by Shilov and other Soviet groups – published primarily in Russian-language journals – initially attracted relatively little attention, and much of that was rather dubious: how could such "ordinary" metal complexes effect so unprecedented a transformation under near-ambient conditions? The first appearances of definitive examples of alkane activation at transition metal centers, around a decade later, did not really dispel these doubts. Activating species such as $[(C_5Me_5)(PMe_3)Ir^{I}]$, in Bergman's pioneering work [5], were coordinatively unsaturated, often photogenerated, and very electron-rich. What correspondingly extraordinary properties do these chloroplatinate salts have to offer? Many believed that this was actually heterogeneous catalysis, with the chemistry taking place at the surface of colloidal metallic platinum, not at a discrete, soluble metal complex.

All such suspicion proved unfounded: detailed mechanistic work, carried out both by Shilov and his collaborators in the 1970s and by other groups starting in the late 1980s, has conclusively demonstrated that Shilov's original proposal *was* correct and provided at least a partial explanation of just what is special about the Shilov system: the interplay between low-valent Pt(II) and high-valent Pt(IV) species, exploiting their differing chemical properties, is crucial in making this remarkable chemistry work.

Here, we examine the roles played by high-valent Pt complexes, not only in the Shilov system itself but also in the many subsequent examples of C–H activation that have been studied as models for and/or improvements upon the original work. To be sure, this topic has previously been addressed to some degree in general reviews of C–H activation (these are much too numerous for a complete listing, but for historical reasons we cite two by Shilov himself [6, 7]). More to the

$$R\text{–}H + [Pt^{II}Cl_4]^{2-} + [Pt^{IV}Cl_6]^{2-} \xrightarrow[H_2O]{120^\circ C} R\text{–}OH + R\text{–}Cl$$

Scheme 1

point, several reviews specifically cover the Shilov and mechanistically related systems [8] and/or C–H activation chemistry of platinum [9, 10] and provide quite thorough pictures of the state of understanding at the time they were written. Hence, in the following sections, we focus on work subsequent to the last of those three reviews (2005) with an emphasis on the role of Pt(IV) in C–H bond activation and functionalization. We highlight the main developments of earlier work for background, but make no attempt at comprehensive coverage or in-depth analysis.

2 Formation and Decomposition of RPt(IV) in the Shilov System

The overall mechanism shown in Scheme 2, outlined by Shilov at an early stage in the research, has been essentially validated by all subsequent work. The reaction begins with activation of a C–H bond at a Pt(II) center. (There are examples of arene, but not alkane, activation by Pt(IV); these probably involve "classical" electrophilic routes via π-complexes and Wheland intermediates [10].) This fact seems incontrovertible since Pt(II) by itself catalyzes H/D exchange; the detailed mechanism of the activation is much less obvious, as discussed in Sect. 3. The resulting RPt(II) complex is *extremely* sensitive to electrophilic cleavage – no $[RPt^{II}Cl_x(H_2O)_{3-x}]^{(x-1)-}$ species can be observed in the presence of any proton source – so using Pt(II) alone, no alkane conversion beyond isotopic exchange would be feasible. However, $[Pt^{IV}Cl_6]^{2-}$ effects oxidation to RPt(IV), which is virtually completely inert to protonolysis but quite susceptible to nucleophilic

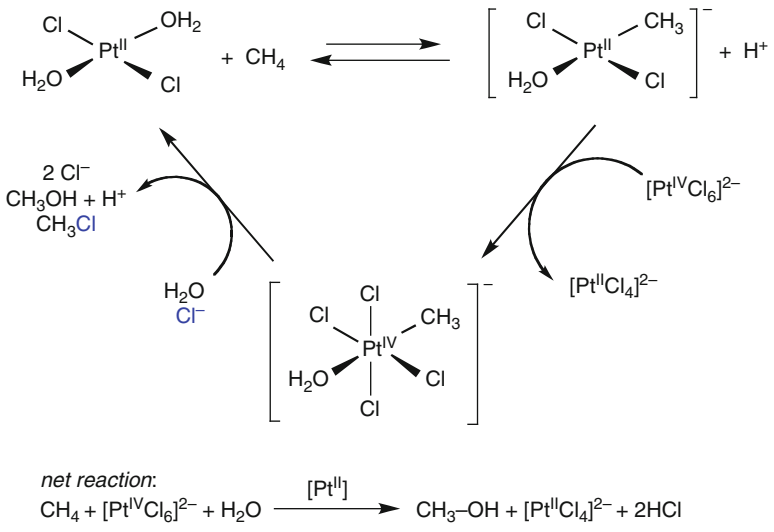

Scheme 2

attack by water or chloride, leading to the organic products and regenerating Pt(II). The intermediacy of RPt(IV) also appears incontrovertible: species such as $[MePt^{IV}Cl_5]^{2-}$ can be synthesized independently and undergo the appropriate transformations under the conditions of the Shilov system. (Observation of an NMR signal corresponding to the latter complex, in a cooled-down solution from a methane oxidation reaction, has even been reported [11]; however, the failure to observe any such signal from a working reaction, at temperature in a pressurized NMR tube [12], casts some doubt on that claim.)

The two keys to the success of the system, then, are (1) the remarkable rapidity of the oxidation step, which can outcompete protonolysis even though the latter is too fast to measure independently; and (2) the complete "umpolung" of the C–Pt bond, from $R^{\delta-}$–$Pt(II)^{\delta+}$ to $R^{\delta+}$–$Pt(IV)^{\delta-}$, which facilitates functionalization rather than simple protonolytic reversion to alkane. In the following two sections, we discuss each of these steps.

2.1 Conversion of RPt(II) to RPt(IV)

The reaction of RPt(II) with $[Pt^{IV}Cl_6]^{2-}$ could proceed by either electron transfer or alkyl-chloride exchange; the two alternatives could be distinguished by enriching one or the other of the reactants with ^{195}Pt, if an authentic RPt(II) species were available. This experiment was eventually accomplished by two different means. First, oxidation of Zeise's salt ($[(C_2H_4)Pt^{II}Cl_3]^-$) to $[(HOCH_2CH_2)Pt^{IV}Cl_5]^{2-}$ was shown, by kinetics analysis, to proceed via the intermediate $(HOCH_2CH_2)Pt(II)$ species [13]; then an insoluble salt of $[(CH_3)Pt^{II}Cl_3]^{2-}$, obtained by reduction in an aprotic solvent, was oxidized to $[(CH_3)Pt^{IV}Cl_5]^{2-}$ when added to a solution of $[Pt^{IV}Cl_6]^{2-}$ [14]. In both cases, the label showed up entirely in inorganic Pt(II), not RPt(IV) (Scheme 3), establishing the electron transfer route.

That finding implies it should be possible to replace Pt(IV) with any suitable oxidant and thus escape the requirement for stoichiometric consumption of Pt in the original Shilov reaction; however, there are two severe constraints on what counts as "suitable". Oxidation of RPt(II) must be fast enough to compete with protonolysis, but the oxidant must not be so powerful as to also oxidize inorganic Pt(II), which is needed to carry out the C–H activation step. The rapidity of the oxidation step with $[Pt^{IV}Cl_6]^{2-}$ appears quite remarkable: while the absolute rate cannot be measured, the relative rate of oxidation to protonolysis can be estimated from the amounts of the corresponding products obtained when $[(CH_3)Pt^{II}Cl_3]^{2-}$ is generated transiently from nucleophilic attack of Cl^- at a methyl of $[(CH_3)_2Pt^{IV}Cl_4]^{2-}$ in an aqueous

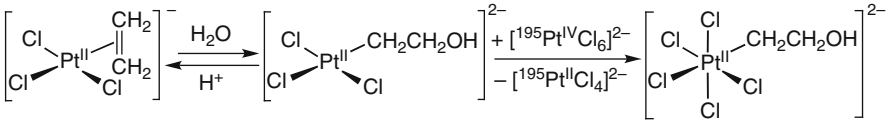

Scheme 3

solution of $[Pt^{IV}Cl_6]^{2-}$, giving a rate constant ratio of around 20 in favor of oxidation at 95°C [15, 16]. The ratio is likely to be still higher at the Shilov operating temperature of 120°C, as a similar experiment using the insoluble $[(CH_3)Pt^{II}Cl_3]^{2-}$ salt mentioned above gave a ratio close to unity at room temperature [14, 16].

Knowing that protonolysis is so fast that $[(CH_3)Pt^{II}Cl_3]^{2-}$ can never be observed in protic solvents, we can estimate that its oxidation by $[Pt^{IV}Cl_6]^{2-}$ is at least several orders of magnitude faster than the closely related exchange reaction of $[Pt^{II}Cl_4]^{2-}$ with $[Pt^{IV}Cl_6]^{2-}$ [17]. The electron-releasing properties of a methyl ligand compared to those of chloride should make the RPt(II) easier to oxidize kinetically as well as thermodynamically, but an effect of that size seems surprising. Presumably, the oxidation takes place via the inner-sphere "chloronium ion transfer" mechanism of Scheme 4, as was demonstrated for redox reactions of related N-ligated complexes [18], so the ability of alkyl ligands to facilitate substitution reactions may also play a role, although it does not appear that a true *trans* effect can come into play.

The mechanism of Scheme 4 (which is somewhat specific to a Pt(II)/Pt(IV) couple or something very closely related) suggests there might be some question whether we could replace $[Pt^{IV}Cl_6]^{2-}$; but in fact there is ample evidence that we can. A number of reports have demonstrated oxidative functionalization of aliphatic C–H bonds using catalytic Pt(II) and stoichiometric oxidants such as chlorine [12], hydrogen peroxide [19], peroxydisulfate [20], and the anode of an electrochemical cell [21]. Most interesting are Wacker-like systems that use catalytic amounts of an oxidant that can in turn be reoxidized by dioxygen, making the latter the stoichiometric oxidant; significant numbers of turnovers have been achieved with both $Cu^{II}Cl_2$ [22] and a polyoxometalate [23]. Recently, a microfluidic device was used for rapid screening of methane oxidation by Pt/cocatalyst/O_2 combinations; Fe(III)

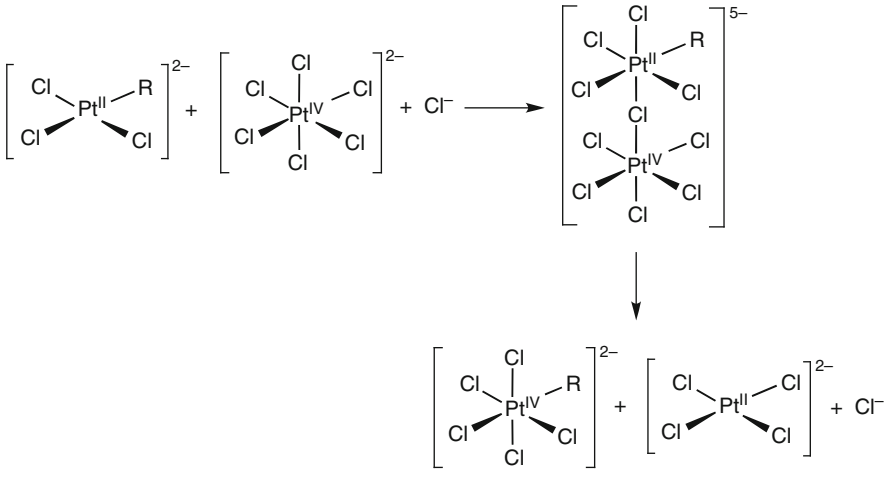

Scheme 4

was found to be the best cocatalyst (a polyoxometallate also showed some success), giving a mixture of methanol and formic acid in up to 50 turnovers [24].

The successful use of these alternate oxidants implies that they rapidly oxidize RPt(II) while not oxidizing inorganic Pt(II). (H_2O_2 does not need to satisfy the second of these criteria: it is both an oxidant and a reductant, so a sufficient steady-state concentration of inorganic Pt(II) can be maintained, albeit at the cost of highly inefficient oxidant consumption [19].) Indeed, $Cu^{I}Cl$ has been shown to be oxidized by $[Pt^{IV}Cl_6]^{2-}$ [25], so the reverse reaction would not take place. The (relative) oxidation rates have been measured for several oxidants using the methods described above. Rather unexpectedly, $Cu^{II}Cl_2$ was found to oxidize $[(CH_3)Pt^{II}Cl_3]^{2-}$ *faster* than $[Pt^{IV}Cl_6]^{2-}$, by around an order of magnitude at 95°C; $Fe^{III}Cl_3$ is somewhat less reactive [16].

One might presume that Cu(II) acts as a one-electron oxidant, which would require a two-step oxidation sequence (the reaction of $Cu^{I}Cl$ with $[Pt^{IV}Cl_6]^{2-}$ appears from kinetics to be stepwise, although the results were not completely conclusive [25]), making this finding even more remarkable. Conceivably, the actual oxidant involves a cluster of Cu(II) centers, as has been suggested for other oxidations of Pt(II) by Cu(II), where the intermediacy of Pt(III) may appear unattractive [26]; similar considerations may apply to the reoxidation of Pd(0) in the Wacker system (a step that is not very well characterized mechanistically). Mixed Pt(II)–Cu(II) clusters are also known [27] and might play a part here. However, other one-electron oxidants such as $[Ir^{IV}Cl_6]^{2-}$ and Ce(IV), where such clustering seems most unlikely, also oxidize $[(CH_3)Pt^{II}Cl_3]^{2-}$ at rates competitive with protonolysis [16].

A two-step sequential sequence would imply an RPt(III) intermediate. Organoplatinum species in that oxidation state have been shown to be rather unstable in one system: oxidation of a (diimine)$Pt^{II}Me_2$ complex with ferrocenium affords only MePt(II) and $Me_3Pt(IV)$ species, the result of disproportionation by methyl transfer. The two-electron oxidation products, $Me_2Pt(IV)$, are observed only when electrochemical oxidation is carried out at higher potentials (Scheme 5) [28]. However, it is quite possible that the instability is largely due to the second methyl group and that a monomethyl-Pt(III) species might be sufficiently long-lived to undergo a second one-electron oxidation more efficiently.

The high reactivity of RPt(II) toward a variety of oxidants, while still unexplained, offers considerable encouragement for ultimately devising practical

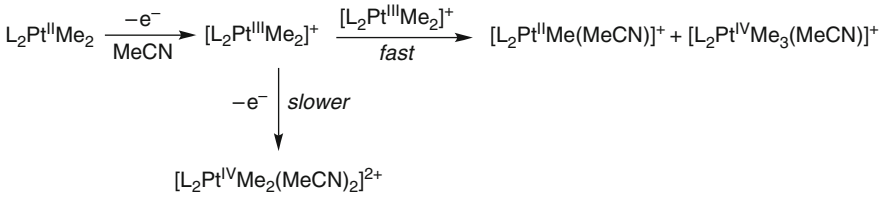

Scheme 5

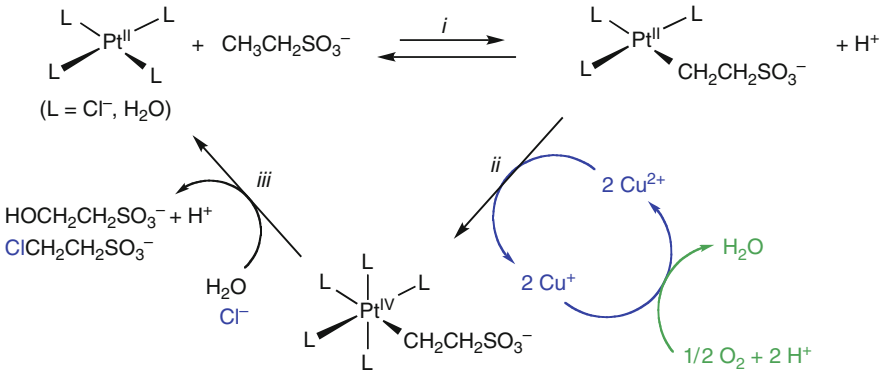

Scheme 6

applications of the Shilov chemistry. Unfortunately, O_2 by itself does not affect the needed rapid oxidation of $[RPt^{II}Cl_3]^{2-}$, although obviously it is thermodynamically competent to do so, since it reoxidizes Cu(I) to Cu(II) and the latter does oxidize RPt(II). (Oxidations of several N-ligated alkyl-Pt(II) species by O_2 have been observed; see Sect. 4.3) To date the most promising modification of the Shilov system has been the Wacker-like system of $[Pt^{II}Cl_4]^{2-}/Cu^{II}Cl_2/O_2$, which oxidizes water-soluble substrates such as ethylsulfonic acid and *p*-tolylsulfonic acid to the corresponding aliphatic alcohols and alkyl chlorides (Scheme 6), with turnover numbers in excess of 100 based on Pt [22, 29]. Of particular interest is the fact that these catalytic systems do not deactivate by precipitation of Pt metal, which is the eventual fate of virtually every experiment using the original Shilov system or most of the alternate oxidants enumerated above; instead, all of the Pt in solution is eventually converted to $[Pt^{IV}Cl_6]^{2-}$ [16, 29]. Since, as noted above, Cu(II) by itself is not capable of oxidizing Pt(II) to Pt(IV), there must be some stronger oxidant generated by the combination of Cu and O_2 under the reaction conditions; further mechanistic study on this catalytic combination might well prove rewarding.

2.2 *Formation of R–X from RPt(IV)*

Stoichiometrically, the liberation of RX from R–Pt(IV)–X amounts to reductive elimination; however, mechanistically, there are issues. Does the reaction proceed directly from six-coordinate Pt(IV), or is prior dissociation of a ligand required? There have been extensive studies on the mechanism of reductive elimination from Pt(IV) in general, especially with regard to C–C bond formation, where preformation of a five-coordinate intermediate is required, although some (kinetically more favored) C–H eliminations from Pt(IV) appear to proceed directly

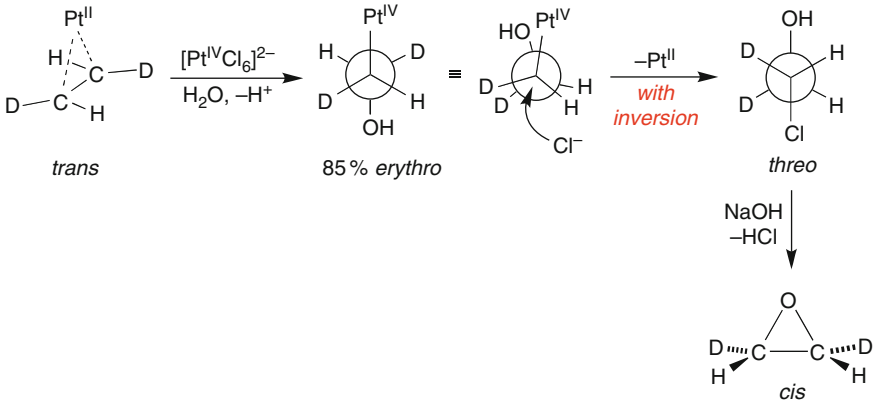

Scheme 7

from the six-coordinate state. This topic has been well reviewed [30] and is not further considered here.

For RX generation, there is the additional question of whether the C–X bond is formed via "straightforward" intramolecular reductive elimination, or by nucleophilic attack by external X^-. Model studies, such as Goldberg's classic work with $(dppe)Pt^{II}(X)(Me)_3$ complexes (X = I or OR), all point toward external nucleophilic attack on a five-coordinate intermediate [31, 32]. Early work on the actual Shilov intermediate, $[(CH_3)Pt^{IV}Cl_5]^{2-}$, strongly supports external nucleophilic attack; for example, in the presence of added bromide, methyl bromide forms faster than the substitution of Br^- for Cl^- in the coordination sphere [33]. A later study demonstrated that Walden inversion accompanies formation of 2-chloroethanol from $[(HOCH_2CH_2)Pt^{IV}Cl_5]^{2-}$ (Scheme 7), a clear sign of nucleophilic displacement; it also provided evidence from kinetics that nucleophilic attack takes place at a five-coordinate intermediate, $[RPt^{IV}Cl_4]^-$ [13]. One implication of these findings, if they are indeed universal, is that a catalytic alkane functionalization scheme via any similar route will have to generate a Pt(IV) intermediate with at least one readily dissociable ligand – most probably in the position *trans* to the strongly labilizing R group – which may place additional constraints on viable candidates for such a catalyst.

3 Does C–H Activation in the Shilov System Involve Pt(IV) Intermediates?

Oxidative addition is the most common mode of reaction of C–H bonds with low-valent transition metal centers; but Pt(II), especially with hard ligands such as chloride and water, does not appear to be particularly low-valent or electron-rich. Hence, alternate mechanisms have been considered as perhaps more probable, the

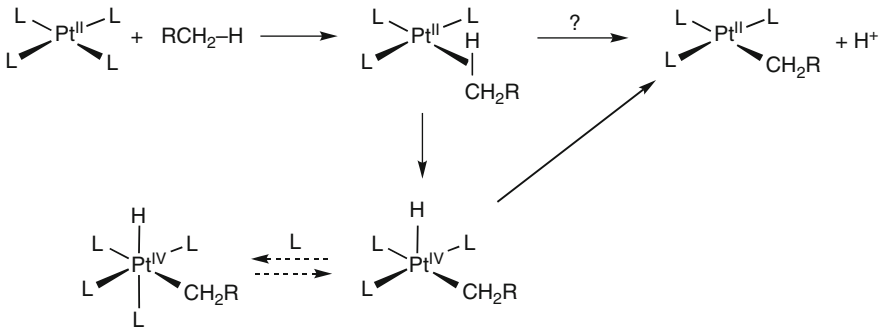

Scheme 8

most common being direct deprotonation of an alkane sigma complex, by analogy to the known acidity of dihydrogen sigma complexes. The two main alternatives (including the intermediacy of a sigma complex in the oxidative addition route, implicated in a very large number of studies on a variety of metal complexes), are shown in Scheme 8; other variants, such as something akin to the sigma bond metathesis mechanism common for d^0 complexes, could also be envisioned. Shilov's earliest papers postulated oxidative addition, on no particular grounds [2]; later he appeared to have changed his mind in favor of the sigma complex deprotonation route, again with no clear reason stated [11]. Another early paper proposed an "S_E2-mechanism with base assistance" [34]; most likely it would have been described as deprotonation of a sigma complex, but the possibility of the latter had not been recognized at the time.

Of course, we now know that RPt(IV) hydrides can be isolated from reactions of alkanes at Pt(II) under the right circumstances, as first demonstrated by Goldberg (Scheme 9); here, the ambidentate nature of the Tp ligand facilitates stabilization of six-coordinate Pt(IV) [35]. However, assessing the generality of that route, and its applicability to cases where RPt(IV)H is *not* observable, is far from straightforward. It should be noted that there is a huge body of work, of which we can only scratch the surface, that bears on this question; we recommend that readers interested in a deeper exploration consult the afore-mentioned reviews (particularly the 2006 review by Lersch and Tilset [10], which is specifically devoted to this topic).

3.1 Studies on Protonolysis of R–Pt(II)

The daunting prospects of achieving direct experimental support for either alternative in the actual Shilov system, given the instability of the RPt(II) species formed, led us to an indirect approach involving study of protonolysis of ligand-stabilized RPt(II) complexes, models for the microscopic reverse of C–H activation. Depending on the choice of ligand L, solvent, and reaction temperature, we

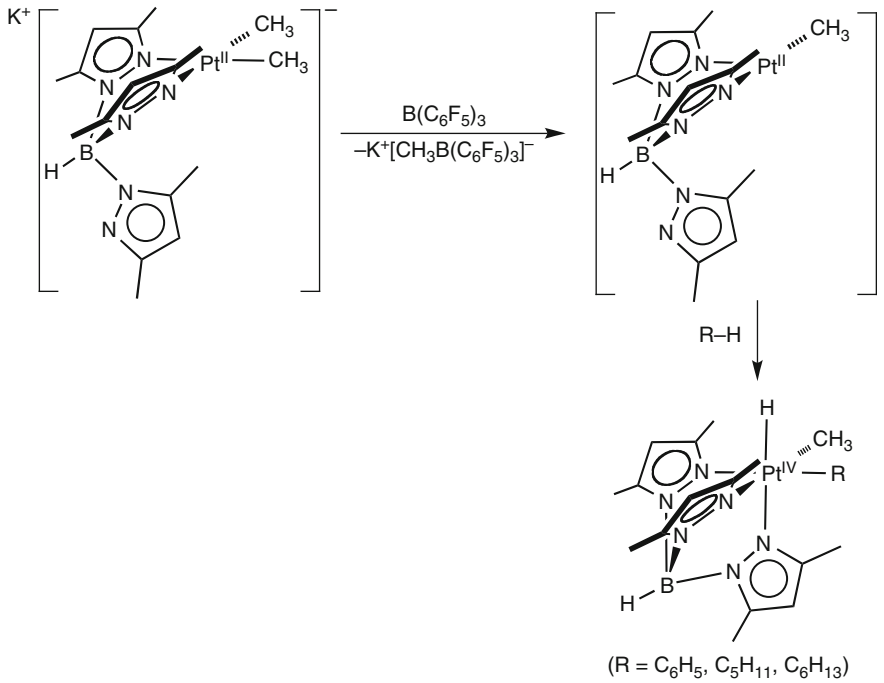

Scheme 9

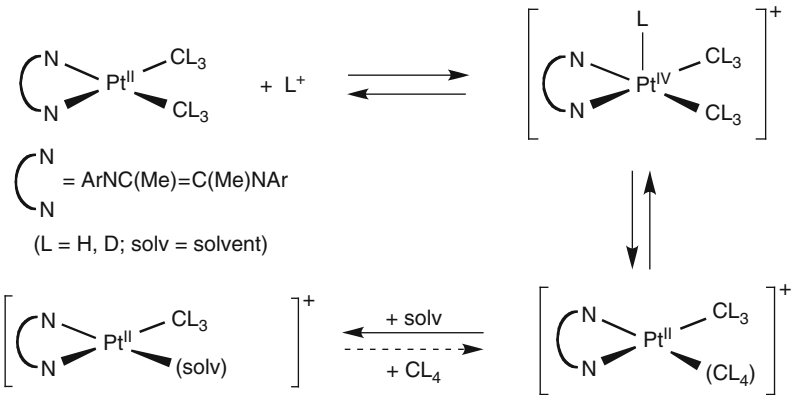

Scheme 10

observed (by NMR) a metastable RPt(IV)H prior to loss of methane; use of deuterated solvent often resulted in extensive H/D scrambling in the liberated alkane and, in some cases, the RPt(IV) group as well [36]. Similar results have since been obtained for a number of other systems [10]. These results strongly support the mechanism shown in Scheme 10, involving protonation at Pt,

reductive coupling to form a sigma alkane complex, and dissociation of alkane; the reversibility of the first two steps accounts for the observed isotopic exchange, with the extent depending on the relative rates of the various processes. The principle of microscopic reversibility implies that C–H activation follows the oxidative addition route.

There are several caveats that must be kept in mind. First, of course, these studies were carried out on models, not the "real" Shilov system; conceivably, the use of stabilizing ligands could alter the mechanism. Some evidence against that possibility is provided by the observation of H/D exchange in the deuterolysis of transiently generated $[(CH_3)Pt^{IV}Cl_5]^{2-}$ in CD_3OD (but not in D_2O, possibly because the loss of methane, which proceeds by associative displacement, may be considerably faster in the presence of the better ligand water), suggesting that the mechanisms are closely related [36]. On the basis of isotope distributions, Zamashchikov also argued for the intermediacy of an ethyl-Pt(IV) hydride in the loss of ethane accompanying decomposition of $[(CH_3)_2Pt^{IV}Cl_4]^{2-}$ [37]; his analysis relied on the (questionable) assumption of no isotope effect on alkane sigma complex stability.

Another possibility is that the observed RPt(IV)H species do not actually lie on the main pathway. One could imagine a situation such as that shown in Scheme 11, where RPt(IV)H is formed reversibly but has nowhere else to go; protonolysis (and isotope exchange) proceed only via direct protonation of the Pt–C bond. This seems extremely unlikely, given the ample evidence of facile interconversion between M(R)(H) and M(η^2-RH) for the vast majority of C–H activation systems, but it is hard to exclude rigorously for the Shilov system. However, it can be ruled out for some of the model systems. Consider, for example, the two reactions shown in Scheme 12: the isotopic scrambling in the protonolysis (top) reaction [38] might conceivably follow the scenario of Scheme 11, but that in the benzene activation [39] clearly could not. Further support is provided by the reaction shown in Scheme 13, where the ratio of RPt(II) to RPt(IV)H products decreased with

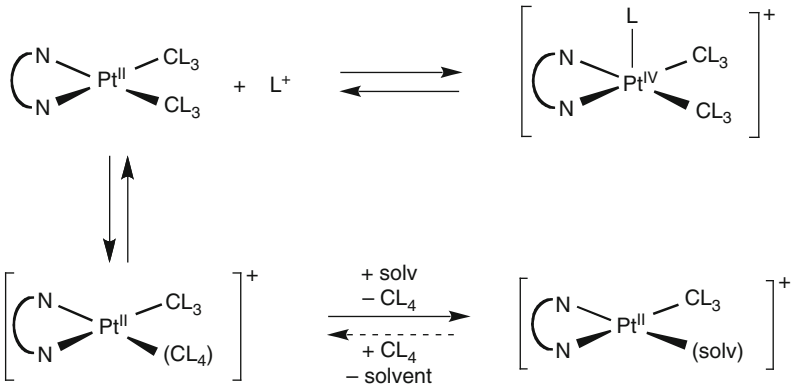

Scheme 11

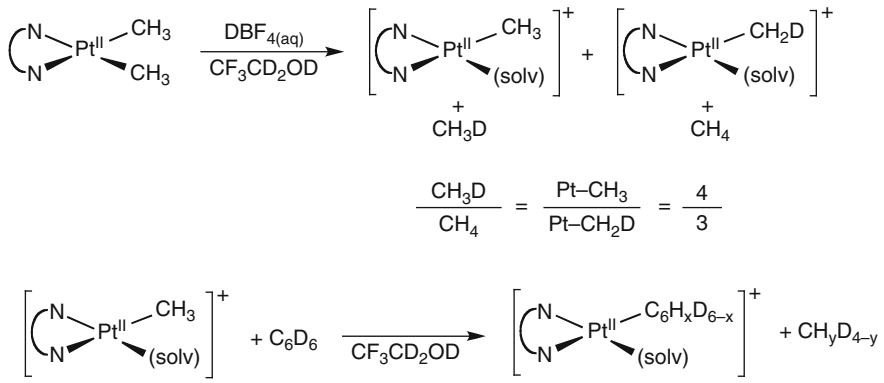

Scheme 12

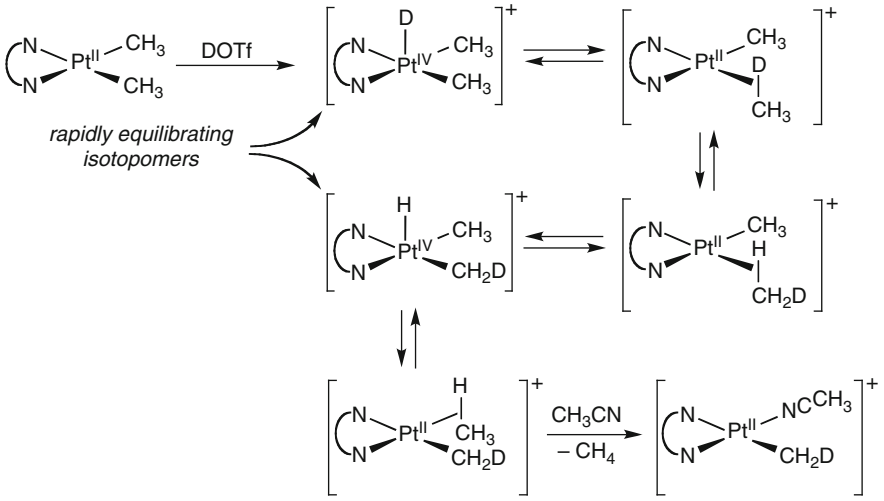

Scheme 13

increasing amounts of trapping ligand MeCN. Such a result is consistent with reductive coupling of RPt(IV)H to Pt(II)(η^2-RH) competing with trapping, but not with the latter being the sole relevant intermediate on the protonolysis pathway [40].

A good deal of work has been invested in determining KIEs for protonolysis of metal alkyls, including those of Pt(II), but definitive mechanistic conclusions have proven very hard to attain: there are just too many complications, as discussed by a number of commentators and well summarized in an earlier review [10]. Indeed, one of the leading researchers in this field, toward the end of a major paper surveying KIE and other experiments, comes close to giving up on the possibility

of distinguishing between the alternative mechanisms: "In conclusion, the similarity of the energy profiles . . . describing the coordinate reaction for a rate determining proton transfer to the substrate, suggests that, under these circumstances, any discussion of the site of proton attack risks becoming semantic in nature [41]".

A more recent observation, however, may offer new opportunities: protonolysis of one particular Pt(II) complex, (COD)$Pt^{II}Me_2$, along with that of several related alkyl-Pd(II) species, was found to exhibit an abnormally large KIE, around 18 at room temperature [42]. Such a value is normally associated with the presence of a large tunneling component, a conclusion also supported by the large temperature dependence of the KIEs. No Pt(IV) hydride species could be detected on protonation at low temperature, nor was any H/D exchange observed, in contrast to the earlier studies on analogs with N-centered ligands; the KIE for one example of the latter, (tmeda)Pt^{II}MeCl, is normal in both room temperature value (around 4.4) and temperature dependence [43]. These results suggest, as a working hypothesis, that the appearance of KIEs, characteristic of tunneling, might be signaling a mechanistic switch: the earlier cases, with N- and P-centered ligands, proceed via protonation at metal to give RPt(IV)H, but the initial site of protonation in (COD)$Pt^{II}Me_2$ is the Pt–C bond to directly form an alkane complex, which loses alkane without ever going through a Pt(IV) species. This is consistent with the greater electron-withdrawing power of the π-accepting bis(olefin) ligand, in comparison to the stronger donor amine and phosphine ligands, as well as with the fact that abnormal KIEs are also observed with the Pd analogs, for which the tetravalent state will be less accessible.

Theoretical studies also agree with this proposal. DFT calculations on the above two examples indicate that the lowest-energy pathways for the two alternative mechanisms are those shown in Scheme 14. For (COD)$Pt^{II}Me_2$, the overall barrier calculated for the top pathway, protonation at Pt–C, is lower than that for the bottom one, protonation at Pt ($\Delta G^{\ddagger}$ = 26.9 and 32.5 kcal/mol respectively), whereas for (tmeda)Pt^{II}MeCl, the reverse result is obtained (30.1 and 29.0 kcal/mol, respectively) [43]. To be sure, the differences are not large (especially for the latter case)

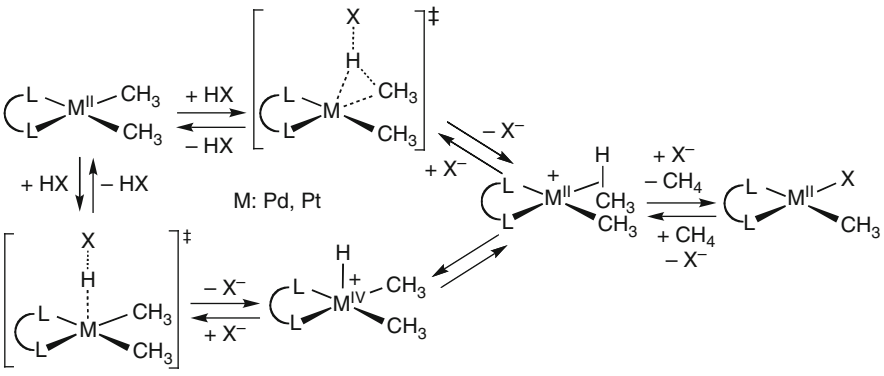

Scheme 14

and complicated by a number of features common to computational studies of this class of reaction (see following section), but the overall pattern is at least suggestive.

No experimental results for the actual Shilov system point clearly in any direction. Analysis of the methane obtained when $[MePt^{IV}Cl_5]^{2-}$ was reduced in a mixture of H_2O/D_2O indicated a KIE around 9 at 0°C, a borderline number, and one whose interpretation is made more difficult by the possible involvement of so-called fractionation factors [36]. Further study, perhaps making use of the $[MePt^{II}Cl_3]^{2-}$ salt described above, might be worthwhile, although complicated by the necessarily heterogeneous reactions of this insoluble material.

3.2 Computational Studies on the Shilov System

Given the difficulty of obtaining direct experimental evidence as outlined above, computation would seem the obvious way to go. A useful and thorough review of computational studies on C–H activation has recently appeared [44]. However, there are problems here too, arising in particular from the fact that the reaction involves ionic species in water. Handling solvation often challenges computational chemists, especially when, as here, one may need to take into account hydrogen-bonding interactions of solvent molecules with coordinated ligands as well as more general effects. The first computational study to tackle the Shilov system recognized and devoted particular attention to these difficulties. For the actual C–H bond cleavage step, their DFT calculations predicted that two different mechanisms were very close in energy: the oxidative addition route via RPt(IV)H and a sigma bond metathesis-like mechanism in which an H atom of a coordinated methane transfers directly to an adjacent chloride. These are closely related to the reverse processes corresponding to the bottom and top mechanisms in Scheme 14, respectively; the calculations actually showed a small preference for the oxidative addition route, but the authors tended to prefer the other, although not definitively [45].

More recently, Ziegler has examined the effect of the detailed structure of the Pt species participating in C–H activation (which is, of course, not known from any definitive experimental results). The calculated transition state for C–H activation leads to the intermediate resulting from the oxidative addition mechanism; it is not clear whether the methodology used would have identified and compared any alternatives. For species $[Pt^{II}Cl_x(H_2O)_{4-x}]^{(x-2)-}$, the rate-determining step was always found to be coordination of methane by ligand displacement, rather than the actual C–H activation itself [46] (contrary to the findings of the earlier study [45]). Replacing chloride with other anionic ligands leads to a decreased barrier for methane coordination (and hence for the overall reaction) as the ligand becomes a stronger *trans* director; but for really strong ones, such as cyanide, the C–H activation barrier increases and becomes rate-limiting [47]. A subsequent study examined the effect of neutral ligands (alcohols, amines, and phosphines) and reached a similar conclusion [48].

These latest results imply that direct study of the kinetics of C–H activation in the original Shilov system to probe the participation of Pt(IV) would be not only extremely difficult, as has already been remarked, but also largely irrelevant, since that step is apparently rarely, if ever, rate-determining. Indeed, most of the mechanistic studies, as well as of the attempted approaches to a more practical alkane functionalization catalyst, have been directed at ligand-substituted Pt(II) complexes, the subject of the following sections.

4 Pt(IV) in Alkane Activation and Functionalization by Ligand-Substituted Complexes

In the discussion of mechanistic studies of protonolysis, the microscopic reverse of C–H activation, it was noted that the requirement for complexes bearing stabilizing ligands raises a potential issue: to be comfortable with the implicit assumption that these species *really* do model the Shilov system, one should show that they can themselves effect C–H activation. The first such demonstration was achieved using $[(tmeda)Pt^{II}Me(C_5F_5N)]^+$, which reacts with benzene at 85°C to give methane and the corresponding phenyl complex, taking advantage of the weakly coordinating (and hence readily displaced during alkane coordination) pentafluoropyridine ligand [49]. A large number of related examples followed, of which the cationic complexes $[(diimine)Pt^{II}Me(TFE)]^+$ (TFE = CF_3CH_2OH) [50] have perhaps been the most fruitful in terms of mechanistic study, while $(bipym)Pt^{II}Cl_2$ (bipym = bipyrimidine) [51] is unquestionably the most encouraging in terms of potential practical applicability. Again, we have space only to highlight a small fraction of this work.

4.1 The Catalytica System

Following up on their earlier report of surprisingly selective mercury-catalyzed oxidation of methane to methyl bisulfate by sulfuric acid (which was also the reaction medium) [52], Periana and coworkers discovered that a bipyrimidine complex of Pt(II) worked even better, generating the same product in over 70% yield – a remarkable achievement, given that "selective" oxygenation of methane to methanol or derivatives thereof rarely surpasses yields of a few percent. A mechanism closely akin to that of the Shilov system was proposed (Scheme 15), with SO_3 replacing Pt(IV) as the oxidant to convert RPt(II) to RPt(IV); whether the initial C–H activation involved an RPt(IV)H intermediate or not was left an open question [52].

As with the Shilov system (even more so, given the conditions: typically around 200°C in fuming sulfuric acid!), a direct experimental assault on the mechanism

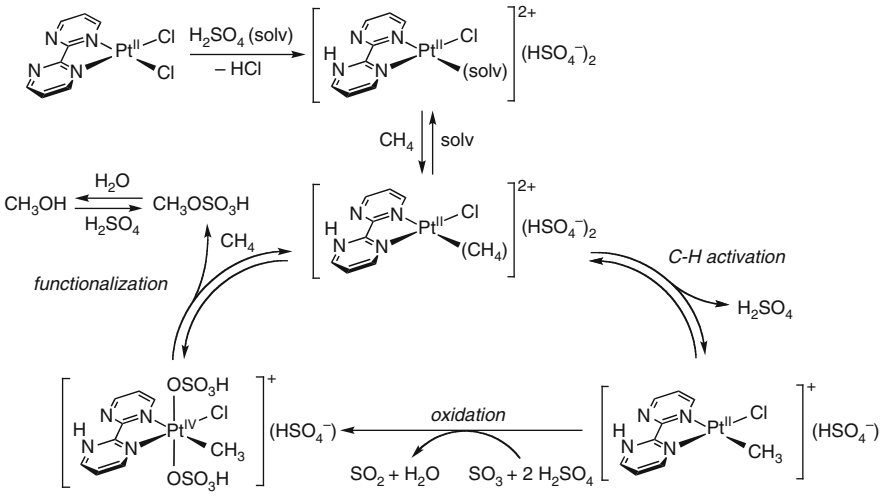

Scheme 15

seems unattractive; but several groups have addressed the problem through computational studies, on both the actual bipym catalyst and the simplified analog $(NH_3)_2Pt^{II}Cl_2$. Perhaps not too surprisingly, the conclusions depend on the structure of the activating complex, which is not known experimentally; besides the question of whether chloride remains attached to Pt or is replaced by bisulfate, there is the further issue of whether the free N centers of the bipym ligand are un-, singly, or doubly protonated, and whether the bisulfate ligand (if present) is further protonated to become coordinated sulfuric acid, in such a strongly acidic medium. One study found that the oxidative addition path is slightly favored if the precursor methane complex is $[(bipym)Pt^{II}Cl(CH_4)]^+$, whereas a deprotonation route is substantially favored if it is $[(bipym)Pt(OSO_3H)(CH_4)]^+$. The authors came down in favor of a nonoxidative route via $[(bipymH_2)Pt^{II}(OSO_3H)]^{3+}$ [53]. Another group argued that the methane-activating complex has a chloride, not a bisulfate ligand, and an unprotonated bipym, but agreed that the deprotonation route is preferred, avoiding a discrete Pt(IV)–H intermediate [54]. More recent calculations by that group, however, seem to prefer the oxidative addition route [55]. Both groups, as well as another [56], find that the barrier to coordination of methane is higher than that for C–H activation, as in most of the findings for the Shilov system itself (see above). An attempt to assess the probable effect of protonation of a free N in bipym by comparing the reactivity (for H/D exchange) of the N-methylated complex was thwarted by the facile demethylation observed under reaction conditions [57].

There appears to be considerable residual uncertainty about the detailed course of C–H activation – probably not too surprising, in view of the difficulty of dealing with solvation and related issues in this far-from-innocent medium. It is perhaps more important to note that all of these studies indicate that – in *contrast*

to the original Shilov system – oxidation of RPt(II) to RPt(IV) is rate-limiting, although the calculated relative barrier heights can depend to a significant extent on the exact nature of the catalytic intermediates; as might be expected, protonation of a ligand makes oxidation considerably more difficult [56]. Such sensitivity to positive charge has also been observed in related experimental studies: [(diimine)Pt^{II}Me(solvent)]$^+$ is much more difficult to oxidize than the corresponding neutral (diimine)$Pt^{II}Cl_2$, despite the fact that replacing Cl with Me generally makes oxidation much more favorable [18]. The prediction that oxidation is the slow step also accords with the experimental observations that H/D exchange is much more pronounced for the Catalytica system and that $(NH_3)_2Pt^{II}Cl_2$ is actually *more* active, at least initially, than the bipym catalyst [52], since all the calculations suggest that the bis(ammine) catalyst is more readily oxidized to Pt(IV). Unfortunately, it is much less stable, decomposing within minutes under reaction conditions (one set of calculations [58] even indicates that methane coordinates by displacing an ammonia ligand, which would be expected to be detrimental to stability). Because one of the drawbacks to the Catalytica system that make it uncompetitive with existing technology for converting methane to methanol (via syngas) is the low rate, these findings suggest an approach to optimization, by designing ligands that improve access to Pt(IV) without sacrificing the stability to harsh reaction conditions imparted by bipym. Unfortunately, to date no such combination has been developed.

Lowering the barrier for C–H activation *should* give an improved H/D exchange catalyst; following leads provided by computation, Periana showed that a Pt(II) picolinate complex catalyzes exchange between C_6H_6 and CF_3COOD at 70°C, about 300 times faster than the original bipym-based complex [59]. It is worth remarking, though, that the observation of aromatic H/D exchange in the presence of a combination of a metal complex and an acid does *not* necessarily demonstrate that C–H activation is taking place at the metal; it is at least conceivable that simple acid-catalyzed exchange could be involved, resulting from lowering the pK_a of the acid by coordination to the metal. Only rarely have explicit tests of such a possibility (for example, by changing the acid strength of the D source [60]) been carried out.

Another limitation is the fact that the reaction requires fuming sulfuric acid; the catalyst is deactivated by even small amounts of water (a reaction byproduct). One explanation, based on calculations, is that the presence of SO_3 is required because H_2SO_4 is not a competent oxidant [56]; another suggests that coordination of methane is much more facile when it occurs via displacement of a protonated H_2SO_4 ligand rather than water [55]. The introduction of an ionic liquid cosolvent has been proposed to circumvent the problem; experimental [61] and theoretical [62] studies (not including the bipym ligand in either case) have been reported for that approach, which shows some modest improvement in stability to water, but with no clear indication of why it works. (Still another economic hurdle is the cost of carrying huge quantities of sulfuric acid through a multistep process; there does not appear to be any way to fix that through better understanding of mechanism.)

4.2 Stoichiometric C–H Activation at Ligated Pt(II)

As noted above, a good deal of mechanism-oriented work has been carried out on C–H activation reactions of $[(\text{diimine})\text{Pt}^{\text{II}}\text{Me}(\text{TFE})]^+$, which as shown in Scheme 16 can lead to a variety of products: isotopic methyl exchange with $^{13}CH_4$ [63]; aryl complexes with arenes [39, 50]; η^3-benzyl complexes with alkyl-substituted arenes [38, 64]; and cationic olefin hydride complexes with linear or cyclic alkanes [65]. Studies strongly indicate a common basic mechanism (Scheme 17), in which the C–H activation step proceeds via oxidative addition to give an RPt(IV)H intermediate – demonstrated, for example, by the isotopic exchange shown in Scheme 12 above.

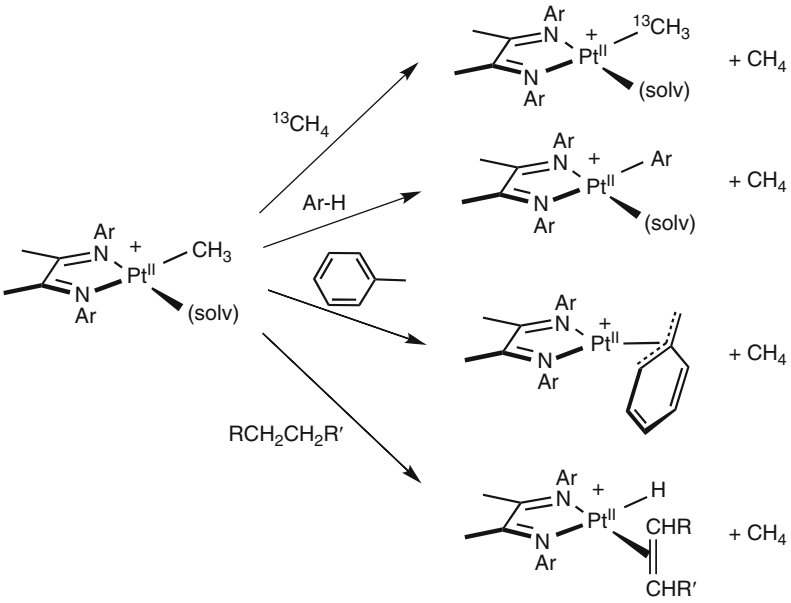

Scheme 16

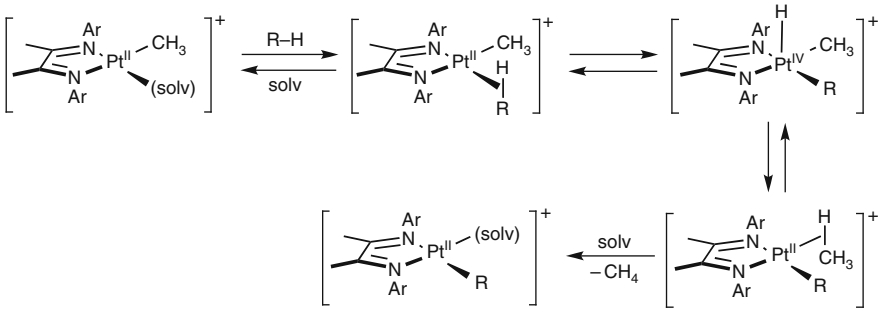

Scheme 17

For the latter, one *could* invoke instead a sigma bond metathesis-like mechanism (also described as a sigma-complex-assisted metathesis, or σ-CAM), in which H or D passes from Ar–H to R without ever *completely* breaking all C–H bonds, thus avoiding a discrete Pt(IV)–H intermediate. Calculations suggest such a process might be favorable for the case of activation of benzene by a phenyl complex, where the isotopic scrambling takes place between two aryl groups, although in such a case the involvement of *p* orbitals at *both* sites was thought to play a key role; for alkane activation, the oxidative addition pathway would be more likely [66]. It might be noted that a Pt(IV) hydride can be observed (stabilized by coordination of acetonitrile as a sixth ligand) during low-temperature protonolysis of a diphenyl complex [67]. Calculations accompanying experimental study of the gas-phase reaction of $[(bipy)Pt^{II}Me]^+$ with $C_6D_xH_{6-x}$ showed no strong preference for either of the two mechanisms [68].

In any case, it is usually formation of the sigma complex Pt(II)(η^2-R–H) and *not* the actual C–H activation that is rate-determining; interconversion between the sigma complex Pt(II)(η^2-R–H) and RPt(IV)H is typically quite rapid. Only for the formation of aryl complexes of sterically undemanding diimine ligands is there evidence for rate-determining C–H activation, presumably because of the better coordinating ability of arenes [39]. In the large majority of cases – in particular, all that involve aliphatic C–H bonds – formation of a sigma complex by displacement of coordinated solvent is the slow step. (Formation of an alkyl-Pt(IV)H has been calculated to be the most energetically demanding step in the case of intramolecular benzylic C–H activation, but there the formation of the sigma complex is relatively much more favorable, as an agostic interaction [69].) Hence, while a wide array of interesting mechanistic complexities and subtleties are revealed in these studies, they are mostly unrelated to the behavior of the Pt(IV) intermediates.

More recently, C–H activation has been extended to inorganic Pt centers, better analogs of the original Shilov system, although the chemistry is limited to substrates that lead to π-stabilized products – η^3-benzyls, η^3-allyls, or other chelated alkene-hydrocarbyls. Dicationic $[(diimine)Pt^{II}(TFE)_2]^{2+}$ reacts with ethylbenzene (but not toluene!) and other arenes and olefins as shown in Scheme 18 [70]; a similar set of transformations can be effected by the dimers $[(diimine)Pt(\mu_2\text{-}OH)]_2^{2+}$ [71]. The reactions are generally considerably slower than the corresponding reactions of $[(diimine)Pt^{II}Me(TFE)]^+$, reflecting tighter binding of TFE to the dicationic Pt(II) center, which slows coordination of the C–H bond by ligand displacement. One might expect the C–H activation step to be slower as well, assuming that the oxidative addition route continues to operate; however, there is no evidence that it ever becomes rate-limiting. Hence, again, this chemistry does not provide much access for probing the detailed involvement of high-valent Pt.

Vedernikov has made extensive use of ambidentate (or "semilabile") ligands to modulate interconversion of Pt(II) and Pt(IV) species, exploiting the same principle as the (κ^2- or κ^3-Tp)Pt example discussed earlier, where a dangling arm in a Pt(II) precursor coordinates to and stabilizes a Pt(IV) product. A dimethyl-Pt(II) complex of a sulfonated dipyridyl ligand not only undergoes facile H/D exchange with deuterated solvent, but can be converted to a stable Pt(IV) hydride in a nonpolar

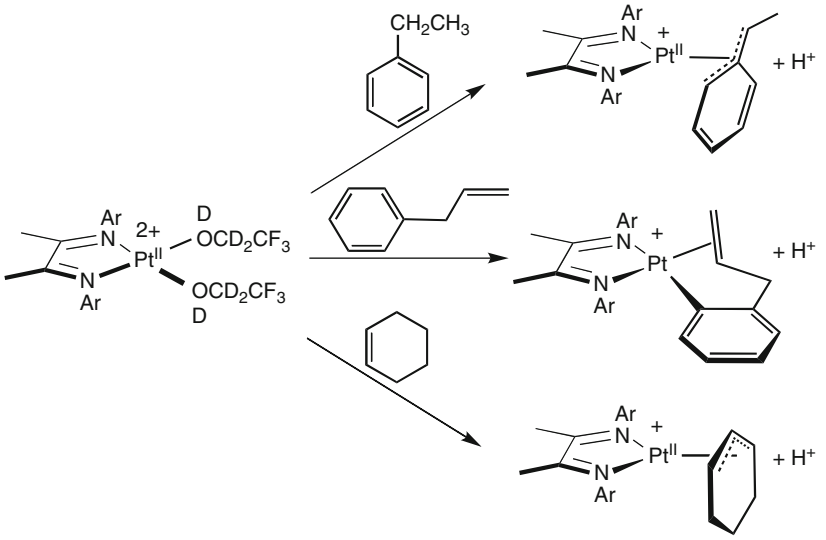

Scheme 18

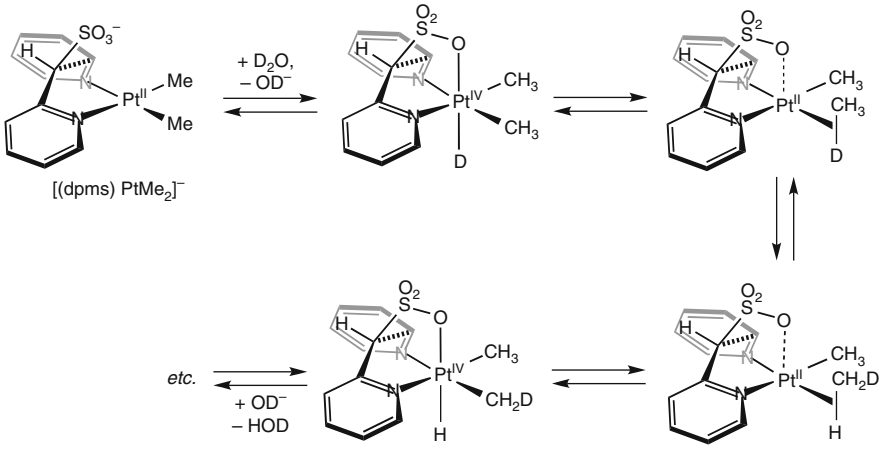

Scheme 19

medium; loss of methane is considerably slower (Scheme 19). Clearly, the formation of the Pt–O bond stabilizes six-coordinate Pt(IV), resulting in a situation where the energies of the several species – (κ^2-dpms)$Pt^{II}Me_2$, (κ^3-dpms)Pt^{IV}(H)Me_2, and (dpms)Pt^{II}Me(η^2-Me–H) – are balanced closely enough to allow exceptionally facile scrambling. In a nonpolar solvent, dissociation of the Pt–O bond is disfavored sufficiently to permit isolation of the Pt(IV) hydride [72].

While C–H activation has not been reported for complexes based on dmps, it has been observed with a dimethyldi(2-pyridyl)borate ligand, even though it lacks the

potentially coordinating extra arm: in the presence of small amounts of water, $[(dmdpb)Pt^{II}Me_2]^-$ reacts with benzene or cycloalkanes to afford the products shown in Scheme 20. The reaction is thought to proceed via protonation to Pt(IV) H followed by reductive coupling, loss of methane, and activation of C–H by the resulting Pt(II) center; in the absence of an appended ligating group, the Pt(IV) intermediates are probably stabilized by coordination of hydroxide. That proposal is supported by the fact that the reaction rate is highly dependent on the counterion, being much faster for the Na^+ than $^nBu_4N^+$ salt [73]. Perhaps the most interesting aspect of the dpms and dmdpb systems is their support of facile oxidation by O_2, which is covered in the next section.

Structurally related species that exhibit C–H activation include the bis(pyrazolyl) borate complex in Scheme 21, for which (as in the above dmdpb system) protonation (or methide abstraction) generates an intermediate that reacts readily with benzene [74]; the bis(azaindolyl)methane complex in Scheme 22, which activates both aromatic and benzylic C–H bonds [75, 76] (some stable Pt(IV) complexes based on the same architecture have also been isolated and shown to undergo reductive elimination of MeX [77]); and complexes based on anionic bidentate ligands such as 2-(2′-pyridyl)indolide [78]. Intramolecular C–H activation was observed for one example of a series of *N*-heterocyclic carbene complexes of Pt(II); distortions induced by steric crowding appear to influence reactivity strongly [79].

A substantial body of C–H activation chemistry can be initiated by reductive elimination from Pt(IV) species: either of ethane from stable, five-coordinate (β-diketiminate)$Pt^{IV}Me_3$ or of alkane from six-coordinate $TpPt^{IV}HR_2$. In some cases, usually involving arene activation, new stable Pt(IV) products are obtained; the course of benzene activation by the TpPt system has been examined theoretically [80]. For alkane activation, the final product is often a Pt(II)–olefin hydride

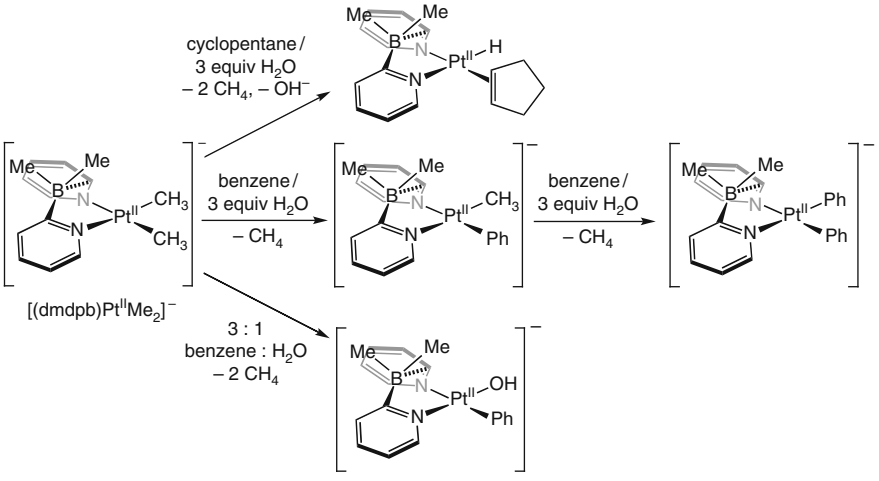

Scheme 20

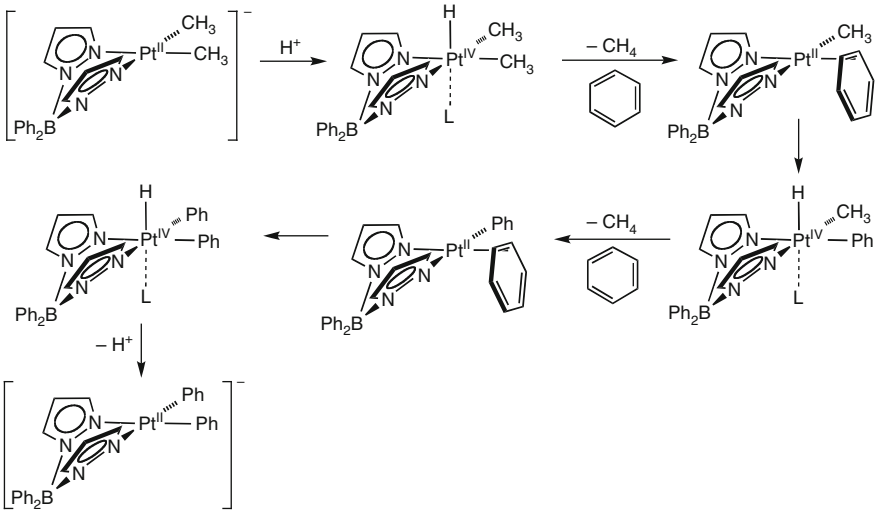

Scheme 21

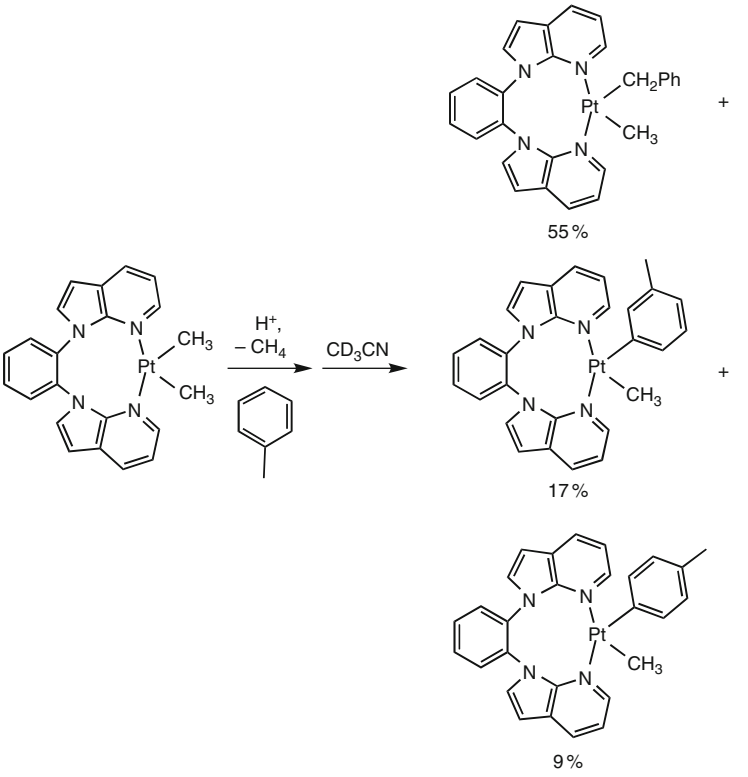

Scheme 22

complex resulting from β-hydride elimination, but there is no reason to doubt that the actual C–H activation involves oxidative addition to give an RPt(IV)H intermediate. This work has been the main topic of an earlier review [81] as well as another chapter in this volume [82] and is not examined further here.

4.3 Oxidation by Dioxygen

Only a very few oxidations of inorganic Pt(II) to Pt(IV) by O_2 have been reported (reviewed in [9], as well as a more recent feature article on O_2 oxidations [83]); as noted earlier, the Shilov intermediate, $[(CH_3)Pt^{II}Cl_3]^{2-}$, is not oxidized (at least not rapidly) by O_2 either. In contrast, N-ligated complexes of alkyl-Pt(II), especially ones having two methyl groups, show much greater reactivity toward O_2. Presumably, this reactivity is largely a consequence of the electron-donating power of methyl substituents (as well as the N-centered ligand); unquestionably methyl substituents do foster oxidizability. For example, electrochemical oxidation of (diimine)$Pt^{IV}Me_4$ (which ultimately leads to homolytic Pt–Me cleavage) is just about as easy as that of (diimine)$Pt^{II}Me_2$, even though the complexes are formally Pt(IV) and Pt(II), respectively [84].

Reactions of $Me_xPt(II)$ with O_2 can be classified into two groups: those in which O_2 inserts into a Pt–C bond and those in which Pt(IV) is generated. (A somewhat fanciful biochemical analogy would be to call these oxygenase-like and oxidase-like, respectively.) There are two well-characterized examples of the former, both light-promoted. The first (Scheme 23) involves a cationic monomethyl-Pt(II) species, which is not expected to be easily oxidized, and indeed there is no indication that any Pt(IV) species is involved; rather it appears that the terpyridine-based ligand sensitizes generation of singlet oxygen, which undergoes insertion much as an olefin might; the resulting methylperoxo complex is also light-sensitive, decomposing to formaldehyde and Pt–OH [85]. The second (Scheme 24) is much slower and probably proceeds via a radical chain pathway (the ligand in this case is unlikely to support formation of singlet O_2); again there is no evidence for participation of Pt(IV) [86]. Insertion of O_2 into a Pt(IV)–H bond is also known (Scheme 25); the

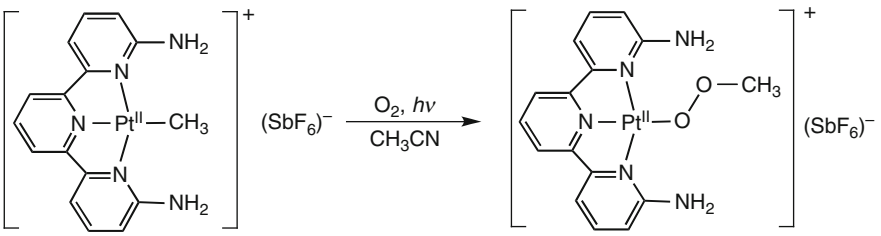

Scheme 23

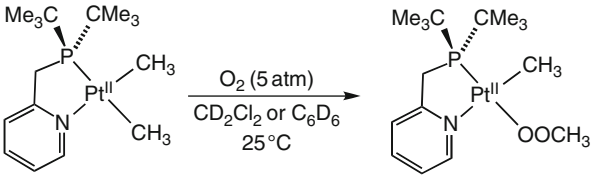

Scheme 24

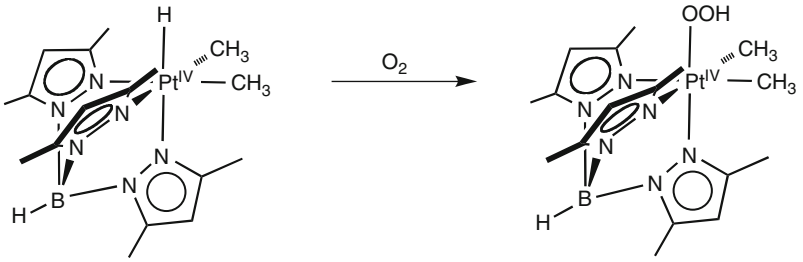

Scheme 25

initially proposed radical chain pathway [87] has been confirmed by recent detailed mechanistic studies [88].

Oxidation to Pt(IV) by O_2 was first reported for (tmeda)$Pt^{II}Me_2$ and related (phen) and (diimine) complexes; the reaction proceeds by the two-step sequence shown in Scheme 26. Neither the monomethyl ((tmeda)Pt^{II}MeCl) nor the diphenyl ((tmeda)-$Pt^{II}Ph_2$) analog reacts with O_2. The mechanism of formation of intermediate Pt(IV)–OOH is not clear; observation (under some conditions) of highly colored species suggests a radical pathway, although (in contrast to the above insertion reactions) there does not appear to be any effect of light [89, 90]. A dimeric Pt(II) complex of a related ligand has recently been reported to react with O_2; while the product was not clearly characterized, it reacts further with MeOTf to produce dimethyl peroxide and a new Pt(IV) dimer (Scheme 27) [91]. (Me_3TACN)$Pt^{II}Me_2$ is oxidized by (moist) air to give a cationic Pt(IV) hydroxo complex, $[(Me_3TACN)Pt^{IV}(OH)Me_2]^+$ [92].

As noted earlier, the semilabile ligand systems introduced by Vedernikov exhibit interesting O_2 chemistry [83]. The dimethyl-Pt(II) complex, $[(dmps)Pt^{II}Me_2]^-$, is the most reactive, undergoing oxidation to Pt(IV) in minutes at room temperature in water [72]. The related monomethyl analogs (dmps)Pt^{II}Me(HX) react similarly but more slowly, probably because they are neutral (actually zwitterionic); it is probable that O_2 actually reacts with a small equilibrium concentration of the corresponding conjugate base $[(dmps)Pt^{II}MeX]^-$ [93, 94]. The mechanism of oxidation appears to be similar to that of the related tmeda system, involving an intermediate Pt(IV)–OOH species that oxidizes another molecule of Pt(II). In all cases, the stereochemistry of the product corresponds to addition of OH and coordination of the sulfonate arm in the original axial positions of the Pt(II) square planar complex (Scheme 28). The analogous phenyl complexes are similarly oxidized by O_2, but more slowly [95]. (dmps)Pt(II)(olefin) complexes also react with O_2; here (as in the oxidation of Zeise's

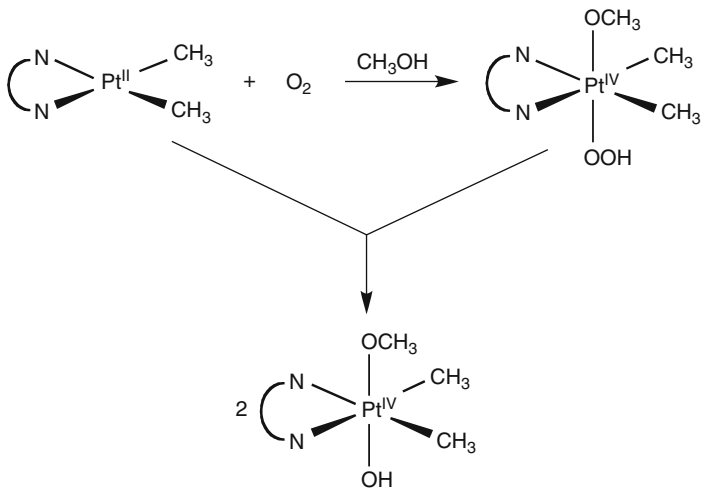

Scheme 26

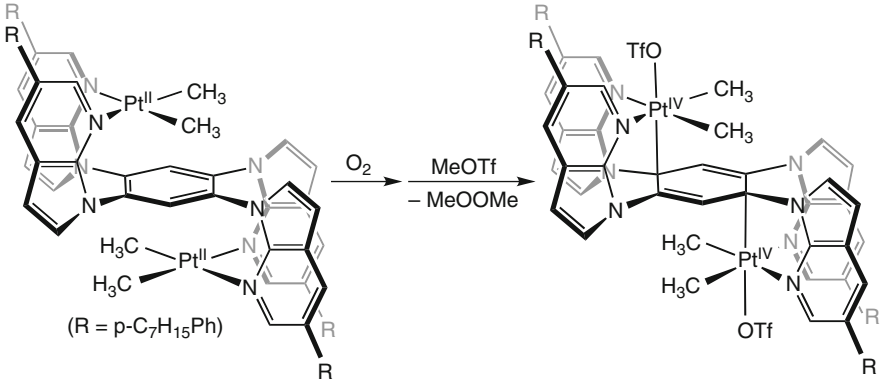

Scheme 27

salt, discussed earlier), the reactive species are (2-hydroxyalkyl)Pt(II) complexes, and products include (2-hydroxyalkyl)Pt(IV), Pt(IV)-oxetanes, or epoxides, depending on the olefin and reactions conditions [96, 97].

Reductive elimination of methanol, the last step in a hypothetical methane functionalization scheme, can be observed from the monomethyl-Pt(IV) species, but only at elevated temperature; mechanistic studies indicate that the formation of methanol is preceded by isomerization, as shown in Scheme 29 [73]. This finding is in accord with earlier studies on C–X bond formation, which require dissociation of a ligand *trans* to the alkyl group before nucleophilic attack at C in the five-coordinate intermediate. The original oxidation product has a pyridine ligand *trans* to

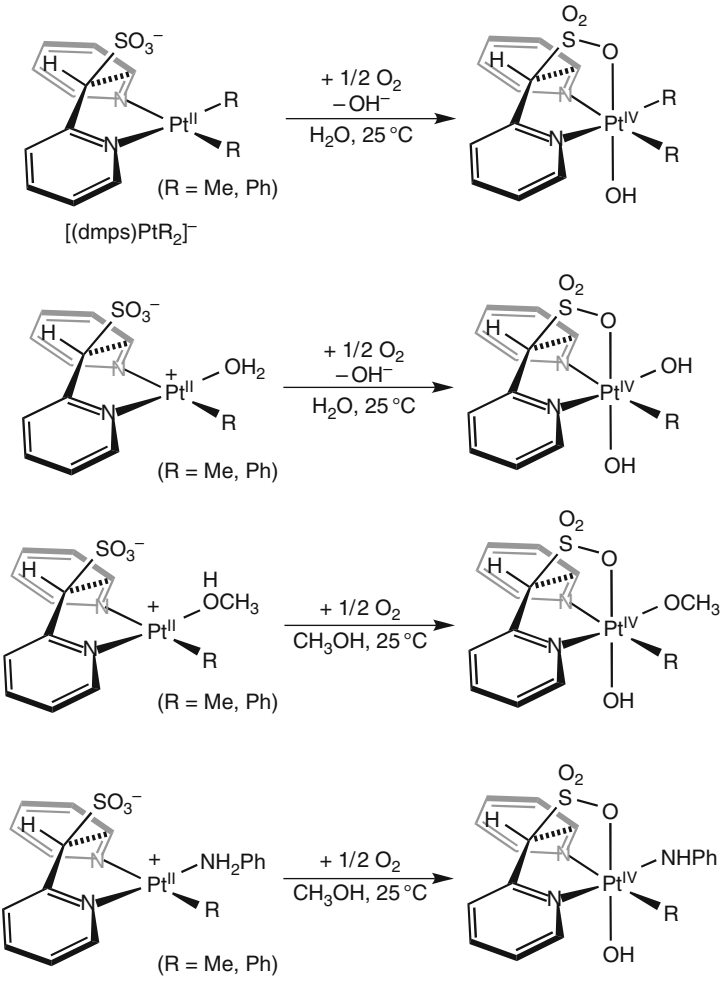

Scheme 28

methyl, strongly disfavoring dissociation. Protonation of a hydroxy ligand is also required; no methanol forms in neutral solution. Some of the C–O bond formation involves a bimolecular pathway, in which OH (or OMe, in which case some dimethyl ether is formed) coordinated to one Pt attacks a methyl group on another.

The related complex $[(dmdpb)Pt^{II}Ph_2]^-$ likewise reacts readily with O_2 in alcoholic solvent, but in a very different manner: a methyl group moves from B to Pt, leaving an opening for RO to add to B and occupy the sixth coordination site in the Pt(IV) product (Scheme 30) [98]. Presumably the absence of a potential sixth ligand in intact dmdpb (in contrast to dpms) accounts for this unexpected behavior. No C–X bond formation has been reported for this system.

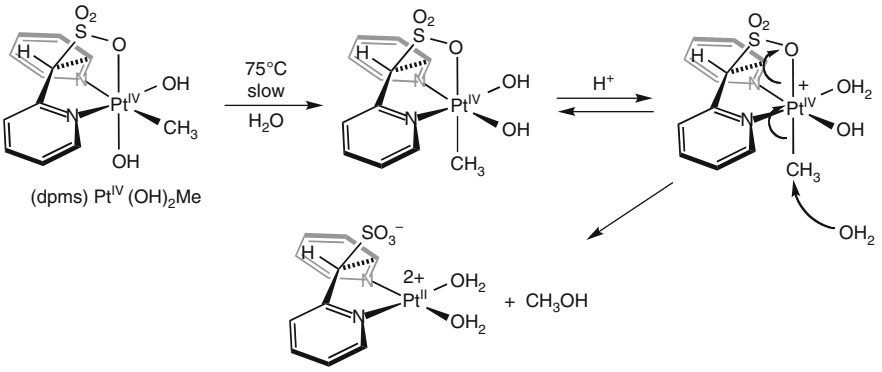

Scheme 29

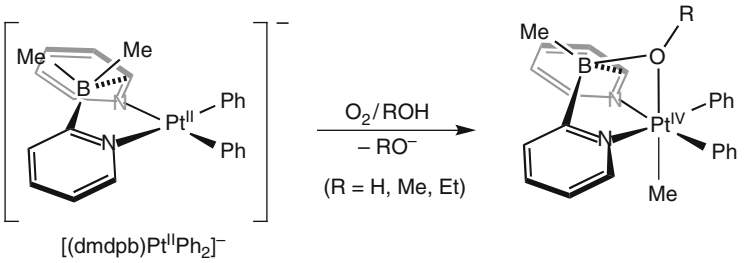

Scheme 30

5 Conclusions and Prospects

Obviously, the main reason for interest in all of this chemistry is the potential for mild, selective, catalytic functionalization of alkanes. There have been a number of transformations based on C–H activation at Pt, including a stoichiometric dehydrogenation in a natural product synthesis [99] and some hydroarylations of olefins [100, 101]. With regard specifically to catalytic oxidative functionalization via high-valent Pt intermediates, while many examples of the individual steps that would likely be involved in such processes – activation of C–H, redox chemistry of alkyl-Pt species, formation of C–X bonds, as well as dehydrogenation – have been demonstrated and (reasonably) well understood mechanistically, finding a single system that can effect *all* of them sufficiently well to add up to a practical catalyst remains elusive. There are, of course, systems that are catalytic, but not yet practical: the original Shilov system is too slow and unstable; the catalyst in the Catalytica system is stable, but the reaction is still too slow, and there are other problems as discussed earlier. Incorporation of ligands often improves one step, but only at the cost of retarding another.

Two issues seem to be ubiquitous. First, the redox chemistry needs to be finely balanced: oxidation of RPt(II) has to be fast to compete with protonolytic cleavage and selective, so that the Pt(II) species that activates the C–H bond is not itself oxidized. Second, the RPt(IV) species has to be able to undergo facile dissociation, so that a five-coordinate intermediate needed to facilitate nucleophilic C–X bond formation is readily accessible; for complexes of multidentate ligands, this criterion will probably require the ability to isomerize easily, as in Scheme 29 above. And, of course, all of this must be achieved within the context of maintaining a Pt(II) center capable of activating the C–H bond.

Nonetheless, recent accomplishments provide ample grounds for encouragement. For example, C–H bonds can be activated by aquo- and hydroxo-Pt(II) complexes (Scheme 18). The oxidation/functionalization sequence of Schemes 28 and 29 ends by producing such a complex; while complexes of the dmps ligand do not also effect C–H activation, it does not seem unreasonable that some other ligand might support all of the steps. One possibly promising approach is the introduction of "pincer" ligands, which have been shown to have interesting properties in C–H activations and other chemistry involving metals other than Pt. The pincer complex in Scheme 31 was shown to catalyze oxidation of 1-propanol to a mixture of 1,3- and 1,2-propanediol, using H_2O_2 as oxidant and Pt(IV) or Cu(II) as cocatalyst – an interesting result, although there are several limitations: only a few turnovers could be obtained; the combination of Cu(II) and O_2 did not work; and the pincer ligand itself is partially chlorinated under reaction conditions [102]. The cationic pincer complex $[(\text{triphos})\text{Pt}^{\text{II}}\text{Me}]^+$ shown in Scheme 32 undergoes facile protonolysis even with very weak acids, in contrast to cationic methyl complexes that lack the tridentate ligand structure; the enhanced reactivity was attributed to torsional strain [103], which (by microscopic reversibility) could conceivably be exploited to accelerate C–H activation reactions as well.

In addition, of course, many of the principles established for Pt may be (and have been) extended to other metals, Pd in particular; we do not have space to address

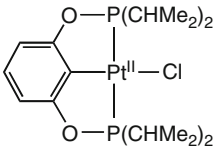

Scheme 31

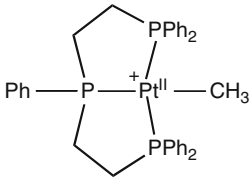

Scheme 32

any of that comparative chemistry here. With the high level of current research activity, including the continuous introduction of novel ligand architectures, it seems highly probable that the right combination of metal, ligand, and reaction-environment will eventually pay off.

References

1. Garnett JL, Hodges RJ (1967) J Am Chem Soc 89:4546
2. Gol'dshleger NF, Tyabin MB, Shilov AE, Shteinman AA (1969) Zh Fiz Khim 43:2174
3. Kukushkin VYu (2007) Coord Chem Rev 251:1
4. Gol'dshleger NF, Es'kova VV, Shilov AE, Shteinman AA (1972) Zh Fiz Khim 46:1353
5. Janowicz AH, Bergman RG (1982) J Am Chem Soc 104:352
6. Shilov AE, Shul'pin GB (1987) Russ Chem Rev 56:442
7. Shilov AE, Shul'pin GB (1997) Chem Rev 97:2879
8. Stahl SS, Labinger JA, Bercaw JE (1998) Angew Chem Int Ed Engl 37:2180
9. Fekl U, Goldberg KI (2003) Adv Inorg Chem 54:259
10. Lersch M, Tilset M (2005) Chem Rev 105:2471
11. Kushch LA, Lavrushko VV, Misharin YuS, Moravsky AP, Shilov AE (1983) Nouv J Chem 7:729
12. Horváth IT, Cook RA, Millar JM, Kiss G (1993) Organometallics 12:8
13. Luinstra GA, Wang L, Stahl SS, Labinger JA, Bercaw JE (1995) J Organomet Chem 504:75
14. Wang L, Stahl SS, Labinger JA, Bercaw JE (1997) J Mol Catal A 116:269
15. Zamashchikov VV, Popov VG, Litvenenko SL (1993) Russ Chem Bull 42:352
16. Weinberg DR, Labinger JA, Bercaw JE (2007) Organometallics 26:167
17. Rich RL, Taube H (1954) J Am Chem Soc 76:2608
18. Scollard JD, Day M, Labinger JA, Bercaw JE (2001) Helv Chim Acta 84:3247
19. Devries N, Roe DC, Thorn DL (2002) J Mol Catal A 189:17
20. Basickes N, Hogan TE, Sen A (1996) J Am Chem Soc 118:13111
21. Freund MS, Labinger JA, Lewis NS, Bercaw JE (1994) J Mol Catal 87:L11
22. Lin M, Shen C, Garcia-Zayas EA, Sen A (2001) J Am Chem Soc 123:1000
23. Bar-Nahum I, Khenkin AM, Neumann R (2004) J Am Chem Soc 126:10236
24. Kreutz JE, Shukhaev A, Du W, Druskin S, Daugolis O, Ismagilov RF (2010) J Am Chem Soc 132:3128
25. Moodley KG, Nicol MJ (1977) J Chem Soc Dalton Trans 239
26. Van Beek JAM, van Koten G, Wehman-Ooyevaar ICM, Smeets WJJ, van der Sluis P, Spek AL (1991) J Chem Soc Dalton Trans 883
27. Moret M-E, Chen P (2010) Eur J Inorg Chem 438
28. Johansson L, Ryan OB, Rømming C, Tilset M (1998) Organometallics 17:3957
29. Baker RT, Brown GH, Carpenter J, Davis ME, Labinger JA, Bercaw JE, unpublished results
30. Crumpton-Bregel DM, Goldberg KI (2003) J Am Chem Soc 125:9442 and references therein
31. Goldberg KI, Yan J, Winter EL (1994) J Am Chem Soc 116:1573
32. Williams BS, Goldberg KI (2001) J Am Chem Soc 123:2576
33. Zamashchikov VV, Litvenenko SL, Uzhik ON, Galat VF (1986) Zh Obshch Khim 56:2417
34. Tret'yakov VP, Rudakov ES, Galenin AA, Rudakova RN (1975) Dokl Akad Nauk SSSR 225:583
35. Wick DD, Goldberg KI (1997) J Am Chem Soc 119:10235
36. Stahl SS, Labinger JA, Bercaw JE (1996) J Am Chem Soc 118:5961
37. Zamashchikov VV, Popov VG, Rudakov ES (1994) Kinet Catal 35:339
38. Heyduk AF, Driver TG, Labinger JA, Bercaw JE (2004) J Am Chem Soc 126:15034
39. Zhong AH, Labinger JA, Bercaw JE (2002) J Am Chem Soc 124:1378

40. Wik BJ, Lersch M, Tilset M (2002) J Am Chem Soc 124:12116
41. Romeo R, D'Amico G (2006) Organometallics 25:3435
42. Bercaw JE, Chen GS, Labinger JA, Lin BL (2008) J Am Chem Soc 130:17654
43. Bercaw JE, Chen GS, Labinger JA, Lin BL (2010) Organometallics 29:4354
44. Balcells D, Clot E, Eisenstein O (2010) Chem Rev 110:749
45. Siegbahn PEM, Crabtree RH (1996) J Am Chem Soc 118:4442
46. Zhu H, Ziegler T (2006) J Organomet Chem 691:4486
47. Zhu H, Ziegler T (2008) Organometallics 27:1743
48. Zhu H, Ziegler T (2009) Organometallics 28:2773
49. Holtcamp MR, Labinger JA, Bercaw JE (1997) Inorg Chim Acta 119:848
50. Johansson L, Ryan OB, Tilset M (1999) J Am Chem Soc 121:1974
51. Periana RA, Taube DJ, Gamble S, Taube H, Satoh T, Fujii H (1998) Science 280:560
52. Periana RA, Taube DJ, Evitt ER, Loffler DG, Wentrcek PR, Voss G, Masuda T (1993) Science 259:340
53. Gilbert TM, Hristov J, Ziegler T (2001) Organometallics 20:1183
54. Kua J, Xu X, Periana RA, Goddard WA (2002) Organometallics 21:511
55. Ahlquist M, Periana RA, Goddard WA (2009) Chem Commun 2373
56. Paul A, Musgrave CB (2007) Organometallics 26:793
57. Villalobos JM, Hickman AJ, Sanford MS (2010) Organometallics 29:257
58. Mylvaganam K, Bacskay GB, Hush NS (2000) J Am Chem Soc 122:2041
59. Ziatdinov VR, Oxgaard J, Mironov OA, Young KJH, Goddard WA, Periana RA (2006) J Am Chem Soc 128:7404
60. Hickman AJ, Villalobos JM, Sanford MS (2009) Organometallics 28:5316
61. Cheng JH, Li ZW, Haught M, Tang YC (2006) Chem Commun 4617
62. Xu Z, Oxgaard J, Goddard W (2008) Organometallics 27:3770
63. Owen JS, Labinger JA, Bercaw JE (2006) J Am Chem Soc 128:1055
64. Driver TG, Day MW, Labinger JA, Bercaw JE (2005) Organometallics 24:3644
65. Chen GS, Labinger JA, Bercaw JE (2007) Proc Natl Acad Sci USA 104:6915
66. Li J-L, Geng C-Y, Huang X-R, Zhang X, Sun C-C (2007) Organometallics 26:2203
67. Parmene J, Krivokapic A, Tilset M (2010) Eur J Inorg Chem 1381
68. Butschke B, Schröder D, Schwarz H (2009) Organometallics 28:4340
69. Marrone A, Re N, Romeo R (2008) Organometallics 27:2215
70. Driver TG, Williams TJ, Labinger JA, Bercaw JE (2007) Organometallics 26:167
71. Williams TJ, Caffyn AJM, Hazari N, Oblad PF, Labinger JA, Bercaw JE (2008) J Am Chem Soc 130:2418
72. Vedernikov AN, Fettinger JC, Mohr F (2004) J Am Chem Soc 126:11160
73. Khaskin E, Zavalij PY, Vedernikov AN (2006) J Am Chem Soc 128:13054
74. Thomas CM, Peters JC (2006) Organometallics 24:5858
75. Zhao S-B, Song D, Jia W-L, Wang S (2005) Organometallics 24:3290
76. Zhao S-B, Wu G, Wang S (2006) Organometallics 25:5979
77. Zhao S-B, Wang R-Y, Wang S (2009) Organometallics 28:2572
78. Karshtedt D, McBee JL, Bell AT, Tilley TD (2006) Organometallics 25:1801
79. Fortman GC, Scott NM, Linden A, Stevens ED, Drta R, Nolan SP (2010) Chem Commun 46:1050
80. Vastine BA, Webster CE, Hall MB (2007) J Chem Theory Comput 3:2268
81. West NM, Templeton JL (2009) Can J Chem 87:288
82. Grice KA, Scheuermann ML, Goldberg KI (2011) Five-coordinate platinum(IV) complexes. Top Organomet Chem 35:1–28
83. Vedernikov AN (2009) Chem Commun 4781
84. Wik BJ, Tilset M (2007) J Organomet Chem 692:3223
85. Taylor RA, Law DJ, Sunley GJ, White AJP, Britovsek GJP (2009) Angew Chem Int Ed Engl 48:5900
86. Grice KA, Goldberg KJ (2009) Organometallics 28:953

87. Wick DD, Goldberg KJ (1999) J Am Chem Soc 121:11900
88. Look JL, Wick DD, Mayer JM, Goldberg KJ (2009) Inorg Chem 48:1356
89. Rostovtsev VV, Labinger JA, Bercaw JE, Lasseter TL, Goldberg KI (1998) Organometallics 17:4530
90. Rostovtsev VV, Henling LM, Labinger JA, Bercaw JE (2002) Inorg Chem 41:3608
91. Zhao S-B, Cui Q, Wang S (2010) Organometallics 29:998
92. Prokopchuk EM, Puddephatt RJ (2003) Can J Chem 81:476
93. Vedernikov AN, Binfield SA, Zavalij PY, Khusnutdinova JR (2006) J Am Chem Soc 128:82
94. Khusnutdinova JR, Zavalij PY, Vedernikov AN (2007) Organometallics 26:3466
95. Khusnutdinova JR, Zavalij PY, Vedernikov AN (2009) Can J Chem 87:110
96. Khusnutdinova JR, Zavalij PY, Vedernikov AN (2007) Organometallics 26:2402
97. Khusnutdinova JR, Newman L, Zavalij PY, Lam Y-F, Vedernikov AN (2008) J Am Chem Soc 130:2174
98. Khaskin E, Zavalij PY, Vedernikov AN (2007) Angew Chem Int Ed Engl 46:6309
99. Johnson JA, Li N, Sames D (2002) J Am Chem Soc 124:6900
100. Luedtke AT, Goldberg KI (2008) Angew Chem Int Ed Engl 47:7694
101. McKeown BA, Foley NA, Lee JP, Gunnoe TB (2008) Organometallics 27:4031
102. Wang Z, Sugiarti S, Morales CM, Jensen CM, Morales-Morales D (2006) Inorg Chim Acta 359:1923
103. Feducia JA, Campbell AN, Anthis JW, Gagné MR (2006) Organometallics 25:3114

Top Organomet Chem (2011) 35:61–84
DOI: 10.1007/978-3-642-17429-2_3

Carbon–Heteroatom Bond-Forming Reductive Elimination from Palladium(IV) Complexes

Joy M. Racowski and Melanie S. Sanford

Abstract This work provides a comprehensive review (1986–2010) of the synthesis, characterization, and reactivity of palladium(IV) complexes that undergo carbon–heteroatom bond-forming reductive elimination reactions. In cases where mechanistic information is available, the molecular pathway for C–X bond formation is described in detail. Examples of catalytic transformations that may involve this mechanistic manifold are also presented.

Keywords Catalysis · C–H activation · High oxidation state · Olefin functionalization · Oxidation · Palladium · Reductive elimination

Contents

J.M. Racowski and M.S. Sanford (✉)
Department of Chemistry, University of Michigan, Ann Arbor, MI 48109, USA
e-mail: mssanfor@umich.edu

1 Introduction

Carbon–heteroatom bond-forming reductive elimination from transient Pd^{IV} intermediates has been proposed as the product release step of a variety of important Pd-catalyzed transformations, including arene and alkane C–H bond functionalization [1, 2], allylic acetoxylation [3], alkene borylation [4], and olefin difunctionalization [5]. Over the past 25 years, a variety of Pd^{IV} model complexes have been synthesized to study reductive elimination reactions at Pd^{IV} centers. For instance, in 1986, Canty reported the first example of a crystallographically characterized organometallic Pd^{IV} complex, *fac*-[(bpy)$Pd^{IV}(CH_3)_3(I)$] (bpy = 2,2′-bipyridine) (**1**). In addition, his group has demonstrated that this species undergoes facile C–C bond-forming reductive elimination to release ethane (Eq. 1) [6].

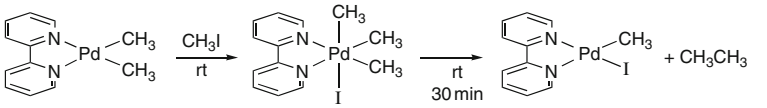

(1) (1)

Since this seminal report, numerous examples of C–C bond-forming reductive elimination from Pd^{IV} complexes have been demonstrated [7–11]. In contrast, carbon–heteroatom bond-forming reactions from Pd^{IV} species remain much rarer. This chapter presents a comprehensive review of the synthesis and reactivity of detectable Pd^{IV} complexes that undergo carbon–heteroatom coupling. Furthermore, mechanistic aspects of these reductive elimination reactions are discussed in detail.

2 Mechanistic Considerations

While the mechanism of many of the transformations described herein has not been investigated in detail, there are several examples where the reductive elimination pathway has been thoroughly evaluated via experiment and/or theory. Ultimately, a molecular-level mechanistic understanding of these processes should provide insights into the factors that control the relative and absolute rates of C–X bond-formation (and other fundamental organometallic transformations) at Pd^{IV}. This, in turn, will serve as critical data to inform the rational design of new catalytic transformations via the $Pd^{II/IV}$ manifold.

Neutral Pd^{IV} complexes are typically octahedral and contain two L-type and four X-type ligands. As summarized in the following lines, four general mechanisms are most commonly proposed for carbon–heteroatom (C–X) bond-forming reductive elimination from these species.

1. *Direct*. Direct mechanisms proceed via direct C–X bond formation from the octahedral starting material *without* dissociation of any other ligands.
2. *Dissociative Ionic* (D_I). D_I mechanisms involve dissociation of an X-type ligand to generate a cationic five-coordinate Pd^{IV} intermediate prior to C–X bond formation.

3. *Dissociative Neutral* (D_N). D_N transformations proceed via initial dissociation of an L-type ligand to form a neutral five-coordinate Pd^{IV} adduct, which is followed by C–X bond-forming reductive elimination.
4. *Radical*. Radical mechanisms entail homolytic cleavage of the Pd^{IV}–C bond to generate a carbon-based radical (C•). C–X bond formation then occurs by subsequent reactions of C•.
5. *Carbocation*. Carbocation mechanisms involve heterolytic cleavage of the Pd^{IV}–C bond to generate Pd^{II} and a carbocation (C^+). Nucleophilic attack on this free carbocation then yields the C–X coupled product.

3 Carbon–Chalcogen Bond Formation

3.1 Carbon–Chalcogen Bond-Forming Reactions in Oxidative Pd Catalysis

As early as 1971, C–O bond-forming reductive elimination from a $Pd^{IV}(Ph)(OAc)$ species was implicated in the $Pd(OAc)_2$-catalyzed oxidation of benzene with $K_2Cr_2O_7$ (Eq. 2) [12].

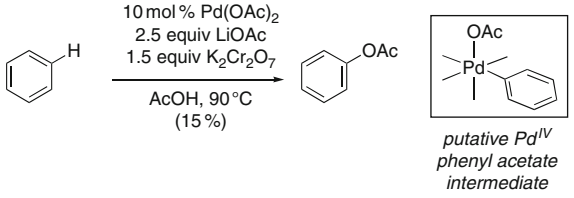

(2)

Subsequently, similar mechanisms have been proposed for benzene acetoxylation with $K_2S_2O_8$ [13] and $PhI(OAc)_2$ [14]. In addition, the ligand-directed oxygenation of sp^2 and sp^3 C–H bonds with $PhI(OAc)_2$ [15, 16], Oxone [17, 18], $K_2S_2O_8$ [17], IOAc [19], $CH_3CO_2O^tBu$ [20], lauroyl peroxide [20], and O_2 [21] (see Eq. 3 for a representative example) have all been suggested to proceed via $Pd^{II/IV}$ pathways in which C–O bond-forming reductive elimination serves as the product-forming step of the catalytic cycle.

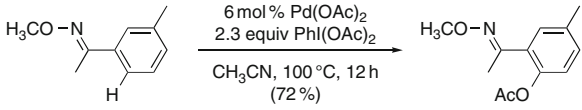

(3)

Numerous Pd-catalyzed olefin difunctionalization reactions are also hypothesized to involve C–O bond-forming reductive elimination from Pd^{IV} as a key step. For example, diverse α-olefins have been shown to undergo Pd-catalyzed dioxygenation

with oxidants including $PhI(OAc)_2$ [22, 23], O_2 [24, 25], and peracetic acid [26] via a putative $Pd^{II/IV}$ pathway (Eq. 4). In addition, the Pd-catalyzed aminooxygenation of olefins with $PhI(OAc)_2$ is thought to involve C–OAc bond formation at Pd^{IV} as the product release step (Eq. 5) [27–29].

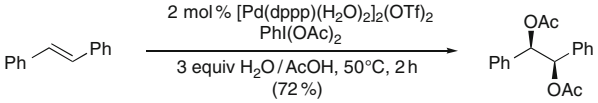

(4)

[dppp = diphenylphosphinopropane]

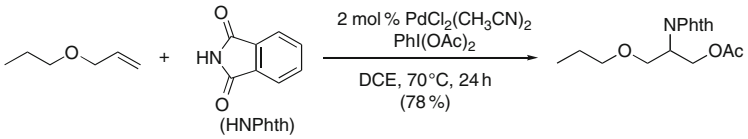

(5)

In contrast to C–O bond-forming reactions, C–S and C–Se coupling are rare in oxidative Pd catalysis. However, a recent report by Dong and coworkers demonstrated the Pd-catalyzed ligand-directed sulfonylation of arylpyridine, arylpyrazole, and aryloxime ether derivatives with $ArSO_2Cl$ (Eq. 6) [30]. The authors speculated that a $Pd^{II/IV}$ mechanism (involving oxidative addition into the S–Cl bond and subsequent C–S bond-forming reductive elimination from Pd^{IV}) was potentially operative.

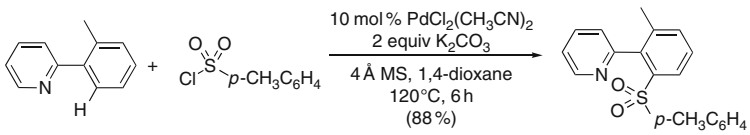

(6)

As discussed earlier, all of the reactions in eqs. (2–6) have been proposed to proceed via $Pd^{II/IV}$ catalytic cycles. Thus, it is of great interest and potential relevance to establish the viability of carbon–chalcogen bond-forming reductive elimination from Pd^{IV} centers. In addition, it is important to understand the effects of steric and electronic factors as well as the influence of ancillary ligands on the mechanisms of reductive elimination from Pd^{IV} to design improved catalytic transformations.

3.2 C–S and C–Se Bond Formation

The earliest reports of carbon–chalcogen bond formation from detectable Pd^{IV} intermediates appeared in 1998. In the first example, the Canty group demonstrated that the reaction of $[TpPd^{II}(CH_3)_2]^-$ (Tp = tris(pyrazol-1-yl)borate) with $(SePh)_2$ at 0°C in acetone-d_6 afforded a transient intermediate assigned as $TpPd^{IV}(CH_3)_2(SePh)$ (**2**) (Eq. 7) [31]. This complex was characterized by ^1H NMR spectroscopy, and its structure was assigned based on the synthesis of a Pt analog. The

corresponding thiophenolate complex $TpPd^{IV}(CH_3)_2(SPh)$ (**3**) was prepared via an analogous procedure, but at lower temperature (−10°C, Eq. 7).

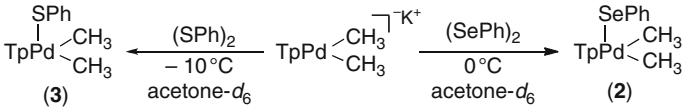

[Tp = tris(pyrazol-1-yl)borate] (7)

Upon standing in acetone solution at 0°C (complex **2**) or −10°C (complex **3**), these Pd^{IV} species underwent competing carbon–chalcogen and C–C bond-forming reductive elimination to form ethane and CH_3–XPh (X = S or Se). The yields of nongaseous organic products were determined by NMR spectroscopy and GCMS and are shown in Eq. 8.

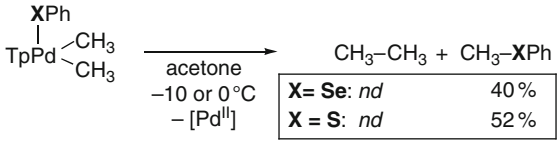

[*nd = not determined*] (8)

Canty conducted more detailed studies of related reductive elimination reactions from $(N\sim N)Pd^{IV}(CH_3)_2(XPh)_2$ [N~N = 1,10-phenanthroline (phen) or 2,2′-bipyridine (bpy), X = Se and S] [32]. In general, the bpy and phen complexes showed similar reactivity; thus, the current discussion will focus on the bpy analogs for conciseness. As shown in Eq. 9, $(bpy)Pd^{IV}(CH_3)_2(SePh)_2$ (**4**) was prepared in 73% yield via the reaction of $(bpy)Pd^{II}(CH_3)_2$ with $(SePh)_2$ in acetone at low temperature (below −25°C). Complex **4** was stable for at least 1 week at −20°C in the solid state, and it was characterized by ^1H and ^{13}C NMR spectroscopy (at −20°C) as well as X-ray crystallography. The sulfur analog of **4** [$(bpy)Pd^{IV}(CH_3)_2(SPh)_2$, **5**] was prepared in a similar fashion (Eq. 9). However, due to the lower reactivity of $(SPh)_2$, this reaction had to be conducted at 20°C (conditions where reductive elimination is fast). Thus, complex **5** was detected transiently by ^1H NMR spectroscopy, but was not isolated.

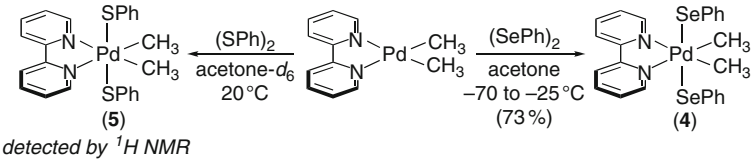

(9)

Warming solutions of **4** and **5** to above 0°C resulted in fast reductive elimination to form mixtures of CH_3–CH_3 and CH_3–XPh. The nongaseous organic products

were quantified by NMR spectroscopy and GCMS, and CH_3–XPh was formed in 17–50% yield, as shown in Eq. 10.

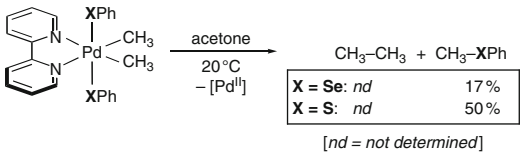

(10)

Mechanistic studies implicated a D_I mechanism for these transformations. In particular, the authors used Eyring analysis to establish a $\Delta S^{\ddagger}$ of −40.7 cal M^{-1} K^{-1} for reductive elimination from **4** in $CDCl_3$. This large, negative value suggests a highly ordered transition state, which is consistent with dissociation of $PhSe^-$ to generate an ion pair [**6**, (Eq. 11)] with highly ordered solvation. In addition, the activation energy (E_a) for the transformation was ~11 kcal mol^{-1}, which is significantly lower than the homolytic bond energy for Pd^{IV}–CH_3 (estimated at ~31 kcal mol^{-1}) [33]. As such, this piece of data suggests strongly against a radical mechanism.

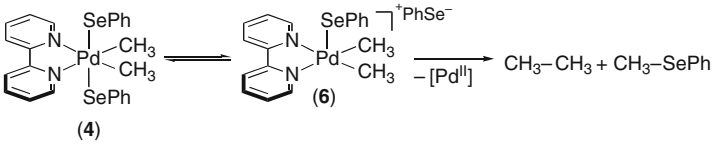

(11)

A final set of studies by Canty focused on C–Se bond formation from the mixed alkyl/aryl Pd^{IV} complex (bpy)$Pd^{IV}(CH_3)(p\text{-}CH_3OC_6H_4)(p\text{-}ClC_6H_4Se)_2$ (**7**) [34]. Complex **7** was prepared in 93% yield by oxidative addition of $(p\text{-}ClC_6H_4Se)_2$ to (bpy)$Pd^{II}(CH_3)(p\text{-}CH_3OC_6H_4)$ at −40°C (Eq. 12). Complex **7** allowed for direct comparison of the relative rates of sp^2 versus sp^3 C–Se bond-forming reductive elimination. As shown in Eq. 12, only the CH_3–Se(p-ClC_6H_4) was detected, demonstrating that sp^3 C–Se coupling is considerably faster in this system.

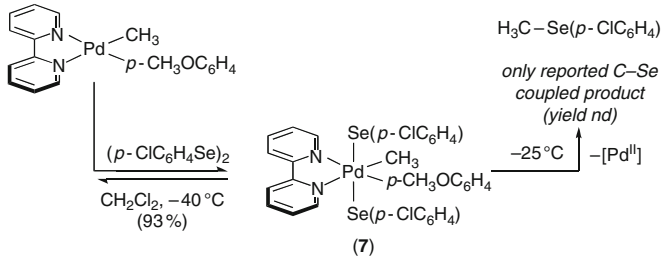

(12)

3.3 C–O Bond Formation

In 2001, Canty reported that the complex (bpy)$Pd^{II}(CH_3)_2$ reacts with $(PhCO_2)_2$ to generate the C–O coupled product CH_3O_2CPh [35]. Although this transformation appears similar to the analogous reactions of (bpy)$Pd^{II}(CH_3)_2$ with $(ArX)_2$

(X = S, Se; eqs. 9, 10), the authors demonstrated that C–O coupling proceeds via a different pathway. When the reaction between (bpy)$Pd^{II}(CH_3)_2$ and $(PhCO_2)_2$ was monitored at −70°C by ^1H NMR spectroscopy, (bpy)$Pd^{IV}(CH_3)_2(O_2CPh)_2$ (**8**) was not detected (Eq. 13). Instead, this species apparently underwent fast disproportionation with residual (bpy)$Pd^{II}(CH_3)_2$ to generate the Pd^{IV} complex (bpy)$Pd^{IV}(CH_3)_3(O_2CPh)$ (**9**) and the Pd^{II} complex (bpy)$Pd^{II}(CH_3)(O_2CPh)$ (**10**) (Eq. 13, step ii). Warming this mixture to −30°C resulted in C–C bond-forming reductive elimination from **9** to liberate ethane and a second equivalent of **10** (Eq. 13, step iii). Finally, at −10°C, **10** underwent reaction with $(PhCO_2)_2$ to generate the C–O coupled product CH_3O_2CPh (Eq. 13, step iv). While this latter transformation may proceed by a Pd^{IV} intermediate, none was detected [36]. This work illustrates the complexities inherent to high oxidation state palladium chemistry, and it shows that extreme caution should be exercised in extrapolating reactivity observed in one system to even closely related transformations.

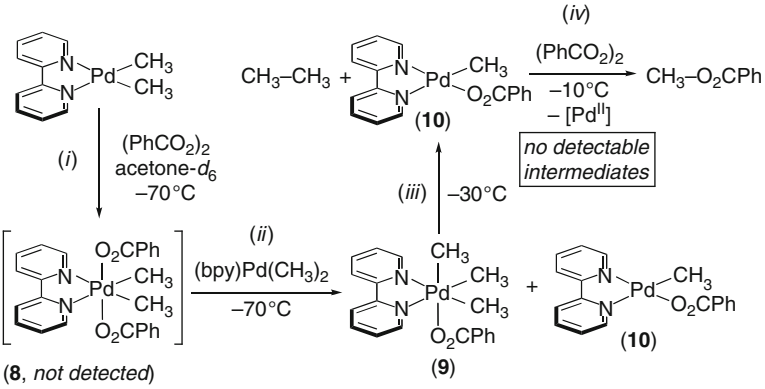

(13)

In 2002, Yamamoto published the first account of C–O bond-forming reductive elimination from an isolated Pd(IV) complex (**11**) [37]. As shown in Eq. 14, **11** was synthesized by the reaction of $Pd_2(dba)_3$ (dba = dibenzylideneacetone), tetrachloro-1,2-benzoquinone, and benzonorbornadiene, followed by the addition of pyridine. This Pd^{IV} adduct is stable in the solid state to >100°C and was characterized by ^1H and ^{13}C NMR spectroscopy as well as X-ray crystallography [38].

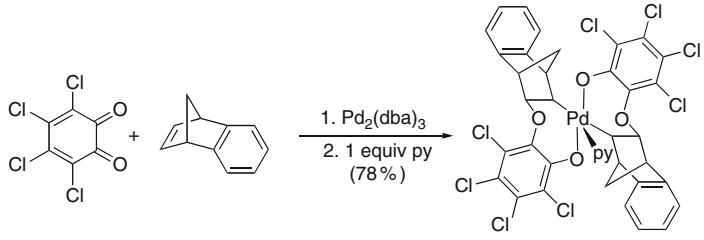

(14)

Heating **11** at 70°C for 4 h in benzene resulted in complete decomposition of the starting material. The major organic product was benzonorbornadiene (43% yield); however, minor quantities of C–O coupled products **12** (12%) and **13** (4%) were also formed (Eq. 15). The thermal decomposition of **11** was inhibited by pyridine, for example, in the presence of 5 equiv of pyridine, the reaction took 50 h (versus 4 h) to reach completion (Eq. 15).

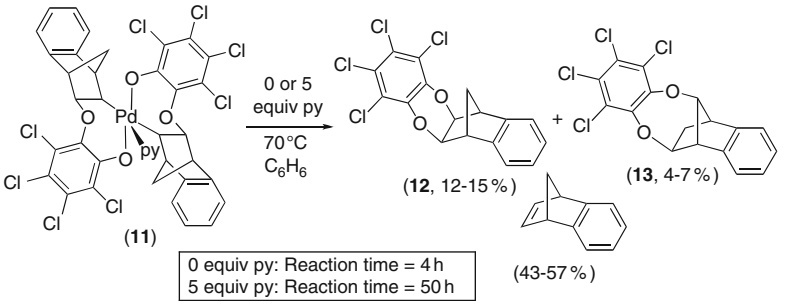

(15)

On the basis of this data, the authors proposed that C–O coupling from **11** proceeds via a dissociative neutral (D_N)/carbocation mechanism. The proposed pathway involves pre-equilibrium dissociation of the pyridine ligand to generate the neutral four-coordinate Pd^{IV} intermediate **14** (Eq. 16). Heterolytic cleavage of the Pd^{IV}–C bond then releases [Pd^{II}] and carbocation **15**, which can be trapped by the intramolecular phenoxide (to form **12**) or undergo rearrangement followed by trapping (to afford **13**).

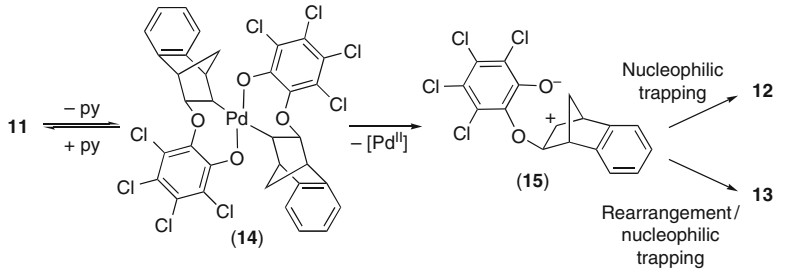

(16)

Most recently, our group has studied C–O bond-forming reductive elimination from Pd^{IV} complexes of general structure **16** (Eq. 17) [39]. Complex **16** was synthesized by reaction of $(phpy)_2Pd^{II}$ (phpy = 2-phenylpyridine) with the hypervalent iodine oxidant $PhI(OAc)_2$ in CH_2Cl_2 for 1 min at room temperature. This Pd^{IV} species was stable for at least 12 months at −35°C and was characterized by ^1H NMR and IR spectroscopy as well as X-ray crystallography.

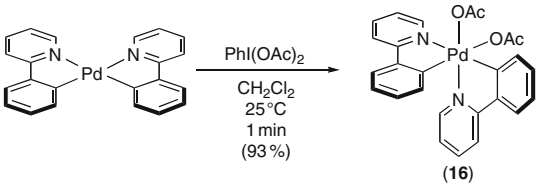

(17)

Complex **16** and derivatives thereof undergo clean C–O bond-forming reductive elimination upon thermolysis in a variety of solvents. For example, heating samples of **16** at 80°C for 30 min in CH_3CN resulted in C–O coupling to afford **17** in 95% yield (Eq. 18). Interestingly, none of the product derived from C–C bond-forming reductive elimination from **16** (**18** in Eq. 18) was detected under these conditions. The high-yielding formation of a single organic product in this system facilitated the first detailed mechanistic investigation of carbon–chalcogen bond formation at Pd^{IV}.

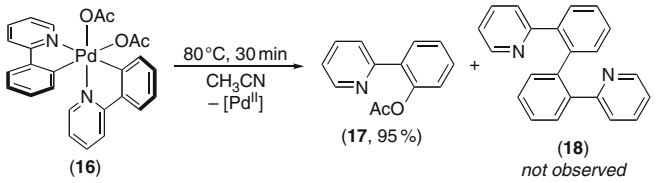

(18)

An original communication on this work suggested a D_N mechanism involving pre-equilibrium dissociation of one of the pyridine ligands followed by C–O coupling [39]. A subsequent DFT study proposed that direct C–O bond-forming reductive elimination from **16** was operative [40]. However, a very recent thorough experimental mechanistic analysis implicated a dissociative ionic (D_I) pathway (Eq. 19) for C–O bond-forming reductive elimination from **16** and its derivatives [41]. In the proposed mechanism, fast pre-equilibrium dissociation of AcO^- (step i) is followed by slow C–O bond formation (step ii) to release **17**.

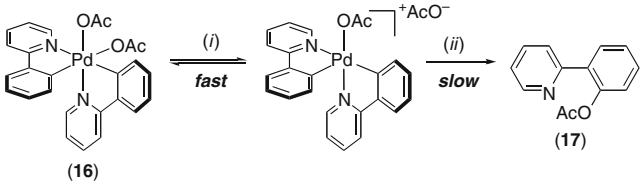

(19)

Numerous pieces of data supported the proposed D_I mechanism. First, complex **16** underwent facile carboxylate exchange with $Bu_4N(O_2C_{10}H_{19})$ in acetone-d_6 at 25°C over 5 min. In contrast, C–O bond-forming reductive elimination required heating at 80°C for 30 min. This result indicates that step i of the mechanism in Eq. 19 is fast and reversible.

Second, the carboxylate exchange process showed similar solvent effects and activation parameters to reductive elimination. For example, $\Delta S^{\ddagger}$ for C–O bond-forming reductive elimination in $CDCl_3$ was -1.4 ± 1.9 cal M^{-1} K^{-1}, while $\Delta S^{\ddagger}$ for carboxylate exchange was -7.2 ± 3.0 cal M^{-1} K^{-1}. In addition, Brønsted acids (like AcOH) and Lewis acids (like AgOTf) accelerated both reductive elimination and carboxylate exchange to similar extents. All of these results are consistent with the two processes being mechanistically linked in a D_I pathway.

Substituent effects on both the carboxylate and the arylpyridine coupling partner were also studied to gain insights into the electronic character of the C–O bond-forming step. A ρ value of -1.36 was obtained for *para*-X-substituted benzoate derivatives (**19** in Eq. 20), consistent with RCO_2^- acting as the nucleophilic coupling partner during C–O bond formation. With complexes containing *para*-Y-substituted arylpyridines (**20** in Eq. 20), a poor Hammett correlation was observed between the rate of reductive elimination and σ, σ^+ or σ^-; however, qualitatively the reactions were fastest with electron withdrawing substituents (Y).

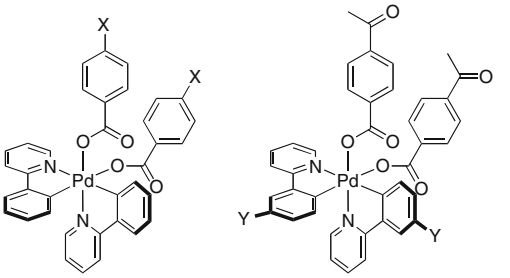

(**19**) (**20**) (20)

It is important to note that the electronic effects in this system are complicated by the fact that there are two different carboxylate ligands and two different arylpyridine ligands, each of which plays a different role in the C–O bond-forming process. However, overall, the data are consistent with a transition state like **21** or **22** for this transformation (Eq. 21). Notably, reductive elimination could also occur with the other (inequivalent) phenylpyridine ligand.

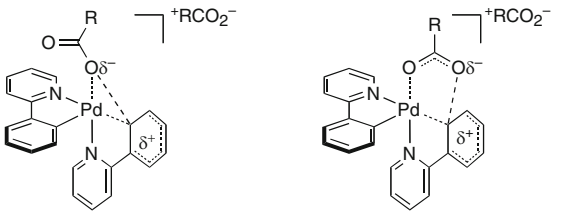

(**21**) (**22**) (21)

Interestingly, moving from the phenylpyridine complex **16** to the more rigid benzo[*h*]quinoline (bzq) complex **23** resulted in a reversal of chemoselectivity for reductive elimination. With **23**, the product of C–C bond-forming reductive elimination (**25**) was favored under most conditions (particularly in acetone and benzene). Mechanistic analysis suggests that C–C bond formation in this system proceeds via a direct mechanism.

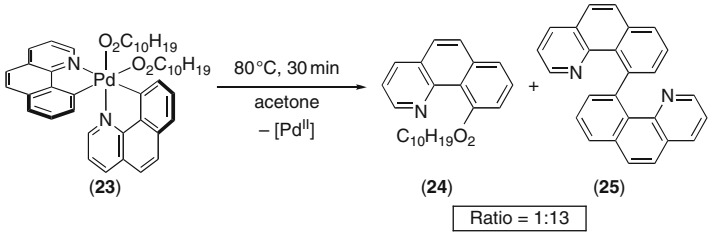

(22)

4 Carbon–Halogen Bond Formation

4.1 Carbon–Halogen Bond-Forming Reactions in Oxidative Pd Catalysis

A wide variety of Pd-catalyzed ligand-directed C–H halogenation reactions have been reported over the past 20 years. For example, C–H iodination with *N*-iodosuccinimide (NIS) [42], IOAc/Bu_4NI [43], and I_2/$PhI(OAc)_2$ [44]; C–H bromination with *N*-bromosuccinimide (NBS) [42], $Cu(OAc)_2$/$CuBr_2$ [45], BrOAc/Bu_4NBr [46], and $CuBr_2$/LiBr [47, 48]; C–H chlorination with Cl_2 [49], *N*-chlorosuccinimide (NCS) [42], $PhICl_2$ [42], and $Cu(OAc)_2$/$CuCl_2$ [45, 48]; and C–H fluorination with *N*-fluoropyridinium reagents [50, 51] have all been applied to both arene and alkane substrates (e.g., see eqs. 23–25). The structures of reactive Pd intermediates in these transformations have not been definitively elucidated. However, $Pd^{II/IV}$ mechanisms that involve carbon–halogen bond formation from transient Pd^{IV} intermediates have been proposed in many of these systems.

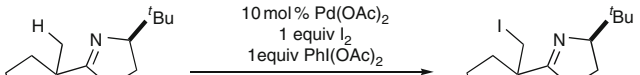

(23)

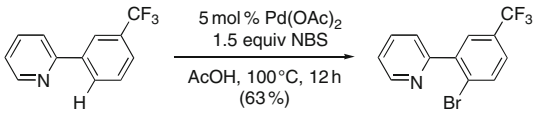

(24)

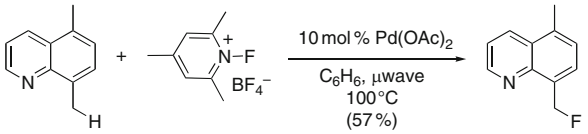

(25)

Numerous Pd-catalyzed olefin difunctionalization reactions have also been terminated by oxidative carbon–halogen bond formation. For example, both intra- and intermolecular aminohalogenations with NCS [52], NIS [53], $CuCl_2$ [54, 55], $CuBr_2/O_2$ [56], and $AgF/PhI(O_2C^tBu)_2$ [57] have been achieved (Eq. 26). Henry has reported a related synthesis of halohydrins via oxypalladation/C–X coupling (Eq. 27) [58]. In addition, the arylhalogenation of diverse α-olefins with $PhICl_2$, $CuCl_2$, and $CuBr_2$ was recently disclosed (Eq. 28) [59, 60]. Although the reactive intermediates in these transformations have not been characterized, carbon–halogen bond-formation from Pd^{IV} intermediates has been suggested in many cases.

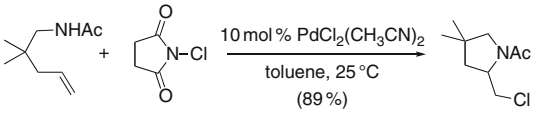

(26)

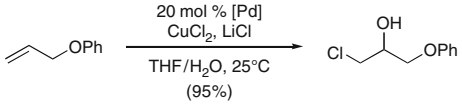

(27)

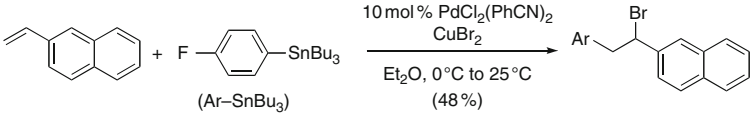

(28)

Based on the extensive proposals of carbon–halogen bond-forming reductive elimination from Pd^{IV} in catalysis, many groups have pursued model studies to investigate the viability and mechanism of such transformations. These studies are detailed in the following lines, and are arranged on the basis of the type of C–X bond that is being constructed (C–I, C–Br, C–Cl, and C–F, respectively).

4.2 C–I Bond Formation

The first example of C–I bond-forming reductive elimination from Pd^{IV} was reported by Elsevier and coworkers in 1994 (Eq. 29) [61]. They synthesized (*p*-Tol-BIAN)$Pd^{IV}(CH_3)_3I$ (**26**) (*p*-Tol-BIAN = bis(*p*-tolylimino)acenaphthene) by the oxidation of (*p*-Tol-BIAN)$Pd^{II}(CH_3)_2$ with CH_3I. Complex **26** was

characterized by NMR spectroscopy and elemental analysis, and this complex underwent reductive elimination at 20°C in $CDCl_3$. The major product (~85%) was ethane; however, significant quantities of CH_3I (~15%) were also formed. This reaction is quite unusual because (N~N)$Pd^{IV}(CH_3)_3(X)$ complexes typically undergo highly selective C–C bond-forming reductive elimination. In the current system, the authors hypothesize that carbon–iodine coupling is driven in the forward direction by the reaction of the inorganic product of C–I bond-formation [(*p*-tolyl-BIAN)$Pd^{II}(CH_3)_2$] with $CHCl_3$ to irreversibly generate (*p*-Tol-BIAN) $Pd^{II}(CH_3)(Cl)$ (which was detected in equimolar quantities to CH_3I).

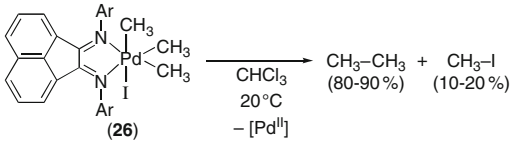

(29)

This same report also described the synthesis of diorgano Pd^{IV} complex (*p*-Tol-BIAN)$Pd^{IV}(CH_3)_2(I)_2$. It was characterized by ^1H and ^{13}C NMR spectroscopy and elemental analysis. The authors report that this species is unstable at room temperature in solution. While the decomposition products were not studied in detail, they are likely to include compounds derived from C–I bond-forming reductive elimination.

Subsequent studies from the Canty group showed that C–I bond-forming reductive elimination occurs in modest yield from palladacyclopentane complex **27** (Eq. 30) [62]. Complex **27** was prepared in a similar fashion to **26** [by oxidative addition of ethyl iodide to (bpy)$Pd^{II}(C_4H_8)$], and was characterized by NMR spectroscopy. As with **26**, thermolysis of **27** in $CDCl_3$ produced predominantly C–C coupled products [as a mixture of hexenes (48%), hexane (38%), butenes (3.5%), and butane (1.5%)]. However, a significant quantity of iodohexane (9%) was also detected by NMR and GCMS analysis (Eq. 30). Notably, similar reactivity was also observed with the analogous Pd^{IV} methyl complex (bpy)$Pd^{II}(C_4H_8)(CH_3)(I)$.

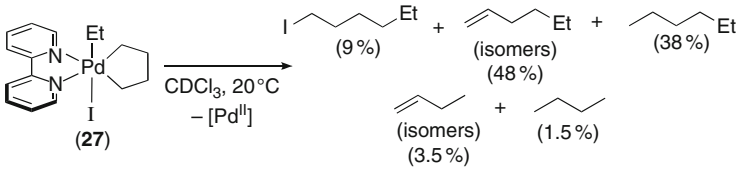

(30)

Most recently, Canty and coworkers demonstrated that the oxidation of (bpy) $Pd^{II}(CH_3)_2$ with I_2 at −50°C in acetone-d_6 affords the diorgano Pd^{IV} complex **28**. The ^1H NMR spectrum of **28** displayed symmetry consistent with the trans geometry shown in Eq. 31 [36]. This species was too unstable to isolate, and, upon warming to −10°C, it underwent clean and highly selective C–I bond-forming reductive elimination to generate CH_3I and (bpy)$Pd^{II}(CH_3)(I)$.

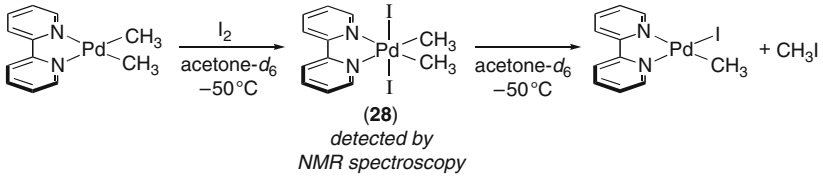

(31)

4.3 C–Br Bond Formation

In 1989, Canty and coworkers demonstrated that the thermolysis of **29**, which was formed by the reaction of (bpy)$Pd^{II}(CH_3)_2$ with phenacyl bromide, yielded traces of CH_3Br (Eq. 32) [63]. However, as expected, the predominant decomposition pathway for this triorgano Pd^{IV} complex involved C–C coupling to generate mixtures of ethane and ethylmethylketone (Eq. 32).

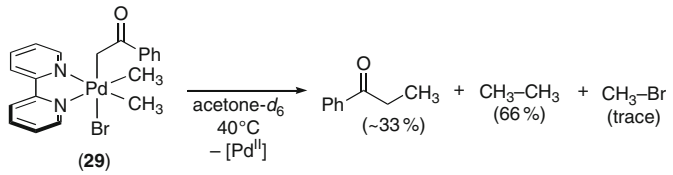

(32)

Later work by Elsevier revealed that the diorgano Pd^{IV} complex **31** undergoes more selective C–Br coupling (Eq. 33) [64]. This complex was prepared by oxidative addition of Br_2 to palladacycle **30** and was characterized by NMR spectroscopy and elemental analysis. At −73°C in CH_2Cl_2 solution, it reacts via C–Br bond-forming reductive elimination to afford **32**. While the low stability of **31** precluded experimental mechanistic investigations, computational studies suggested a direct reductive elimination pathway with $\Delta G^{\ddagger}$ of 23.4 kcal mol^{-1} [65].

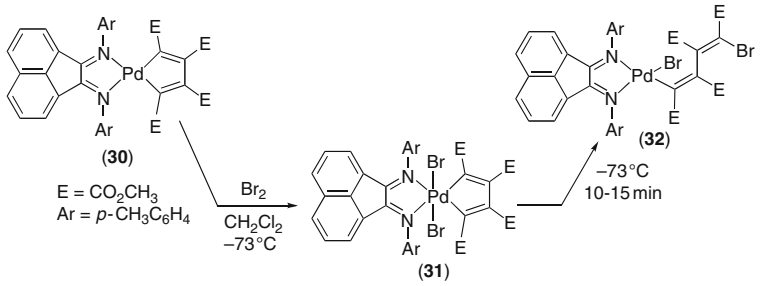

(33)

Most recently, the cyclometalated Pd^{IV} adduct **34** was reported by Daugulis (Eq. 34) [66]. Complex **34** was synthesized by the oxidation of **33** with Br_2 at −78°C in CH_2Cl_2 and was characterized by X-ray crystallography. This Pd^{IV}

adduct decomposed within hours at 0°C in CH_2Cl_2 solution and over days in the solid state. Although no products were identified or characterized, it is likely that sp^3 C–Br bond-forming reductive elimination is a major decomposition pathway.

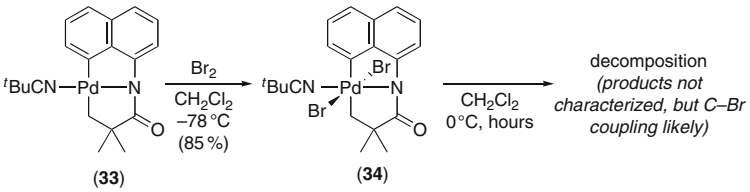

(34)

4.4 C–Cl Bond Formation

The first literature example of C–Cl bond-forming reductive elimination from Pd^{IV} involved the mono-organo Pd^{IV} complex **36** (Eq. 35) [67]. This pincer adduct was accessed by van Koten and coworkers via oxidation of the Pd^{II} precursor (**35**) with excess Cl_2 at room temperature in $CHCl_3$. The Pd^{IV} trichloride intermediate was characterized by ^1H NMR spectroscopy, but underwent fast reductive elimination to form **37**. However, the decomposition was not very clean, which the authors attributed to the presence of excess dissolved Cl_2.

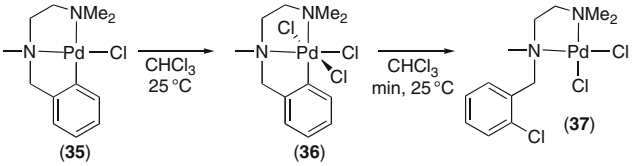

(35)

van Koten and coworkers reported a related reaction of bimetallic Pd^{IV} complex **39** [68]. As shown in Eq. 36, **39** was synthesized by the oxidation of **38** with $PhICl_2$ at room temperature in $CHCl_3$. Complex **39** was characterized by ^1H NMR spectroscopy and could be isolated in low yield. It underwent fast decomposition in solution. Although the organic product was not definitively identified, it was proposed to be **40**.

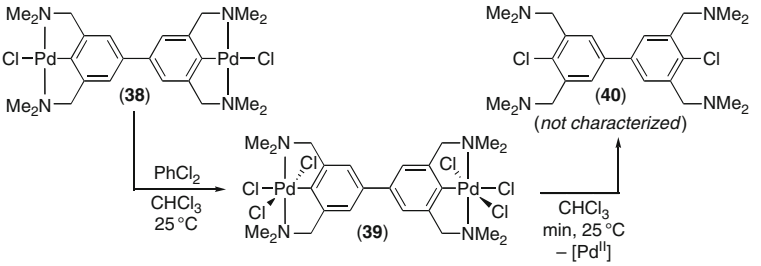

(36)

Another example of C–Cl bond-forming reductive elimination involved the bimetallic complex **42** (Eq. 37) [69]. This species was proposed as an intermediate in the oxidation of **41** with Cl_2 at −30°C. Complex **42** could be detected by NMR spectroscopy but not isolated. It underwent selective sp^3 C–Cl coupling to generate **43** within 50 min at −25°C.

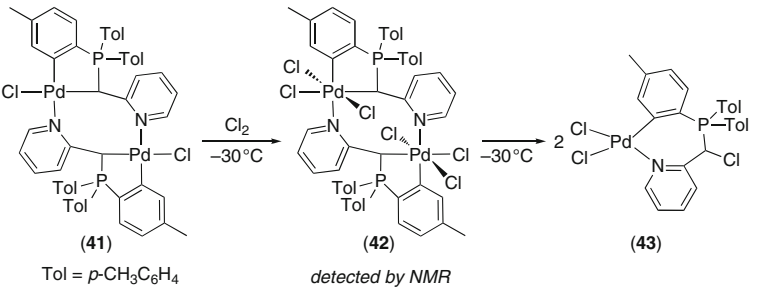

(37)

Whitfield and Sanford investigated C–Cl bond formation from two isolated Pd^{IV} complexes. $PhICl_2$ and *N*-chlorosuccinimide were used to oxidize $(phpy)_2Pd^{II}$ to form stable Pd^{IV} species **44** and **45** (Eq. 38) [70]. These complexes were stable in solution for several hours at room temperature and were characterized by ^1H and ^{13}C NMR spectroscopy and X-ray crystallography (**45**).

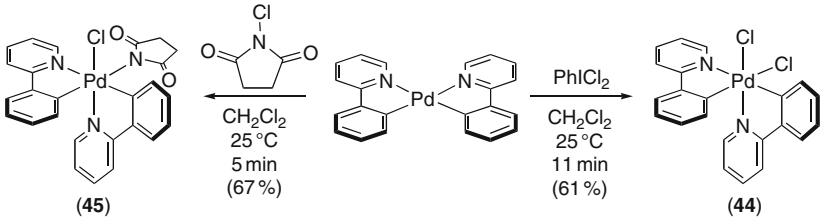

(38)

The distribution of reductive elimination products from **44** and **45** varied depending on the solvent. For example, when **44** was heated at 80°C for 12 h in pyridine, C–C coupling predominated; in contrast, C–Cl bond-forming reductive elimination was favored in AcOH and CH_3CN (Eq. 39). The best selectivity for **46** over **47** was observed in AcOH, where these products were formed in a 5:1 ratio.

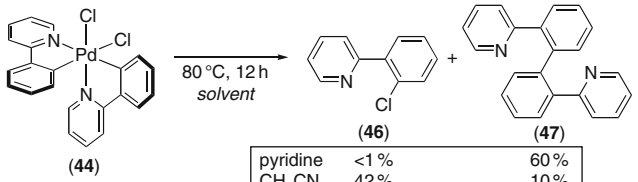

pyridine	<1 %	60 %
CH_3CN	42 %	10 %
AcOH	49 %	7 %

(39)

Complex **45** is a particularly interesting case because the following three different reductive elimination reactions are possible: C–Cl, C–C and C–N coupling to generate products **46**, **47**, and **48**, respectively. As shown in Eq. 40, the ratio of these products was again highly dependent on the reaction medium, with AcOH favoring **46** and pyridine leading to preferential formation of **47**. Intriguingly, significant quantities (~8%) of the C–N coupled product **48** were also formed in pyridine. The mechanism of this transformation as well as the mechanistic origin of these intriguing solvent effects is not known at this time.

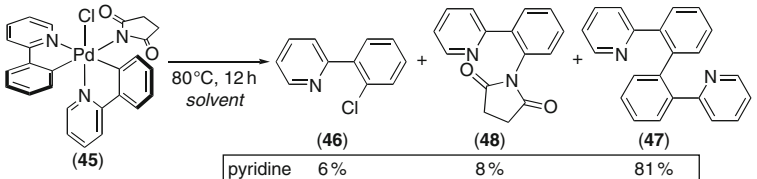

	(46)	(48)	(47)
pyridine	6%	8%	81%
CH_3CN	8%	<1%	20%
AcOH	67%	<1%	5%

(40)

Finally, Arnold and Sanford have reported C–Cl bond formation from the Pd^{IV} *N*-heterocyclic carbene complex **50** (Eq. 41) [71]. Complex **50** was prepared by oxidation of **49** with $PhICl_2$ at −35°C in CH_3CN and was characterized by ^1H and ^{13}C NMR spectroscopy and X-ray crystallography. This complex could potentially undergo $C_{carbene}$–C_{bzq}, C_{bzq}–O, $C_{carbene}$–Cl, or C_{bzq}–Cl bond-forming reductive elimination. Remarkably, only the latter was observed to generate **51** in 75% yield.

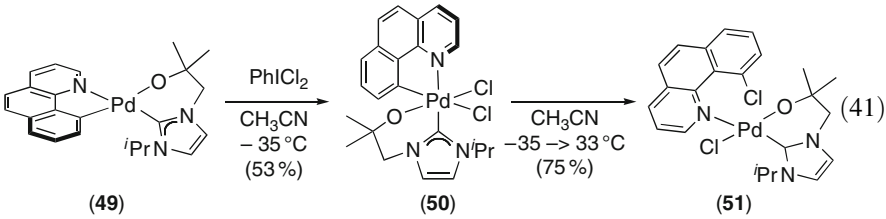

(41)

4.5 C–F Bond Formation

The most recently discovered carbon–halogen coupling reactions at Pd^{IV} centers involve the formation of sp^2 C–F bonds. These transformations are particularly notable because, until very recently [72], Aryl–F bond-forming reductive elimination had not been achieved from any transition metal center [73].

Ball and Sanford showed that the treatment of **52** with XeF_2 at 70°C for 2.5 min afforded the mono-aryl Pd^{IV} complex **53** in modest 35% yield (Eq. 42) [74]. This

species was characterized by NMR spectroscopy and X-ray crystallography and was stable for hours in solution at room temperature.

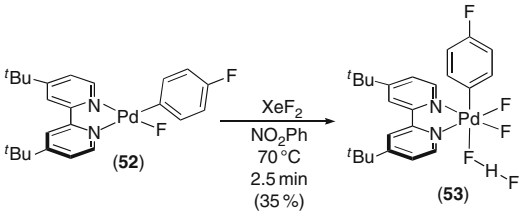

(42)

Intriguingly, thermolysis of **53** at 80°C for 1 h in nitrobenzene did *not* lead to significant quantities of aryl fluoride **54** (Eq. 43a). Instead, biaryl **55** was the major organic product (35% yield). Compound **55** could be formed via several different pathways, including (1) transmetalation followed by C–C bond-forming reductive elimination, (2) generation of Ar• and subsequent radical coupling, or (3) a bimetallic reductive elimination process.

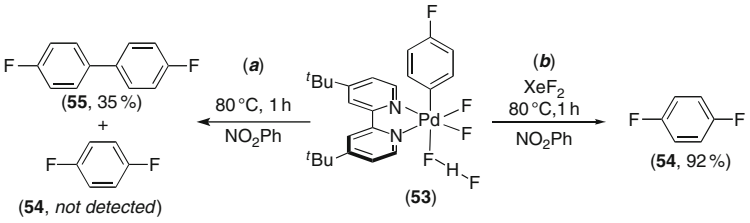

(43)

In contrast, C–F bond-formation was observed when **53** was treated with an excess of electrophilic fluorinating reagents (e.g., XeF_2) at 80°C in nitrobenzene (Eq. 43b). Under these conditions, <5% of the biaryl product **55** was produced. The mechanism of this transformation (particularly the role of the F^+ reagents in promoting C–F coupling) has not been fully elucidated.

A very thorough mechanistic study of C–F bond-forming reductive elimination from Pd^{IV} complexes **57**, **58**, and **59** was conducted by Ritter and coworkers. Initial oxidation of **56** with Selectfluor™ at 23°C in CH_3CN formed **57** [75, 76]. The subsequent addition of pyridine then led to **58**, while the use of NMe_4F produced **59** (Eq. 44). The solution structures of cationic complexes **57** and **58** were established through detailed one- and two-dimensional ^1H, ^{13}C, and ^{19}F NMR analysis. The solid state structure of difluoride **59** was determined using X-ray crystallography, and NMR analysis showed that **59** adopts the same structure in CH_3CN solution [76].

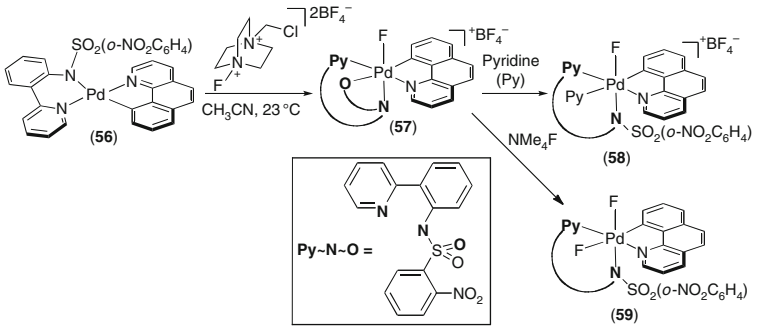

(44)

Heating complex **57** at 50°C in CH_3CN resulted in rapid and clean C–F bond-forming reductive elimination to afford **60** (Eq. 45). The addition of pyridine trapped the Pd-containing product as the cationic bis-pyridine adduct **61** (Eq. 45). Very similar reactivity was observed with the pyridine-ligated Pd^{IV} starting material **58**.

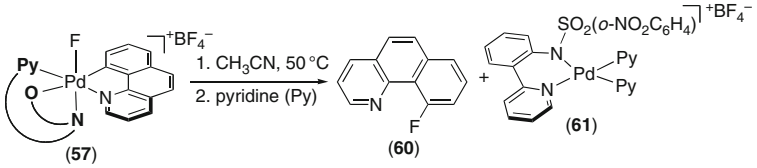

(45)

A full mechanistic analysis was conducted of C–F bond-forming elimination from complexes **57** and **58** [77, 78]. The authors studied the activation parameters, k_{obs} as a function of the reaction medium, and k_{obs} as a function of substituents X, Y, Z, and L (see complex **62** in Eq. 46). As detailed below, all of these experiments were consistent with a D_N pathway for reductive elimination, involving fast pre-equilibrium dissociation of the sulfonyl or pyridine ligand (step 1) followed by rate limiting C–F coupling (step 2, Eq. 47). For clarity, the mechanistic discussion below will focus primarily on complex **57**; however, in general, similar results were obtained in both cases.

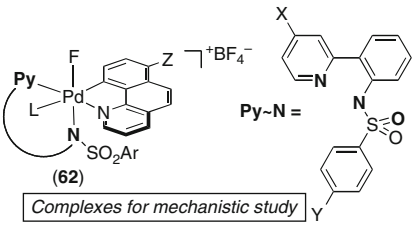

(46)

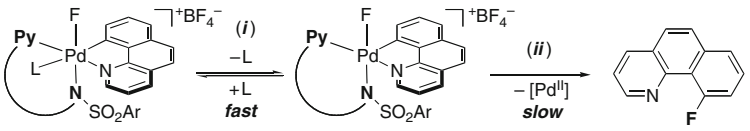

(47)

C–F reductive elimination from **57** showed a $\Delta S^{\ddagger}$ of 12.4 cal M^{-1} K^{-1}, consistent with a dissociative mechanism, in which the transition state is less ordered than the starting material. The rate of reductive elimination was independent of the dielectric of the solvent (which was modified through the addition of Bu_4NBF_4 to CH_3CN). This suggests that the polarity/charge of the transition state is similar to that of the ground state, which is again consistent with the mechanism in Eq. 47.

Hammett plots were constructed by variation of each of the substituents X, Y, and Z in complex **62** (Eq. 46). The ρ values obtained from this analysis were as follows: $\rho_X = -0.22$, $\rho_Y = -0.19$, and $\rho_Z = +0.61$ [78]. These values are consistent with reductive elimination occurring through a transition state like that shown in Eq. 48, involving nucleophilic attack of the fluoride on the σ-aryl group. DFT calculations (particularly the computed natural charges) showed a very similar transition state, providing additional support for the proposed mechanism. The authors suggest that the electronic requirements for C–F bond formation in this system are similar to those for nucleophilic aromatic substitution reactions.

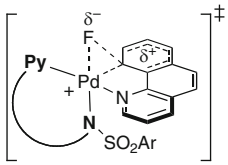

(48)

Two final strong pieces of evidence in support of the D_N mechanism were obtained in studies of the pyridine-ligated complex **58**. First, equilibration between **57** and **58** was found to be fast at 25°C (49 s^{-1}), a temperature well below that required for C–F reductive elimination (Eq. 49).

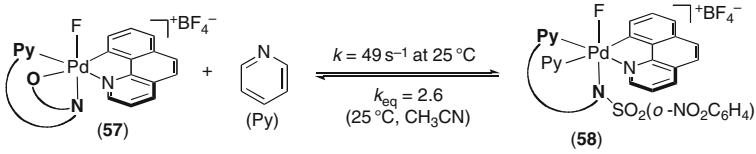

(49)

Second, studies of the rate of C–F coupling in the presence of added pyridine showed an inverse first-order dependence on this additive. These results are both indicative of rapid pyridine dissociation that occurs prior to the rate-determining step of the reaction.

The difluoride complex **59** was significantly more thermally stable than either **57** or **58**. Nonetheless, this complex did undergo C–F bond-forming reductive

elimination under forcing conditions. For example, heating **59** for 5 min at 150°C in DMSO provided C–F coupled product **60** in nearly quantitative yield (97%). In addition, reductive elimination proceeded neatly in the solid state (98% yield after 4 h at 100°C) (Eq. 50).

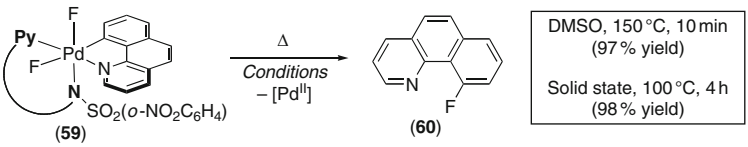

(50)

However, at lower temperatures, the yield of **60** decreased dramatically (e.g., 38% yield of **60** was obtained in DMSO at 50°C). Under these conditions, F_2 reductive elimination appears to be competitive, as the other benzoquinoline-containing product is **63** (Eq. 51). While the origin of these effects and the mechanism of reductive elimination from **59** have not been studied in detail, the authors propose that the change in product distribution as a function of temperature may be due to a large difference in $\Delta S^{\ddagger}$ between the C–F and F–F bond-forming processes.

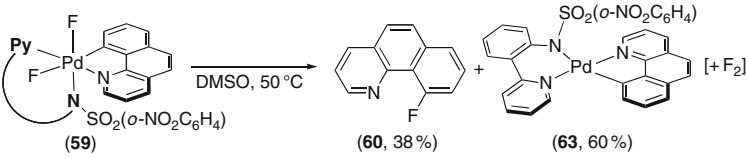

(51)

5 Conclusions and Future Directions

Over the last 20 years, numerous reagents have been utilized to oxidize Pd^{II} model complexes to Pd^{IV} species. Furthermore, a wide variety of supporting ligands have been shown to stabilize these Pd^{IV} adducts. In many cases, the Pd^{IV} compounds decompose via carbon–heteroatom bond-forming reductive elimination, thereby establishing the potential feasibility of such transformations in catalytic oxidation. However, in these model systems, C–C bond-forming reductive elimination is frequently a competing decomposition pathway. This has often hampered efforts to conduct detailed mechanistic investigations of C–X bond formation at Pd^{IV}.

Several recent studies have begun to uncover the molecular mechanisms of carbon–heteroatom bond-forming reductive elimination from Pd^{IV} centers. This recent work has addressed such fundamental questions as the electronic requirements of C–X coupling, the effects of ancillary ligands, the influence of solvent and additives, and the relative rates of competing transformations. The future of this field is bright, as there are still many outstanding mechanistic questions to be

answered. For example, the stereochemical outcome (retention vs. inversion) and stereospecificity of sp^3 carbon–heteroatom reductive elimination from Pd^{IV} are of great interest, since both are crucial for developing well-controlled asymmetric catalytic transformations. In addition, it is important to understand the influence of ligand structure, solvent, and additives on competing carbon-heteroatom bond-forming processes, since organometallic Pd^{IV} species containing different heteroatom X-type ligands are likely present during many catalytic processes. Finally, studies of C–X reductive elimination from Pd^{IV} mono-organo complexes are important future targets, since such adducts more closely resemble putative catalytic intermediates than most of the complexes discussed herein. Efforts in all of these areas are sure to inform the development and optimization of novel catalytic transformations.

Acknowledgments The authors thank the US National Science Foundation for support of the Sanford group's work described herein. In addition, Professor Polly Arnold as well as Dr. Allison Dick, Dr. Salena Whitfield, Dr. Stephen Pearson, and Nicholas Ball are gratefully acknowledged for their important contributions.

References

1. Lyons TW, Sanford MS (2010) Chem Rev 110:1147–1169
2. Dick AR, Sanford MS (2006) Tetrahedron 62:2439–2463
3. Aydin J, Larsson JM, Selander N, Szabo KJ (2009) Org Lett 11:2852–2854
4. Selander N, Willy B, Szabo KJ (2010) Angew Chem Int Ed 49:4051–4053
5. Muniz K (2009) Angew Chem Int Ed 48:9412–9423
6. Byers PK, Canty AJ, Skelton BW, White AH (1986) J Chem Soc Chem Commun: 1722–1723.
7. Canty AJ (1992) Acc Chem Res 25:83–90
8. Canty AJ, van Koten G (1995) Acc Chem Res 28:406–413
9. Canty AJ (2009) Dalton Trans 47:10409–10417
10. Xu LM, Li BJ, Yang Z, Shi ZJ (2010) Chem Soc Rev 39:712–733
11. Sehnal P, Taylor RJK, Fairlamb IJS (2010) Chem Rev 110:824–889
12. Henry PM (1971) J Org Chem 36:1886–1889
13. Eberson L, Jonsson L (1974) J Chem Soc Chem Commun: 885–886.
14. Yoneyama T, Crabtree RH (1996) J Mol Catal A 108:35–40
15. Dick AR, Hull KL, Sanford MS (2004) J Am Chem Soc 126:2300–2301
16. Desai LV, Hull KL, Sanford MS (2004) J Am Chem Soc 126:9542–9543
17. Desai LV, Malik HA, Sanford MS (2006) Org Lett 8:1141–1144
18. Reddy BVS, Reddy LR, Corey EJ (2006) Org Lett 8:3391–3394
19. Wang DH, Hao XS, Wu DF, Yu JQ (2006) Org Lett 8:3387–3390
20. Giri R, Liang J, Lei JQ, Li JJ, Wang DH, Chen X, Naggar IC, Guo C, Foxman BM, Yu JQ (2005) Angew Chem Int Ed 44:7420–7424
21. Zhang J, Khaskin E, Anderson NP, Zavalij PY, Vedernikov AN (2008) Chem Commun 31:3625–3627
22. Li Y, Song D, Dong VM (2008) J Am Chem Soc 130:2962–2964
23. Wang WF, Wang FJ, Shi M (2010) Organometallics 29:928–933
24. Zhu MK, Zhao JF, Loh TP (2010) J Am Chem Soc 132:6284–6285
25. Wang AZ, Jiang HF, Chen HJ (2009) J Am Chem Soc 131:3846–3847

26. Park CP, Lee JH, Yoo KS, Jung KW (2010) Org Lett 12:2450–2452
27. Alexanian EJ, Lee C, Sorensen EJ (2005) J Am Chem Soc 127:7690–7691
28. Liu GS, Stahl SS (2006) J Am Chem Soc 128:7179–7181
29. Desai LV, Sanford MS (2007) Angew Chem Int Ed 46:5737–5740
30. Zhao X, Dimitrijevic E, Dong VM (2009) J Am Chem Soc 131:3466–3467
31. Canty AJ, Jin H (1998) J Organomet Chem 565:135–140
32. Canty AJ, Jin H, Skelton BW, White AH (1998) Inorg Chem 37:3975–3981
33. Byers PK, Canty AJ, Crespo M, Puddephatt RJ, Scott JD (1988) Organometallics 7:1363–1367
34. Canty AJ, Denny MC, Patel J, Sun H, Skelton BW, White AH (2004) J Organomet Chem 689:672–677
35. Canty AJ, Done MC, Skelton BW, White AH (2001) Inorg Chem Commun 4:648–650
36. Canty AJ, Denney MC, Skelton BW, White AH (2004) Organometallics 23:1122–1131
37. Yamamoto Y, Ohno T, Itoh K (2002) Angew Chem Int Ed 41:3662–3665
38. Yamamoto Y, Kuwabara S, Matsuo S, Ohn T, Nishiyama H, Itoh K (2004) Organometallics 23:3898–3665
39. Dick AR, Kampf JW, Sanford MS (2005) J Am Chem Soc 127:12790–12791
40. Fu J, Li Z, Liang S, Guo Q, Lui L (2008) Organometallics 27:3736–3742
41. Racowski JM, Dick AR, Sanford MS (2009) J Am Chem Soc 131:10974–10983
42. Kalyani D, Dick AR, Anani WQ, Sanford MS (2006) Tetrahedron 62:11483–11498
43. Giri R, Chen X, Yu JQ (2005) Angew Chem Int Ed 44:2112–2115
44. Giri R, Chen X, Hao XS, Li JJ, Liang J, Fan ZP, Yu JQ (2005) Tetrahedron: Asymmetry 16:3502–3505.
45. Wan X, Ma Z, Li B, Zhang K, Cao S, Zhang S, Shi Z (2006) J Am Chem Soc 128:7416–7417
46. Mei TS, Giri R, Maugel N, Yu JQ (2008) Angew Chem Int Ed 47:5215–5212
47. Savitha G, Felix K, Perumal PT (2009) Synlett 2079–2082.
48. Bedford RB, Mitchell CJ, Webster RL (2010) Chem Commun 46:3095–3097
49. Fahey DR (1970) J Chem Soc Chem Commun: 417.
50. Hull KL, Anani WQ, Sanford MS (2006) J Am Chem Soc 128:7134–7135
51. Wang X, Mei TS, Yu JQ (2009) J Am Chem Soc 131:7520–7521
52. Michael FE, Sibbald PA, Cochran BM (2008) Org Lett 10:793–796
53. Doroski TA, Cox MR, Morgan JB (2009) Tetrahedron Lett 50:5162–5164
54. Lei A, Lu X, Liu G (2004) Tetrahedron Lett 45:1785–1788
55. Christie SDR, Warrington AD, Lunniss CJ (2009) Synthesis 148–154.
56. Manzoni MR, Zabawa TP, Kasi D, Chemler SR (2004) Organometallics 23:5618–5621
57. Wu T, Yin G, Lui G (2009) J Am Chem Soc 131:16354–16255
58. El-Qisairi AK, Henry PM (2000) J Organomet Chem 603:50–60
59. Kalyani D, Satterfield AD, Sanford MS (2010) J Am Chem Soc 138:8419–8427
60. Kalyani D, Sanford MS (2008) J Am Chem Soc 130:2150–2151
61. van Asselt R, Rijnberg E, Elsevier CJ (1994) Organometallics 13:706–720
62. Canty AJ, Hoare JL, Davies NW, Traill PR (1998) Organometallics 17:2046–2051
63. Canty AJ, Watson AA, Skelton BW, White AH (1989) J Organomet Chem 367:C25–C28
64. van Belzen R, Hoffmann H, Elsevier CJ (1997) Angew Chem Int Ed Engl 36:1743–1745
65. van Belzen R, Elsevier CJ, Dedieu A, Veldman N, Spek AL (2003) Organometallics 22:722–736
66. Shabashov D, Daugulis O (2010) J Am Chem Soc 132:3965–3972
67. Alsters PL, Engel PF, Hogerheide MP, Copijn M, Spek AL, van Koten G (1993) Organometallics 12:1831–1844
68. Lagunas MC, Gossage RA, Spek AL, van Koten G (1998) Organometallics 17:731–741
69. Vincente J, Chicote MT, Lagunas MC, Jones PG, Bembenek E (1994) Organometallics 13:1243–1250
70. Whitfield SR, Sanford MS (2007) J Am Chem Soc 129:15142–15143
71. Arnold PL, Sanford MS, Pearson SM (2009) J Am Chem Soc 131:13912–13913

72. Watson DA, Su MJ, Teverovskiy G, Zhang Y, Garcia-Fortanet J, Kinzel T, Buchwald SL (2009) Science 325:1661–1664
73. Grushin VV (2010) Acc Chem Res 43:160–171
74. Ball ND, Sanford MS (2009) J Am Chem Soc 131:3796–3797
75. Furuya T, Ritter T (2008) J Am Chem Soc 130:10060–10061
76. Furuya T, Ritter T (2008) J Am Chem Soc 130:12834
77. Furuya T, Benitez D, Tkatchouk E, Strom AE, Tang P, Goddard WA III, Ritter T (2010) J Am Chem Soc 132:3793–3807
78. Furuya T, Benitez D, Tkatchouk E, Strom AE, Tang P, Goddard WA III, Ritter T (2010) J Am Chem Soc 132:5922

Top Organomet Chem (2011) 35:85–110
DOI: 10.1007/978-3-642-17429-2_4

Palladium(IV) Complexes as Intermediates in Catalytic and Stoichiometric Cascade Sequences Providing Complex Carbocycles and Heterocycles

Helena C. Malinakova

Abstract Palladium-catalyzed multicomponent coupling and annulation reactions have become important tools in organic synthesis. Recently, palladium(IV) complexes have been proposed as intermediates in catalytic cycles of these transformations, although experimental evidence for their involvement is frequently lacking. Examples of such catalytic annulation reactions are discussed, followed by a review of studies performed with stoichiometric isolable or semistable palladium(IV) complexes seeking experimental evidence for feasibility of the participation of palladium(IV) intermediates in cascade carbon–carbon and carbon–heteroatom bond-forming sequences.

Keywords Annulation reaction · Oxidative addition · Palladacycle · Palladium(IV) complex

Contents

H.C. Malinakova
Department of Chemistry, The University of Kansas, Lawrence, KS 66045, USA
e-mail: hmalina@ku.edu

1 Introduction

A rapid construction of complex carbocyclic or heterocyclic frameworks constitutes one of the most challenging goals of synthetic organic chemistry. In recent years, palladium-catalyzed cascade reactions became recognized as a powerful tool in the construction of carbocycles and heterocycles due to the capability of palladium complexes to mediate sequential bisfunctionalization of one substrate creating multiple carbon–carbon or carbon–heteroatom bonds in one operation (Scheme 1) [1]. Advances in our fundamental understanding of the chemistry of palladium complexes in higher oxidation states have led to an ever increasing number of reports on palladium-catalyzed multicomponent annulation reactions in which palladium(IV) complexes were implicated as key catalytic intermediates. However, unequivocal experimental evidence for the involvement of palladium (IV) complexes in such transformations is often lacking.

Studies performed with stoichiometric palladium complexes have been frequently employed to explore feasibility of the individual steps of the catalytic cycles proposed for the novel catalytic annulation reactions. Herein, evolution of the sophistication of such palladium-catalyzed annulation protocols is demonstrated on selected examples, along with a discussion of the existing evidence for the participation of palladium(IV) complexes. Subsequently, studies performed with stoichiometric isolable or semistable palladium(IV) complexes seeking evidence for the involvement of well-defined palladium(IV) intermediates in analogous cascade carbon–carbon and carbon–heteroatom bond formations are discussed in detail.

2 Processes Catalytic in Palladium

One of the first palladium-catalyzed annulation protocols, in which the involvement of palladium(IV) intermediates had been proposed, was published by Dyker in the early 1990s. A homocoupling of *ortho*-iodoanisole afforded 6*H*-dibenzo[*b*,*d*]pyran, and a cross-coupling of *ortho*-iodoanisole with vinyl bromides provided benzo[*b*] furans (Scheme 2) [2, 3]. The mechanistic rationale put forward for these processes invoked an initial Csp^3–H activation induced by the palladium(II) center, followed by the formation of palladium(IV) intermediates via oxidative addition of aryl iodide or vinyl halide building blocks. Dyker's reports inspired synthetic chemists

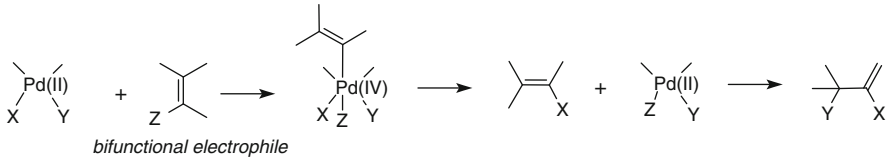

Scheme 1 Bisfunctionalization via a Pd(II)–Pd(IV) cycle

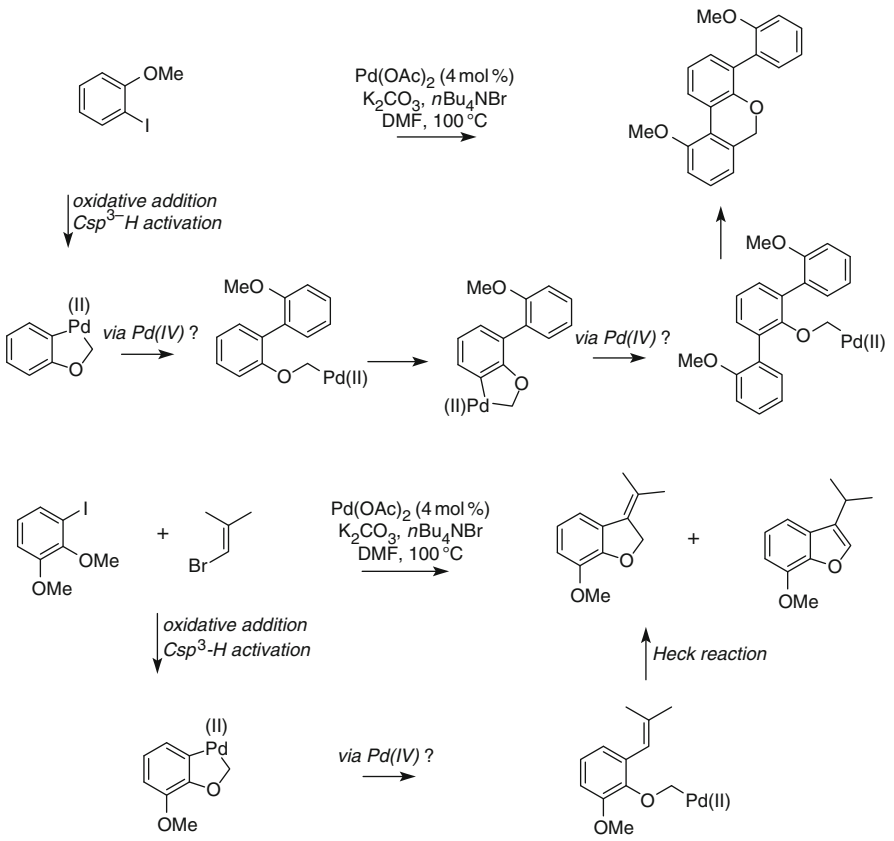

Scheme 2 Dyker's homocoupling and cross-coupling of two organohalides

to broaden their conceptual thinking about pathways that could be employed in palladium catalysis; however, the occurrence of palladium(IV) intermediates in these transformations had been questioned (*vide infra*).

A highly versatile palladium-catalyzed multicomponent coupling and annulation reaction proposed to feature palladium(IV) intermediates has been introduced by Catellani [4]. Since the original report, numerous variations on the key concept have been reported by Lautens and others [5, 6]. The process was rationalized by a catalytic cycle involving an initial oxidative addition to a palladium(0) complex followed by a migratory insertion of norbornene to form a palladium(II) complex, which was poised for an intramolecular C–H activation to form a pallada(II)cycle. The pallada(II)cycle then reacted with a second organohalide to form a palladium (IV) complex that underwent reductive elimination and migratory deinsertion of norbornene to form a new organopalladium(II) complex capable of participating in a variety of cascade-terminating carbon–carbon bond-forming steps that regenerated the palladium(0) form of the catalyst (Scheme 3). Most recent applications

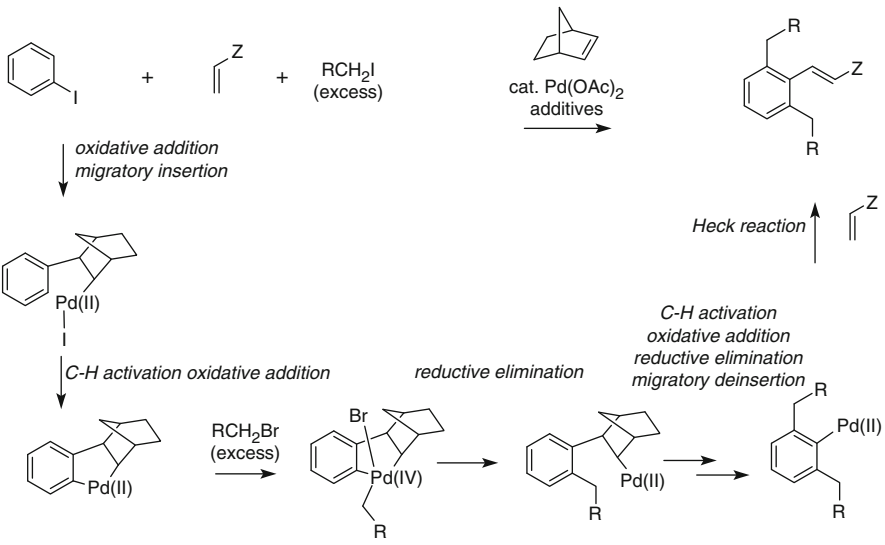

Scheme 3 Mechanism of Catellani's multicomponent norbornene-mediated annulations

of this concept in catalytic transformations reported by Lautens are shown in Scheme 4 [5, 6]. Catellani performed studies with stoichiometric palladium complexes that demonstrated the feasibility of the formation of the pallada(II) cycle incorporating norbornene, as well as the oxidative addition of an aliphatic organohalide to the pallada(II)cycle leading to the formation of a Csp^2–Csp^3 bond (*vide infra*).

The impressive chemoselectivity of the transformations shown in Scheme 4 relies on the fact that oxidative addition of aryl halides into palladium(0) complexes at ambient temperature is faster than oxidative addition of alkyl halides, as well as the demonstrated feasibility of oxidative addition of alkyl halides to palladium(II) complexes providing palladium(IV) intermediates [7].

An intriguing variation of Catellani's reaction accomplished a selective cross-coupling of two different aryl halides and methyl acrylate (Scheme 5) [8, 9]. It was suggested that a difference in the rates of oxidative additions of the two differentially substituted aryl halides with the palladium(0) and the palladium(II) complexes accounted for the reported reactivity. However, the mechanistic rationale invoking palladium(IV) intermediates have not been supported by either an experiment or computations.

Recently, mechanistic and computational studies aiming to establish whether organic electrophiles bearing halides on a sp^2-hybridized carbon could indeed undergo an oxidative addition leading to palladium(IV) complexes, and to uncover alternative pathways that could account for the formation of the observed products, have appeared in the literature. In a representative study, Echavarren reported DFT calculations comparing the feasibility of a direct oxidative addition of vinyl halides to pallada(II)cycles analogous to those proposed in Dyker's and Catellani's

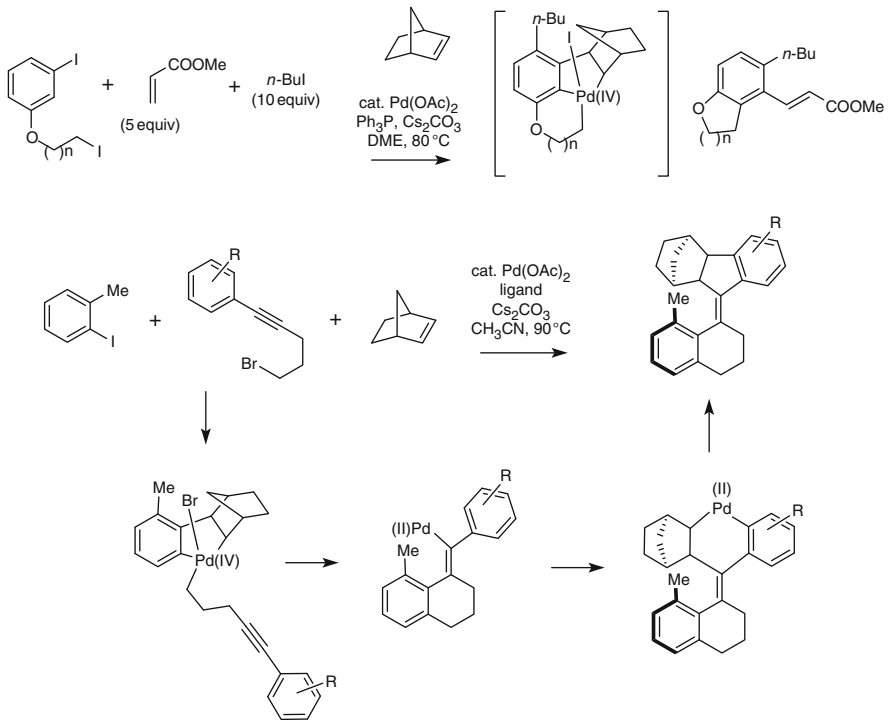

Scheme 4 Applications of the norbornene-mediated annulation developed by Lautens

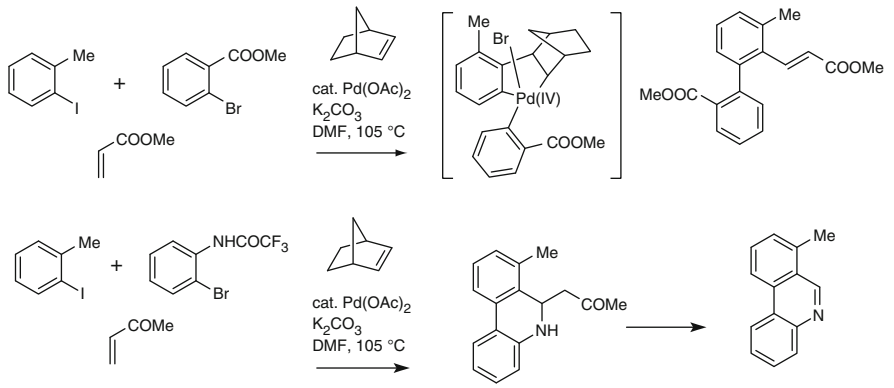

Scheme 5 Cross-coupling variants of Catellani's norbornene-mediated annulation

reactions, with an alternative pathway involving Pd–Pd transmetalation, e.g., an aryl transfer between two palladium(II) centers (Scheme 6) [10]. The study concluded that an easy formation of bridged dinuclear complexes allows for a facile intramolecular transmetalation of organic ligands between two palladium(II) centers. For organic electrophiles featuring Csp^2–halide bonds, the transmetalation

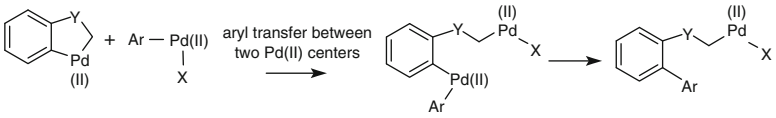

Scheme 6 Aryl transfer between two Pd(II) centers

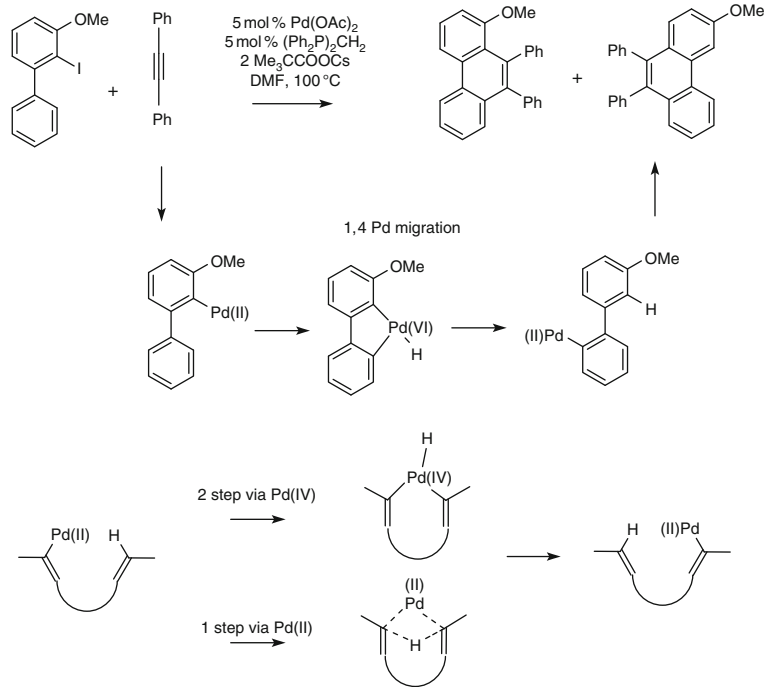

Scheme 7 Larock's bisfunctionalization of alkynes and its possible mechanistic pathways

process was found to be significantly more favorable than the formation of palladium(IV) intermediates that were found to possess relatively higher energies.

Larock reported a palladium-catalyzed annulation reaction that effectively achieves a bisfunctionalization of a symmetrical alkyne with *ortho*-iodobiaryls (Scheme 7) [11]. The transformation has been proposed to involve a 1,4-palladium (II) migration featuring an unprecedented hydridopallada(IV)cycle (Scheme 7). To date no experimental evidence is available to confirm the involvement of palladium (IV) intermediates in this process. The catalytic process inspired a computational study on the mechanism of 1,*n*-palladium migrations in aromatic hydrocarbons. The study assessed feasibility of competitive palladium(II) and palladium(IV) pathways [12] and concluded that in the 1,4-migration relevant to Larock's annulation, the palladium(IV) and palladium(II) mechanisms (Scheme 7) become competitive.

Novel palladium-catalyzed cross-coupling/annulation sequences performed under oxidative conditions have been designed to construct complex nitrogen-containing heterocycles (Schemes 8 and 9). The reaction reported by Li achieved an intra/intermolecular bisfunctionalization of a propargyl amide with an arene and phthalimide [13]. The proposed catalytic cycle involves an intermolecular amino-palladation of the alkyne mediated by a palladium(II) complex. The resulting palladium(II) intermediate is then oxidized to a palladium(IV) complex by the PhI $(OAc)_2$ oxidant. Subsequent intramolecular electrophilic palladation of the aromatic ring by the palladium(IV) complex gives a palladium(IV) metalacycle that forms the organic product via reductive elimination. However, a precise timing for the palladium(II) to palladium(IV) oxidation could not be established, and an oxidation to palladium(IV) might be occurring after the electrophilic aromatic palladation. Furthermore, an alternative sequence of the elemental steps starting with electrophilic palladation of the aromatic ring and followed by an intramolecular carbopalladation, oxidation to palladium(IV), and terminated by the C–N coupling could not be ruled out. Prior studies by others on the palladium-catalyzed oxidative bisamination reactions [14] and aminoacetoxylation [15] laid the foundation for the mechanistic proposals described above.

In a recent variant on this process reported by Michael [16], a palladium(II)-mediated intramolecular aminopalladation is followed by an oxidation of the palladium(II) intermediate by the $FN(SO_2Ph)_2$ oxidant to give a palladium(IV) complex. The palladium(IV) complex then mediates an intermolecular electrophilic aromatic substitution followed by C–C bond formation via reductive elimination (Scheme 9).

The selected examples of palladium-catalyzed annulation reactions discussed herein highlight the synthetic potential of catalytic processes proposed to feature palladium intermediates in higher oxidation states in the construction of complex carbocyclic and heterocyclic systems.

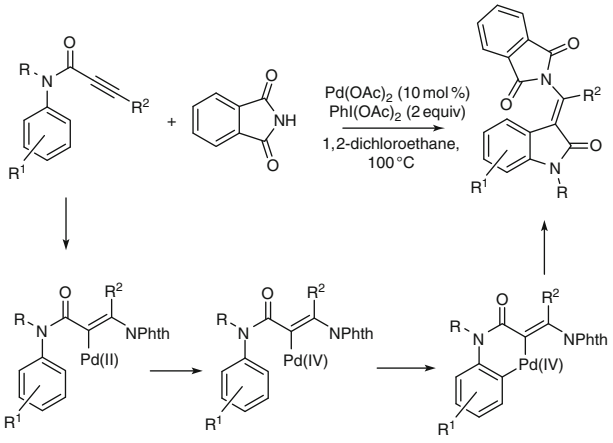

Scheme 8 Sequential C–N/C–C bisfunctionalization of alkynes under oxidative conditions

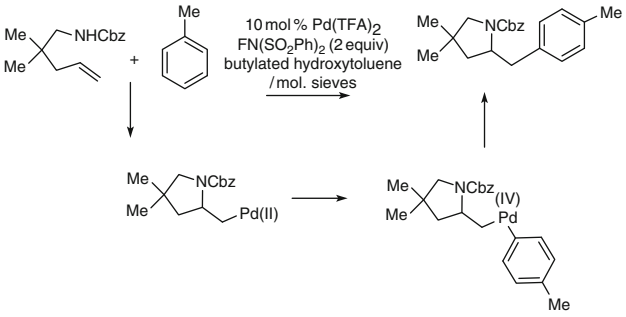

Scheme 9 Sequential C–N/C–C bisfunctionalization of alkenes under oxidative conditions

3 Processes Stoichiometric in Palladium

3.1 Oxidative Addition Reactions of Palladacyclopentanes

Herein, investigations of the synthesis, structure, and reactivity of stoichiometric palladium(IV) complexes, aiming to provide relevant insights into the mechanism of the catalytic annulation protocols described above, are discussed. Palladium(II) complexes featuring two carbon–palladium bonds constitute a logical starting point for exploring oxidative transformations that form two new carbon–carbon or carbon–heteroatom bonds in a tandem fashion via intermediates possessing palladium in higher oxidation states (Scheme 10). The presence of the two carbon–palladium(II) bonds within a single bidentate ligand comprising a five-membered ring stabilizes the resulting pallada(II)cycles, rendering them ideal templates for stoichiometric studies.

A seminal exploration of decomposition pathways of pallada(II)cyclopentanes in the presence of organic oxidants was published by Canty [17]. In particular, studies on the reactivity of pallada(II)cyclopentanes with allylic halides opened up an opportunity for future design of annulation protocols. Canty synthesized allyl palladium(IV) complex $PdBrC_4H_8(CH_2CH{=}CH_2)(bpy)$ via oxidative addition of allyl bromide to pallada(II)cyclopentane (L–L = bipyridine) (Scheme 10). The palladium(IV) complex proved to be stable in solution at room temperature and was characterized by ^1H NMR spectroscopy and elemental analysis. A single stereoisomer shown in Scheme 11 was formed as indicated by the ^1H NMR analysis. However, X-ray crystallographic data could not be secured. Decomposition of the allylpalladium(IV) complex in $CDCl_3$ solution afforded 88% of cyclobutane and less than 12% of butanes and propenes. The allyl ligand was recovered bonded to palladium in the form of the $Pd(II)(CH_2CH{=}CH_2)(bpy)Br$ complex (Scheme 11).

In the same report, a mechanism for the reductive decomposition of a series of palladium(IV) complexes bearing diverse R groups (R = Me, Et, Bn, Scheme 10) was proposed. An initial halide dissociation from the palladium(IV) complex and isomerization was proposed, followed by the development of an agostic interaction of a C–H

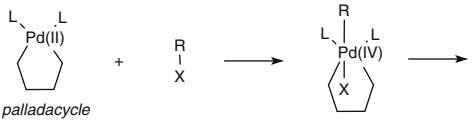

Scheme 10 Oxidation of pallada(II)cycles with organic oxidants – a general outline

Scheme 11 Allylpalladium (IV) complex prepared by Canty

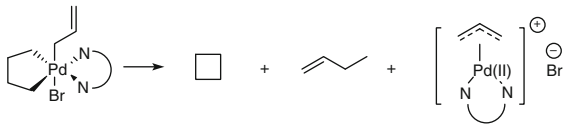

bond from the R group in an equatorial position to the palladium(IV) center, while the cyclobutane ligand occupies the apical and equatorial positions. These steps were proposed to precede the carbon–carbon bond-forming reductive elimination. The lack of the carbon–carbon bond-forming reductive elimination between the cyclobutane ligand and the allyl ligand has been rationalized by the inability of the allyl ligand to form a C–H agostic interaction with the palladium center after the departure of the halide, possibly due to the preference for the η^3-bonding of the allyl complex. In a related study on the reactivity of an allylpalladium(IV) complex $Me_2Pd(CH_2CH{=}CH_2)Br(bpy)$, the formation of $Pd(II)(\eta^3\text{-}CH_2CH{=}CH_2)Br$ was also favored over carbon–carbon bond-forming processes [18, 19].

3.2 *Synthesis of 1,3-Dienes from Palladacyclopentadienes*

Elsevier prepared functionalized 1,3-dienes from stable isolated pallada(II) cyclopentadiene and organohalides (R^1X) via a proposed oxidation yielding palladium(IV) complexes as unstable intermediates, which underwent a rapid reductive elimination forming a new carbon–carbon bond. A subsequent cross-coupling reaction of the stable palladium(II) complexes with organostannanes $(R^2)_4Sn$ (Scheme 12) afforded the 1,3-dienes [20]. No spectroscopic evidence

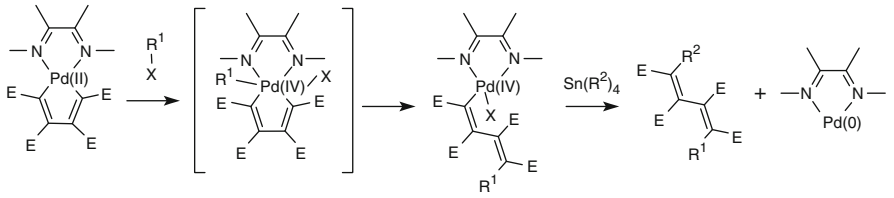

Scheme 12 Synthetic application of pallada(II)cyclopentadienes – a stepwise stoichiometric protocol

for the involvement of the proposed palladium(IV) complexes have been secured, although the formation of the corresponding palladium(II)dienehalide complex has been confirmed for reactions with MeI, BnBr, and PhI. In the light of evidence discussed above in the context of the catalytic processes, the involvement of the palladium(IV) complexes in the reactions with PhI seems doubtful [10].

The study emphasized the importance of the rigid bidentate amine ligands in facilitating the oxidative addition reactions providing the presumed palladium (IV) intermediates, noting that analogous reactions with complexes bearing phosphine ligands failed. Taking advantage of the fact that oxidative addition of the alkyl halide to the pallada(II)cyclopentadiene is strongly favored over the oxidative addition of the organohalide to palladium(II)dienehalide, a catalytic variant of the three-component coupling of RI, $RSnBu_3$, and EtOC(O)C≡CC(O)OEt has been successfully demonstrated [20]. In a most recent study, Elsevier investigated the mechanistic details of the oxidative addition/reductive elimination sequence of his pallada(II)cyclopentadienes bearing rigid bidentate nitrogen ligands with molecular halogens [21]. The authors recorded a low temperature ^{1}H NMR spectra on a red complex precipitated at low temperature from the reaction of the pallada(II)cyclopentadiene with bromide. The spectral features supported the proposed structure of the palladium(IV) complex featuring the two bromines in the apical positions and therefore possessing C_{2v} symmetry. At higher temperatures, the complex converts into a butadienyl palladium(II) complex with a new Csp^2–Br bond. The complex was characterized by X-ray crystallography; DFT-B3LYP calculations confirmed the feasibility of the proposed pathway.

3.3 Norbornene-Derived Palladacycles

Catellani has supported the mechanism proposed for her unique palladium-catalyzed and norbornene-mediated catalytic cascade protocols (Scheme 3) by the preparation of stable pallada(II)cycles incorporating the norbornene scaffold and rigid phenanthroline ligands. The pallada(II)cycle was reacted with *p*-nitrobenzyl bromide to give rise to a new complex, which is believed to represent the palladium (IV) intermediate. The complex was stable in solution for several hours and slowly underwent a regioselective transformation into the palladium(II) bromide complex featuring a new aryl–benzyl bond (Scheme 13) [22]. The new palladium(II) bromide complex was isolated and fully characterized by X-ray crystallography. The presumed palladium(IV) intermediate has been assigned the structure including the stereochemistry as shown in Scheme 13 on the basis of the ^{1}H NMR spectroscopic data, including data from NOE experiments, and considerations of the ring current effects caused by the phenanthroline rings. The authors pointed out that reductive elimination from the octahedral palladium(IV) intermediate proceeded with a complete regioselectivity, favoring the formation of a new Csp^3–Csp^2 bond.

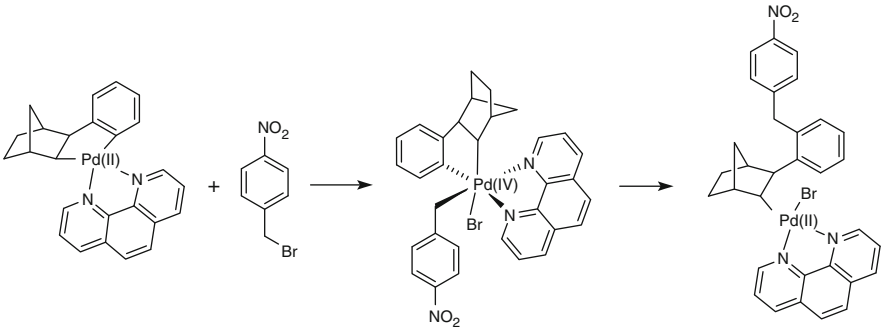

Scheme 13 Intermediate isolated from a stoichiometric variant of Catellani's reaction

It was noted that shielding caused by the phenanthroline ligand might have prevented the alkyl migration toward the norbornane ring. In agreement with earlier observations by Canty, halide dissociation was proposed to occur prior to a rearrangement of the complex allowing for the reductive elimination to occur between groups in an equatorial–axial arrangement with respect to the plane defined by palladium and the phenanthroline ligand. However, experimental evidence for the detailed mechanism of reductive elimination has not been provided.

In a recent mechanistic study, Catellani investigated the kinetics of the oxidative addition of benzyl halides to norbornene-derived pallada(II)cycles via electrochemical techniques [23]. Kinetic measurements indicated that the oxidative addition was first order with respect to both the pallada(II)cycle and the benzyl bromide, and the oxidative addition of benzyl bromide ($k_1Br = 3.6\ M^{-1}\ s^{-1}$, DMF, 29 °C) was 600 times faster than the oxidative addition of benzyl chloride (6×10^{-3}, $M^{-1}s^{-1}$, DMF 29 °C), both features being consistent with S_N2-like mechanism. The rate constant for a slow subsequent reductive elimination ($6(\pm)1 \times 10^{-4}\ s^{-1}$, DMF, 29 °C) converting the palladium(IV) complex into the palladium(II) bromide complex was found to be zero order with respect to the concentration of benzyl bromide. The data are in agreement with the mechanism proposed above, but this study did not shed more light on the nature of the rearrangements of the ligand sphere prior to reductive elimination. The authors concluded that alternative mechanistic pathways lacking palladium(IV) intermediates were likely to operate when phenyl iodide was used as the organic electrophile in these transformations.

Norbornene has also been utilized in a one-step construction of C2-symmetrical pallada(IV)spirocycle complexes featuring one palladium(IV)–Csp^3 bond and one palladium(IV)–O bond in each palladacyclic ring (Scheme 14) [24]. Oxidative cyclization of norbornene or benzonorbornadiene with chloranil and $Pd_2(dba)_3$ (dba = dibenzylideneacetone) afforded new palladium(IV) complexes bearing various Lewis basic ligands (L = pyridine, THF, and diethyl ether). Selected complexes were characterized by X-ray crystallography. Notably, these palladium (IV) complexes proved to be stable for prolonged periods of time at room temperature, both in the solid state and in solution. The complexes decomposed upon

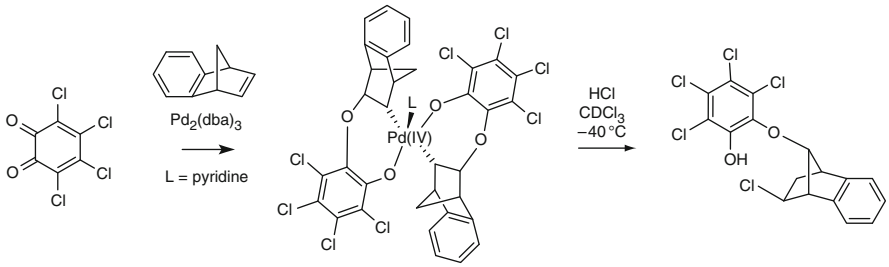

Scheme 14 Synthesis of a pallada(IV)spirocycle

heating in solution or upon treatment with an acid, producing mixtures of products, some of which resulted from the carbon–oxygen coupling between the norbornene and chloranil ligands (Scheme 14).

3.4 Synthesis of Benzoxepines, Benzopyrans, and Benzofurans from Oxapalladacycles

3.4.1 Intermediates on the Pathway from Oxapalladacycles to Benzoxepines, Benzopyrans, and Benzofurans

Studies described above highlighted the potential of pallada(II)cyclopentanes to participate in oxidative annulation protocols, assuming that suitable biselectrophilic organic oxidants could be identified (Schemes 1 and 10). This concept motivated systematic explorations of the reactivity of stable functionalized oxapallada(II) cyclopentanes with bifunctional electrophiles in the author's laboratory [25, 26]. Oxapallada(II)cycles possessing both sp^2-hybridized and sp^3-hybridized carbons bonded to palladium have been constructed with the goal to elucidate the effect of hybridization and substitution at the palladium-bonded carbons in the presumed palladium(IV) intermediates. A sequence of oxidative addition of palladium(0) complex ($Pd_2(dba)_3$) to an aryl iodide in the presence of bidentate ligands bearing nitrogen heteroatoms (*N,N,N′N′*-tetramethylethylenediamine, *N,N′*-dicyclohexylethylenediimine, or bipyridine) followed by base-mediated intramolecular displacement of the iodide at the palladium(II) center afforded the corresponding oxapallada(II)cycles as stable solids (Scheme 15). Various additional ligands, including monodentate and bidentate phosphines, could be introduced to the oxapallada(II)cycles via an exchange for the *N,N,N′N′*-tetramethylethylenediamine ligand. Oxapallada(II)cycles featuring auxiliary ligands with tight five-membered chelate rings with two nitrogen or two phosphorus (diphenylphosphinoethane) atoms were stable both in solution and as solids. An increase in the chelate size (diphenylphosphinobutane), the presence of two monodentate phosphine ligands, or an increase in the steric bulk at the palladium(II)-bonded sp^3-hybridized carbon

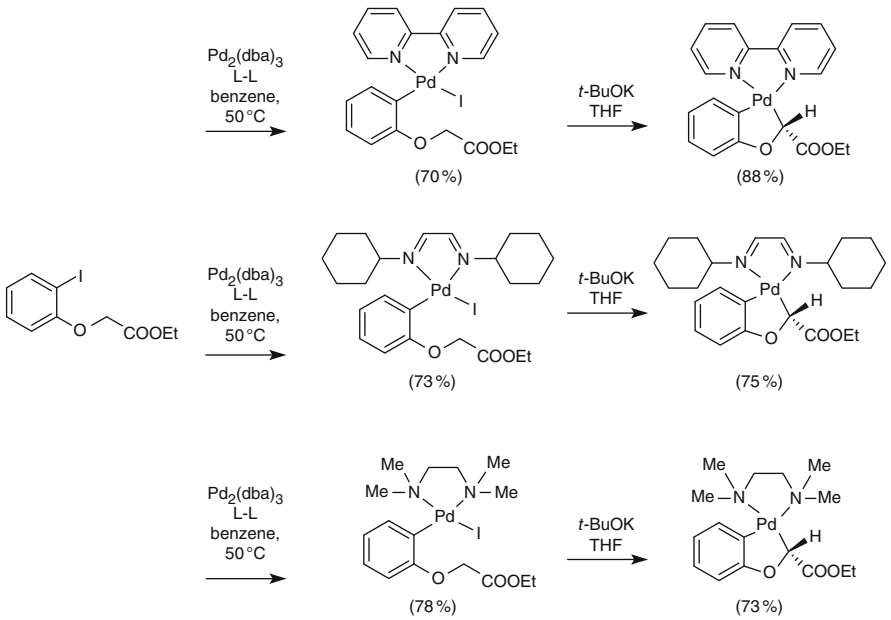

Scheme 15 Preparation of oxapallada(II)cycles

arising from branching of the carbon chain at that position notably diminishes the stability of the oxapallada(II)cycles [27]. X-ray crystallographic analyses revealed that the oxapallada(II)cycles possessed undistorted square planar coordination spheres and differed in the extent of shielding of the space above and below the square planar coordination spheres caused by different ligands (Fig. 1).

Next, oxapallada(II)cycles were reacted with a series of organic electrophiles possessing two electrophilic centers, including a carbon-bonded leaving group and a double bond. It was anticipated that an annulation reaction would occur and realize an effective bisfunctionalization of the organic electrophile with the organic fragment present in the oxapallada(II)cycles (Schemes 1 and 10). The appropriate organic oxidants would be capable of generating a palladium(IV) complex, which would then undergo a reductive elimination generating palladium(II) intermediates that would engage the second reactive functionality in the electrophile to complete the annulation process and release a palladium(0) complex.

Initially, the reactivity of oxapallada(II)cycles bearing *N*,*N*,*N*′,*N*′-tetramethylethylenediamine, 2,2′-bipyridine, *N*,*N*′-dicyclohexylethylenenediimine, 1,2-bis(diphenylphosphino)ethane, and two triphenylphosphine auxiliary ligands with a series of potential bifunctional electrophiles including acroyl chloride, allyl bromide, 3-iodo-2,3-cyclohexenone, 2-iodo-1,2-cyclohexene, vinyl(phenyl)iodonium tetrafluoroborates, and 4-methyl-1-pentyne-1yl(phenyl)iodonium tetrafluoroborate was screened. No reaction was detected when oxapallada(II)cycles were treated with the vinyl halides, and no isolable products were formed from the reactions of oxapalla(II)cycles bearing monodetante or bidentate phosphine ligands with any of

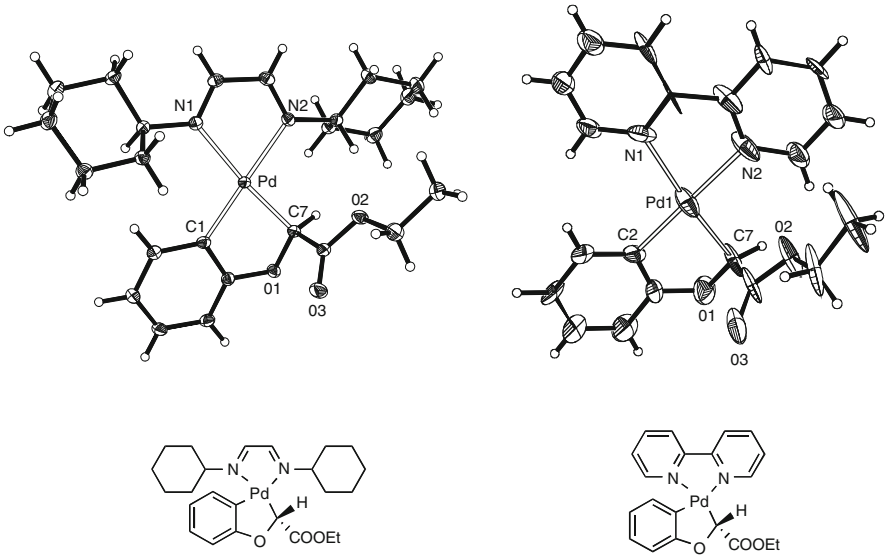

Fig. 1 Molecular structures of palladacycles established by X-ray crystallography

the electrophiles. In contrast, acroyl chloride, allyl bromide, and the hypervalent iodonium salts converted the oxapallada(II)cycles bearing the 2,2′-bipyridine or ethylenediimine ligands either into new palladium(II) complexes or into isolable heterocycles, including a benzoxepine (from acroyl chloride), a benzopyran (from allyl bromide), and benzofurans (from the vinyl and alkynyl iodonium salts). Detailed investigations of the reactions between oxapallada(II)cycles and allyl bromides and vinyl and alkynyl(phenyl)iodonium salts are discussed herein.

Oxapallada(II)cycle **1a** featuring *N*,*N*′-dicyclohexylethylenediimine ligand reacted more rapidly with substituted allyl bromides than the oxapallada(II)cycle **1b** bearing the 2,2′-bipyridine ligand. The reactions afforded racemic heterocycles **2a,b**, **3a,b**, and **4** in a single step (Scheme 16) [25]. Notably, in contrast to the report by Canty [17], the allyl fragment did engage in the carbon–carbon bond-forming reactions. Two equivalents of the allylic electrophiles were incorporated into the annulation products via an additional functionalization of a Csp^2–H bond in the aromatic rings. Bases, additives, and elevated temperatures (80–100 °C), either in solution (6–10 equiv of allyl bromides, 1,2-dichloroethane, or acetonitrile) or in neat allyl bromide, were employed to facilitate the intramolecular cyclization. Results summarized in Scheme 16 demonstrate how the substitution pattern in the allyl bromides controls the cyclization mode switching from an unexpected 7-endo-trig cyclization to 6-exo-trig cyclization with more substituted allyl bromides. Palladium was recovered as palladium(II) dibromide and as a bisallylpalladium(II) complex from reactions run in neat allyl bromides (Scheme 16), as confirmed by X-ray crystallographic analyses of the recovered palladium complexes.

When both the oxapallada(II)cycles **1a** and **1b** were reacted with 1-octenyl(phenyl)iodonium tetrafluoroborate at room temperature in 1,2-dichloroethane,

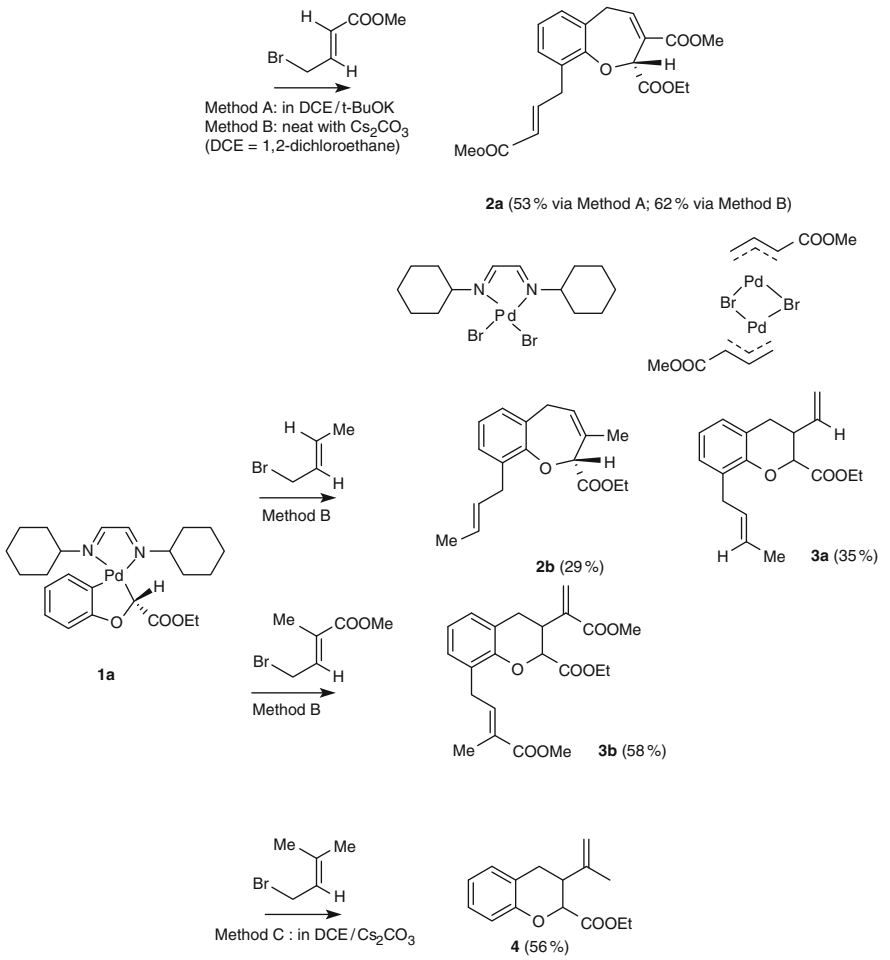

Scheme 16 Reactions of oxapallada(II)cycle **1a** with allyl bromides

benzofuran **5a** was formed. The reaction with oxapallada(II)cycle **1b** afforded the best result providing benzofuran **5a** in 74% yield lacking an undesired benzofuran by-product arising from a decarboxylation (Scheme 17) [26]. The treatment of oxapallada(II)cycle **1b** with functionalized vinyl(phenyl)iodonium salts bearing a phenyl and 4-methyl-1-pentyne-1-yl functional group and with an alkynyl(phenyl) iodonium salt (4-methyl-1-pentyne-1-yl(phenyl)iodonium tetrafluoroborate) caused a rapid consumption of the oxapallada(II)cycle at ambient temperature (for vinyl iodonium salts) or at 0 °C (for alkynyl iodonium salt), but anticipated heterocyclic products could not be detected. To facilitate the ring-closing via the intramolecular Heck-type migratory insertion reaction, suitable additives had to be added. Employing a mixture of PPh_3, Bu_4NCl and triethylamine, 3-benzyl-substituted benzofuran **5b**, and a mixture of two benzofurans **5c** and **6** bearing the alkynyl substituent were

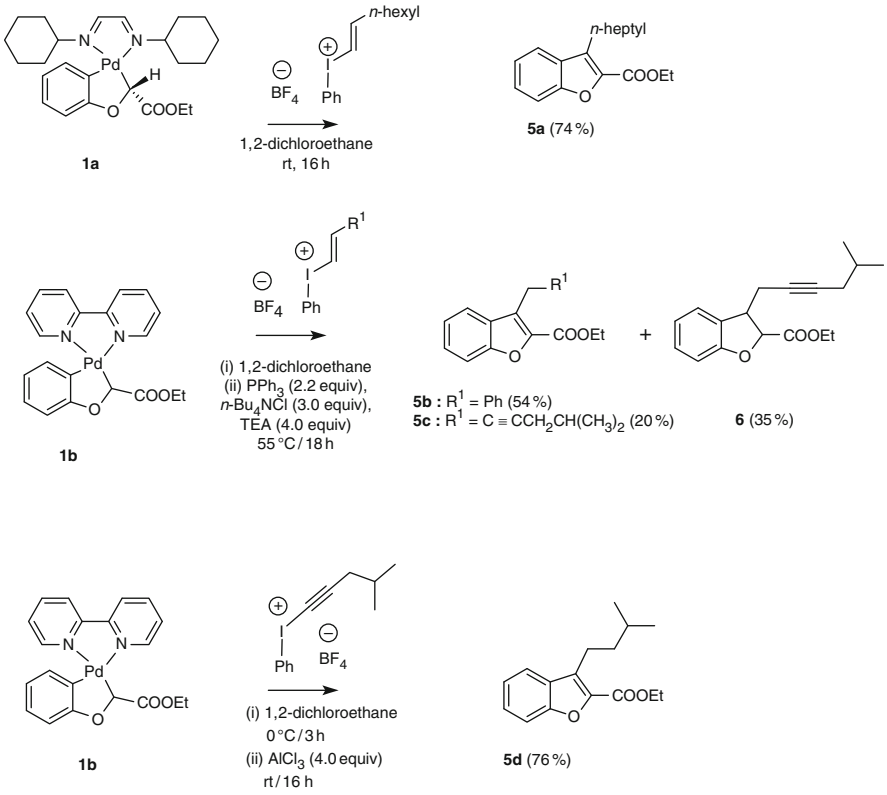

Scheme 17 Reactions of oxapallada(II)cycles **1a** and **1b** with vinyl- and alkynyl(phenyl)iodonium salts

obtained (Scheme 17) [26]. The desired annulation reaction of oxapallada(II)cycle **1b** with alkynyl iodonium salt was achieved by the addition of Lewis acids ($AlCl_3$) to a second stage of a one-pot/two-step protocol, providing benzofuran **5d** (Scheme 17). At the completion of reactions with 1-*n*-octene-yl(phenyl)iodonium tetrafluoroborates, palladium was recovered as a black precipitate of Pd(0). Mixtures of poorly soluble complexes of palladium were isolated from reactions employing the sequential addition of additives.

The outcome of these annulation reactions could be rationalized by a Pd(II)–Pd(IV)–Pd(II)–Pd(0) cycle consisting of oxidative addition giving palladium(IV) complexes (highlighted in Scheme 18) followed by reductive elimination and intramolecular 6-exo or 7-endo or 5-exo Heck reactions. Incorporation of two equivalents of the allyl into the annulation products suggests the involvement of two distinct palladium(IV) complexes (Scheme 18), the second one arising via an intramolecular palladation of the aromatic ring followed by an oxidative addition of a second equivalent of the allyl bromide.

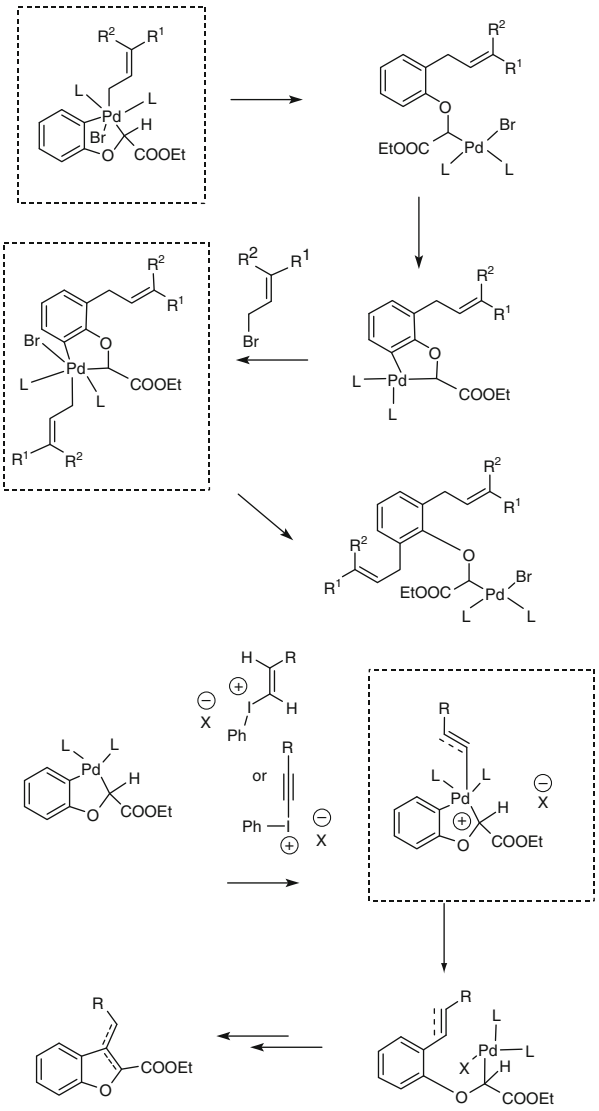

Scheme 18 Proposed intermediates in the reactions of oxapallada(II)cycles with allyl halides and vinyl- and alkynyl(phenyl)iodonium salts

The main goal of these studies was isolation and characterization of organopalladium intermediates present on the pathway from oxapallada(II)cycles to the heterocyclic products. When the reaction of oxapallada(II)cycle **1a** with neat methyl 4-bromo-2-butenoate was performed at decreased temperature (45 °C) for a limited time period (30 min), a new palladium(II) complex **7a** was isolated, and its structure was fully assigned via X-ray crystallographic analysis (Scheme 19). Reacting

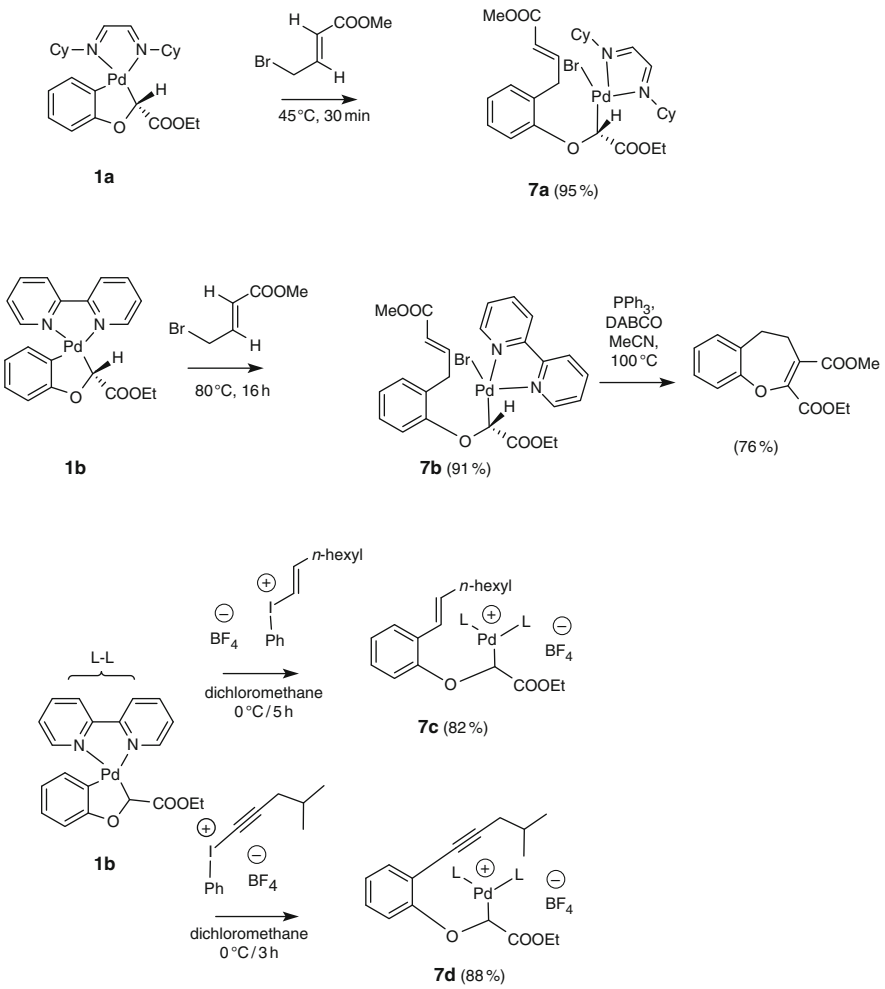

Scheme 19 Stable organopalladium(II) intermediates isolated from the reactions of oxapallada (II)cycles **1a** and **1b** with allyl halides and vinyl- and alkynyl(phenyl)iodonium salts

oxapallada(II)cycle **1a** with neat methyl 4-bromo-2-butenoate under the same conditions but for an extended time (45 °C, 20 h) afforded benzoxepine **2a** [25].

Oxapallada(II)cycle **1b** bearing the planar and more rigid 2,2′-bipyridine ligand reacted more slowly with methyl 4-bromo-2-butenoate (2.0 equiv, 16 h, 80 °C) to afford a stable and robust arylpalladium(II) bromo complex **7b** (Scheme 19), the molecular structure of which was confirmed by X-ray crystallography. The conversion of complex **7b** into a new benzoxepine via an intramolecular 7-endo-trig Heck cyclization required additives (PPh_3, DABCO) and rather strenuous conditions (MeCN, 100 °C). Despite the loss of the stereogenic

center in the benzoxepine product via a double bond isomerization, the high-yielding formation of benzoxepine demonstrates that complex **7b** engages in the reaction steps analogous to those occurring from the more labile complex **7a** and leading to the benzoxepine and benzopyran products described in Scheme 15 (*vide supra*). As anticipated, reactions of palladacycle **1b** with the more reactive vinyl iodonium salt or an alkynyl iodonium salt (Scheme 19) had to be performed at lower temperatures (0 °C, 3–5 h) to allow for isolation of the corresponding cationic palladium(II) complexes **7c** and **7d** as solids via precipitation from cold solutions in dichloromethane with diethyl ether [26]. Cationic complexes **7c** and **7d** were fully characterized via ^{1}H and ^{13}C NMR spectroscopic techniques. In all cases, the new carbon–carbon bond formation occurred between the sp^2-hybridized carbon of the aromatic ring and the allylic sp^3-hybrizidized, the sp^2-hybridized, or the *sp*-hybridized carbon originating from the vinylic or the alkynyl oxidant.

3.4.2 Spectroscopic and Crystallograhic Characterization of the Palladium(IV) Intermediates

Isolation and full characterization of the palladium(IV) complexes formed en route from palladacycles **1** to palladium(II) complexes **7** would constitute a key piece of evidence for the mechanism of the annulation reaction proposed in Scheme 18. Although several palladium(IV) complexes bearing three carbon–palladium bonds have been characterized by X-ray crystallography [28], the isolation and characterization of intermediates capable of productive, complexity increasing carbon–carbon bond-forming reactions remain rare [29, 30]. The challenge of this undertaking consists in the selection of appropriate auxiliary ligands that would provide sufficient stabilization to the reactive palladium(IV) intermediates, but at the same time permit the entire annulation sequence to proceed.

Aiming to provide spectroscopic evidence for the formation of the putative palladium(IV) intermediate, *in situ* monitoring of the reaction between palladacycle **1b** and (*E*)-1-octenyl(phenyl)iodonium tetrafluoroborate in 1:1.1 molar ratio was performed utilizing low temperature ^{1}H NMR (400 MHz) spectroscopy [26]. Experiments conducted at –10 °C indicated an immediate formation of a 1:1 mixture of complex **7c** with a new organopalladium intermediate distinct from the palladacycle **1b**. A complete clean conversion of the new intermediate, tentatively assigned the structure of organopalladium(IV) complex **8** (Fig. 2), into complex **7c** occurred within 1 h at –10 °C. Subsequently, the temperature for the reaction monitoring experiment was lowered to −50 °C (Fig. 2). Under these conditions, palladacycle **1b** (trace a, Fig. 2) was again immediately converted into an intermediate identical to the complex detected at −10 °C and distinct from the complex **7c** (trace d, Fig. 2). The putative complex **8** proved to be stable in solution at temperatures −50 °C to −40 °C, and an ^{1}H NMR spectra of an essentially pure (contains phenyl iodide) complex **8** was recorded (trace b, Fig. 2). The first signals indicating the conversion of complex **8** into the “open

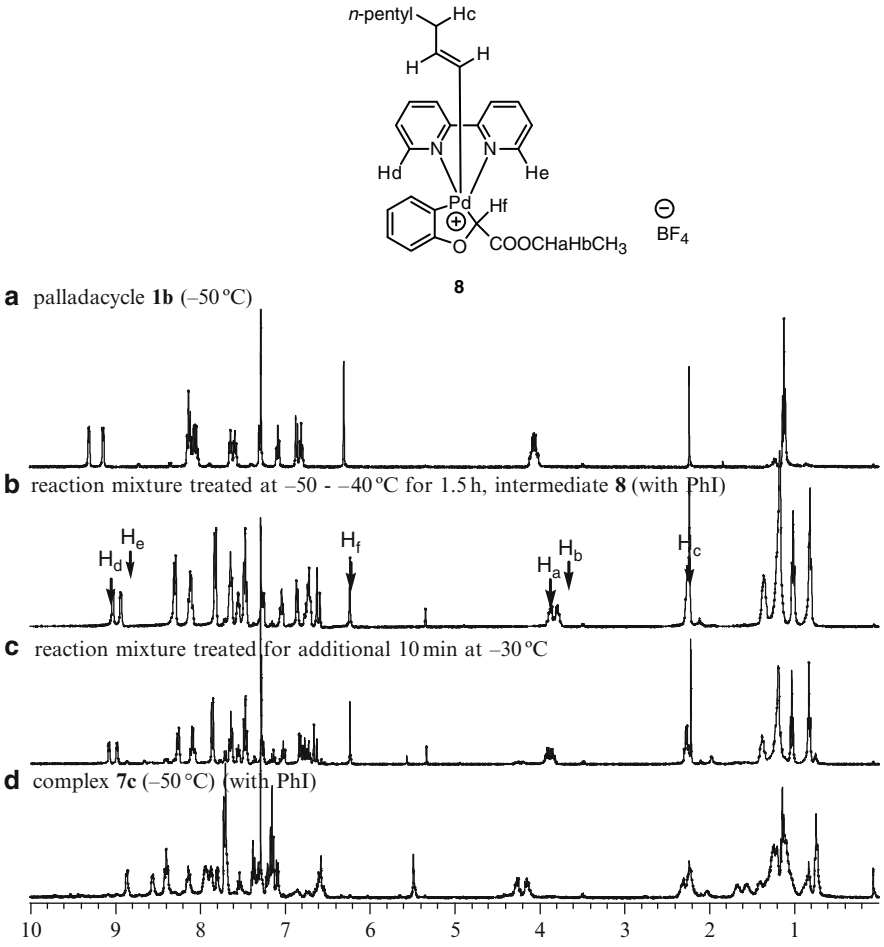

Fig. 2 Low-temperature ^{1}H NMR (400 MHz, $CDCl_3$) monitoring of the reaction between palladacycle **1a** and (*E*)-1-octenyl(phenyl)iodonium tetrafluoroborate

form" complex **7c** were detected following the treatment of the reaction mixture for 10 min at –30 °C (trace c, Fig. 2). The proposed structure of the intermediate **8** is further supported by the observation of the characteristic signals for protons labeled Ha–Hf in the structure of complex **8** in ^{1}H NMR spectra of the intermediate (trace b in Fig. 2).

However, all attempts at low temperature crystallization of the cationic complex **8**, or an exchange of the tetrafluoroborate for iodide anticipating the formation of a stabilized octahedral complex that could be isolated as a solid, proved to be unsuccessful [26].

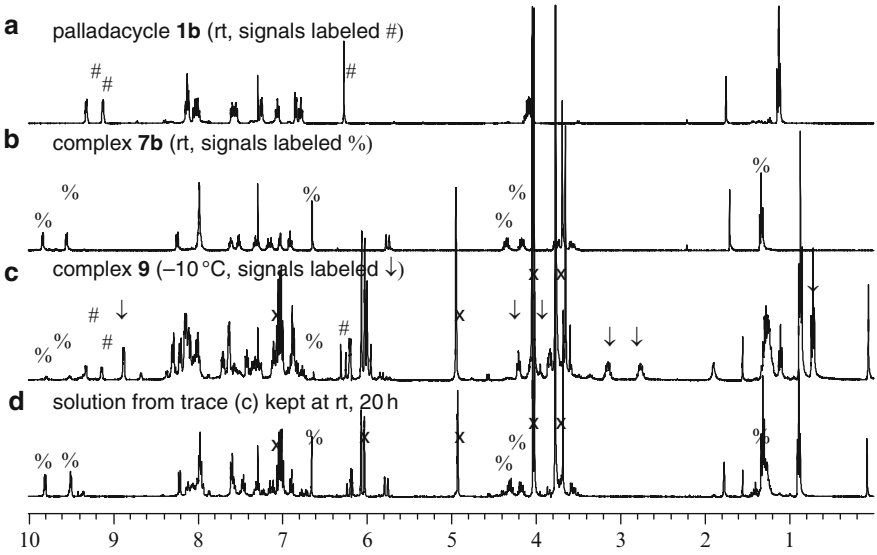

Fig. 3 ^{1}H NMR (400 MHz, $CDCl_3$) of substrates and intermediates en route from **1b**

In a similar manner, oxapallada(II)cycle **1b** bearing the rigid and therefore stabilizing bipyridine ligand was chosen for ^{1}H NMR monitoring experiments aiming to detect and isolate the presumed palladium(IV) intermediate that might operate en route from palladacycle **1b** to complex **7b** [25]. Thus, palladacycle **1b** was treated with neat methyl-4-bromo 2-butenoate at 0 °C (8.5 h) during which time a cloudy solution turned clear. Precipitation with pentane and a solvent decantation performed rapidly at –10 °C afforded a yellow solid, the ^{1}H NMR spectrum of which was recorded at –10 °C (see trace c in Fig. 3). In addition to indicative signals for the remaining palladacycle **1b** (labeled # in traces a and c, Fig. 3) and the emerging "open form" **7b** (labeled % in traces b and c, Fig. 3), as well as residual signals for allylic bromide and/or alcohol (labeled x in trace c), signals (labeled ↓) indicating the presence of a significant concentration of a distinct palladium complex containing the allyl substituent ($CH_2CH{=}CHCO_2Me$) were detected (compare traces a, b and c, Fig. 3). On standing at room temperature, the $CDCl_3$ solution of the yellow solid (shown in trace c, Fig. 3) was cleanly converted to a solution of complex **7b** (compare the spectral traces b, c, and d, Fig. 3). The key ^{1}H NMR signals (labeled ↓ in trace c, Fig. 3) were assigned as follows: proton at 6.02 ppm (s, 1 H) as OC**Ha**(COOEt)Pd; protons at 4.22 ppm (t, $J = 7.2$ Hz, 1 H) and 3.85 (ddd, $J = 15.6$ Hz, 10.0 Hz, 6.8 Hz, 1 H) as the two protons **Hb** and **Hc** in the allyl fragment -C**HbHc**–CH=CHCOOMe; and protons at 3.15 ppm (dq, $J =$ 7.2 Hz, 3.2 Hz, 1 H) and 2.82 (dq, $J = 7.2$ Hz, 2.8 Hz, 1 H) as methylene protons **Hf** and **Hg** in the ethyl ester group –C(=O)OC**HfHg**CH_3 in the structure of the

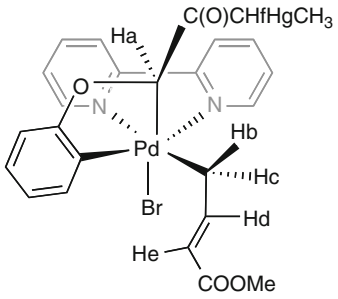

9

Fig. 4 Structure of the palladium(IV) complex isolated at –10 °C

proposed palladium(IV) complex **9** (Fig. 4) operating as an intermediate en route from palladacycle **1b** to complex **7b**.

Encouraged by these results, purification and further characterization of complex **9** was attempted. The yellow solid obtained by the protocol described above was subjected to low-temperature (−30 °C) diffusion-controlled crystallization (ethyl acetate/pentane or ethyl acetate/hexane) to afford small and twinned single crystals of a palladium complex, distinct from the palladacycle **1b** and the "open form" complex **7b**. Single-domain crystals were obtained for two different solvent polymorphs. The asymmetric unit for one of these polymorphs contains two crystallographically independent palladium(IV)-containing molecules, and the asymmetric unit of the second polymorph contains just one. Gratifyingly, the X-ray crystallographic analysis unequivocally indicated that a *cis*-isomer of the proposed allylpalladium(IV) intermediate **9** was indeed formed (Fig. 4). All three molecules of **9** possess a distorted octahedral geometry with the phenyl-*o*-(ethoxycarbonylmethyleneoxo) groups forming a five-membered chelate ring that contains the palladium and two [sp^3-hybridized carbon atom C7 and sp^2-hybridized carbon atom C(2)] of the three carbon atoms bonded to it. The five nonhydrogen atoms comprising this chelate ring in each of these three molecules are slightly noncoplanar (rms deviations from the respective least-squares mean planes range from 0.07 to 0.14 Å). The sp^3-hybridized carbon atom C7 deviates the most from each mean plane (ranging from 0.11 to 0.23 Å) in one direction, and the oxygen atom has the next largest deviation (ranging from 0.10 to 0.19 Å) but in the opposite direction from the least-squares mean plane. The allyl substituent in complex **9** resides *cis* to the bromide ligand and *cis* to the aromatic carbon (C2) of the chelate ring. Both the allyl group and the coordinated aromatic carbon (C2) are positioned *trans* to the nitrogen atoms of the 2,2′-bipyridine ligand. The Pd–N, Pd–Br, and Pd–CH_2(allyl) bond lengths are in agreement with those found in related complexes, and the Pd–Csp^2(aryl) and Pd–Csp^3 (methylene) bond lengths Pd–C2 and Pd–C7, respectively, as well as the Pd–N bond lengths, are comparable to those found for the analogous square planar pallada(II)cycle **1b** (Fig. 5).

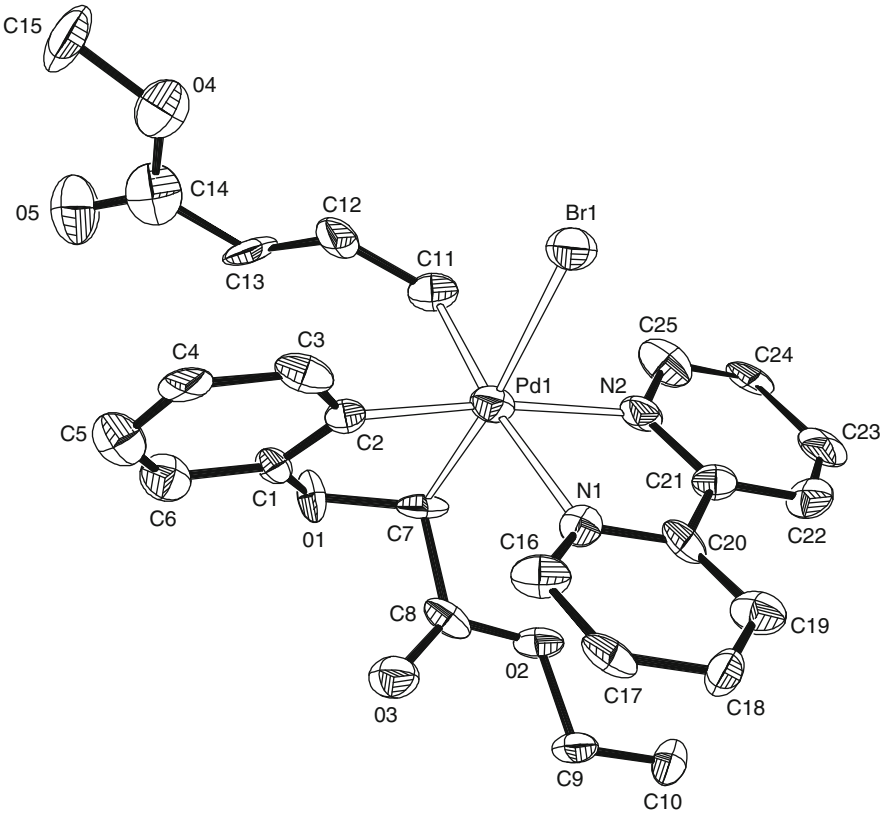

Fig. 5 Thermal ellipsoids diagram of allylpalladium(IV) complex 9. The ellipsoids are drawn at the 50% probability level. Selected bond lengths (Å) and angles (deg): Pd(1)–C(2) 2.002(13); Pd (1)–C(7) 2.029(12); Pd(1)–C(11) 2.079(12); Pd(1)–N(1) 2.179(10); Pd(1)–N(2) 2.139(11); Pd (1)–Br(1) 2.606(2); C(2)–Pd(1)–C(7) 78.6(6); C(2)–Pd(1)–Br(1) 97.1(4); C(2)–Pd(1)–C(11) 88.4 (5); C(11)–Pd(1)–N(2) 96.7(5); N(2)–Pd(1)–N(1) 75.7(4); N(1)–Pd(1)–C(2) 99.3(5)

The preferential formation of the *cis*-isomer of complex **9** is in agreement with the *cis*-structure assigned for a related benzylpallada(IV)cyclic complex by Catellani on the basis of NMR spectroscopic studies [22], but contrasts with the generation of *cis*/*trans* isomer mixtures detected by NMR in reactions of pallada(II) cyclopentane with [Ph_2I][OTf] [31]. ^{1}H NMR spectra recorded on $CDCl_3$ solutions of the single crystals of complex **9** at low temperatures (−10 °C) (Fig. 6) showed signals identical to those highlighted in trace (c) (Fig. 3) and revealed that no isomerization of complex **9** occurred for 5 h at subzero temperature in the $CDCl_3$ solution. Rather, a slow conversion of complex **9** into complex **7b** was detected to occur even at subzero temperatures. In the spectra of pure crystallized complex **9** (Fig. 6), further assignments of the indicative ^{1}H NMR signals could be made for protons **Hd** (7.36 ppm, dt, J = 15.2 Hz, 9.0 Hz, 1 Hd) and **He** (6.00 ppm, d, J = 15.2 Hz) in the allyl fragment (–CH_2C**Hd**=C**He**COOMe). Palladium(IV)

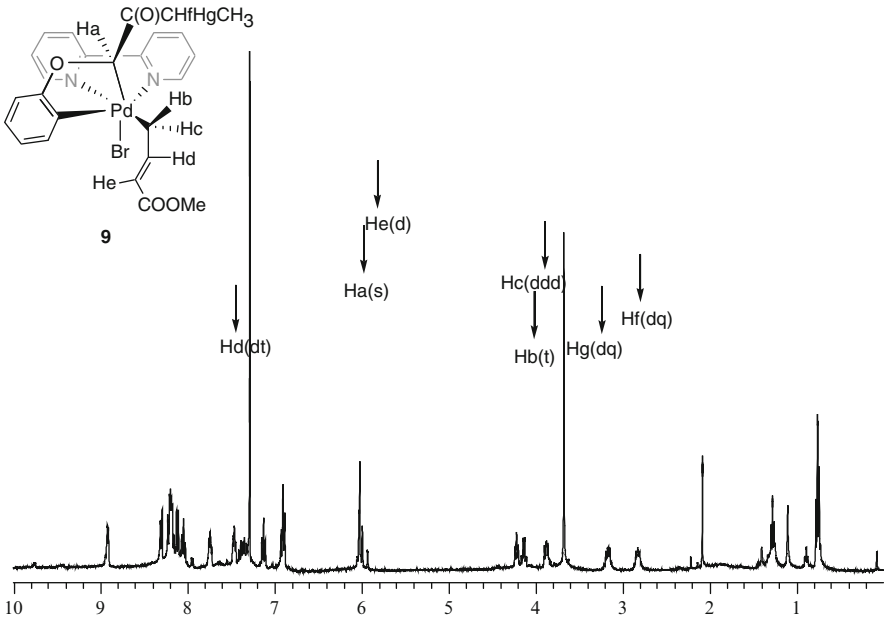

Fig. 6 ^{1}H NMR spectra recorded for the crystallized complex 9 (400 MHz, $CDCl_3$, – 10 °C)

complex **9** was sufficiently stable in solution to permit the collection of ^{13}C NMR data ($CDCl_3$ – 10 °C), and the solid complex **9** could be handled at room temperature for short time periods, although prolonged standing of solid **9** at room temperature resulted in its conversion to complex **7b**.

4 Concluding Remarks

Studies described above successfully demonstrated the operation of palladium(IV) complexes as intermediates in key carbon–carbon bond-forming events in diverse palladium-catalyzed cascade protocols. The spectroscopic and X-ray crystallographic characterization of the semistable palladium(IV) complexes yielded valuable structural data on these still rare organometallic entities. The future challenges for the research on the structure and reactivity of semistable complexes of palladium in higher oxidation states include the design of new types of auxiliary ligands that would impart sufficient stability to the organopalladium intermediates and at the same time would model as closely as possible the ligand sphere present in the actual catalytic transformations. Identification of conditions under which binuclear complexes of palladium in higher oxidation states are operating and furnishing structural data on these novel complexes have recently emerged as an important research direction [29, 32]. Finally, extensive future studies with semistable palladium(IV)

complexes can be expected to uncover cases when palladium(IV) complexes may participate in elemental steps other than reductive elimination [33, 34].

References

1. Negishi EI, Coperet C, Ma S, Liou SY, Li F (1996) Chem Rev 96:365
2. Dyker G (1992) Angew Chem Int Ed Engl 31:1023
3. Dyker G (1993) J Org Chem 58:6426
4. Catellani M (2003) Synlett 298
5. Lautens M, Pache S (2003) Org Lett 5:4827
6. Gerike KM, Chai DI, Bieler N, Lautens M (2009) Angew Chem Int Ed 48:1447
7. Sehnal P, Taylor RJK, Farilamb IJS (2010) Chem Rev 110:824
8. Faccini F, Motti E, Catellani M (2004) J Am Chem Soc 126:78
9. Dell Ca N, Motti E, Mega A, Catellani M (2010) Adv Synth Catal 352:1451
10. Cardenas DJ, Marin-Matute B, Echavarren AM (2006) J Am Chem Soc 128:5033
11. Larock RC, Campo MA (2002) J Am Chem Soc 124:14326
12. Mota AJ, Dedieu A (2006) Organometallics 25:3130
13. Tang S, Peng P, Pi SF, Liang Y, Wang NW, Li JH (2008) Org Lett 10:1179
14. Muniz K, Hovelmann CH, Streuff J (2008) J Am Chem Soc 130:763
15. Liu G, Stahl SS (2006) J Am Chem Soc 128:7179
16. Rosewall CF, Sibbald PA, Liskin DV, Michael FE (2009) J Am Chem Soc 131:9488
17. Canty AJ, Hoare JL, Davies NL, Traill PR (1998) Organometallics 17:2046
18. Byers PK, Canty AJ, Traill PR, Watson AA (1990) J Organomet Chem 390:399
19. Brown DG, Byers PK, Canty AJ (1990) Organometallics 9:1231
20. van Belzen R, Klein RA, Kooijman H, Veldman N, Spek AL, Elsevier CJ (1998) Organometallics 17:1812
21. van Belzen R, Elsevier CJ (2003) Organometllics 22:722
22. Bocelli G, Catellani M, Ghelli S (1993) J Organomet Chem 458:C12
23. Amatore C, Catallani M, Deledda S, Jutand A, Motti E (2008) Organometallics 27:4549
24. Yamamoto Y, Kuwabara S, Matsuo S, Ohno T, Nishiyama H, Itoh K (2004) Organometallics 23:3898
25. Guo R, Portscheller JL, Day VW, Malinakova HC (2007) Organometallics 26:3874
26. Datta Chaudhuri P, Guo R, Malinakova HC (2008) J Organomet Chem 693:567
27. Lu G, Portscheller JL, Malinakova HC (2005) Organometallics 24:945
28. Canty AJ (1992) Acc Chem Res 25:83
29. Powers DC, Ritter T (2009) Nat Chem 1:302
30. Racowski JM, Dick AR, Sanford MS (2009) J Am Chem Soc 131:10974
31. Canty AJ, Patel J, Rodemann T, Ryan JH, Skelton BW, White AH (2004) Organometallics 23:3466
32. Caty AJ, Gardiner MG, Jones RC, Rodemann T, Sharma M (2009) J Am Chem Soc 131:7236
33. Pilarski, LT, Selander N, Böse D, Szabó KJ (2009) Org Lett 11:5518
34. Aydin J, Larsson JM, Selander N, Szabó KJ (2009) Org Lett 11:2852

Top Organomet Chem (2011) 35:111–128
DOI: 10.1007/978-3-642-17429-2_5

η^1-Alkynyl Chemistry for the Higher Oxidation States of Palladium and Platinum

Allan J. Canty and Manab Sharma

Abstract This chapter reviews the organometallic chemistry of palladium and platinum, in which the metal atom is bonded to alkynyl ligands and the formal oxidation state of the metal atom is greater than two. Several synthetic methods have been reported, where the most generally applicable involve oxidation of alkynylmetal(II) complexes and reactions of organometal(II) complexes with alkynyl(aryl)iodine(III) reagents. Metal(IV) complexes obtained have octahedral geometry and some have been shown to decompose via reductive elimination processes to generate carbon–carbon bonds. Unsymmetrical metal–metal bonded species formally represented as Pt^{III}–Pt^{III} ↔ Pt^{IV}–Pt^{II} have been characterised as intermediates in oxidation of Pt^{II} to Pt^{IV}. Potential implications for mechanisms of organic reactions mediated by higher oxidation state metal centres are discussed.

Keywords Acetylides · Pt–Pt bonds · Alkynyl complexes · Alkynyliodonium · Organopalladium · Organoplatinum · Oxidation chemistry · Palladium(IV) · Platinum(III) · Platinum(IV)

Contents

A.J. Canty (✉) and M. Sharma
School of Chemistry, University of Tasmania, Hobart, Tasmania 7001, Australia
e-mail: Allan.Canty@utas.edu.au

1 Introduction

η^1-Alkynyl complexes have become a prominent feature of palladium(II) and platinum(II) chemistry [1, 2]. Recent research in higher oxidation state chemistry has been stimulated partly by early suggestions of the involvement of η^1-alkynylpalladium(IV) species in catalysis [3–9], oxidatively induced reactions of η^1-alkynylplatinum(II) complexes in stoichiometric organic synthesis [10–12], and in the generation of Pt^{II} species as catalysts for hydrosilylation reactions [13]. There are few reports of spectroscopically detected or isolated complexes, limited to bis(η^1-alkynyl)platinum(IV) [14, 15], mono(η^1-alkynyl)metal(IV) species [16–25], and binuclear platinum complexes [24, 25]. In view of the paucity of reports, early work is reviewed together with recent advances. In this review, "alkynyl" refers to the η^1-anionic ligand $[RC{\equiv}C]^-$, where R may include alkyl, aryl, and similar groups such as trimethylsilyl and $MC{\equiv}CC_6H_4^-$, but does not include motifs such as $M(C{\equiv}C)_nM$ and $M(C{\equiv}C)_nR$. The alkynyl group may be generally regarded as a strong field ligand with a trans influence between that of C(sp^2, sp^3) and chloride groups [26] and exhibiting little evidence of π-backbonding [26, 27].

There are few reported synthetic routes to higher oxidation state alkynyl complexes for palladium and platinum. Synthetic methods include the reaction of an aryl azide with an alkynylplatinum(II) complex [14], reaction of $MeO_2CC{\equiv}CCO_2Me$ with a stannylplatinum(IV) metallacycle [16, 17], and reaction of phenylacetylene with an amidoplatinum(IV) complex [23]. Demonstrated synthetic routes that appear suitable for general application are limited to iodine as an oxidant for alkynylplatinum(II) complexes [15] and alkynyl(aryl)iodine(III) reagents ("iodonium reagents") that oxidise platinum(II) and palladium(II) complexes with concomitant transfer of $[RC{\equiv}C]^+$ to the metal centre [18–22, 24, 25]. In view of this, and the emerging role of iodonium reagents in $Pd^{III/IV}$-mediated organic synthesis [21, 25, 28–30], including alkynyl(aryl)iodine(III) reagents [29], this chapter is structured in terms of bis(alkynyl)platinum, mono(alkynyl)platinum, and iodonium chemistry. This sequence also broadly reflects the chronological development of the field. Electrochemical indications of higher oxidation state species are discussed within these sections, except for the complex ions $[Pt(C{\equiv}CR)_4]^{2-}$ for which cyclic voltammetry has been interpreted in terms of a metal-centred oxidation from Pt^{II} to Pt^{III} [31].

2 Bis(η^1-alkynyl)metal Chemistry

Beck and coworkers reported a reaction in which dinitrogen is eliminated from 4-nitrophenyl azide on reaction with *trans*-$[Pt(C{\equiv}CPh)_2(PEt_3)_2]$ (**1**) to give a Pt^{IV} complex containing a dianionic 2-tetrazene-1,4-diyl ligand, $Pt(C{\equiv}CPh)_2\{1,4\text{-}(4\text{-}(NO_2)C_6H_4)_2N_4\text{-}N,N'\}(PEt_3)_2$ (**2**) (Eq. 1), characterised by X-ray crystallography

[Pt–C 1.99(1), 2.00(1) Å, C≡C 1.20(2), 1.19(2) Å, Pt–C≡C 172.5(9), 177.4(7)°] [14].

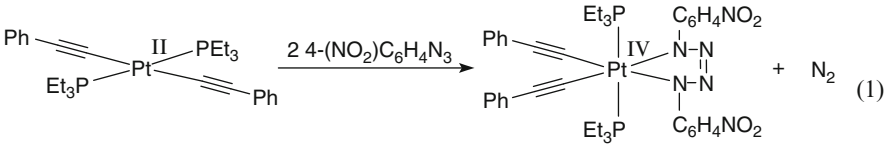

(1) (2) (1)

This early report of a well-characterised trialkylphosphine complex has been followed by recent electrochemical studies of phosphine complexes, providing evidence for oxidation occurring primarily at the metal centre in polymeric *trans*-[{Pt(μ-C≡CC$_6$H$_4$C≡C)(PBu$_3$)$_2$}$_n$] (**3**), *trans*-[Pt{C≡C–(η^6-C$_6$H$_5$)Cr(CO)$_3$}$_2$(PBu$_3$)$_2$ (**4**), a copolymer containing both –C≡CC$_6$H$_4$C≡C– and –C≡C{η^6-(C$_6$H$_4$)Cr(CO)$_3$}C≡C– bridges linking *trans*-[Pt^{II}(PBu$_3$)$_2$] groups [32], and a complex containing –C≡C{C$_6$H$_4$–(1,3-C$_2$ON$_2$)–C$_6$H$_4$}C≡C– bridges linking *trans*-[Pt^{II}(C≡CAr)(PEt$_3$)$_2$] groups (**5**) (Scheme 1) [33].

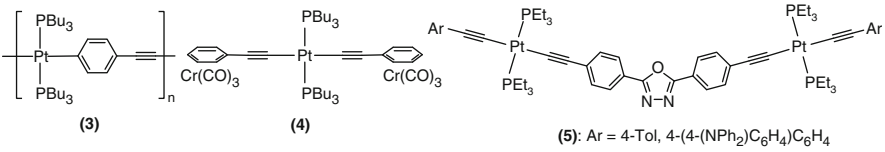

(3) (4) (5): Ar = 4-Tol, 4-(4-(NPh$_2$)C$_6$H$_4$)C$_6$H$_4$

Scheme 1 Pt^{II}(C≡CR^1)$_2$ complexes examined by electrochemical methods

Complex **6** reacts with iodine to form heterocycle **7** [10], where it is assumed that the process of carbon–carbon bond formation is a result of oxidatively induced reductive elimination (Eq. 2). This protocol has been developed as a key step in the stoichiometric synthesis of a range of macrocycles, including interlocked π-conjugated macrocycles (catenanes) [10–12].

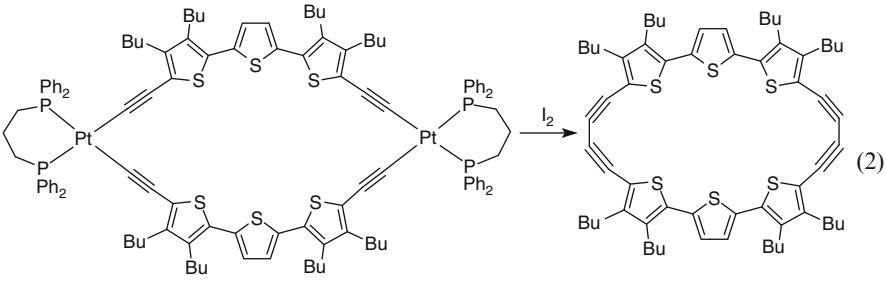

(6) (7) (2)

Evidence for the role of bis(alkynyl)platinum(IV) species as precursors in catalytic processes has also been presented [13]. Complexes Pt(C≡CR)$_2$(COD) (R usually aryl, COD = 1,5-cyclooctadiene) exhibit useful properties as pre-catalysts for hydrosilylation reactions in cross-linking of polyorganosiloxanes containing Si–H and vinyl groups. Of particular value, the complexes are inactive as

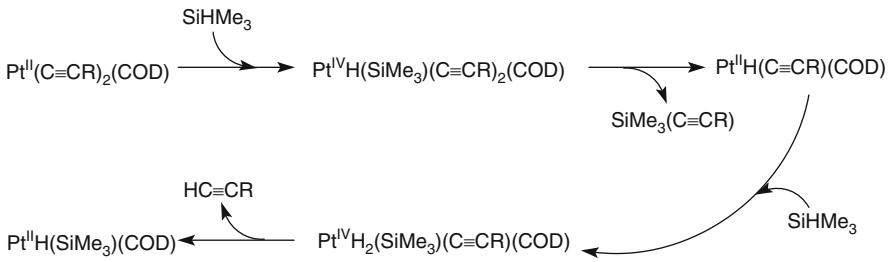

Scheme 2 Proposed mechanism for the generation of "$Pt^{II}H(SiMe_3)$" from $Pt(C{\equiv}CR)_2(COD)$, for subsequent participation in hydrosilylation catalysis

pre-catalysts at ambient temperature, and high curing rates are obtained above a kick-off temperature that can be tuned by choice of R. Computational studies using $SiHMe_3$ as a model for silyl groups in polyorganosiloxanes suggest that this may occur via either a sequence of oxidative additions of $SiHMe_3$ and reductive eliminations of $SiMe_3(C{\equiv}CR)$ and $RC{\equiv}CH$ (Scheme 2), or more directly without Pt^{IV} intermediates by a reductive coupling from Pt^{II} that is induced by alkene coordination to form "$Pt^{II}(C{\equiv}CR)_2(COD)(alkene)$" in the first step. For both processes, the initial step is rate-determining with a computed barrier of 27 kcal mol^{-1} and results in formation of the "$Pt^{II}H(SiMe_3)$" motif for entry into the Chalk– Harrod mechanism for hydrosilylation. Experimental evidence favours oxidative addition of an Si–H bond, e.g. $Me_3Si–O–SiHMe_2$ reacts with $Pt(C{\equiv}CC_6H_4–4\text{-}SiMe_3)_2(COD)$ at moderate temperatures, but a related polysiloxane containing alkene groups but without an Si–H bond does not react up to 120°C [13].

In a related manner, it has been suggested that palladium(IV) species "$PdCl_2(SnMe_3)(C{\equiv}CMe)(PBu_3)_2$" and "$PdCl(SnMe_3)(C{\equiv}CMe)_2(PBu_3)_2$" may be involved in the reaction of *trans*-$[PdCl_2(PBu_3)_2]$ with $SnMe_3(C{\equiv}CMe)$ to form *trans*-$[PdCl(C{\equiv}CMe)(PBu_3)_2]$, $SnClMe_3$, and $SnMe_3(C{\equiv}CMe)$ [34]. However, direct evidence for higher oxidation state bis(alkynyl)palladium species is lacking, except for electrochemical studies of *trans*-$[Pd\{C{\equiv}CC_6H_4C{\equiv}C–RuCl(dppe)_2\}_2(PBu_3)_2]$ (dppe = 1,2-bis(diphenylphosphino)ethane) (**8**) and *trans*-$[Pd\{C{\equiv}CC_6H_4C{\equiv}C–(\eta^5\text{-}C_5H_4)Fe(\eta^5\text{-}C_5H_5)\}_2(PBu_3)]$ (**9**) [35]. Cyclic voltammetry and voltammetry with a rotating platinum electrode for both **8** and **9** are interpreted as indicating oxidation of the Ru^{II} centres in **8** and Fe^{II} centres in **9** to M^{III} and, at higher potentials, Ru^{IV}/Ru^{III} for **8** and Pd^{III}/Pd^{II} for both **8** and **9** [35].

Complex **2** (Eq. 1) and complex **11** in the reaction sequence shown in (Eq. 3) reported by James and coworkers [15] appear to be the only isolated bis(alkynyl) platinum(IV) complexes. Complex **11**, assumed to have the configuration shown by analogy with **2** and related $PtI_2Me_2(bpy)$ (bpy = 2,2′-bipyridine), was obtained in quantitative yield and is stable over weeks in the solid state but slowly decomposes in solution by reductive elimination to form **12** (Eq. 3). The reaction of (Eq. 3) can be viewed as a suitable model for the chemistry of (Eq. 2), implicating Pt^{IV}

intermediate(s) containing the "$PtI_2C_2P_2$" kernel followed by C–C bond formation for the sequence **6**→**7**.

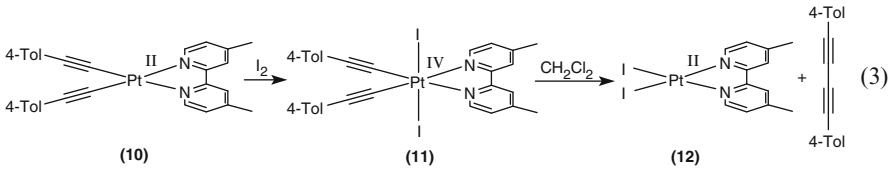

(3)

Electrochemical studies of $Pt(C{\equiv}CPh)_2(Bu_2^t$-bpy), which would be confidently anticipated to react with iodine in the same manner as **10**, reveal an irreversible and ill-defined oxidation process in *N*,*N*-dimethylformamide [36] and one irreversible oxidation in dichloromethane assigned as a HOMO-centred process ["metal and alkynyl(s)"] [37].

3 Mono(η^1-alkynyl)metal Chemistry

There is extensive interest in the electrochemical behaviour of mono(alkynyl) platinum(II) complexes, in particular for complexes of substituted terpyridines **13** [38–43], and related species including **14** [44], **15** [45], **16** and **17** (Scheme 3) [46], and a complex containing the bridging group in **5** linking two *trans*-$[PtCl(PPh_3)_2]$ units [33]. Processes involving the unsaturated ligands, and the rhenium kernel in **16** and **17**, occur for these complexes but, in general, irreversible oxidation can also be ascribed to the palladium and platinum centres as predominantly metal-centred M^{III}.

Introduction of a second organyl donor, forming M^{II}(alkynyl)(organyl), allows the study of the influence of *cis*- and *trans*-dispositions of the organyl groups (Scheme 4). Complexes **18** show one reversible and one irreversible anodic wave in cyclic voltammetry, assigned as iron-centred and platinum-centred, respectively [47]. Complexes corresponding to one-electron oxidation by DDQ or ferrocenium are isolable (**19**, **20**). A Mössbauer spectrum of **19** (R = Me) is characteristic of the

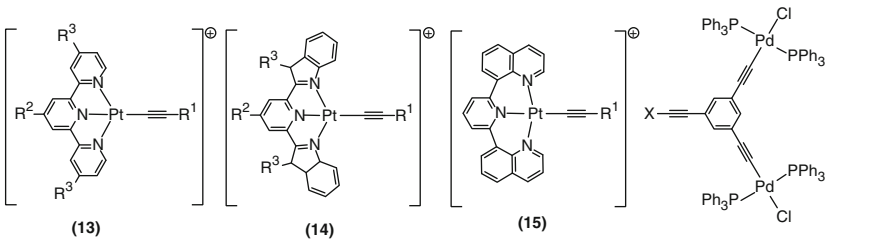

Scheme 3 $Pt^{II}(C{\equiv}CR^1)$ and $Pd^{II}(C{\equiv}CR^1)$ complexes examined by electrochemical methods

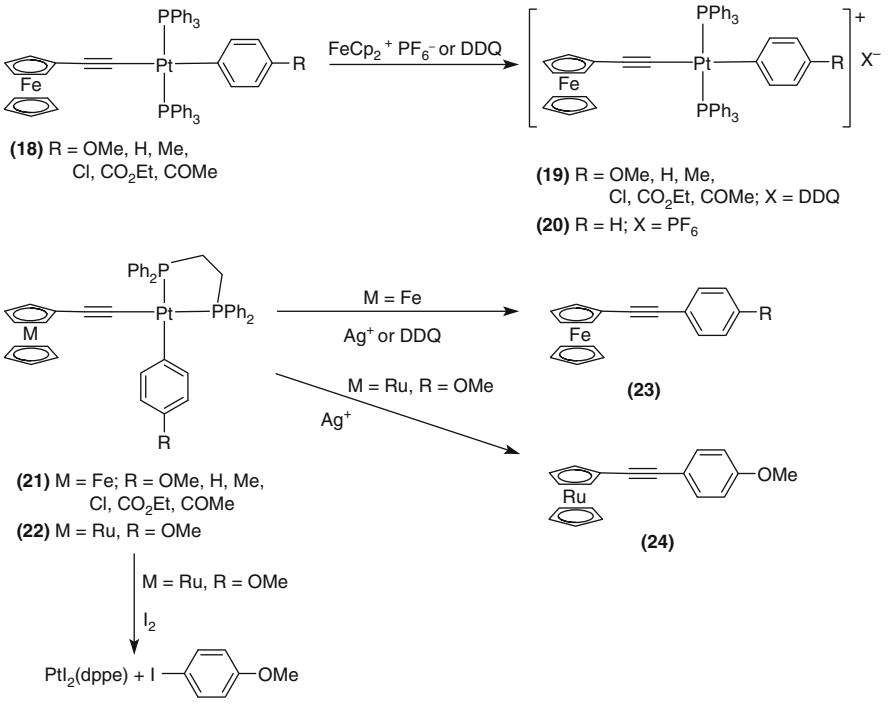

Scheme 4 Oxidation chemistry of *trans*- and *cis*-$Pt^{II}(\eta^1$-alkynyl)(aryl) complexes; *DDQ* = 2,3-dichloro-4,5-dicyanobenzoquinone

ferrocenium ion, and thus the cations are best regarded as Pt^{II} species. The ruthenium analogues of **18** (R = OMe, H, Me, Cl, CO_2Et) exhibit very high anodic potentials, consistent with the observed absence of oxidation on addition of Ag^+ or the substituted benzoquinone DDQ [48]. Iron complexes with the *cis*-configuration (**21**) give cyclic voltammetry, suggesting that one-electron oxidised species undergo a fast reaction to produce the C–C coupling product (**23**) [49], and these coupling products could be obtained by reaction with $AgBF_4$ via an oxidatively induced reductive elimination [48]. The oxidant DDQ also facilitates this reactivity for iron but not for the ruthenium analogue, and the ruthenium complex reacts with iodine to give PtI_2(dppe) and 4-methoxyiodobenzene together with traces of the C–C coupling product **24** and a trace amount of the Glaser coupling product $[C{\equiv}C{-}(\eta^5\text{-}C_5H_4)Ru(\eta^5\text{-}C_5H_5)]_2$.

Complex **25** reacts with excess alkyne to give **26** in 52% yield together with **27**, **28**, and an uncharacterised dimethyltin(II) product **29** (Scheme 5). Complex **26** is, apparently, the first reported mono(alkynyl)platinum(IV) complex and has an extraordinary configuration containing an *sp*(alkynyl), an sp^2(alkenyl), and two sp^3(methyl) groups (**26**). The complex has been characterised by NMR spectroscopy and X-ray diffraction [Pt–C(*sp*) 2.09(1) Å, C≡C 1.178(14) Å, Pt–C≡C 178.3 (9)°] [16, 17]. Complex **25** is an inefficient catalyst for the reaction of $(Me_2SnSe)_3$

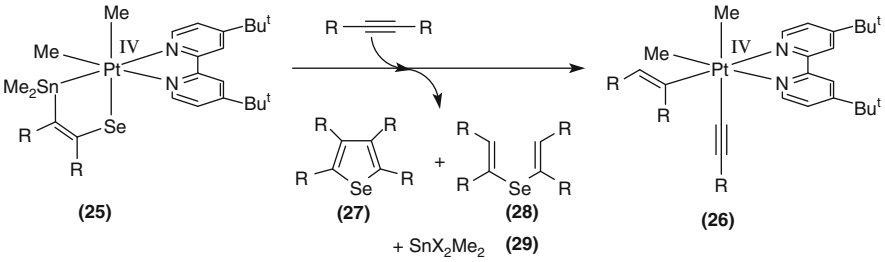

Scheme 5 Reaction of metallacycle **25** with excess alkyne to form complex **26** together with organoselenium compounds and an unidentified dimethyltin(II) product, R = CO_2Me

with $MeO_2CC{\equiv}CCO_2Me$ to form the organoselenium products **27** and **28** with **29** in 1:1:2 ratio. The mechanisms of these reactions have not been elucidated. ^{13}C NMR data for **25** illustrate significant differences in $^1J_{PtC}$ coupling, following the sequence *sp* (901 Hz) > sp^2 (780 Hz) > sp^3 (477 (trans to Se), 575 Hz (trans to nitrogen)) [17].

More recently, Gunnoe and coworkers, in exploring amidoplatinum(IV) chemistry [23] using [2,6-bis{(pyrazol-1-yl)methyl}phenyl-*N*,*C*,*N*]$^-$ as a flexible ancillary ligand [50], found that the amido complex **27** reacts with phenylacetylene at 60°C in benzene to form **28** (Eq. 4). The X-ray crystal structure of **28** shows some similarities with **26**, exhibiting a "PtC_4N_2" kernel containing *sp*, sp^2, and two sp^3 groups [Pt–C(*sp*) 2.062(5) Å, C≡C 1.180(8) Å, Pt–C≡C 179.4(6)°].

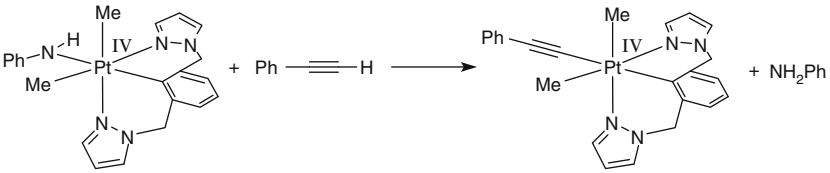

(4)

Alkynyl(aryl)platinum(II) complexes **29–33** where the aryl group is a planar intramolecular coordinating group undergo irreversible oxidation processes when examined by cyclic voltammetry in dichloromethane (**29**, **31**) [51], *N*,*N*-dimethylformamide (**30**) [52], and tetrahydrofuran (**32–34**) [53, 54] (Scheme 6). The potentials for **32–34** are shifted by ca. 200 mV to more negative values from the chloro-analogue $Pt^{II}Cl(N,C,N)$, which could be interpreted as indicating that the electron density on the platinum centre has increased and is thus easier to oxidise [53]. The total current was measured for the cathodic process for **32** (R^1 = $SiMe_3$), suggesting that two electrons are removed irreversibly. The oxidative process for the binuclear complex **34** is consistent with the removal of four electrons in two simultaneous irreversible oxidation steps [54].

An attempted synthesis of a higher oxidation state complex using iodine as an oxidant for **35** in tetrahydrofuran led to the formation of the iodoplatinum(II)

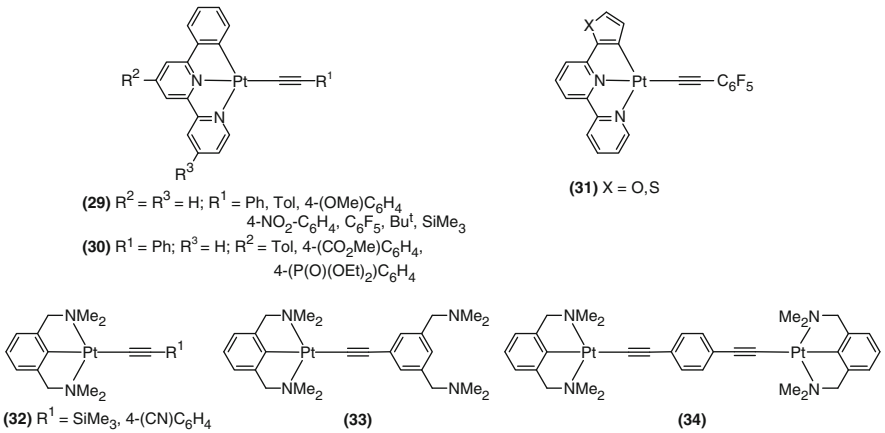

Scheme 6 $Pt^{II}(C{\equiv}CR^1)$(CNN)and $Pt^{II}(C{\equiv}CR^1)$(NCN) complexes examined by electrochemical methods

complex **36** and I–C≡C–$SiMe_3$ (Eq. 5) [53]. In contrast, Pt^{II}(NCN)(Tol) reacts with iodine to form $Pt^{IV}I_2$(NCN)(Tol) [55]. The application of alkynyliodonium reagents as oxidants that formally transfer a $[RC{\equiv}C]^+$ group to $Pt^{II}(O_2CAr)$(NCN) give Pt^{IV} products is discussed in the following section.

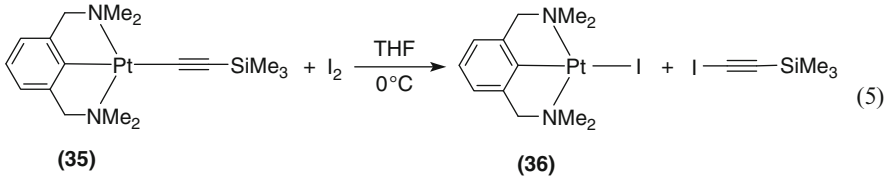

(5)

4 Mono(η^1-alkynyl)metal Chemistry Derived from Iodonium Reagents

The mechanism of reaction of alkynyl(aryl)iodonium reagents as oxidants leading to the formation of metal–carbon bonds is much less understood than for oxidative addition reactions of alkyl or aryl halides [21]. Evidence for free radical processes has been reported for diaryliodine(III) reagents, e.g. for reactions with [Fe(η^5-C_5H_5)$(CO)_2]_2$ [56], Fe(TPP) (TPP = tetraphenylporphyrinato-dianion) [57], $[Mn(CO)_5]^-$ [58], YbI_2 and SmI_2 [59], and for alkynyl(aryl)iodine(III) reagents, e.g. for reactions with triphenylphosphine [60]. Some guidance is also provided by mechanistic studies of reactions of diaryliodine(III) and alkynyl(aryl)iodine(III) with organic nucleophiles [61, 62]. Mechanisms established for reactions of organic nucleophiles include radical processes, although, in most cases, reactions are interpreted in terms of the nucleophile interacting with the electrophilic iodine(III)

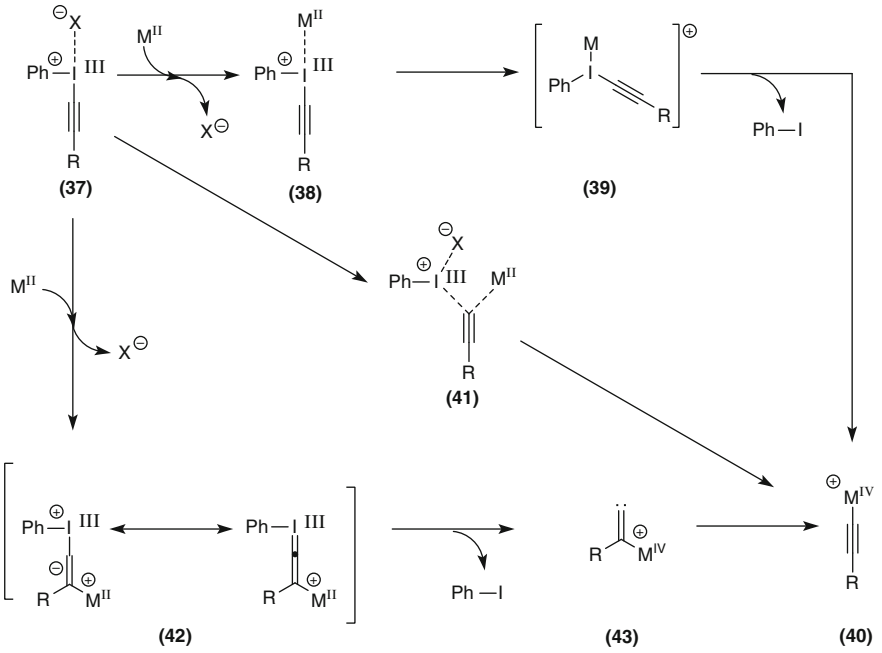

Scheme 7 Proposed mechanisms for reaction of metal(II) nucleophiles with alkynyl(phenyl) iodine(III) reagents, omitting free radical processes

centre followed by reductive elimination to form Nu–Ar and ArI. For organometallic transformations with [RC≡C] as the transferred group, the mechanism may be represented by the sequence **37**→**38**→**39**→**40**, together with recent DFT calculations for both aryl and [RC≡C] transfer [63], consistent with direct transfer via **41** to a Pd^{II} centre without involving a Pd···I interaction (Scheme 7).

The potential process **37**→**42**→**43**→**40** recognises the polarity of the alkynyl group of **37**, $-C^{\delta-}\equiv C^{\delta+}-R$, and strong evidence for the intermediacy of species analogous to **42** and **43** from reactivity studies using organic nucleophiles [61]. Although mechanisms have not been rigorously established for organometallic substrates reacting with alkynyl(aryl)iodine(III) reagents, Scheme 7 acts as a "working model" for Pt^{II} and Pd^{II} substrates, although to date there appears to be no evidence discounting the occurrence of free radical processes.

In contrast to the reaction of (Eq. 5) that does not lead to detection of a Pt^{IV} product, closely related carboxylato-complexes $Pt^{II}(O_2CAr)(NCN)$ react with IPh(C≡CR)(OTf) at room temperature in acetone to form Pt^{IV} species $Pt^{IV}(O_2CAr)$(OTf)(C≡CR)(NCN) (**44**) characterised by ^1H NMR spectroscopy (Scheme 8) [20]. An unstable Pd^{IV} complex (**45**) has been detected at −50°C. Platinum complexes **44** react with sodium iodide to give isolable iodo-complexes (**46**) in 78–93% yield, one of which (R = $SiMe_3$, Ar = 4-$(CF_3)C_6H_4$) has been characterised by X-ray crystallography [Pt–C(*sp*) 1.951(3) Å, C≡C 1.205(4) Å, Pt–C≡C 172.7(3)°] [19, 20].

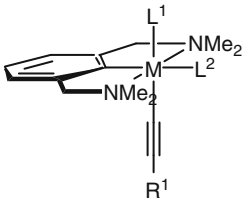

$L^1 = O_2CAr$, $L^2 = OTf$

(44) M = Pt, $R^1 = SiMe_3$, Ph,
Ar = Ph, 4-CF_3-C_6H_4

(45) M = Pd, $R^1 = SiMe_3$, Ar = Ph

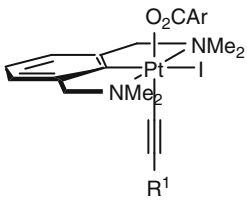

(46) $R^1 = SiMe_3$, Ph,
Ar = Ph, 4-CF_3-C_6H_4

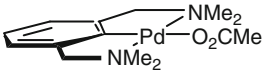

(47)

+IPh(C≡CSiMe3)(OTf)
–PhI

$\Delta E^{\ddagger}$ = +15.2 kcal mol^{-1}
ΔE = –18.4 kcal mol^{-1}

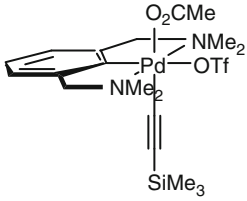

(48)

Scheme 8 M^{IV}(NCN) complexes **44–46** synthesised using alkynyl(phenyl)iodine(III) reagents and DFT calculations for the reaction of $Pd^{II}(O_2CMe)$(NCN) (**47**→**48**); configuration of L^1 and L^2 not established

Szabó and coworkers have reported DFT studies of this system for palladium, as noted above, using as a model the interaction of $Pd(O_2CMe)$(NCN) (**47**) with I(C≡CSiMe$_3$)Ph(OTf) to form "$Pd(O_2CMe)(OTf)(C{\equiv}CSiMe_3)$(NCN)" (**48**) (Scheme 8) [63]. The reaction is highly exothermic with a moderate activation barrier. Calculations for the analogous reaction of IPh_2(OTf) are less favourable although overall exothermic and supportive of the proposed involvement of Pd^{IV} intermediates in the coupling of alkenes with IAr_2(OTf) catalysed by Pd^{II} pincer complexes, e.g. **47** and Pd(OTf){2,6-$(Ph_2PO)_2C_6H_3$-*P*,*C*,*P*} [64].

The synthesis of the Pd^{IV} complex **45** [20] using I(C≡CSiMe$_3$)Ph(OTf) is also a model reaction for related emerging organic synthesis involving IAr_2(X) oxidation of monoarylpalladium(II) intermediates, where the latter intermediates are generally [28, 65–68], but not always [66], present as intramolecularly coordinated species Pd^{II}(L-*C*,*N*) formed by cyclopalladation reactions.

Diorganoplatinum(II) complexes of 1,2-bis(dimethylphosphino)ethane (dmpe) react readily with IPh(C≡CSiMe$_3$)(OTf) at −50°C in acetone-d_6 to form Pt^{IV} complexes **49–52**, characterised by ^{1}H and ^{31}P NMR spectroscopy, although the configuration of **52** has not been determined (Scheme 9) [20, 22]. In contrast with **50** and **51**, NMR spectra indicate that the triflate ligand in **49** and **52** is in equilibrium with acetone-d_6 as ligand and that pyridine and acetonitrile fully displace triflate. Complexes **49–51**, and the pyridine and acetonitrile species $[PtMe_2(C{\equiv}CSiMe_3)$(dmpe)(L)$]^+$, decompose in solution when warmed to ca. −10°C, forming ethane

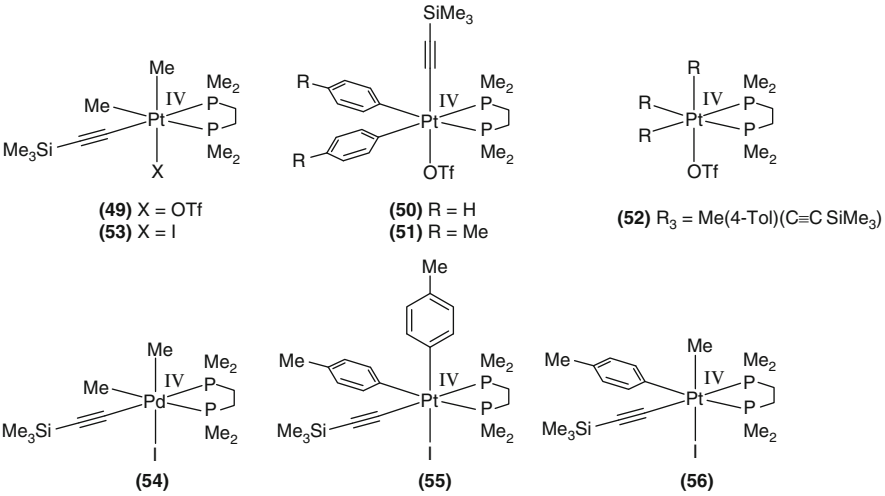

Scheme 9 Metal(IV) complexes containing a bidentate phosphine donor

from the $Pt^{IV}Me_2(C{\equiv}CSiMe_3)$ motif (**49**), $(Ar)_2$ from **50** and **51**, and Me-Tol from $Pt^{IV}Me(Tol)(C{\equiv}CSiMe_3)$ (**52**). Although a range of factors are expected to play a role in determining the selectivity in C–C coupling, the preferences for $C(sp^3)$–$C(sp^3)$ over $C(sp^3)$–$C(sp)$ (**49**), $C(sp^2)$–$C(sp^2)$ over $C(sp^2)$–$C(sp)$ (**50**), and $C(sp^3)$–$C(sp^2)$ over both $C(sp^3)$–$C(sp^2)$ and $C(sp^3)$–$C(sp)$ (**52**) follow a trend with higher values of n in sp^n preferred for coupling partners.

Addition of sodium iodide to the triflate complexes gives iodo complexes **53**, **54**–**56**, where the $Pt^{IV}(Tol)_2(C{\equiv}CSiMe_3)$ complexes have different configurations (**50**, **51**, and **55**). The X-ray crystal structure of **56** has been determined and, as expected, the Pt–C(Tol) distance is longer than the Pt–C(alkynyl) distance, where both groups are opposite a phosphorus donor [Pt–$C(sp^2)$ 2.155(18) Å, Pt–C(*sp*) 2.04(2) Å, C≡C 1.14(3) Å, Pt–C≡C 167.6(19)°] [22]. The iodoplatinum(IV) complexes (**53**, **55**, and **56**) are more stable than the triflato-complexes, decomposing at 25°C to give Me–Me (**53**) and at 50°C to give $(4\text{-Tol})_2$ (**55**, **56**), $Me_3SiC{\equiv}C(Tol)$ (**55**), and Me–Tol and $Me_3SiC{\equiv}C(Tol)$ (**56**).

The Pd^{IV} complex **54** detected at −50°C and characterised by ^1H and ^{31}P NMR comparison with the platinum analogue, decomposed at low temperature [20], with the *fac*-$Pd^{IV}IC_3P_2$ configuration, is a model for frequently proposed and undetected intermediates in palladium catalysis in the presence of phosphine donors.

In early work studying the reactivity of Pt^{II} substrates towards alkynyl(phenyl) iodine(III) reagents, Pt^{IV} complexes with 2,2′-bipyridine ligands were readily isolated in 78–90% yield from room temperature reactions, including a platina (IV)cycle (**64**) and formulations exhibiting a mixture of isomers (**59a**, **b**; **60a**, **b**) (Scheme 10) [18, 20].

For $Pt^{IV}IR_2(C{\equiv}CSiMe_3)$(dmpe) (**53**, **54**, **55**, **56**) and complexes of 2,2-bipyridines (**59**–**62**, **64**) shown in Schemes 9 and 10, the configuration with the alkynyl group trans to phosphorus or nitrogen is preferred.

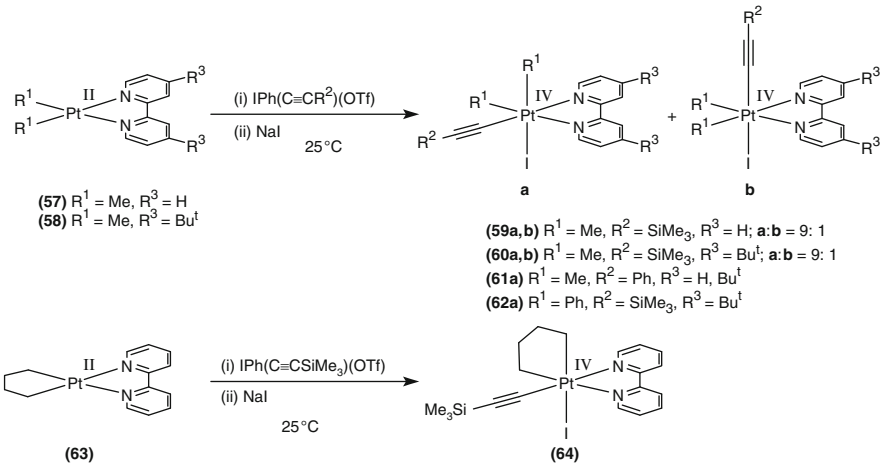

Scheme 10 Platinum(IV) complexes obtained at room temperature on reactions of Pt^{II} 2,2′-bipyridine complexes

These early reports [18, 20] provide support for the proposed role of Pd^{IV} in stoichiometric synthesis of benzofurans involving reaction of pallada(II)cyclic Pd(L-*C*,*C*)(bpy) (L = $[2\text{-}(EtO_2CCHO)C_6H_4]^{2-}$)with I(C≡CR)Ph($BF_4$) [69, 70]. Palladium(IV) intermediates were not detected in this study, but NMR monitoring of reactions of closely related alkenyl reagents I(CH=CHR)Ph(BF_4) led to detection of a Pd^{IV} intermediate [69, 70].

The reaction of $Pt^{II}Me_2$(bpy) (**57**) in acetone-d_6 has been examined at low temperature by ^{1}H NMR spectroscopy at −80°C, resulting in detection of an intermediate characterised as binuclear **65** (Scheme 11) [24]. Unreacted IPh(C≡CSiMe$_3$)(OTf) is present on formation of **65** and, on warming to −20°C, is consumed with formation of the Pt^{IV} product **66**. Intermediate **65** reacts with excess sodium iodide at −80°C to form crystalline **67** in 85% yield, and iodide also reacts to remove unreacted IPh(C≡CSiMe$_3$)(OTf) oxidant. The iodo derivative (**67**) exhibits NMR spectra identical to the triflate precursor (**65**) and decomposes at −20°C to form a 1:1 ratio of $Pt^{IV}IMe_2$(C≡CSiMe$_3$)(bpy) and $Pt^{II}Me_2$(bpy). The Pt^{IV} products are present as isomers in 9:1 ratio (**59a**, **59b**), identical to that obtained in the room temperature reaction (Scheme 10) and also on addition of sodium iodide to Pt^{IV}(OTf)Me_2(C≡CSiMe$_3$)(bpy) (**66**) (Scheme 11).

The X-ray crystal structure determination for binuclear **67** shows an essentially ionic composition [24], with the Pt···I distance [3.4198(6) Å] about 0.3 Å below van der Waals contact [71] but considerably longer than typical Pt–I bond lengths, e.g. 2.7631(4) Å in $Pt^{IV}IMe_2Ph$(bpy) [72, 73]. The "$PtMe_2$(bpy)" units are twisted about the Pt–Pt bond by ca. 40°, the "Si–C≡C–Pt–Pt" axis is approximately linear [Si–C≡C 175.4(6), C≡C–Pt 175.9(6), C–Pt–Pt 176.54(17)°], and the geometry for the alkynylplatinum group [Pt–C(*sp*) 1.964(7) Å, C≡C 1.212(10) Å] is similar to that in the four reported mononuclear Pt^{IV} complexes [**2**, **26**, **28**, **46** (R = SiMe$_3$,

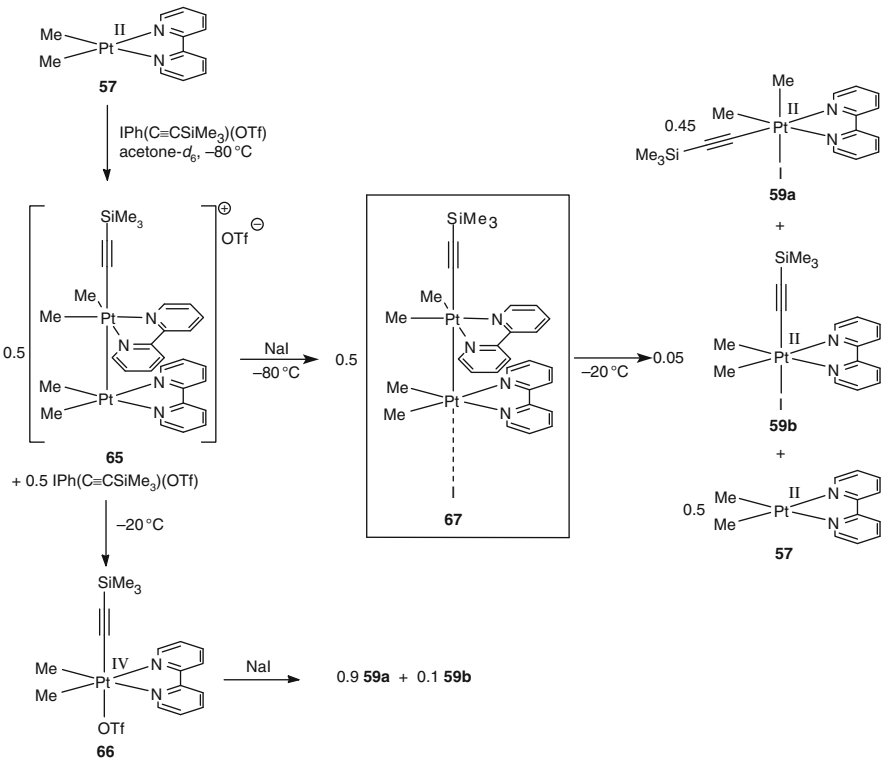

Scheme 11 Reaction of $Pt^{II}Me_2(bpy)$ with IPh(C≡CSiMe$_3$)(OTf) (**57**→**65**→**66**), involving stepwise oxidation to Pt^{IV} via binuclear **65**, and isolation of the iodide salt (**67**) that decomposes to give products with a 1:1 ratio for Pt^{IV}(**59a**,**59b**):Pt^{II}(**57**)

Ar = 4-(CF_3)C_6H_4)]. The Pt–Pt distance, 2.7639(4) Å, is similar to that observed for Pt^{III} binuclear complexes that do not have bridging groups, i.e. symmetrical complexes with octahedral geometry at platinum in (L-*C*,*N*)$_2$ClPt–PtCl(L-*C*,*N*)$_2$ (L = deprotonated 2-phenylpyridine, [2-C_6H_4py]$^-$, [2.7269(3) Å]) [74] and (L-*N*, *N*′)$_2$ClPt-PtCl(L-*N*,*N*′)$_2$ (L = deprotonated C_8-carbocyclic α-dioxime, [C_8H_{12}(=NO)$_2$H]$^-$, 2.6969(5) Å]) [75]. Related symmetrical Ir^{II} dimers have similar Ir–Ir bond lengths, 2.826(2) [76] and 2.6622(3) Å [77].

In view of the unsymmetrical environment for the two platinum atoms in **65** and **67**, the cation may be best regarded as Pt^{III}–Pt^{III} ↔ Pt^{IV}–Pt^{II}, where the average higher oxidation state centre is octahedral and contains the alkynyl group. At one extreme, the lower oxidation state centre can be regarded as Pt^{II} acting as a donor ligand for an electrophilic Pt^{IV} centre, in a manner similar to coordination of Pt^{II} to Cd^{II} in [(bpy)Me_2Pt–Cd(cyclen-N_4)]$^{2+}$ [cyclen = (CH_2CH_2NH)$_4$] [Pt–Cd = 2.6101 (8) Å] [78] and to Cu^{I} in (N~N)Me_2Pt–Cu(OTf) [Pt–Cu = 2.3992(16) Å, N~N = (2,6-$Cl_2C_6H_4N$=CMe)$_2$] [79]. In addition, with this interpretation, it is feasible that coordination Pt^{II}→Pt^{IV} prevents oxidation of the Pt^{II} centre until the temperature is

raised, leading to reaction of **65** to give **66** (Scheme 11). More speculative is the potential roles of assembly of two $Pt^{II}Me_2(bpy)$ units prior to commencement of oxidation by $IPh(C{\equiv}CSiMe_3)(OTf)$, the role of a dimer "$[PtMe_2(bpy)]_2$" in increasing the nucleophilic character of Pt^{II}, or assembly commencing as the (unknown) mechanism of oxidation begins to form an electrophilic platinum centre.

5 Concluding Remarks

Although an alkynylplatinum(IV) complex was first described over 20 years ago [14], to date there are only four crystal structures reported for Pt^{IV}, and none for Pd^{IV}. The structures depict different motifs at the Pt^{IV} centre, one of which is a dialkynyl complex (**2**) and three are monoalkynyl complexes [**26**, **28**, **46** (R = $SiMe_3$, Ar = 4-$(CF_3)C_6H_4$)], and there is one additional structure of a binuclear complex viewed as containing "Pt^{III}–Pt^{III}↔Pt^{IV}–Pt^{II}" with an alkynyl group bonded to the higher oxidation state centre (**67**). Other isolated complexes, or detected in solution by NMR spectroscopy, fall into the same general classes as those characterised crystallographically and include monoalkynylpalladium(IV) species. As for related triorganometal(IV) complexes [69], bis(organyl)(alkynyl) metal(IV) complexes have the *fac*-MC_3 configuration, and diorganometal(IV) complexes have the "*cis*-MC_2" configuration. Rare examples of transition metal complexes containing three classes of organyl donor [C(*sp*), C(sp^2), and C(sp^3)] are represented (**26**, **28**, and **56**), together with the "$Pt^{IV}C_4N_2$" motif (**26**, **28**). There are few well-characterised examples for each of the new classes of complex, suggesting that subtleties in reactivity remain to be detected and that new structural types and synthetic methods may be feasible.

Stoichiometric reactions of Pt^{II} and Pd^{II} complexes illustrate that the higher oxidation states are feasible as undetected intermediates in some organic synthesis procedures, as noted throughout this review, although some reaction protocols that achieve the higher oxidation state are not those proposed in catalysis. Of particular interest in platinum chemistry are the oxidative addition–reductive elimination sequence in (Eq. 3) and C–C reductive elimination reactions of Pt^{IV} phosphine complexes [**55**, **56** (Scheme 9)] as models for the transformation in (Eq. 2). For palladium, reaction of $IPh(C{\equiv}CSiMe_3)(OTf)$ with $Pd^{II}(NCN)(O_2CPh)$ to form a Pd^{IV} species **45** (Scheme 8) is a model for the reaction of "$IAr_2(X)/Pd^{II}$/N~CH" to form N~CAr via cyclopalladation, oxidation by $IAr_2(X)$, and C–C reductive elimination from Pd^{IV} [28, 65, 67, 68]; and for the initial oxidation step in reactions of $IAr_2(X)$ with alkenes mediated by pincer complexes such as **47** and $Pd^{II}(OTf)$\{2,6-$(Ph_2PO)_2C_6H_3$-*P*,*C*,*P*\}, the feasibility of the proposed intermediate "$Pd^{IV}(OTf)_2Ar$\{2,6-$(Ph_2PO)_2C_6H_3$-*P*,*C*,*P*\}" is also encouraged by detection of the bis(phosphine) species "$Pd^{IV}IC_3P_2$" (**54**) (Scheme 9).

Characterisation of binuclear **65** (Scheme 11) as an intermediate in oxidation of Pt^{II} to Pt^{IV} has been a timely discovery [24, 25], concurrent in 2009 with detection of symmetric binuclear Pd^{III}–Pd^{III} complexes that decompose by C–X bond

formation [80–83] and proposals that the reaction of "$IAr_2(X)/Pd^{II}$/N~CH" to form N~CAr referred to above may occur via related dimeric species [68].

The relatively unexplored field of higher oxidation state alkynylmetal (III/IV) chemistry of palladium and platinum, in particular when compared with alkylmetal (IV) chemistry, is providing fascinating examples of new motifs at higher oxidation state centres and model systems supporting proposed roles of the higher oxidation states in organic synthesis. Wider implications are also apparent. As one example of the potential for further exploration of alkynyl chemistry to probe mechanisms in organometallic chemistry, binuclear **67** (Scheme 11) is isoelectronic with a proposed unsymmetrical ion-pair "$(bpy)Me_2(PhS)Pt–PtMe_2(bpy)\cdot PhS$" intermediate in the reaction of $PtMe_2(bpy)$ with PhSSPh to form $Pt^{IV}(SPh)_2Me_2(bpy)$ [84].

Acknowledgements The authors acknowledge the Australian Research Council and the University of Tasmania for supporting our research over an extended period in higher oxidation state organometallic chemistry of palladium and platinum.

References

1. Belluco U, Bertani R, Michelin RA, Mozzon M (2000) J Organomet Chem 600:37
2. Long NJ, Williams CK (2003) Angew Chem Int Ed 42:2586
3. Gevorgyan V (2002) In: Negishi E-I (ed) Handbook of organopalladium chemistry for organic synthesis, vol 1. Wiley, New York, p 1463
4. Trost BM, Chan C, Ruhter G (1987) J Am Chem Soc 109:3486
5. Alper H, Saldana-Maldonado M (1989) Organometallics 8:1124
6. Catellani M, Marmiroli B, Chiara Fagnola M, Acquotti D (1996) J Organomet Chem 507:157
7. Herrmann WA, Reisinger C-P, Öfele K, Broβmer C, Beller M, Fischer H (1996) J Mol Catal A 108:51
8. Naka A, Okada T, Ishikawa M (1996) J Organomet Chem 521:163
9. Trost BM, Sorum MT, Chan C, Harms AE, Rühter G (1997) J Am Chem Soc 119:698
10. Fuhrmann G, Debaerdemaeker T, Bäuerle P (2003) Chem Commun 948
11. Ammann M, Rang A, Schalley CA, Bäuerle P (2006) Eur J Org Chem 1940
12. Bäuerle P, Ammann M, Wilde M, Götz G, Mena-Osteritz E, Rang A, Schalley CA (2007) Angew Chem Int Ed 46:363
13. Jagadeesh MN, Thiel W, Köhler J, Fehn A (2002) Organometallics 21:2076
14. Geisenberger J, Nagel U, Sebald A, Beck W (1983) Chem Ber 116:911
15. James SL, Younus M, Raithby PR, Lewis J (1997) J Organomet Chem 543:233
16. Janzen MC, Jenkins HA, Jennings MC, Rendina LM, Puddephatt RJ (1999) J Chem Soc Dalton Trans 1713
17. Janzen MC, Jenkins HA, Jennings MC, Rendina LM, Puddephatt RJ (2002) Organometallics 21:1257
18. Canty AJ, Rodemann T (2003) Inorg Chem Commun 6:1382
19. Canty AJ, Rodemann T, Skelton BW, White AH (2005) Inorg Chem Commun 8:55
20. Canty AJ, Rodemann T, Skelton BW, White AH (2006) Organometallics 25:3996
21. Canty AJ, Rodemann T, Ryan JH (2008) Adv Organomet Chem 55:279
22. Canty AJ, Watson RP, Karpiniec SS, Rodemann T, Gardiner MG, Jones RC (2008) Organometallics 27:3203
23. Munro-Leighton C, Feng Y, Zhang J, Alsop NM, Gunnoe TB, Boyle PD, Peterson JL (2008) Inorg Chem 47:6124

24. Canty AJ, Gardiner MG, Jones RC, Rodemann T, Sharma M (2009) J Am Chem Soc 131:7236
25. Canty AJ (2009) Dalton Trans 10409
26. Manna J, John KD, Hopkins HD (1995) Adv Organomet Chem 38:79
27. Louwen JN, Hengelmolen R, Grove DM, Oskam A, DeKock RL (1984) Organometallics 3:908
28. Deprez NR, Sanford MS (2007) Inorg Chem 46:1924
29. Datta Chaudhuri P, Guo R, Malinakova HC (2008) J Organomet Chem 693:567
30. Muñiz K (2009) Angew Chem Int Ed 48:9412
31. Benito J, Berenguer JR, Forniés J, Gil B, Gómez J, Lalinde E (2003) Dalton Trans 4331
32. Morisaki Y, Chen H, Chujo Y (2004) J Organomet Chem 689:2684
33. Chan CKM, Tao C-H, Tam H-L, Zhu N, Yam VW-W, Cheah K-W (2009) Inorg Chem 48:2855
34. Sebald A, Stader C, Wrackmeyer B, Bensch W (1986) J Organomet Chem 311:233
35. Lavastre O, Plass J, Bachmann P, Guesmi S, Moinet C, Dixneuf PH (1997) Organometallics 16:184
36. Hua F, Kinayyigit S, Rachford AA, Shikhova EA, Goeb S, Cable JR, Adams CJ, Kirschbaum K, Pinkerton AA, Castellano FN (2007) Inorg Chem 46:8771
37. Hua F, Kinayyigit S, Cable JR, Castellano FN (2006) Inorg Chem 45:4304
38. Yam VW-W, Tang RP-L, Wong KM-C, Cheung K-K (2001) Organometallics 20:4476
39. Wong KM-C, Tang W-S, Chu BW-K, Zhu N, Yam VW-W (2004) Organometallics 23:3459
40. Chakraborty S, Wadas TJ, Hester H, Flaschenreim C, Schmehl R, Eisenberg R (2005) Inorg Chem 44:6284
41. Shikhova E, Danilov EO, Kinayyigit S, Pomestchenko IE, Tregubov AD, Camerel F, Retailleau P, Ziessel R, Castellano FN (2007) Inorg Chem 46:3038
42. Jarosz P, Lotito K, Schneider J, Kumaresan D, Schmehl R, Eisenberg R (2009) Inorg Chem 48:2420
43. Jarosz P, Du P, Schneider J, Lee S-H, McCamant D, Eisenberg R (2009) Inorg Chem 48:9653
44. Tam AY-Y, Lam WH, Wong KM-C, Zhu N, Yam VW-W (2008) Chem Eur J 14:4562
45. Garner KL, Parkes LF, Piper JD, Williams JAG (2010) Inorg Chem 49:476
46. Chong SH-F, Lam SC-F, Yam VW-W, Zhu N, Cheung K-K, Fathallah S, Costuas K, Halet J-F (2004) Organometallics 23:4924
47. Sato M, Mogi E, Katada M (1995) Organometallics 14:4837
48. Sato M, Mogi E (1996) J Organomet Chem 508:159
49. Sato M, Mogi E, Kumakura S (1995) Organometallics 14:3157
50. Canty AJ, Patel J, Skelton BW, White AH (2000) J Organomet Chem 599:195
51. Lu W, Mi B-X, Chan MCW, Hui Z, Che C-M, Zhu N, Lee S-T (2004) J Am Chem Soc 126:4958
52. Schneider J, Du P, Jarosz P, Lazarides T, Wang X, Brennessel WW, Eisenberg R (2009) Inorg Chem 48:4306
53. Back S, Gossage RA, Lutz M, del Río I, Spek AL, Lang H, van Koten G (2000) Organometallics 19:3296
54. Back S, Lutz M, Spek AL, Lang H, van Koten G (2001) J Organomet Chem 620:227
55. van Beek JAM, van Koten G, Smeets WJJ, Spek AL (1986) J Am Chem Soc 108:5010
56. Nesmeyanov AN, Chapovsky YA, Polovyanyuk IV, Makarova LG (1967) J Organomet Chem 7:329
57. Battioni J-P, Dupré D, Delaforge M, Jaouen M, Mansuy D (1988) J Organomet Chem 358:389
58. Wei C-H, Bockman TM, Kochi JK (1992) J Organomet Chem 428:85
59. Makioka Y, Fujiwara Y, Kitamura T (2000) J Organomet Chem 611:509
60. Ochiai M, Kunishima M, Nagao Y, Fuji K, Fujita E (1987) J Chem Soc Chem Commun 1708
61. Stang PJ, Zhdankin VV (1996) Chem Rev 96:1123
62. Grushin VV (1992) Acc Chem Res 25:529
63. Szabó KJ (2010) J Mol Catal A 324:56
64. Aydin J, Larsson JM, Selander N, Szabó KJ (2009) Org Lett 11:2852

65. Kalyani D, Deprez NR, Desai LV, Sanford MS (2005) J Am Chem Soc 127:7330
66. Deprez NR, Kalyani D, Krause A, Sanford MS (2006) J Am Chem Soc 128:4972
67. Kalberer EW, Whitfield SR, Sanford MS (2006) J Mol Catal A Chem 251:108
68. Deprez NR, Sanford MS (2009) J Am Chem Soc 131:11234
69. Datta Chaudhuri P, Guo R, Malinakova HC (2008) J Organomet Chem 693:567
70. Malinakova HC (2011) Palladium(IV) Complexes as intermediates in catalytic and stoichiometric cascade sequences providing complex carbocycles and heterocycles. Top Organomet Chem 35:85–110
71. Bondi A (1964) J Phys Chem 68:441
72. Bayler A, Canty AJ, Ryan JH, Skelton BW, White AH (2000) Inorg Chem Commun 3:575
73. Canty AJ, Patel J, Rodemann T, Ryan JH, Skelton BW, White AH (2004) Organometallics 23:3466
74. Yamaguchi T, Kubota O, Ito T (2004) Chem Lett 33:190
75. Baxter LAM, Heath GA, Raptis RG, Willis AC (1992) J Am Chem Soc 114:6944
76. Rasmussen PG, Anderson JE, Bailey OH, Tamres M (1985) J Am Chem Soc 107:279
77. Huang H, Rheingold AL, Hughes RP (2009) Organometallics 28:1575
78. Yamaguchi T, Yamazaki F, Ito T (1999) J Am Chem Soc 121:7405
79. Moret M-E, Chen P (2009) J Am Chem Soc 131:5675
80. Powers DC, Ritter T (2009) Nat Chem 1:302
81. Powers DC, Geibel MAL, Klein JEMN, Ritter T (2009) J Am Chem Soc 131:17050
82. Powers DC, Ritter T (2011) Palladium(III) in synthesis and catalysis. Top Organomet Chem 35:129–156
83. Powers DC, Benitez D, Tkatchouk E, Goddard WA, Ritter T (2010) J Am Chem Soc 132:14092–14103
84. Bonnington KJ, Jennings MC, Puddephatt RJ (2008) Organometallics 27:6521

Top Organomet Chem (2011) 35:129–156
DOI: 10.1007/978-3-642-17429-2_6

Palladium(III) in Synthesis and Catalysis

David C. Powers and Tobias Ritter

Abstract While the organometallic chemistry of Pd in its (0), (+II), and (+IV) oxidation states is well established, organometallic Pd(III) chemistry remains widely unexplored. Few characterized Pd(III) complexes are known, which has inhibited detailed study of the organometallic chemistry of Pd(III). In this review, the potential roles of both mono- and dinuclear Pd(III) complexes in organometallic chemistry are discussed. While not widely recognized, Pd in the (+III) oxidation state may play a significant role in a variety of known Pd-catalyzed reactions.

Keywords Bimetallic redox chemistry · C–H functionalization · Metal–metal bonding · Pd(III)

Contents

D.C. Powers and T. Ritter (✉)
Department of Chemistry and Chemical Biology, Harvard University, 12 Oxford Street, Cambridge, MA 02138, USA
e-mail: ritter@chemistry.harvard.edu

1 Introduction

Palladium is among the most widely used metals for catalysis in organic chemistry, and the fundamental organometallic chemistry of palladium in the (0), (+II), and (+IV) oxidation states has been well studied [1]. Organometallic Pd(I) complexes, while relatively less common, have been employed as precatalysts in organic synthesis [2–4]. By comparison, the organometallic chemistry of Pd(III) remains in its infancy. Few authentic Pd(III) complexes are known and the potential role of Pd(III) in catalysis is only now beginning to be elucidated. Herein, we review the organometallic chemistry of Pd(III) and discuss the relevance of Pd(III) intermediates to Pd-catalyzed processes. We review the organometallic chemistry of well-defined, isolated Pd(III) complexes, as well as organometallic chemistry in which the potential role of Pd(III) intermediates is currently more speculative. On the basis of the reports discussed herein, Pd(III) may be much more prevalent in Pd-catalyzed processes than has generally been recognized.

2 Mononuclear Pd(III) Chemistry

2.1 Mononuclear Pd(III) Werner-Type Complexes

Palladium(II) has a d^8 electronic configuration and mononuclear Pd(II) complexes are generally square planar (Fig. 1) [5]. Metal-based oxidation of mononuclear Pd (II) complexes by one electron should result in paramagnetic, low-spin d^7, tetragonally distorted octahedral Pd(III) complexes [6]. Further one-electron oxidation should afford octahedral d^6 Pd(IV) complexes [5].

Unlike complexes based on Pt(III) [7–15], compounds containing Pd(III) are rare. A compound with the empirical formula PdF_3 was originally proposed to contain Pd(III) [16, 17], but was subsequently shown to be more appropriately formulated as $Pd^{2+}[PdF_6]^{2-}$ and contain Pd(II) and Pd(IV) [18, 19]. The polyatomic anions PdF_4^- and PdF_6^{3-} have been prepared by solid-state synthesis [20–22]. Mononuclear coordination complexes containing Pd(III) have been observed by

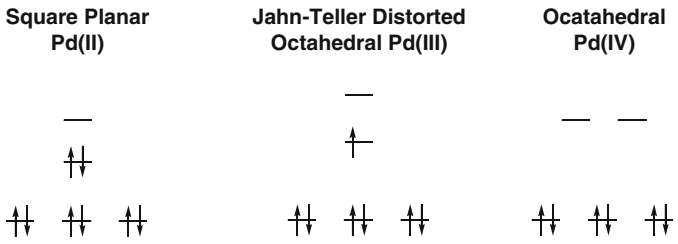

Fig. 1 Electronic structure of mononuclear Pd(II), Pd(III), and Pd(IV)

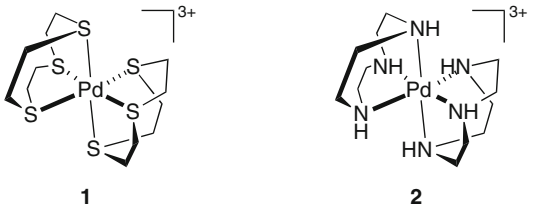

Fig. 2 Crystallographically characterized examples of mononuclear Pd(III) Werner-type complexes

electrochemical measurements as well as EPR spectroscopy [23–30], although assignment of these complexes as containing Pd(III), and not Pd(II) with a singly oxidized ligand framework, has been the source of continuing discussion [31–34]. In 2010, the (+III) oxidation state of Pd was stabilized in a mixed Ni/Pd oligomeric M–X–M–X chain of the formulation $[Ni_{1-x}Pd_x(chxn)Br]Br_2$ (chxn = (1*R*,2*R*)-cyclohexanediamine) by electrochemical oxidation of a mixture of $[Ni(chxn)_2]Br_2$ and $[Pd(chxn)_2]Br_2$ [35, 36].

Two mononuclear Werner-type complexes based on Pd(III) have been characterized by X-ray crystallography. The X-ray crystal structure of mononuclear Pd (III) complex **1**, in which the Pd(III) center is supported by two 1,4,7-trithiacyclononane ligands, was reported in 1987 (Fig. 2) [37–39]. An analogous complex (**2**), supported by 1,4,7-triazacyclononane ligands, was reported a year later [40]. Both complexes contain distorted octahedral Pd centers, as expected for low-spin d^7 Pd (III) [6]. Detailed examination of the electrochemical and spectroscopic properties of Pd(III) complexes supported by macrocyclic polydentate ligands has indicated that the unpaired electron in **1** and **2** resides predominantly in the $4d_{z^2}$ orbital [41–46].

2.2 Mononuclear Pd(III) Complexes in Catalysis

2.2.1 Pd(III) in Pd-Catalyzed Oxidative C–H Coupling Reactions

Palladium is a versatile transition metal for the catalysis of various carbon–carbon and carbon–heteroatom cross-coupling reactions [1]. Traditional C–C cross-coupling reactions employ prefunctionalized substrates – typically containing C–X (X = Cl, Br, I, OTf) and C–M (M = B, Sn, Zn, Mg) bonds, respectively – and are generally accepted to proceed through Pd(0)/Pd(II) catalysis cycles [47]. Direct oxidative coupling of arene C–H bonds has the potential to generate the products of traditional cross-coupling chemistry without the need for prefunctionalized reaction partners (Fig. 3a) [48–53]. A general catalysis cycle for such an oxidative coupling of aryl C–H bonds is outlined in Fig. 3b. Initial C–H palladation at Pd(II) (**3**) would generate an aryl Pd(II) complex (**4**). Subsequently, a second C–H palladation could afford a heteroleptic biaryl Pd(II) complex (**5**), poised to undergo C–C bond-forming reductive elimination. Reoxidation of the thus formed

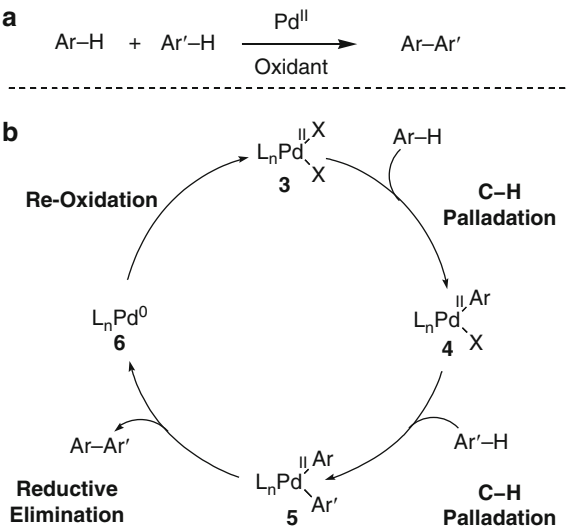

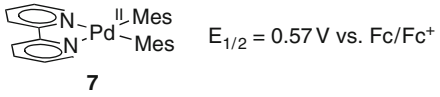

7

Fig. 3 Generic Pd(0)/Pd(II) catalysis cycle for oxidative C–H cross-coupling

Fig. 4 *Bis*-mesityl Pd(II) complex **7**, an analog of intermediate **5**, shows a reversible one-electron oxidation wave for the Pd(II)/Pd(III) couple at 0.57 V

Pd(0) to Pd(II) by an external oxidant would close the catalysis cycle. While biaryl Pd(II) intermediate **5** is typically proposed to undergo direct C–C reductive elimination, in the presence of an external oxidant, **5** could potentially be oxidized to a higher-valent species prior to the C–C bond-forming event [54, 55].

Single-electron oxidation of biaryl Pd(II) complexes to afford Pd(III) species was observed during the electrochemical oxidation of *bis*-mesityl Pd(II) complex **7** (Fig. 4) [56]. Complex **7**, which can be viewed as a model for oxidative C–H coupling intermediate **5** (Fig. 3), undergoes a one-electron oxidation at 0.57 V, assigned to the Pd(II)/Pd(III) redox couple.

Oxidative C–H coupling reactions are frequently carried out in the presence of Ag(I) additives [57–64]. As described below, due to (1) the demonstrated availability of one-electron oxidation processes for compounds such as **7** [56], (2) the propensity of Ag(I) to facilitate one-electron oxidative cleavage of Pd–C bonds [65] (*vide infra*), and (3) the frequency with which Ag(I) additives are employed in Pd-catalyzed cross-coupling chemistry [57–64], the reaction chemistry of Ag(I) salts with organometallic Pd(II) complexes has received experimental scrutiny.

In 2001, Milstein studied the reactivity of Pd(II) aryl complex **8** with one-electron oxidants galvinoxyl radical and AgOTf (Fig. 5) [66]. Treatment of Pd(II)

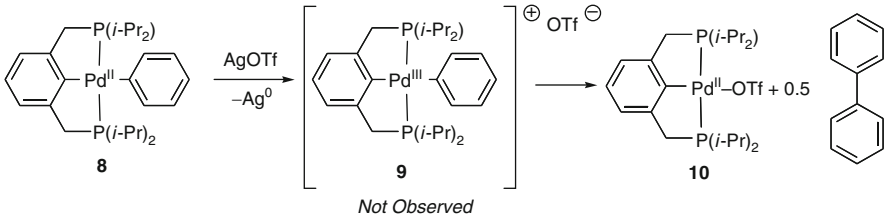

Fig. 5 Treatment of Pd(II) complex **8** with AgOTf generates Pd(II) complex **10** and biphenyl

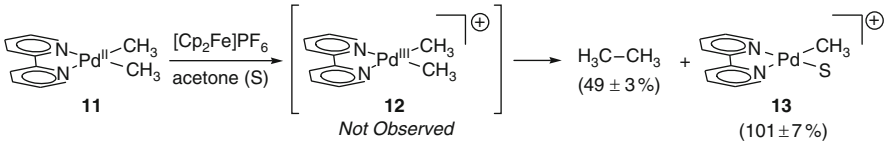

Fig. 6 Treatment of Pd(II) complex **11** with $[Cp_2Fe]PF_6$ (Fc^+) affords ethane and **13**

aryl complex **8** with AgOTf resulted in the formation of biphenyl along with Pd(II) triflate **10**. Similar reactivity was observed upon treatment of **8** with galvinoxyl radical. Milstein proposed that this oxidant-induced reductive coupling of aryl ligands proceeds through Pd(III) intermediate **9**. The authors speculated that Pd (III) aryl intermediate **9** may be better formulated as a Pd(II) complex with a pendant aryl radical ligand, generated by inner-sphere ligand-to-metal electron transfer. No organic products resulting from coupling of free organic radicals with solvent were observed, suggesting that biphenyl is not produced by radical combination of phenyl radicals generated by Pd–C bond homolysis. This observation led to the suggestion that intermediate **9** may be an aryl-bridged dinuclear complex, which can liberate biphenyl without the intermediacy of free radical chemistry [67].

The oxidatively induced reductive coupling of methyl ligands to afford ethane from Pd(II) dimethyl complex **11** was reported in 2009 by Mayer and Sanford [68]. Treatment of dimethyl Pd(II) complex **11** with ferrocenium hexafluorophosphate ($[Cp_2Fe]PF_6$; Fc^+), an outer-sphere, single-electron oxidant, led to the formation of ethane along with cationic Pd(II) complex **13** (Fig. 6). Based on the electrochemical study of closely related *bis*-mesityl Pd(II) complex **7** (Fig. 4) [56], the observed ethane formation was proposed to proceed via initial single-electron oxidation of **11** to Pd(III) complex **12**.

Three mechanisms for the formation of ethane from **12** were considered (Fig. 7). In mechanism A, Pd(III) complex **12** undergoes Pd–C bond homolysis to afford Pd (II) complex **13** and a methyl radical. Subsequent radical combination generates ethane. Similar Pd–C bond homolysis following single-electron oxidation was proposed by Trogler during an independent study of the oxidation chemistry of Pd(II) methyl complexes with Fc^+ [65]. In mechanism B, direct reductive elimination from **12** affords ethane and mononuclear Pd(I) complex **14**, which further reacts with **11** and Fc^+ to generate Pd(II) complex **13**. Analogous chemistry has been proposed for coupling reactions from organonickel complexes [69–75].

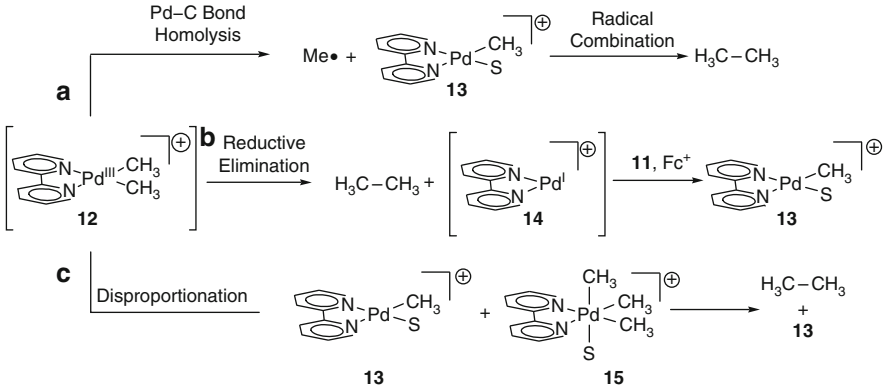

Fig. 7 Mechanisms considered for the formation of ethane from Pd(III) complex **12**

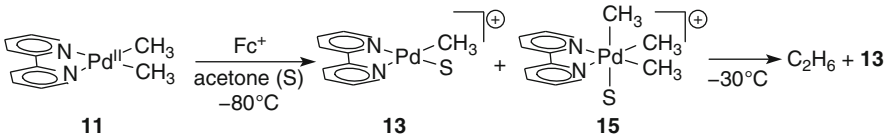

Fig. 8 Pd(II) complex **13** and Pd(IV) complex **15** were observed following oxidation of **11** with Fc^+ at –80°C

In mechanism C, two equivalents of complex **12** undergo disproportionation to afford Pd(II) complex **13** and Pd(IV) intermediate **15**. Subsequent reductive elimination from **15** generates ethane and Pd(II) complex **13**. Similar disproportionation has been proposed from Pt(III) dimethyl complexes [76].

The observation that ethane formation is uninhibited by radical traps such as 1,4-cyclohexadiene and styrene suggests that ethane is not formed by combination of free methyl radicals and is inconsistent with free radical pathway A. To differentiate between pathways B and C, the oxidation of **11** with Fc^+ was carried out at low temperature in order to observe potential reaction intermediates. Treatment of **11** with Fc^+ at –80°C led to the observation of Pd(II) complex **13** and Pd(IV) complex **15** (Fig. 8). Subsequent warming to –30°C led to the formation of ethane. On the basis of these observations, the authors concluded that pathway C is likely responsible for the formation of ethane in the reaction of **11** with Fc^+.

The chemistry of complex **11** with $AgPF_6$ was evaluated because Ag(I) is a common additive in Pd-catalyzed oxidative C–H coupling reactions [57–64] and a potential one-electron oxidant, similar to Fc^+. Treatment of dimethyl Pd(II) complex **11** with $AgPF_6$ resulted in the immediate formation of an intermediate (**16**), as observed by ^1H NMR spectroscopy, which subsequently generated **13**, ethane, and Ag mirror (Fig. 9). The authors proposed that Ag(I) acts as an inner-sphere one-electron oxidant. Initial coordination of Ag(I) to Pd to generate **16**, followed by electron transfer, would furnish proposed Pd(III) intermediate **12**. Disproportionation of Pd(III) intermediate **12** to Pd(II) complex **13** and Pd(IV) intermediate **15**

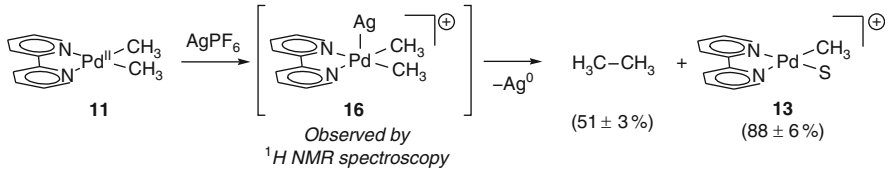

Fig. 9 Treatment of **11** with $AgPF_6$ results in the formation of an intermediate, assigned as **16**, which subsequently generates ethane and **13**

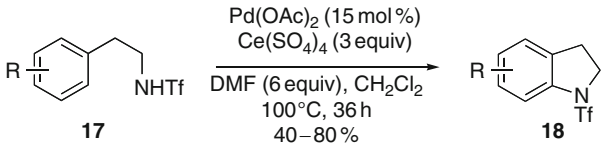

Fig. 10 Pd-catalyzed C–H amidation reported by Yu

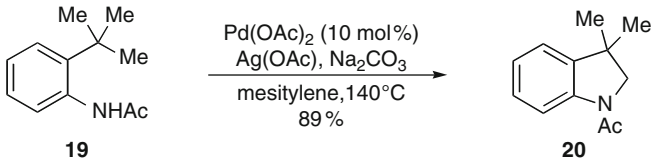

Fig. 11 Pd-catalyzed C–H amidation reported by Glorius

followed by reductive elimination from Pd(IV) complex **15**, as was proposed in the oxidation of **11** with Fc^+, would then generate the observed reaction products.

2.2.2 Pd(III) in Pd-Catalyzed Oxidative Carbon–Heteroatom Bond-Forming Reactions

In 2009, two reports disclosed the use of single-electron oxidants in intramolecular Pd-catalyzed C–H amidation reactions. Yu and coworkers disclosed a Pd-catalyzed *N*-triflyl indoline (**18**) synthesis from *N*-triflyl phenethylamines (**17**) using single-electron oxidant $Ce(SO_4)_2$ (Fig. 10) [77]. The authors proposed that this reaction proceeds through initial oxidation of Pd(II) to Pd(III). Glorius and coworkers reported a Pd-catalyzed *N*-acyl indoline (**20**) synthesis from *N*-acyl anilines (**19**) in the presence of AgOAc (Fig. 11) [78]. While the authors favored a Pd(0)/Pd(II) catalysis cycle, they noted that the intermediacy of higher-valent Pd species could not be discounted given that AgOAc can serve as a single-electron oxidant.

Many questions remain to be addressed regarding the mechanisms of these amidation reactions. Primarily, are high-valent Pd intermediates involved or are classical Pd(0)/Pd(II) catalysis cycles operative? If single-electron oxidation affords Pd(III) intermediates, does C–N bond formation proceed directly from

Pd(III) or are Pd(IV) species, generated by either disproportionation of Pd(III) or further oxidation of Pd(III) to Pd(IV), the competent intermediates for C–N bond formation? Are potential high-valent intermediates mononuclear or is more than one palladium present during oxidation? Answers to these questions provide insights into the potential role of high-valent Pd complexes in C–H amidation reactions.

2.2.3 Pd(III) in Kumada and Negishi Coupling Reactions

Knochel has noted remarkable rate accelerations for both Kumada [79] and Negishi [80] coupling reactions when performed in the presence of isopropyl iodide (Fig. 12).

Oxidative addition of Pd(0) to isopropyl iodide has been shown to proceed via initial single-electron transfer to generate transient Pd(I) intermediates and isopropyl radicals [81, 82]. On the basis of a positive isopropyl iodide-induced radical-clock experiment (Fig. 13), Knochel suggested that the observed rate acceleration in Kumada coupling reactions is due to the participation of a radical pathway and proposed a radical mechanism involving Pd(I) and Pd(III) radical chain carriers (Fig. 14). The proposal of Pd(III) intermediates in Kumada coupling reactions is, to the best of our knowledge, the only proposal of Pd(III) intermediates under reducing conditions.

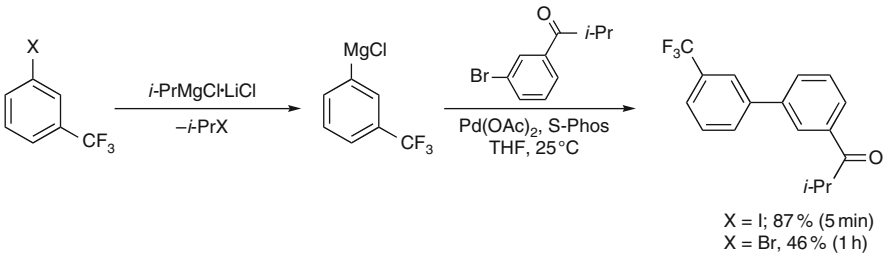

Fig. 12 Isopropyl iodide-catalyzed Kumada coupling reported by Knochel

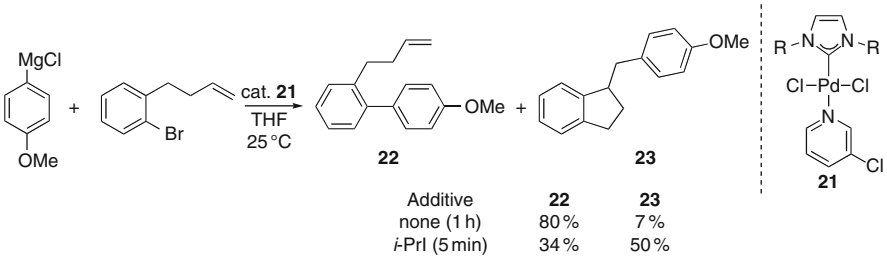

Fig. 13 Observation of isopropyl iodide-induced radical clock (R = 2,6-di-*i*-Pr-C_6H_3)

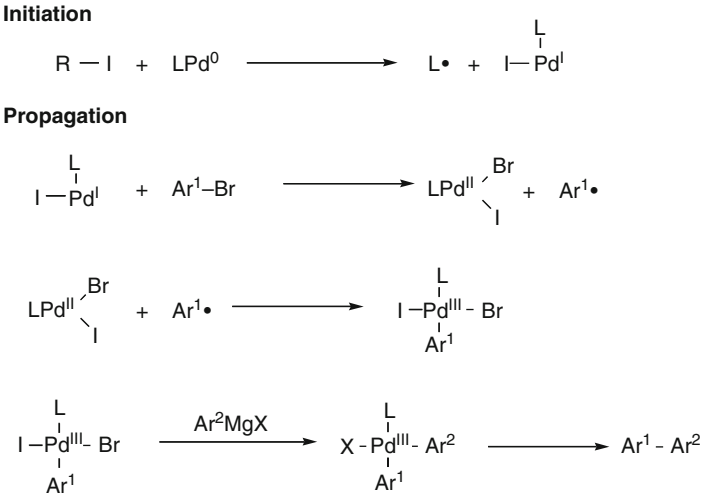

Fig. 14 Mechanism proposed to account for the rate acceleration of cross-coupling observed in the presence of radical promoters

2.2.4 Pd(III) Intermediates in O_2 Insertion Reactions

Goldberg and coworkers proposed Pd(III) intermediates during an investigation of the reaction of dimethyl Pd(II) complex **24** with O_2 (Fig. 15) [83].

Consistent with a radical chain mechanism, the rate of O_2 insertion was found to be sensitive to light, and the addition of radical initiator AIBN was required in order to observe reproducible reaction rates. Based on analysis of the kinetics of O_2 insertion into the Pd–C bond of **24**, a mechanism involving mononuclear Pd(III) intermediates was proposed (Fig. 16). Palladium(III) intermediate **27**, formed by the combination of dimethyl Pd(II) complex **24** with peroxy radical **26** [84], generates the observed Pd(II) peroxide **25** by homolytic Pd–C cleavage to reduce Pd(III) complex **27** and generate radical chain carrier $Me^{\bullet}$.

The mechanism of O_2 insertion into the Pd–C bond of **24** differs from the autoxidation of organic substrates due to the ability of Pd to attain high oxidation state intermediates. In hydrocarbon autoxidation, peroxy radical abstracts hydrogen without the intermediacy of hypervalent intermediates. In the oxidation of **24**, the coordination number of Pd is proposed to increase from four to five upon reaction of Pd(II) complex **24** with peroxy radical (**26**).

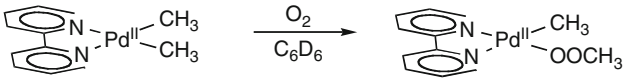

24 **25**

Fig. 15 Pd(II) peroxide **25** is obtained by insertion of O_2 into the Pd–C bond of **24**

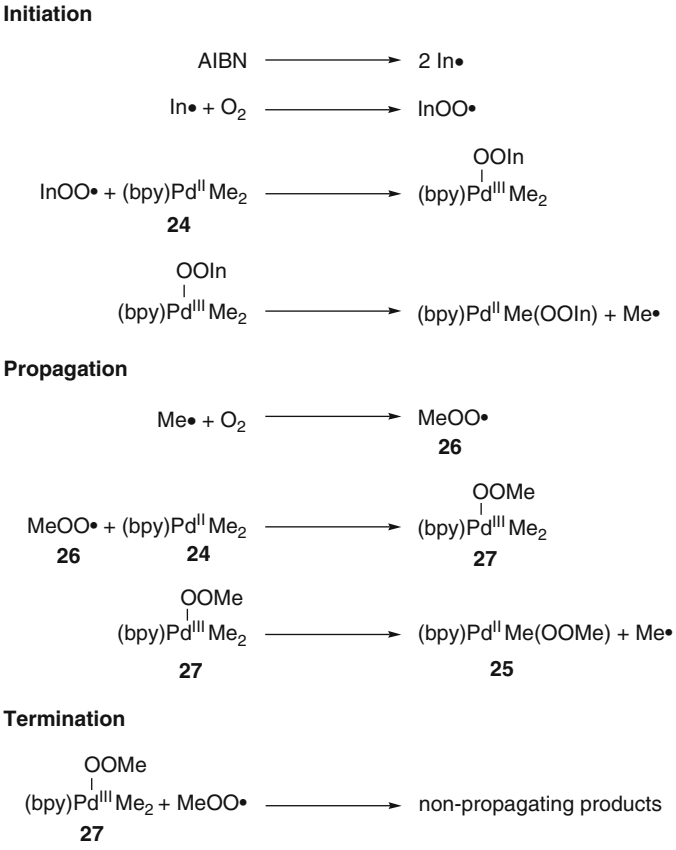

Fig. 16 Proposed mechanism for the insertion of O_2 into the Pd–C bond of **24**

2.3 Organometallic Chemistry of Isolated Pd(III) Complexes

The first example of organometallic chemistry from isolated, well-defined mononuclear Pd(III) complexes was reported by Mirica in 2010 [85]. Organometallic Pd(III) complexes **30** and **31** were prepared by controlled bulk electrolysis of Pd(II) precursors **28** and **29**, respectively (Fig. 17). Complex **33** was prepared by chemical oxidation of **32** with Fc^+. X-ray crystallographic analysis of **30**, **31**, and **33** revealed tetragonally distorted octahedral complexes, consistent with the expected Jahn–Teller distortion for mononuclear, low-spin Pd(III) complexes [6]. A combination of EPR spectroscopy and computational results suggests that the unpaired electron resides in the $4d_{z^2}$ orbital, consistent with the MO description of octahedral Pd(III) in Fig. 1.

Photolysis of **30** afforded a mixture of ethane, methane, and methyl chloride, along with Pd(II) complex **34** (Fig. 18).

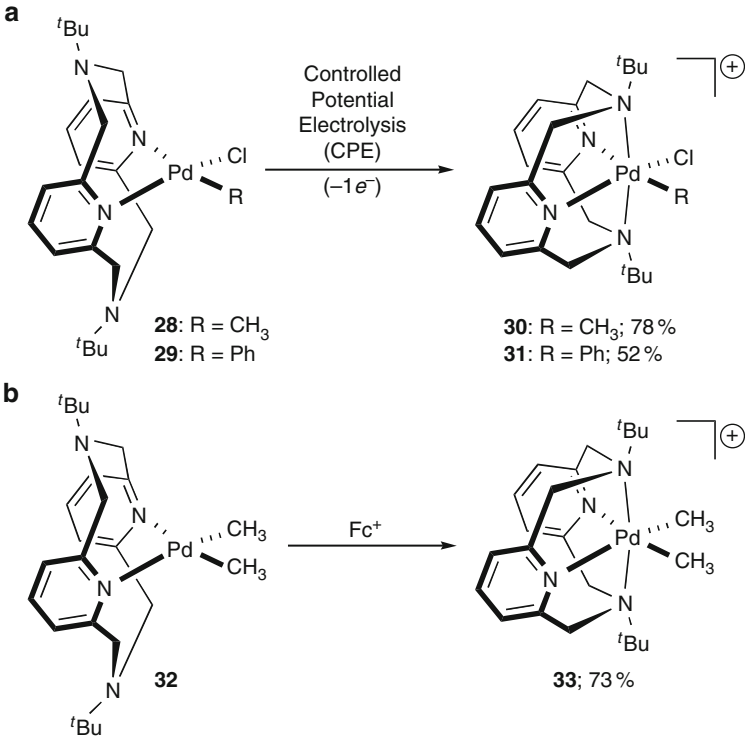

Fig. 17 **a**) Mononuclear Pd(III) complexes **30** and **31** were prepared by controlled potential electrolysis (CPE) of **28** and **29**, respectively. **b**) Complex **33** was prepared by oxidation of **32** with Fc^+

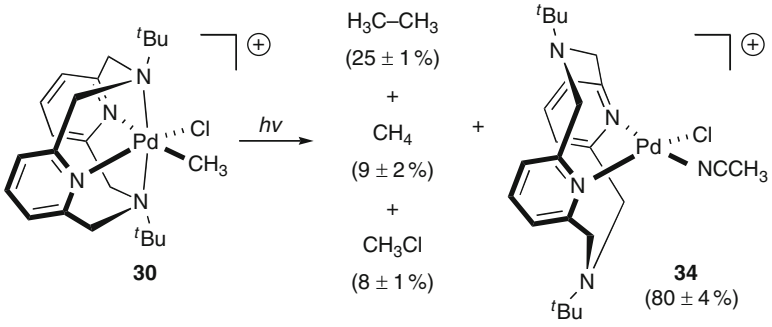

Fig. 18 Photolysis of Pd(III) complex **30** generated ethane, methane, methyl chloride, and Pd(II) complex **34**

The addition of radical scavengers, such as TEMPO, suppressed the formation of ethane, methane, and methyl chloride, instead leading only to the observation of TEMPO-Me (**35**) and Pd(II) complex **34** (Fig. 19). The observed reaction with radical scavengers is consistent with photo-induced homolytic Pd–C bond cleavage

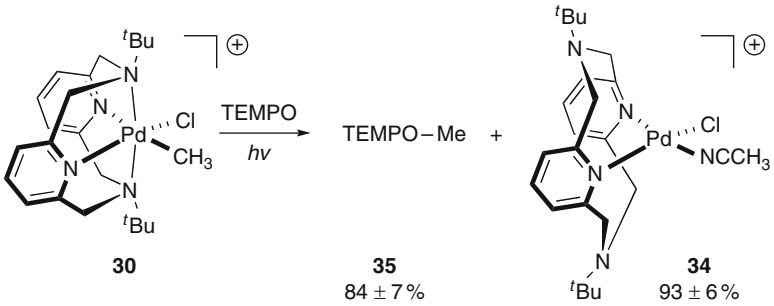

30 **35** 84 ± 7 % **34** 93 ± 6 %

Fig. 19 Photolysis in the presence of radical scavenger TEMPO suppressed formation of ethane, methane, and methyl chloride

as the operative pathway for the formation of the observed organic products, although the observed organic products may also arise from radical combination of $Me^{\bullet}$ with **30** to afford a transient Pd(IV) intermediate, which subsequently generates the observed products.

3 Dinuclear Pd(III) Chemistry

3.1 Dinuclear Pd(III) Complexes

Palladium(II) has a d^8 electronic configuration; the HOMO of mononuclear Pd(II) complexes is typically the d_{z^2} orbital (Fig. 1) [5]. When two palladium nuclei are held in proximity such that electronic communication between the two metals is possible, mixing of the *d* orbitals gives rise to the qualitative molecular orbital picture in Fig. 20 [86]. Bonding and antibonding interactions result from mixing of the d_{z^2}, d_{xy}, d_{xz}, and d_{yz}orbitals; the $d_{x^2-y^2}$ is predominantly metal–ligand bonding and does not significantly participate in metal–metal bonding interactions.

3.1.1 Dinuclear Pd(II) Complexes

Both the metal–metal σ and σ* orbitals should be filled for dinuclear Pd(II) complexes (Fig. 20). On the basis of these considerations alone, no attractive metal–metal interaction is expected; there is no Pd–Pd bond [87]. Second-order, symmetry-allowed mixing of the Pd d_{z^2} orbital with the $5p_z$ and the 5*s* orbital, however, perturbs the molecular orbital diagram based only on *d* orbital interactions [88–91]. In 2010, an evaluation of the bonding interactions between the Pd centers in acetate-bridged, dinuclear Pd(II) complex **36** was reported (Fig. 21) [88]. On the basis of DFT calculations, the authors predicted a weak attractive interaction between the Pd centers in **36** and computed a Pd–Pd bond order of 0.11.

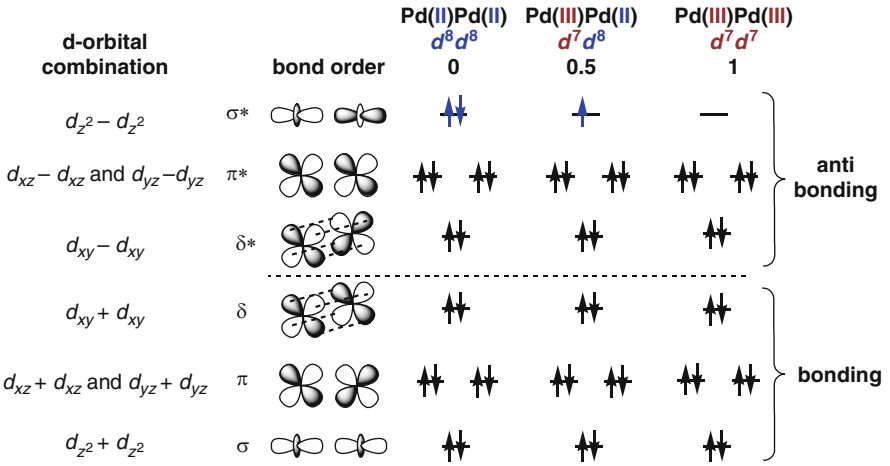

Fig. 20 Qualitative molecular orbital diagram for electronically coupled dinuclear Pd complexes based on *d*-orbital mixing. Oxidation of dinuclear Pd(II) complexes can result in the formation of metal–metal bonds

Fig. 21 Acetate-bridged dinuclear Pd(II) complex **36** is computed to have a Pd–Pd bond order of 0.11, arising from mixing of the $5p_z$ and 5*s* orbitals with the 4*d* orbitals

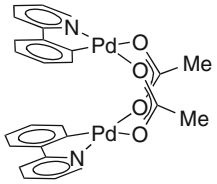

36

Computed Pd–Pd Bond Order: 0.11

3.1.2 Pd(II)/Pd(III) Mixed Valence Complexes

Oxidation of dinuclear Pd(II) complexes by one electron is predicted to afford dinuclear Pd(II)/Pd(III) mixed valence complexes with a Pd–Pd bond order of 0.5 (Fig. 20) [92]. Dinuclear Pd(II)/Pd(III) mixed valence complexes have been detected by EPR spectroscopy, although, similar to mononuclear systems, the unpaired electron is not always metal-centered [87, 93]. Two examples of dinuclear Pd(II)/Pd(III) complexes bearing a metal-centered unpaired electron have been reported [94, 95]. In 1988, Bear reported the EPR spectrum of tetrabridged dinuclear complex **38**, prepared by electrochemical oxidation of **37** (Fig. 22a) [95]. In 2007, Cotton reported the only crystallographically characterized mixed valence Pd (II)/Pd(III) complex (**40**; Fig. 22b) [94]. Both **38** and **40** are paramagnetic and have EPR spectra consistent with a metal-based oxidation. The metal– metal distance in **40** is 0.052 Å shorter than the corresponding distance in Pd(II) complex **39**, consistent with a Pd–Pd bond order of 0.5.

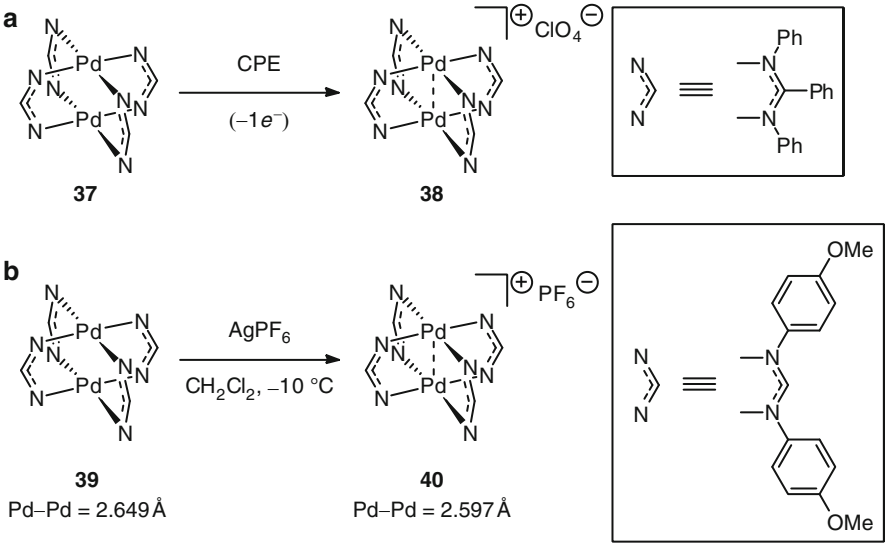

Fig. 22 (**a**) Electrochemical oxidation of **37** afforded mixed valence Pd(II)/Pd(III) complex **38**. (**b**) One-electron oxidation of **39** with $AgPF_6$ afforded **40**. The Pd–Pd distance in **40** is consistent with a Pd–Pd bond order of 0.5

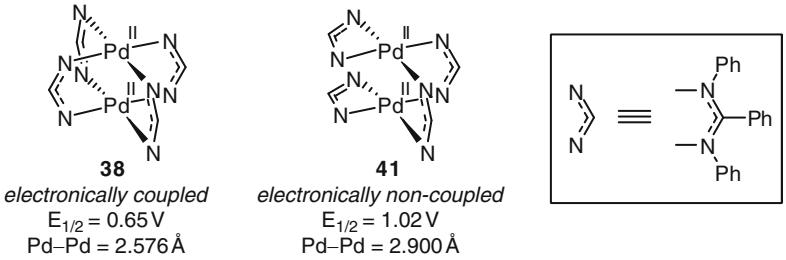

Fig. 23 The HOMO of **38**, in which the Pd centers are electronically coupled, is 370 mV higher in energy than the HOMO of **41**, in which the palladium centers are not electronically coupled

Elegant electrochemical studies related to Bear's report of dinuclear Pd(II)/Pd(III) mixed valence complex **38** emphasize an important difference between the oxidation chemistry of mono- and dinuclear complexes. The electrochemistry of complex **38**, bearing four bridging ligands, and **41**, in which two ligands are bridging and two are chelating, was studied (Fig. 23) [95]. Complex **41** displays oxidation behavior consistent with two electronically isolated Pd centers; a single two-electron oxidation wave was observed at 1.02 V. By contrast, complex **38** displays electrochemical behavior consistent with electronically coupled metal centers; a one-electron oxidation wave is observed at 0.65 V. On the basis of these electrochemical measurements, it was concluded that the electronic interaction between two palladium centers raises the HOMO energy by 370 mV and renders the dinuclear complex easier to oxidize than the complex with noninteracting metal centers. The disparate electrochemical

behavior of **38** and **41** is likely a reflection of relative distances between the Pd centers (in **38**, Pd–Pd = 2.576 Å; in **41**, Pd–Pd = 2.900 Å) [92, 96].

3.1.3 Dinuclear Pd(III) Complexes

Oxidation of dinuclear Pd(II) complexes by two electrons can result in dinuclear Pd(III) complexes with a metal–metal σ bond (Fig. 20). Cotton reported the first dinuclear Pd(III) complex (**43**) in 1998 (Fig. 24) [97]. Complex **43** was obtained by oxidation of dinuclear Pd(II) complex **42** with $PhICl_2$ and is diamagnetic, consistent with the formation of a spin-paired Pd–Pd bond. Further, the metal–metal bond distance in **43** is 2.39 Å, a contraction of 0.16 Å as compared to Pd(II) complex **42** (Pd–Pd = 2.55 Å).

The first organometallic Pd(III) complexes (**44**–**46**) were reported in 2006 (Fig. 25) [98]. Complexes **44**–**47** have been used as precatalysts for both the diborylation of terminal olefins and diborylation/cross-coupling tandem reactions (Fig. 26) [99]. The role of the Pd(III) complexes in these reactions has not been established; the diborane reagents employed have been shown to immediately reduce the dinuclear Pd(III) complexes to Pd(II) species, and thus the Pd(III) complexes may be a precatalyst for lower-valent active catalysts.

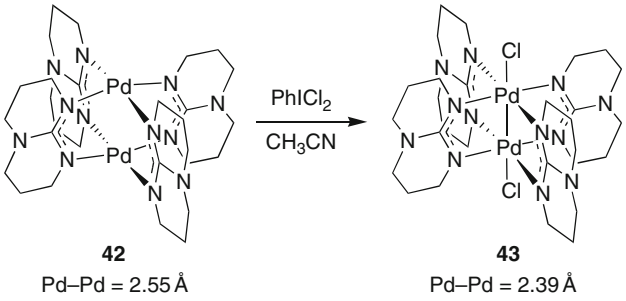

Fig. 24 In 1998, Cotton reported the first dinuclear Pd(III) complex (**43**), obtained by oxidation of **42** with $PhICl_2$

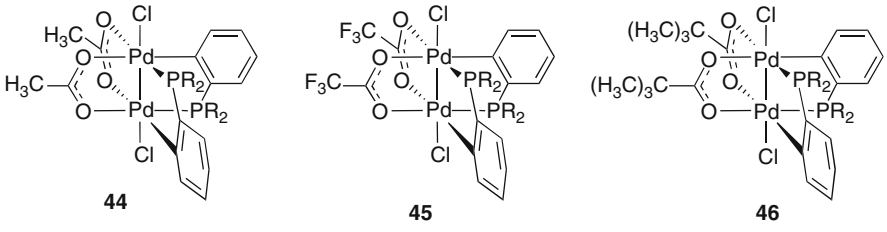

Fig. 25 Early examples of organometallic dinuclear Pd(III) complexes (R = Ph)

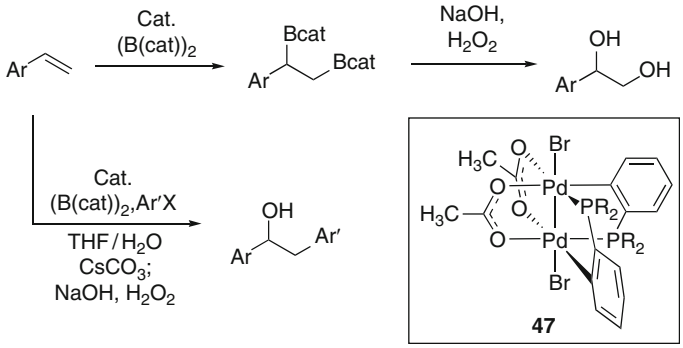

Fig. 26 Dinuclear Pd(III) precatalysts in diborylation and borylation/cross-coupling tandem reactions (R = Ph; $(B(cat))_2$ = bis(pinacolato)diboron)

3.2 Dinuclear Pd(III) Complexes in Catalysis

3.2.1 Pd-Catalyzed C–H Acetoxylation

Palladium-catalyzed aromatic C–H acetoxylation was first reported in 1966 [100, 101]. In 1971, Henry proposed Pd(IV) intermediates in the Pd-catalyzed acetoxylation of benzene with $K_2Cr_2O_7$ in AcOH [102]. Subsequent reports by Stock [103] and Crabtree [104] also discussed the possible intermediacy of Pd(IV) complexes in the acetoxylation of benzene (Fig. 27a). In 2004, Sanford reported the regioselective *ortho*-acetoxylation of 2-arylpyridines and proposed a reaction mechanism involving aromatic C–H metallation at Pd(II), oxidation of the resulting aryl Pd(II) intermediate to a Pd(IV) complex, and product-forming C–O reductive elimination (Fig. 27b) [105–108].

In 2009, we suggested that Pd-catalyzed aromatic C–H acetoxylation may proceed via dinuclear Pd(III) complexes instead of via mononuclear Pd(IV) intermediates [109]. On the basis of dinuclear Pd(II) complex **36**, the product of cyclometallation of 2-phenylpyridine (**48**) with $Pd(OAc)_2$ [110], a synthesis cycle based on dinuclear Pd(III) complexes was established (Fig. 28). Oxidation of **36** with $PhI(OAc)_2$, a common oxidant in Pd-catalyzed aromatic acetoxylation, afforded dinuclear Pd(III) complex **50**. Complex **50** was observed to undergo C–O reductive elimination under pseudocatalytic conditions to generate **49** in 91% yield. The critical dinuclear Pd(III) intermediate (**50**) was crystallographically characterized; the Pd–Pd distance in **50** was measured to be 2.555 Å (compared with 2.872 Å for **36** [111]), consistent with the formation of a Pd–Pd single bond. Dinuclear Pd(III) complex **50** was found to be a kinetically competent catalyst in the acetoxylation of 2-phenylpyridine with $PhI(OAc)_2$.

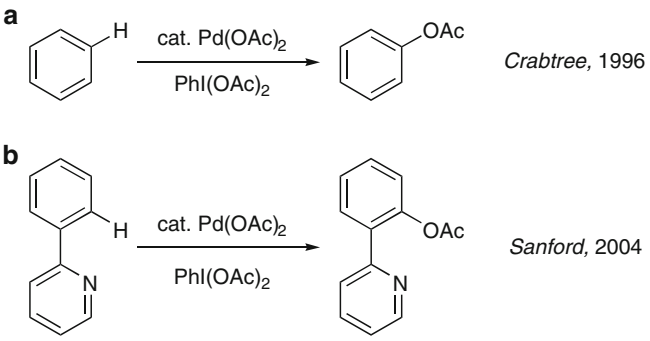

Fig. 27 Pd-catalyzed aromatic C–H acetoxylation reactions with $PhI(OAc)_2$

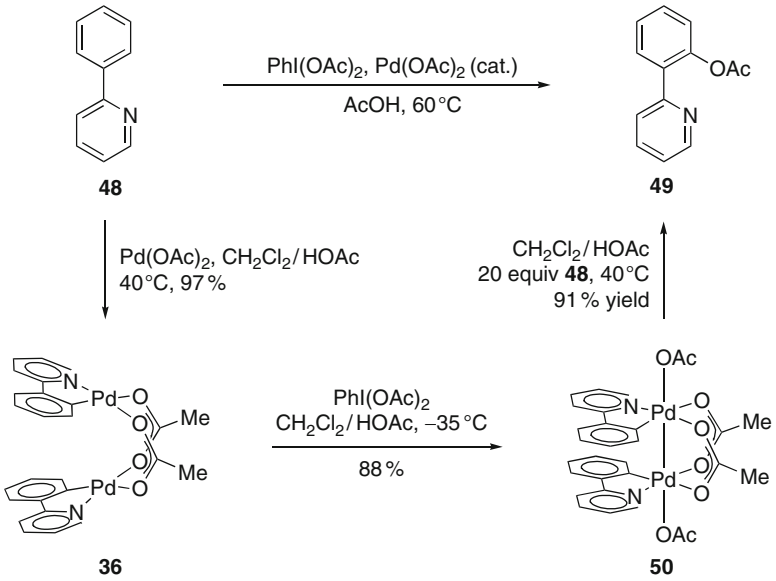

Fig. 28 A synthesis cycle for the acetoxylation of 2-phenylpyridine (**48**) based on dinuclear Pd(III) complex **50** has been established

3.2.2 Pd-Catalyzed C–H Chlorination

Fahey reported the Pd-catalyzed directed aromatic C–H chlorination of azobenzene using Cl_2 in 1970 (Fig. 29) [112, 113], and Sanford reported the Pd-catalyzed directed aromatic C–H chlorination of 2-arylpyridines with *N*-chlorosuccinimide (NCS) in 2004 (chlorination reaction shown in Fig. 30) [105, 114–116].

In 2010, we reported an investigation of the mechanism of the $Pd(OAc)_2$-catalyzed chlorination of benzo[*h*]quinoline (**51**) with NCS (Fig. 30) [96, 117]. Elucidation of the salient features of the mechanism operative in catalysis was

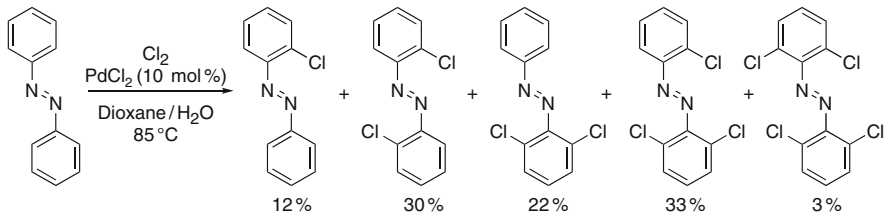

Fig. 29 Chlorination of azobenzene reported by Fahey

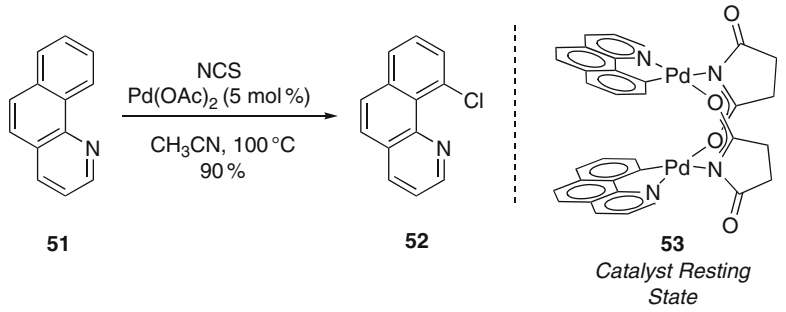

Fig. 30 The resting state of Pd-catalyzed chlorination of benzo[*h*]quinoline (**51**) is succinate-bridged dinuclear Pd complex **53**. Pd–Pd bond length in **53**: 2.8628(4) Å

enabled by identification of the catalyst resting state, which was found to be succinate-bridged dinuclear Pd(II) complex **53**. The two palladium centers in **53** are held in proximity (Pd–Pd = 2.863 Å) by the bridging succinate ligands as established by X-ray crystallography.

Using resting state **53** as the catalyst for the chlorination reaction shown in Fig. 30, the rate law of chlorination was determined to be as follows: rate = k [**53**] [NCS] [AcO^-], which implies that oxidation is the turnover-limiting step in catalysis. Further, the observed first-order dependence on dinuclear resting state **53** implies that two Pd centers participate in oxidation. The unexpected cocatalysis by acetate ions – generated by acetate for succinate exchange during formation of **53** – is consistent with a rate-determining transition state for oxidation in which acetate and NCS each interact with one of the Pd centers of resting state **53**, generating a dinuclear Pd(III) intermediate (Fig. 31).

The experimentally derived rate law for chlorination is consistent with dinuclear Pd(III) complex **54** being the immediate product of oxidation during catalysis. Complex **54** has one apical chloride ligand and one apical acetate ligand and thus, upon thermolysis, could undergo either C–Cl reductive elimination, to generate **52**, or C–O reductive elimination, to generate **55** (Fig. 32). We evaluated and confirmed the kinetic and chemical competence of **54** as an

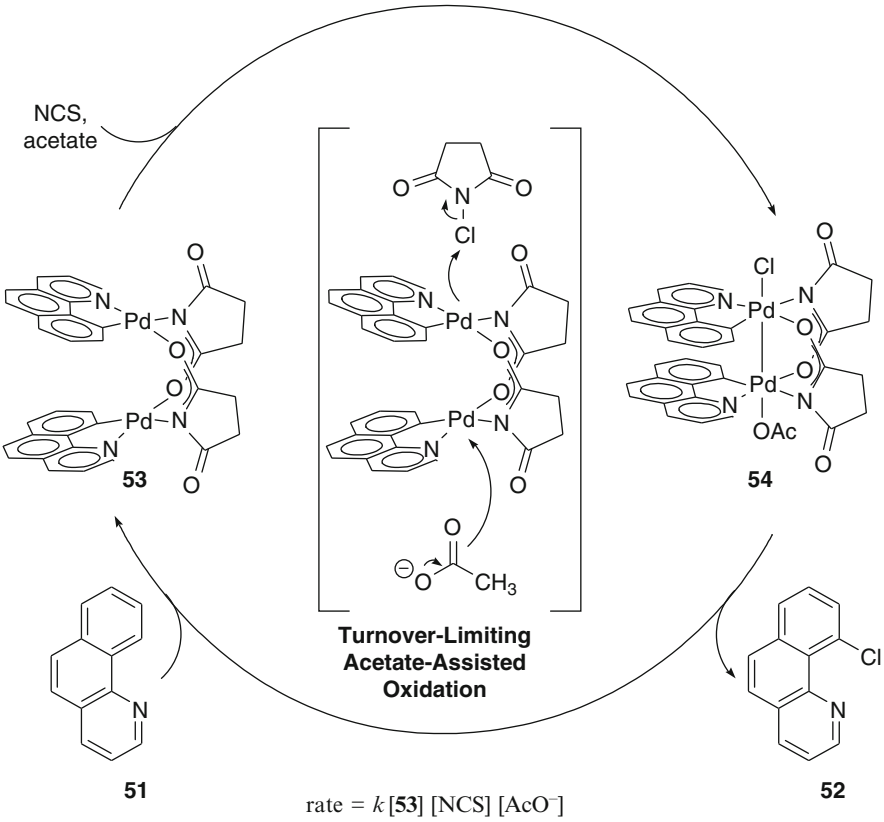

Fig. 31 Proposed acetate-assisted bimetallic oxidation of **53** would afford dinuclear Pd(III) complex **54** immediately following oxidation

intermediate for chlorination. Chemoselective C–Cl reductive elimination from **54** was observed upon warming **54** above –78°C (200:1 ratio of **52** to **55**). The observed ratio of **52** to **55** in the thermal decomposition of preformed **54** is consistent with the product distribution from the $Pd(OAc)_2$-catalyzed chlorination of benzo[*h*]quinoline (**51**). Using 10 mol% $Pd(OAc)_2$, a 200:1 ratio of **52** to **55** was observed (Fig. 32).

3.2.3 Pd-Catalyzed C–H Arylation

Deprez and Sanford reported an investigation of the mechanism of $Pd(OAc)_2$-catalyzed arylation of 2-arylpyridine derivatives with diaryliodonium salt **57** in 2009 (Fig. 33) [118]. The catalyst resting state was proposed to be mononuclear Pd complex **59**. By examining the initial rate of arylation as a function of [$Pd(OAc)_2$],

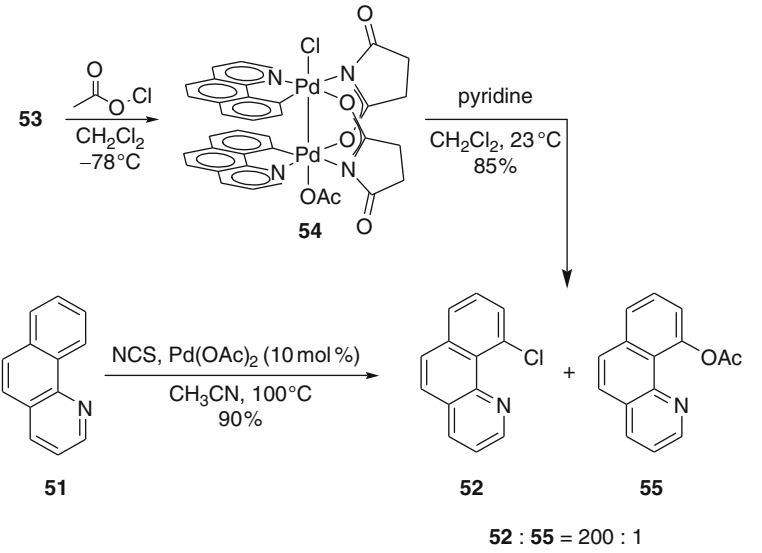

Fig. 32 The ratio of **52** to **55** obtained by thermal decomposition of dinuclear Pd(III) complex **54** is similar to the ratio of **52** to **55** obtained by $Pd(OAc)_2$-catalyzed chlorination of benzo[*h*] quinoline (**51**) with NCS

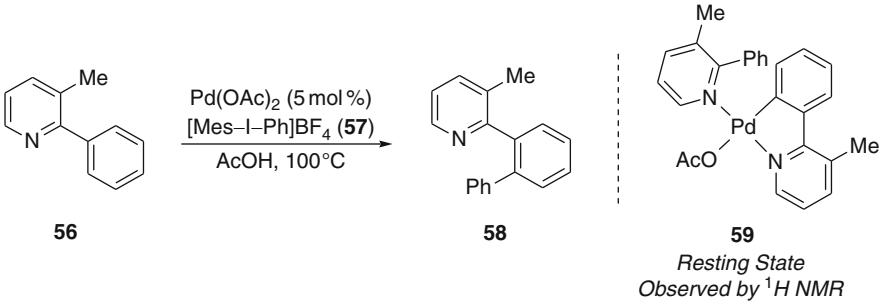

Fig. 33 The catalyst resting state for the $Pd(OAc)_2$-catalyzed arylation of 3-methyl-2-phenylpyridine (**56**) is proposed to be mononuclear Pd(II) complex **59**

the rate law of arylation was determined to be second order in Pd. In combination with the observation that oxidation is the turnover-limiting step in catalysis, the experimentally determined rate law is consistent with two Pd centers participating in oxidation during catalysis.

Sanford proposed the product of oxidation during catalysis to be one of the two constitutional isomers of a high-valent dinuclear Pd complex shown in Fig. 34 and suggested that the second palladium center in either **60** or **61** functions as an auxiliary ligand to the metal center that mediates the C–C bond formation.

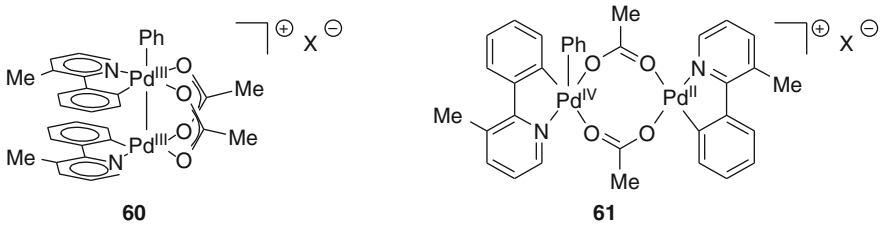

Fig. 34 Formulations of the high-valent, dinuclear Pd complex proposed by Sanford in the arylation of 2-arylpyridine derivatives

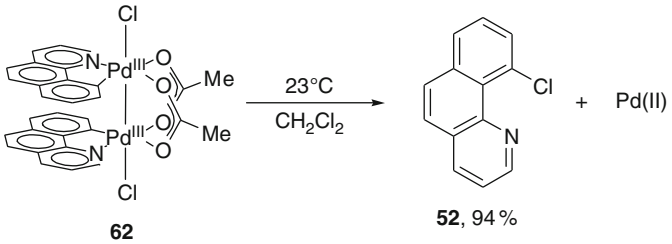

Fig. 35 C–Cl reductive elimination from dinuclear Pd(III) complex **62**

3.3 Role of Dinuclear Core During Redox Chemistry

Carbon–heteroatom reductive elimination from dinuclear transition metal complexes, as was proposed by us [96, 109] as the product-forming step in Pd-catalyzed C–H acetoxylation and chlorination reactions, is rare. The two formulations of the high-valent, dinuclear Pd intermediate in arylation proposed by Sanford (**60** and **61**) highlight that reductive elimination from dinuclear Pd structures could, in principle, proceed with either redox chemistry at both metals (bimetallic reductive elimination; reductive elimination from **60**) or with redox chemistry at a single metal (monometallic redox chemistry; reductive elimination from **61**). While structures **60** and **61** do not differ in composition, they do differ in their respective potentials for metal–metal redox cooperation to be involved in C–C bond-forming reductive elimination.

In 2010, we reported a study regarding the role of the dinuclear core during C–Cl reductive elimination from **62**, an analog of the dinuclear Pd complexes that have been proposed in catalysis (Fig. 35) [96, 119]. Experimental results established that reductive elimination from **62** proceeds without fragmentation of the dinuclear core; C–Cl bond formation proceeds from a dinuclear complex.

To probe the role of the dinuclear core during reductive elimination (i.e., mono- versus bimetallic reductive elimination), the electron binding energies of each Pd center were computed as a function of reaction progress. The electron binding energy is a measure of the energy required to remove an electron from a particular

orbital to infinite separation. The electron binding energy of an electron decreases during reduction and increases during oxidation. For metal centers with similar ligand environments, electron binding energy is well correlated with formal oxidation state [120–124].

The computed electron binding energies of Pd_a and Pd_b during the low-energy reductive elimination pathway from **A**, the computed structure of **62**, monotonically decrease during reduction from Pd(III) (**A**) to Pd(II) (**D**). The observed trends are consistent with simultaneous redox chemistry at both metal centers during C–Cl reductive elimination (Fig. 36).

For comparison, the electron binding energies of the palladium centers during a hypothetical pathway involving a Pd(II)/Pd(IV) mixed valence intermediate were also computed (Fig. 37). For hypothetical reductive elimination via a Pd(II)/Pd(IV) mixed valence complex (**E**), the electron binding energies of Pd_a and Pd_b diverge during Pd(III)/Pd(III) to Pd(II)/Pd(IV) disproportionation (**A** → **E**). Subsequent reductive elimination is accompanied by a convergence of the electron binding energies as both Pd centers are becoming Pd(II) (**E** → **D**). That the electron binding energy profiles for the computed reductive elimination pathway (Fig. 36) and hypothetical monometallic reductive elimination pathways (Fig. 37) are different is consistent with the assertion of metal–metal redox synergy during reductive elimination from **62**.

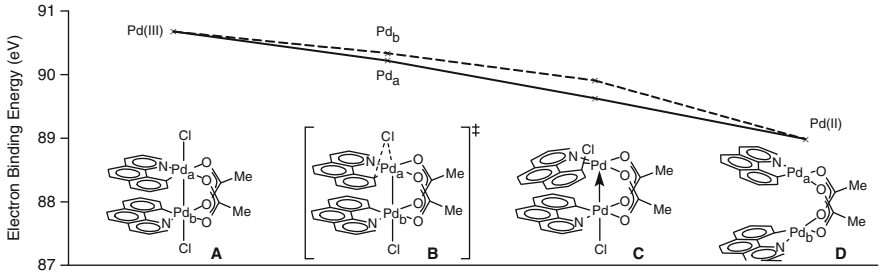

Fig. 36 Electron binding energies as a function of reaction progress for C–Cl reductive elimination from dinuclear Pd(III) structure **A**

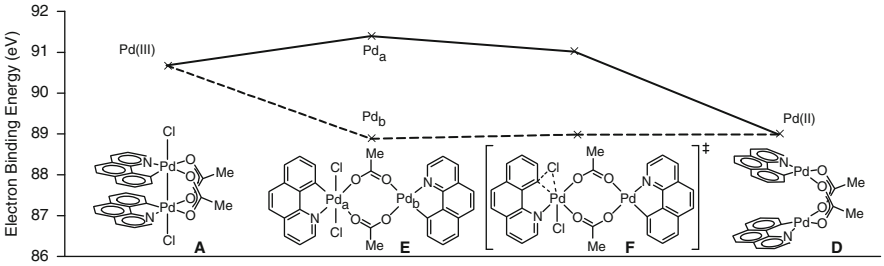

Fig. 37 Electron binding energy as a function of reaction progress for monometallic reductive elimination via a Pd(II)/Pd(IV) mixed valence structure

In addition, the energetic barrier to reductive elimination from **62** has been calculated as a function of metal–metal bond length. As the metal–metal distance is increased, orbital overlap, which mediates redox communication during reductive elimination, is reduced. The barrier to reductive elimination is positively correlated with the metal–metal distance; as the metals are increasingly separated, reductive elimination becomes increasingly energetically demanding. These calculations suggest that metal–metal redox synergy, in which the redox chemistry of reductive elimination is shared by two metals, lowers the energetic barrier to reductive elimination versus related processes involving a single metal.

3.3.1 Discussion of High-Valent Pd Intermediates Relevant in Pd-Catalyzed C–H Oxidations

From the seminal studies regarding the oxidation of benzene by Henry [102], Stock [103], and Crabtree [104], to the vast array of Pd-catalyzed aromatic C–H functionalizations reported in the last 5 years [125–128], it is evident that Pd-catalyzed aromatic C–H oxidation continues to be an area of intense methodological and mechanistic investigation. Early mechanism proposals for the acetoxylation of aromatic C–H bonds invoked Pd(IV) intermediates. While mononuclear Pd(IV) complexes have been prepared and the intimate mechanisms of reductive elimination from these complexes have been elucidated [107, 108, 129–132], the relevance of Pd(IV) complexes to catalysis has not yet been established. Frequently, aromatic C–H palladation is the turnover-limiting step in Pd-catalyzed C–H oxidation reactions [109, 133]. When palladation is turnover limiting, reaction kinetics analysis provides detailed information about the mechanism of metallation, not the mechanism of oxidation, and cannot provide any information regarding the identity of potential high-valent intermediates.

Elucidation of the catalysis cycle that is operative during a given transformation requires direct investigation of the reaction during catalysis. Elucidation of the mechanism of oxidation relevant to catalysis by kinetics analysis requires a reaction in which oxidation is turnover limiting. In both the chlorination [96, 117] and arylation [118] of 2-arylpyridine derivatives, oxidation is the turnover-limiting step of catalysis; in both reactions, kinetics analysis has revealed that two Pd centers are required for oxidation during catalysis. The structures of the proposed dinuclear Pd(III) complexes relevant to chlorination have been established by independent synthesis. A catalysis cycle, which is consistent with the results of all studies in which the identity of high-valent intermediates could be probed, is presented in Fig. 38. Following C–H metallation, nucleophile-assisted bimetallic oxidation affords a dinuclear Pd(III) complex. Subsequent reductive elimination from this high-valent dinuclear complex affords the observed organic fragments and Pd(II). Although the results were obtained during study of the chlorination of benzo[*h*] quinoline, they may be relevant to a variety of other C–H oxidation reactions. While detailed experimentation regarding the specific mechanism of individual reactions

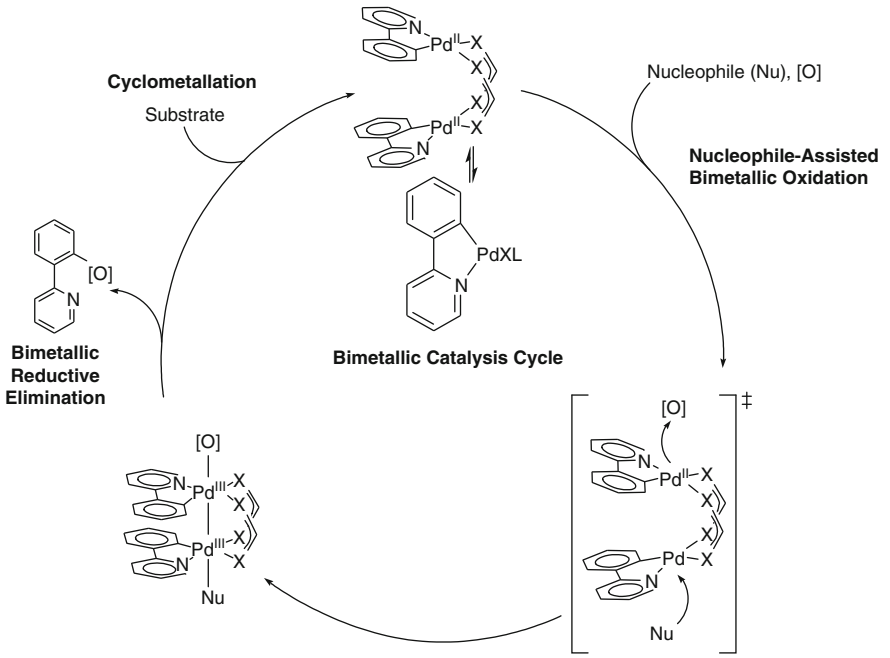

Fig. 38 Proposed bimetallic $Pd(II)_2/Pd(III)_2$ catalysis cycle

remains to be examined, we suggest that a bimetallic redox mechanism based on dinuclear Pd(III) complexes is a viable conceptual framework for Pd-catalyzed aromatic C–H oxidation reactions.

4 Outlook

Herein, we have reviewed the organometallic chemistry of Pd(III), discussing examples of both well-defined Pd(III) complexes that participate in organometallic reactions and examples in which the potential involvement of Pd(III) is more speculative at this time. We have discussed oxidative C–H coupling reactions in which biaryl Pd(II) intermediates may be diverted from the traditional Pd(0)/Pd(II) redox cycle in the presence of one-electron oxidants, allowing access to catalytically relevant mononuclear Pd(III) intermediates. We have also examined the recent proposal that many Pd-catalyzed oxidative C–H functionalization reactions may proceed via dinuclear Pd(III) complexes that undergo product-forming reductive elimination with redox participation of both metal centers. In both oxidative C–H coupling reactions and Pd-catalyzed C–H oxidations, Pd(III) intermediates have been discovered in reactions previously believed to proceed via more traditional two-electron, monometallic Pd redox cycles. On the basis of these proposals,

Pd(III), in both mono- and dinuclear complexes, may play a much more prominent role in catalysis than has previously been appreciated. We anticipate that the unique reactivity of both mono- and dinuclear Pd complexes will provide a foundation for the discovery of new reactions mediated by Pd(III) in the future.

Acknowledgment We gratefully acknowledge financial support for this work from the NIH-NIGMS (GM088237) and the NSF (CHE-0952753). TR is a Sloan Fellow.

References

1. Negishi E (ed) (2002) Handbook of organopalladium chemistry for organic synthesis. Wiley, New York
2. Murahashi T, Kurosawa H (2002) Coord Chem Rev 231:207–228
3. Markert C, Neuburger M, Kulicke K, Meuwly M, Pfaltz A (2007) Angew Chem Int Ed 46:5892–5895
4. Hama T, Hartwig JF (2008) Org Lett 10:1545–1548
5. Albright TA (1982) Tetrahedron 38:1339–1388
6. Miessler GL, Tarr DA (2004) Inorganic chemistry. Pearson Education, Upper Saddle River, New Jersey
7. Canty AJ, Gardiner MG, Jones RC, Rodemann T, Sharma M (2009) J Am Chem Soc 131:7236–7237
8. Bonnington KJ, Jennings MC, Puddephatt RJ (2008) Organometallics 27:6521–6530
9. Roundhill DM, Gray HB, Che CM (1989) Acc Chem Res 22:55–61
10. Matsumoto K, Sakai K (2000) Adv Inorg Chem 49:375–427
11. Lippert B (1999) Coord Chem Rev 182:263–295
12. Zipp AP (1988) Coord Chem Rev 84:47–83
13. Blake AJ, Gould RO, Holder AJ, Hyde TI, Lavery AJ, Odulate MO, Schröder M (1987) J Chem Soc Chem Commun 118–120
14. Usón R, Forniés J, Tomás M, Menjón B, Sünkel K, Bau R (1984) J Chem Soc Chem Commun 751–752
15. Usón R, Forniés J, Tomás M, Menjón B, Bau R, Sünkel K, Kuwabara E (1986) Organometallics 5:1576–1581
16. Nyholm RS, Sharpe AG (1952) J Chem Soc 3579–3587
17. Sharpe AG (1950) J Chem Soc 3444–3450
18. Bartlett N, Rao PR (1964) Proc Chem Soc Lond 393–394
19. Tressaud A, Wintenberger M, Bartlett N, Hagenmuller P (1976) C R Acad Sci Paris 282:1069–1072
20. Tressaud A, Khairoun S, Dance JM, Grannec J, Portier J, Hagenmuller P (1982) J Fluorine Chem 21:28
21. Tressaud A, Khairoun S, Dance JM, Hagenmuller P (1984) Z Anorg Allg Chem 517:43–58
22. Tressaud A, Khairoun S, Grannec J, Dance JM, Hagenmuller P (1985) J Fluorine Chem 29:39
23. Jasper SA, Huffman JC, Todd LJ (1998) Inorg Chem 37:6060–6064
24. Eachus RS, Graves RE (1976) J Chem Phys 65:5445–5452
25. Krigas T, Rogers MT (1971) J Chem Phys 54:4769–4775
26. Raizman A, Barak J, Suss JT (1985) Phys Rev B 31:5716–5721
27. Lane GA, Geiger WE, Connelly NG (1987) J Am Chem Soc 109:402–407
28. Möller E, Kirmse R (1997) Inorg Chim Acta 257:273–276
29. Luca V, Kukkadapu R, Kevan L (1991) J Chem Soc Faraday Trans 87:3083–3089
30. Warren LF, Hawthorn MF (1968) J Am Chem Soc 90:4823–4828

31. Kirmse R, Stach J, Dietzsch W, Steimecke G, Hoyer E (1980) Inorg Chem 19:2679–2685
32. Pandey KK (1992) Coord Chem Rev 121:1–42
33. Ray K, Weyhermüller T, Neese F, Wieghardt K (2005) Inorg Chem 44:5345–5360
34. Motoyama T, Shimazaki Y, Yajima T, Nakabayashi Y, Naruta Y, Yamauchi O (2004) J Am Chem Soc 126:7378–7385
35. Yamashita M, Takaishi S (2010) Chem Commun 46:4438–4448
36. Takaishi S, Wu H, Xie J, Kajiwara T, Breedlove BK, Miyasaka H, Yamashita M (2010) Inorg Chem 49:3694–3696
37. Blake AJ, Holder AJ, Hyde TI, Schröder M (1987) J Chem Soc Chem Commun 987–988
38. Blake AJ, Holder AJ, Hyde TI, Roberts YV, Lavery AJ, Schröder M (1987) J Organomet Chem 323:261–270
39. Matsumoto M, Itoh M, Funahashi S, Takagi HD (1999) Can J Chem 77:1638–1647
40. Blake AJ, Gordon LM, Holder AJ, Hyde TI, Reid G, Schröder M (1988) J Chem Soc Chem Commun 1452–1454
41. McAuley A, Whitcombe TW (1988) Inorg Chem 27:3090–3099
42. Hunter G, McAuley A, Whitcombe TW (1988) Inorg Chem 27:2634–2639
43. Reid G, Blake AJ, Hyde TI, Schröder M (1988) J Chem Soc Chem Commun 1397–1399
44. Blake AJ, Reid G, Schröder M (1990) J Chem Soc Dalton Trans 3363–3373
45. Blake AJ, Crofts RD, de Groot B, Schröder M (1993) J Chem Soc Dalton Trans 485–486
46. Reid G, Schröder M (1990) Chem Soc Rev 19:239–269
47. Hartwig JF (2010) Organotransition metal chemistry. University Science Books, Sausalito, CA, USA
48. Ackermann L, Vicente R, Kapdi AR (2009) Angew Chem Int Ed 48:9792–9826
49. Alberico D, Scott ME, Lautens M (2007) Chem Rev 107:174–238
50. Campeau LC, Fagnou K (2006) Chem Commun 1253–1264
51. McGlacken GP, Bateman LM (2009) Chem Soc Rev 38:2447–2464
52. Pascual S, de Mendoza P, Echavarren AM (2007) Org Biomol Chem 5:2727–2734
53. Stuart DR, Fagnou K (2007) Science 316:1172–1175
54. Kalyani D, Sanford MS (2008) J Am Chem Soc 130:2150–2151
55. Kalyani D, Satterfield AD, Sanford MS (2010) J Am Chem Soc 132:8419–8427
56. Klein A, Niemeyer M (2000) Z Anorg Allg Chem 626:1191–1195
57. Chen X, Goodhue CE, Yu JQ (2006) J Am Chem Soc 128:12634–12635
58. Cho SH, Hwang SJ, Chang S (2008) J Am Chem Soc 130:9254–9256
59. Stuart DR, Villemure E, Fagnou K (2007) J Am Chem Soc 129:12072–12073
60. Takahashi M, Masui K, Sekiguchi H, Kobayashi N, Mori A, Funahashi M, Tamaoki N (2006) J Am Chem Soc 128:10930–10933
61. Potavathri S, Dumas AS, Dwight TA, Naumiec GR, Hammann JM, DeBoef B (2008) Tetrahedron Lett 49:4050–4053
62. Campeau LC, Parisien M, Jean A, Fagnou K (2006) J Am Chem Soc 128:581–590
63. Lebrasseur N, Larrosa I (2008) J Am Chem Soc 130:2926–2927
64. René O, Fagnou K (2010) Org Lett 12:2116–2119
65. Seligson AL, Trogler WC (1992) J Am Chem Soc 114:7085–7089
66. Kraatz HB, van der Boom ME, Ben-David Y, Milstein D (2001) Isr J Chem 41:163–171
67. Ozawa F, Fujimori M, Yamamoto T, Yamamoto A (1986) Organometallics 5:2144–2149
68. Lanci MP, Remy MS, Kaminsky W, Mayer JM, Sanford MS (2009) J Am Chem Soc 131:15618–15620
69. Coronas JM, Muller G, Rocamora M (1986) J Organomet Chem 301:227–236
70. Ceder RM, Granell J, Muller G, Font-Bardía M, Solans X (1996) Organometallics 15:4618–4624
71. Higgs AT, Zinn PJ, Simmons SJ, Sanford MS (2009) Organometallics 28:6142–6144
72. Tsou TT, Kochi JK (1979) J Am Chem Soc 101:7547–7560
73. Matsunaga PT, Hillhouse GL, Rheingold AL (1993) J Am Chem Soc 115:2075–2077
74. Koo K, Hillhouse GL (1995) Organometallics 14:4421–4423

75. Higgs AT, Zinn PJ, Sanford MS (2010) Organometallics 29:5446–5449
76. Johansson L, Ryan OB, Rømming C, Tilset M (1998) Organometallics 17:3957–3966
77. Mei TS, Wang X, Yu JQ (2009) J Am Chem Soc 131:10806–10807
78. Neumann JJ, Rakshit S, Dröge T, Glorius F (2009) Angew Chem Int Ed 48:6892–6895
79. Manolikakes G, Knochel P (2009) Angew Chem Int Ed 48:205–209
80. Kienle M, Knochel P (2010) Org Lett 12:2702–2705
81. Kramer AV, Labinger JA, Bradley JS, Osborn JA (1974) J Am Chem Soc 96:7145–7147
82. Kramer AV, Osborn JA (1974) J Am Chem Soc 96:7832–7833
83. Boisvert L, Denney MC, Hanson SK, Goldberg KI (2009) J Am Chem Soc 131:15802–15814
84. Kamaraj K, Bandyopadhyay D (1999) Organometallics 18:438–446
85. Khusnutdinova JR, Rath NP, Mirica LM (2010) J Am Chem Soc 132:7303–7305
86. Cotton FA, Murillo CA, Walton RA (eds) (2005) Multiple bonds between metal atoms. Springer Science and Business Media, New York
87. Cotton FA, Matusz M, Poli R, Feng X (1988) J Am Chem Soc 110:1144–1154
88. Bercaw JE, Durrell AC, Gray HB, Green JC, Hazari N, Labinger JA, Winkler JR (2010) Inorg Chem 49:1801–1810
89. Xia BH, Che CM, Zhou ZY (2003) Chem Eur J 9:3055–3064
90. Pan QJ, Zhang HX, Zhou X, Fu HG, Yu HT (2007) J Phys Chem A 111:287–294
91. Yip HK, Lai TF, Che CM (1991) J Chem Soc Dalton Trans 1639–1641
92. Berry JF, Cotton FA, Ibragimov SA, Murillo CA, Wang X (2005) Inorg Chem 44:6129–6137
93. Cotton FA, Matusz M, Poli R (1987) Inorg Chem 26:1472–1474
94. Berry JF, Bill E, Bothe E, Cotton FA, Dalal NS, Ibragimov SA, Kaur N, Liu CY, Murillo CA, Nellutla S, North JM, Villagrán D (2007) J Am Chem Soc 129:1393–1401
95. Yao CL, He LP, Korp JD, Bear JL (1988) Inorg Chem 27:4389–4395
96. Powers DC, Ritter T (2009) Nat Chem 1:302–309
97. Cotton FA, Gu J, Murillo CA, Timmons DJ (1998) J Am Chem Soc 120:13280–13281
98. Cotton FA, Koshevoy IO, Lahuerta P, Murillo CA, Sanaú M, Ubeda MA, Zhao Q (2006) J Am Chem Soc 128:13674–13675
99. Penno D, Lillo V, Koshevoy IO, Sanaú M, Ubeda MA, Lahuerta P, Fernández E (2008) Chem Eur J 14:10648–10655
100. Davidson JM, Triggs C (1966) Chem Ind (Lond) 457
101. Tisue T, Downs WJ (1969) J Chem Soc D 410a
102. Henry PM (1971) J Org Chem 36:1886–1890
103. Stock LM, Tse K, Vorvick LJ, Walstrum SA (1981) J Org Chem 46:1757–1759
104. Yoneyama T, Crabtree RH (1996) J Mol Catal A Chem 108:35–40
105. Dick AR, Hull KL, Sanford MS (2004) J Am Chem Soc 126:2300–2301
106. Desai LV, Hull KL, Sanford MS (2004) J Am Chem Soc 126:9542–9543
107. Dick AR, Kampf JW, Sanford MS (2005) J Am Chem Soc 127:12790–12791
108. Racowski JM, Dick AR, Sanford MS (2009) J Am Chem Soc 131:10974–10983
109. Powers DC, Geibel MAL, Klein JEMN, Ritter T (2009) J Am Chem Soc 131:17050–17051
110. Gutierrez MA, Newkome GR, Selbin J (1980) J Organomet Chem 202:341–350
111. Dinçer M, Özdemir N, Günay ME, Çetinkaya B (2008) Acta Crystallogr E Struct Rep Online 64:M381
112. Fahey DR (1970) J Chem Soc D 417
113. Fahey DR (1971) J Organomet Chem 27:283–292
114. Whitfield SR, Sanford MS (2007) J Am Chem Soc 129:15142–15143
115. Kalyani D, Dick AR, Anani WQ, Sanford MS (2006) Org Lett 8:2523–2526
116. Kalyani D, Dick AR, Anani WQ, Sanford MS (2006) Tetrahedron 62:11483–11498
117. Powers DC, Xiao DY, Geibel MAL, Ritter T (2010) J Am Chem Soc 132:14530–14536
118. Deprez NR, Sanford MS (2009) J Am Chem Soc 131:11234–11241
119. Powers DC, Benitez D, Tkatchouk E, Goddard WA, Ritter T (2010) J Am Chem Soc 132:14092–14103
120. Riggs WM (1972) Anal Chem 44:830–832

121. Leigh GJ (1975) Inorg Chim Acta 14:L35–L36
122. Chatt J, Elson CM, Hooper NE, Leigh GJ (1975) J Chem Soc Dalton Trans 2392–2401
123. Cisar A, Corbett JD, Daake RL (1979) Inorg Chem 18:836–843
124. Corbett JD (1983) Inorg Chem 22:2669–2672
125. Lyons TW, Sanford MS (2010) Chem Rev 110:1147–1169
126. Xu L-M, Li B-J, Yang Z, Shi Z-J (2010) Chem Soc Rev 712–733
127. Muñiz K (2009) Angew Chem Int Ed 48:9412–9423
128. Chen X, Engle KM, Wang DH, Yu JQ (2009) Angew Chem Int Ed 48:5094–5115
129. Canty AJ (1992) Acc Chem Res 25:83–90
130. Byers PK, Canty AJ, Crespo M, Puddephatt RJ, Scott JD (1988) Organometallics 7:1363–1367
131. Fu Y, Li Z, Liang S, Guo QX, Liu L (2008) Organometallics 27:3736–3742
132. Furuya T, Benitez D, Tkatchouk E, Strom AE, Tang P, Goddard WA, Ritter T (2010) J Am Chem Soc 132:3793–3807
133. Stowers KJ, Sanford MS (2009) Org Lett 11:4584–4587

Top Organomet Chem (2011) 35:157–184
DOI: 10.1007/978-3-642-17429-2_7

Organometallic Platinum(II) and Palladium(II) Complexes as Donor Ligands for Lewis-Acidic d^{10} and s^2 Centers

Marc-Etienne Moret

Abstract Square-planar palladium(II) and platinum(II) complexes with a high-lying filled d_{z^2} orbital can act as metalloligands for Lewis-acidic metal centers such as d^{10} and s^2 cations. This behavior is promoted by hard ligands such as σ-bound hydrocarbyl ligands. A wide diversity of structural motifs based on this kind of donor–acceptor metal–metal bonds has been discovered in the last decades. This chapter reviews the coordination chemistry of metalloligands derived from alkyl, aryl, alkynyl, and carbene complexes of palladium(II) and platinum(II). The specific reactivity of the resulting bimetallic complexes is also addressed.

Keywords Heterobimetallic Complexes · Metal–metal bonds · Palladium · Platinum · Transmetalation

Contents

M.-E. Moret
Laboratorium für Organische Chemie, ETH Zürich, Wolfgang-Pauli-Str. 10, CH-8093 Zürich, Switzerland
and
Division of Chemistry and Chemical Engineering, California Institute of Technology, 1200 East California Blvd, Pasadena, CA 91125, USA
e-mail: memoret@caltech.edu

1 Introduction

The rich nucleophilic reactivity of square-planar platinum(II) and palladium(II) complexes is well established. One of the most documented examples is the stepwise oxidative addition of alkyl halides to organoplatinum(II) [1] and organopalladium (II) [2, 3] complexes *via* S_N2-type substitution at the sp^3 carbon center. Additionally, electron-rich Pt^{II} centers are subject to protonation at the metal to generate Pt^{IV} hydrides as the first step in the protonolysis of many platinum–carbon bonds [4–7]. With a less reactive Lewis acid such as SO_2, reversible adduct formation is observed [8], and this reaction has been used in the development of sensors [9–11].

From a molecular-orbital point of view, all of these reactions involve the d_{z^2} orbital, which is the highest occupied molecular orbital (HOMO) in the presence of hard donor ligands [12]. Strong ligand-field splitting renders the $d_{x^2-y^2}$ orbital so high in energy that it usually does not play a role in the chemistry of these complexes, which are therefore often referred to as *pseudo closed-shell* compounds [13]. These considerations naturally suggest the possibility for square-planar d^8 complexes to act as two-electron donor metalloligands for Lewis-acidic metals, forming a dative metal–metal bond (Scheme 1).

The first examples of organoplatinum complexes featuring such donor–acceptor bonds were reported in 1982 by the group of van Koten [14–16] and exhibited Pt–Hg or Pt–Ag contacts supported by a formamidino bridge (Scheme 1, left). Of this family of compounds only a mercury adduct was structurally characterized, but the existence of an analogous Pt^{II}–Ag^{I} interaction was confirmed by the

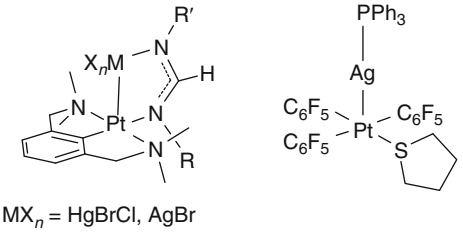

Scheme 1 Early examples of donor–acceptor metal–metal bonds in organoplatinum(II) chemistry

observation of a $^{1}J(^{195}Pt–^{109}Ag)$ coupling constant of 170 Hz in solution [15]. A few years later, Usón and Cotton demonstrated that similar interactions occur without a bridging ligand in the compound $\{[(C_6F_5)_3(tht)Pt]Ag(PPh_3)\}$ (tht = tetrahydrothiophene) (Scheme 1, right), which possesses a short (2.637(1) Å), unsupported Pt–Ag bond [17].

Since these early developments, a wide variety of organometallic platinum(II) and palladium(II) compounds possessing dative metal–metal bonds have been prepared with diverse ligands and acceptor fragments. This chapter provides an overview of the known structural motifs with selected examples and discusses the reactivity of some of these bimetallic species and their possible involvement as intermediates in catalytic systems based on group 10 metals.

2 General Considerations

2.1 Nature of the Donor and Acceptor Moieties

Platinum(II) and palladium(II) compounds are expected to be relatively weak donors as compared to their group 9 congeners in the (+I) oxidation state [16]. Lewis basicity sufficient to form donor–acceptor metal–metal bonds can, however, be achieved by using hard donor ligands on the d^8 metal center, which destabilize the d_{z^2} orbital through repulsive interaction with its equatorial torus. Thus, σ-bonded hydrocarbyl as well as N- or O-donor ligands are often found in the compounds discussed in this chapter. The diffuse nature of the HOMO makes divalent group 10 metal centers rather soft Lewis bases that are ideally suited to form stable adducts with soft acids, as reflected in the fact that unsupported Pt^{II}–Hg^{II} and Pt^{II}–Cd^{II} bonds are known, while the rare examples of Pt^{II}–Zn^{II} bonds [18, 19] are stabilized by one or more bridging ligand(s).

2.2 Binding Modes

Several binding modes for the coordination of platinum(II) fragments to Lewis-acidic metals can be distinguished (Scheme 2). We define type I bonds as consisting solely of a metal–metal interaction, which will in general have the bond axis

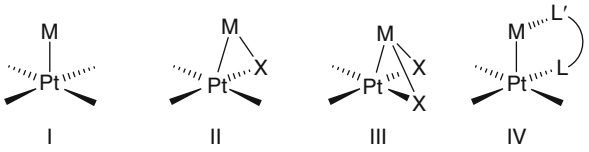

Scheme 2 Possible binding modes of square-planar Pt^{II} complexes to a Lewis-acidic metal M

perpendicular to the coordination plane of the d^8 metal. Type II and III compounds involve additional interaction with respectively one or two of the ligand atoms directly bound to platinum, as typically found for ligands with available π-electron density such as phenyl groups (see Sect. 4.3). Finally, type IV complexes exhibit metal–metal interactions stabilized by one or more covalent bridges. When the bridges are rigid, the existence of an actual attractive metal–metal interaction can sometimes be questioned because the close proximity of the metals is enforced by the ligand(s).

2.3 Synthesis

Since platinum(II) and – to a lesser extent – palladium(II) complexes are kinetically stable, most of the complexes described herein are prepared by reacting a preformed platinum(II) or palladium(II) complex with a salt of a d^{10} or s^2 cation. In some cases, the Lewis-acidic moiety is also a preformed complex containing labile ligands. There are some examples of more complicated reactions in which coordination to a Lewis acid induces changes in the coordination sphere of Pt^{II} to form oligomeric structures that cannot be isolated otherwise (see Sect. 4.2.1).

2.4 Characterization

The most direct way to observe metal–metal bonds is by crystallographic methods, and a vast majority of the complexes discussed here have been characterized by X-ray diffraction. NMR and optical spectroscopic methods have allowed the detection of these interactions in solution.

Pt^{II}–Ag^{I} interactions have been directly characterized by measuring the corresponding ^1J coupling constant by either ^{195}Pt [20] or ^{109}Ag [15] NMR. Alternatively, $^2J(^{31}P–^{195}Pt)$ couplings have been observed for compounds containing a Pt–M–PPh_3 unit (M = Ag, Au) [20, 21]. The formation of Pt^{II}–Cd^{II} or Pt^{II}–Ag^{I} interactions in solution has been found to cause a downfield shift of the ^{195}Pt resonance [22, 23]. The presence of Pt^{II}–M bonds in solution also manifests itself indirectly in several ways, for example by a decrease of the $^2J(^1H–^{195}Pt)$ coupling constant of platinum-bound methyl groups [20, 24, 25] or the appearance of coupling between the acceptor metal nucleus and the *ortho* fluorine atom of platinum-bound perfluorophenyl groups [26].

Lewis-acidic metal complexation often has a marked effect on the optical properties of organoplatinum compounds. Metal–metal-bonded bi- or trimetallic units often constitute a chromophore in themselves, giving rise to low-energy absorption and sometimes luminescence attributed to metal-to-metal charge transfer (MM'CT) transitions [27, 28]. Additionally, a marked blue shift of metal-to-ligand charge transfer (MLCT) absorptions is usually observed upon complexation of a platinum(II)

chromophore to a Lewis-acidic metal [21, 24]; this is easily understood considering that the d_{z^2} orbital from which the charge transfer occurs is stabilized by interaction with the second metal.

3 Alkyl Complexes

3.1 Methyl Complexes

3.1.1 Methylplatinum(II) Complexes

The interaction of alkylplatinum compounds with Lewis-acidic metals was pioneered in 1988 by the group of Puddephatt [20], who showed that the fragment [(bpy)$PtMe_2$] can coordinate to the Ph_3PM fragment (M = Ag, Au) (Scheme 3, upper right). In the same contribution, the formation of a complex of stoichiometry {[(bpy)$PtMe_2$]$_2$Ag}(BF_4) was observed at low temperature. All these compounds were too unstable to be structurally characterized, but the existence of Pt–M interactions was proved by the observation of a direct coupling constant $^1J(^{195}Pt–^{107/109}Ag)$ coupling of 680 Hz in the ^{195}Pt NMR spectrum of {[(bpy)$PtMe_2$]Ag(PPh_3)}(BF_4). Additionally, the geminal $^2J(^1H–^{195}Pt)$ coupling of the methyl protons was found to decrease upon coordination to gold(I) or silver(I).

The first structural characterization of a dative bond involving a dimethylplatinum(II) fragment was reported a decade later by Yamaguchi et al. [22], who

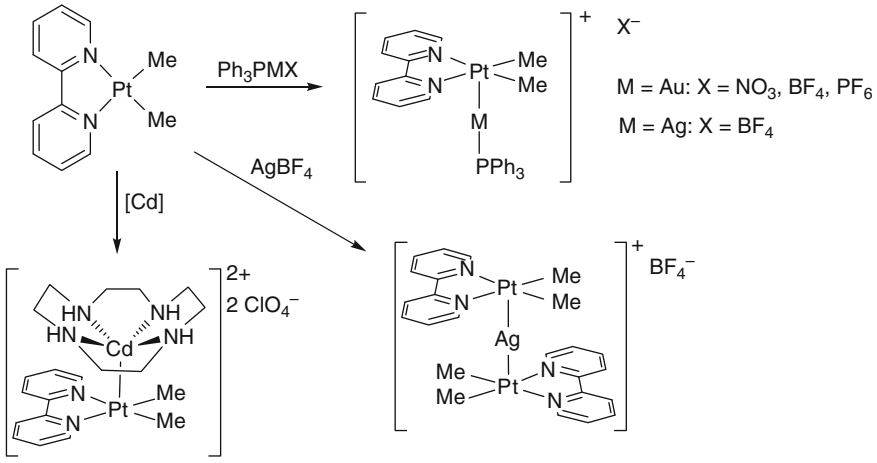

Scheme 3 Complexation of [(bpy)$PtMe_2$] to d^{10} cations

prepared the adduct of [(bpy)$PtMe_2$] with the $[(cyclen)Cd]^{2+}$ (cyclen = 1,4,7,10-tetraazacyclododecane) fragment and showed it to possess a short (2.6101 Å) platinum–cadmium bond of type I (Scheme 3, lower left).

Later, Mak et al. [29] reported the incorporation of the $PtMe_2$ fragment into the macrocyclic complex $[(PNP)_2Pt_2Me_4]$ (PNP = 2,6-bis(diphenylphosphino)pyridine), which is able to encapsulate Cu^I and Tl^I cations *via* two donor–acceptor metal–metal bonds (Scheme 4). Interestingly, copper(I) is additionally bound to the pyridine unit of the PNP ligand, resulting in type IV interactions, while thallium(I) is held only by its interactions with the platinum(II) centers. The same authors also reported that the reaction of $[(PNP)_2Pt_2Me_4]$ with $AgBF_4$ does not yield an analogous Pt_2Ag complex but instead affords the $PtAg_2$ complex depicted in the lower right of Scheme 4, in which one of the dimethylplatinum(II) units has been replaced by a silver atom.

Twenty years after the pioneering work of Puddephatt, we succeeded in isolating and structurally characterizing complexes in which the $PtMe_2$ fragment is bound to monovalent coinage metal centers by unsupported Pt–M bonds [24]. We made use of an α-diimine ligand (hereafter abbreviated NN) incorporating 2,6-dichlorophenyl substituents on the nitrogen atoms (Scheme 5), which offers some steric protection against aggregation and inhibits the oxidative decomposition process described in reference [20]. The complex $[(NN)PtMe_2]$ reacts with $CuOTf{\cdot}\frac{1}{2}C_7H_8$

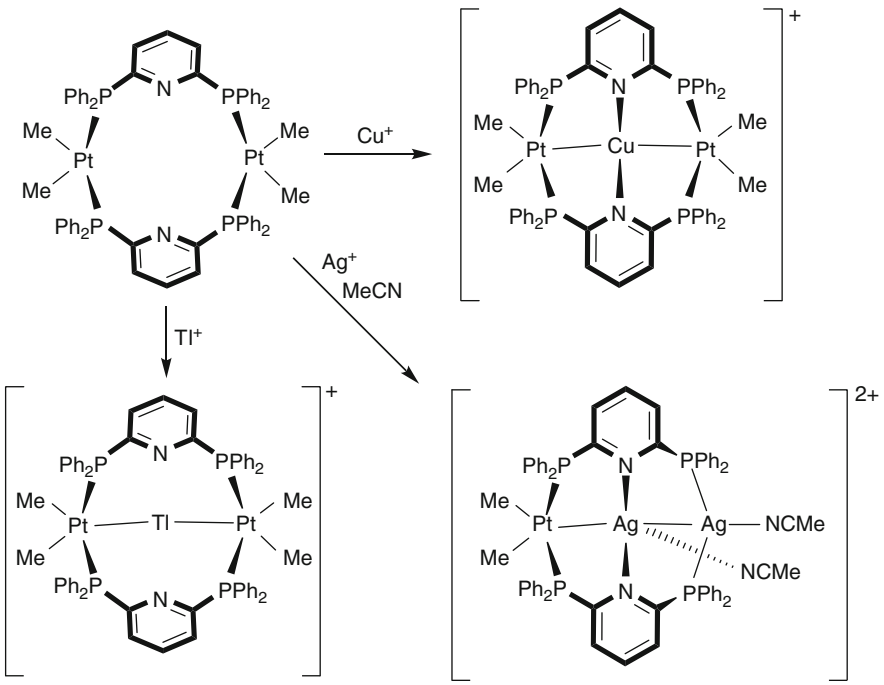

Scheme 4 Metal cation encapsulation by a macrocyclic diplatinum complex

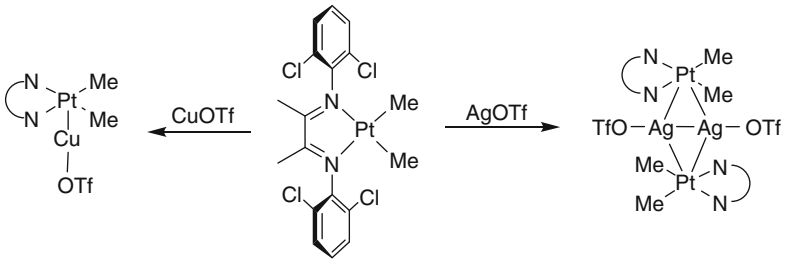

Scheme 5 Reaction of [(NN)PtMe$_2$] (NN = 2,3-bis(2,6-dichlorophenylimino)butane) with monovalent coinage metal triflates

Scheme 6 A methyl-bridged platinum(II)–copper(I) bond

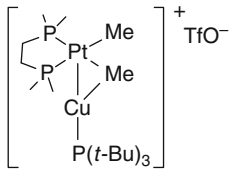

to form the mononuclear adduct {[(NN)PtMe$_2$]CuOTf} (Scheme 5, left), which exhibits a linear Pt–Cu–O geometry with a very short (2.3992 Å), unsupported Pt−Cu contact. In contrast, the reaction with AgOTf yields a tetrametallic compound with four unsupported Pt−Ag contacts and an argentophilic interaction. The existence of [(NN)PtMe$_2$]MOTf (M = Cu, Ag) species in solution was demonstrated by a combination of ^{1}H NMR and UV–Vis spectroscopy. In particular, the monomeric nature of the adducts was confirmed by their diffusion coefficients, as measured by pulsed-field gradient (PFG) NMR techniques.

Extending our study to a P,P chelated dimethylplatinum(II) complex, we isolated and structurally characterized a cationic complex of formula {[(dmpe)PtMe$_2$]Cu[P(*t*-Bu)$_3$]}$^+$ (dmpe = 1,2-bis(dimethylphosphino)ethane) as its triflate salt [25]. This is the first example of a complex involving a methyl group as a bridging ligand between a d^8 and a d^{10} metal (Scheme 6). Its significance as an intermediate for transmetalation is discussed in Sect. 7.2.2.

3.1.2 Methylpalladium(II) Complexes

In comparison with their platinum(II) counterparts, palladium(II) alkyl complexes are generally less stable, and palladium has a lower tendency to involve in donor–acceptor metal–metal bonds [30, 31]. Thus, it comes as no surprise that palladium analogues of the complexes described in this section were unknown until the very recent report of Lanci et al. [32]. In the course of their study on the oxidation of [(^{t}Bu$_2$bpy)PdMe$_2$], they observed that it forms a thermally labile complex with AgPF$_6$ (see Sect. 7.1). Replacing Ag^I with the weaker oxidant Tl^I, the authors succeeded in isolating and structurally characterizing a 3:2 dicationic complex

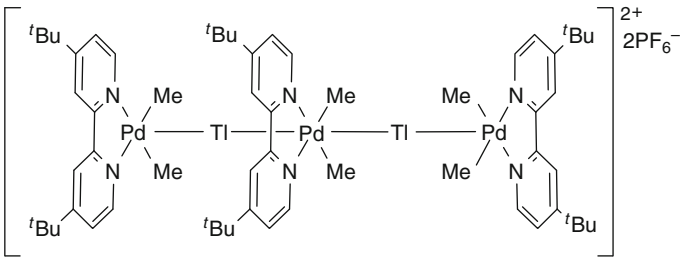

Scheme 7 A pentanuclear complex containing four Pd^{II}–Tl^{I} bonds

(Scheme 7) that features a remarkable linear Pd–Tl–Pd–Tl–Pd chain consisting of four Pd^{II}–Tl^{I} bonds.

3.2 Metallacycles

A simple way to lower the reactivity of metal–alkyl bonds is to incorporate them in a metallacycle. Along these lines, complexes incorporating the *o*-CH_2–C_6H_4–P(*o*-tolyl)$_2$-κ*C*,*P* ligand on platinum have been used as robust building blocks for constructing dative Pt^{II}→Ag^{I} [31, 33] and Pt^{II}→Hg^{II} bonds [34–37].

A recent example [31] from Falvello et al. on bimetallic, pyrazolate-bridged complexes of platinum(II) and palladium(II) is instructive (Scheme 8). These two compounds exhibit differentiated behavior in the presence of silver(I) perchlorate: the platinum complex binds silver through two donor–acceptor metal–metal bonds supplemented by silver–tolyl π interactions, while the palladium complex binds silver through the π-electron density of the pyrazolate ligands.

4 Aryl Complexes

Two classes of stabilized arylplatinum complexes have played a major role in the discovery and the development of Pt→M donor–acceptor bonds: metallacyclic compounds and complexes incorporating pentafluoro- and pentachlorophenyl ligands. In contrast, the use of phenylplatinum complexes for that purpose is only very recent. In this section, we discuss selected recent developments for these three classes of compounds.

4.1 Metallacycles

Metal–aryl bonds that are incorporated in a metallacycle are particularly robust, and thus it is not surprising that compounds of this type have been among the first

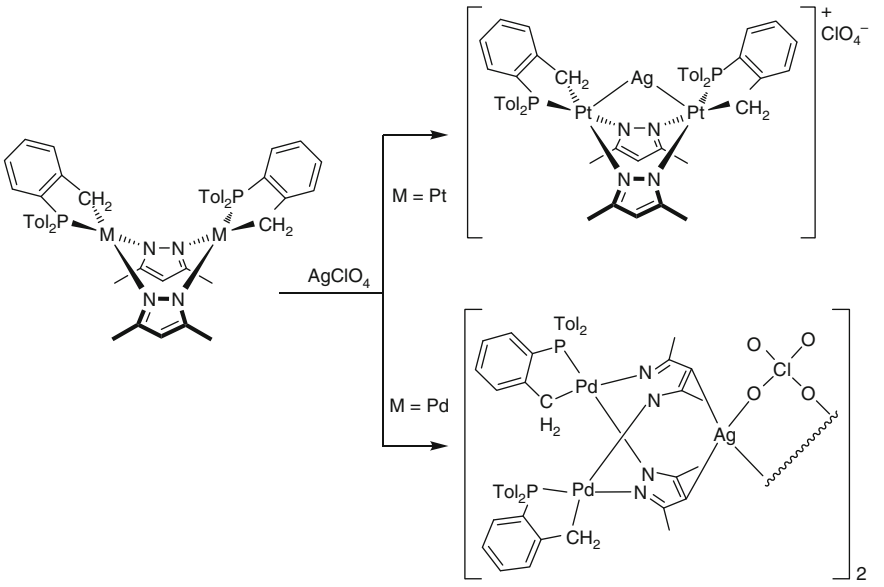

Scheme 8 Silver(I) complexation by dinuclear, pyrazolate-bridged metallacycles

organoplatinum compounds shown to act as Lewis bases for d^{10} metal ions (see Sect. 1). In most group 10 metallacycles, the aryl ligand and the platinum(II) or palladium(II) square coordination are approximately coplanar. As a result, there is little steric bulk around the region above or below the metal center. This geometry is ideally suited for the formation of type I or II complexes, the latter involving interaction of the Lewis acid with the *ipso* carbon atom of the aryl group.

4.1.1 Platinacycles

In the last decade, several reports have appeared that demonstrate the use of platinum(II) complexes of 2-(pyrid-2-yl)phenyl (phpy) and 7,8-benzoquinolate (bzq) as donor ligands for d^{10} metal centers (Scheme 9). First, the neutral, dicyclometallated compound $[(phpy)_2Pt]$ was shown to form a type I complex with the $[(cyclen)Cd]^{2+}$ fragment [22]. In contrast, its reaction with $AgClO_4$ in acetone yielded yellow crystals displaying helical, metal–metal-bonded unidimensional chains featuring both type I and type II interactions [23]. Then, Janzen et al. [38] demonstrated that even the cationic metallacycle $[(phpy)Pt(9S3)]^+$ (9S3 = 1,4,7-trithiacyclononane) can act as a Lewis base toward Ag^I in the tricationic complex $\{[(phpy)Pt(9S3)]_2Ag(NCMe)_2]\}^{3+}$, which was structurally characterized as its PF_6 salt. The donating ability of the platinum(II) center is thought to be enhanced by a weak apical coordination of a sulfur atom of the 9S3 ligand, which destabilizes the d_{z^2} orbital by electronic repulsion. This hypothesis is supported by the shortening of this Pt–S bond from 2.9518 to 2.6870 Å upon coordination to Ag^I.

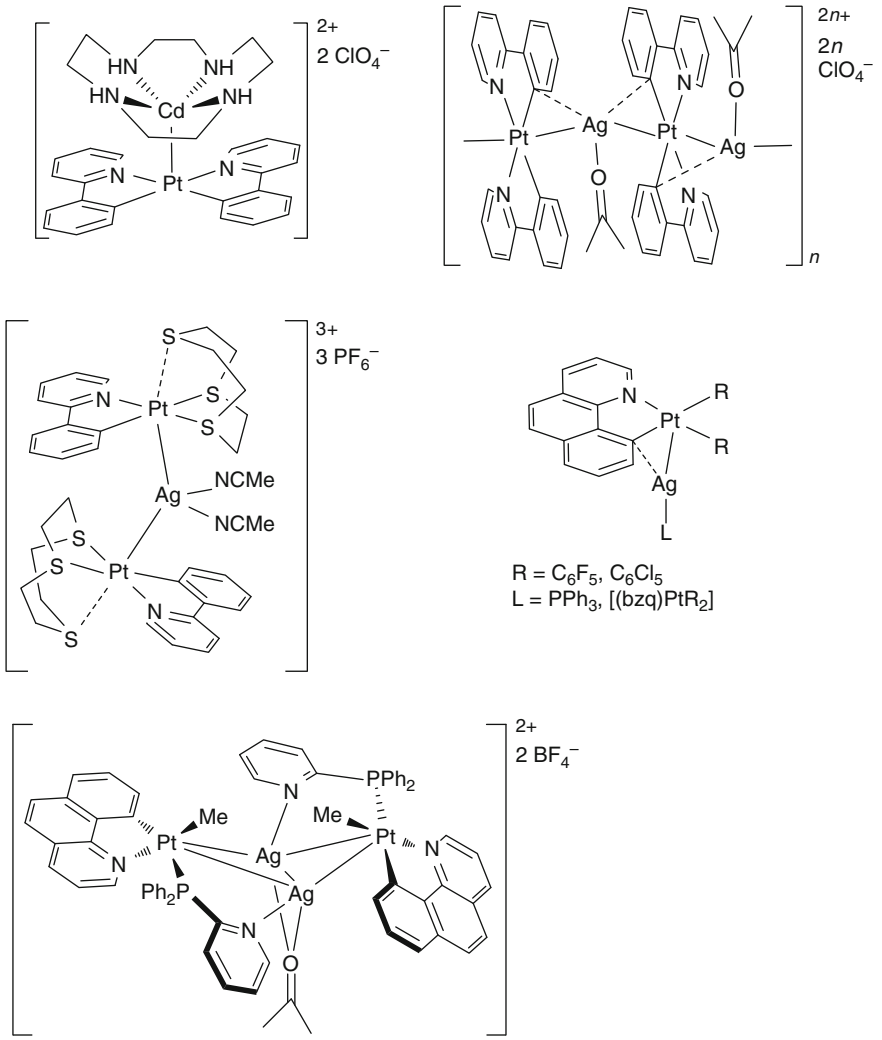

Scheme 9 Compounds involving a donor–acceptor bond from platinum(II) complexes of 2-(pyrid-2-yl)phenyl (phpy) and 7,8-benzoquinolate (bzq)

Subsequently, Forniés et al. [21] presented an extensive study of the coordination of the anionic complexes $[(bzq)PtR_2]^-$ (R = C_6F_5, C_6Cl_5) to silver(I). They prepared and structurally characterized both the homoleptic anions $\{[(bzq)PtR_2]_2Ag\}^-$ and the neutral heteroleptic complexes $\{[(bzq)PtR_2]Ag(PPh_3)\}$, showing that in all cases a type II coordination involving the *ipso* carbon atom of the bzq ligand is preferred. The Pt–Ag bond of the neutral complexes is also present in solution and results in a marked blue shift of the low-energy ^{1}MLCT transition as compared to the free anion $[(bzq)PtR_2]^-$.

Finally, a recent study by Jamali et al. [39] describes the preparation of a tetranuclear butterfly-shaped cluster in which each of two platinum(II) centers binds to two silver(I) cations that are themselves connected by an argentophilic interaction. The cluster is stabilized by bidentate P,N ligands bridging a Pt–Ag bond each. Solution-phase NMR suggests an equilibrium between the butterfly geometry and a planar arrangement similar to that of $\{[(NN)PtMe_2]_2Ag_2(OTf)_2\}$ (see Sect. 3.1.1, Scheme 5).

4.1.2 Palladacycles

There are two structurally characterized examples in which an arylpalladium(II) coordinates to silver(I) in a type II fashion (Scheme 10). First, Kickham and Loeb [40] reported that an attempt to abstract the chloride ligand in a palladated thiacyclophane with two equivalents of silver(I) triflate unexpectedly resulted in the formation of a bimetallic complex in which the silver(I) ion is encapsulated by three oxygen atoms and an interaction with the Pd–C bond. Then, Braunstein et al. [41] synthesized a remarkable one-dimensional coordination polymer by reacting the phosphanyl iminolate palladium complex depicted in Scheme 10 (bottom) with silver(I) triflate.

4.2 Perhalophenyl Complexes

Starting in the mid-1980s, the use of platinum(II) complexes with two or more perhalophenyl complexes as Lewis bases for the construction of donor–acceptor Pt^{II}–Ag^{I} bonds has been extensively studied in the groups of Usón and, later, Forniés. This work has been reviewed [26, 42] and is not discussed in detail here.

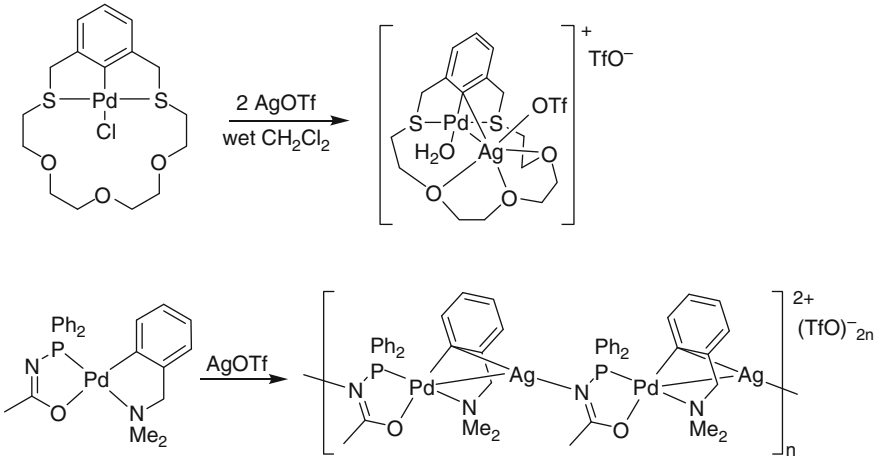

Scheme 10 Aryl palladacycles involved in type II Pd^{II}–Ag^{I} bonds

Recent extensions of this work involve the use of a range of Lewis acids and the synthesis of higher-nuclearity clusters and polymeric structures. Selected examples are presented in this section.

The ability of perhalophenyl ligands to stabilize $Pt^{II} \rightarrow M$ dative bonds can be attributed to several factors. First, being very electron-poor, they allow access to negatively charged metalloligands of type $[Pt(C_6X_5)_3L]^-$ and $[Pt(C_6X_5)_4]^{2-}$, which yield neutral complexes upon Lewis neutralization with Ag^+. Second, the electron-withdrawing halogeno substituents decrease the basicity of the π-electron cloud of the aromatic ring, which therefore does not compete with the platinum center for the Lewis acid. Finally, metal–metal bonds are often additionally stabilized by weak Ag–X interactions.

4.2.1 Discrete Polymetallic Structures

Since the report by Usón and Cotton on the synthesis of the compound $\{[(C_6F_5)_3(tht)Pt]Ag(PPh_3)\}$, which possesses a short, unsupported Pt–Ag bond (2.637 Å) [17], a large number of related complexes of varying nuclearities and geometries have been synthesized. Examples of common structural types in these compounds are depicted in Scheme 11.

In addition to their ability to bind molecular fragments such as $[Ag(SC_4H_8)]^+$ [43] and $[Cd(cyclen)]^{2+}$ [44], the dianionic metalloligands $[Pt(C_6X_5)_4]^{2-}$ (X = F, Cl) can form homoleptic complexes containing a linear Pt–M–Pt chain (Scheme 11A). Examples thereof are the two isoelectronic complexes $\{[(C_6F_5)_4Pt]_2Pb\}^{2-}$ [45] and $\{[(C_6F_5)_4Pt]_2Tl\}^{3-}$ [46], which were prepared as their tetrabutylammonium salts by reacting two equivalents of $[(C_6F_5)_4Pt](NBu_4)_2$ with lead(II) and thallium(I) nitrate, respectively. In addition to the Pt–M bonds, they exhibit eight stabilizing M· · ·F contacts in an axially compressed square-antiprism geometry. Remarkably, two $[(C_6F_5)_4Pt]^{2-}$ units are also able to stabilize thallium(II) in $\{[(C_6F_5)_4Pt]_2Tl\}(NBu_4)_2$, which was the first paramagnetic Tl^{II} complex to be isolated.

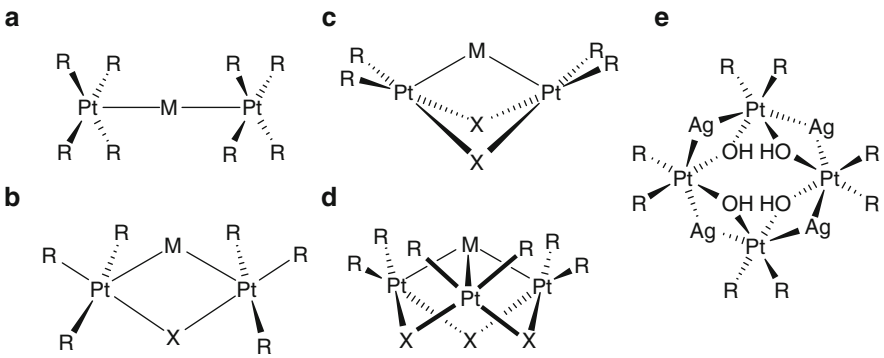

Scheme 11 Structural types for polynuclear complexes containing type I donor–acceptor Pt–M bonds from perhalophenyl platinum(II) complexes. R = C_6F_5, C_6Cl_5; X = Cl, OH, C_6F_5

A few complexes are known in which two platinum(II) centers are bridged by one ligand (Scheme 11B), including $[(C_6F_5)_3Pt(\mu\text{-}Pb)(\mu\text{-}X)Pt(C_6F_5)_3]^-$ (X = Cl, OH) [47] and $[(C_6F_5)_3Pt(\mu\text{-}OH)(\mu\text{-}HgC_6F_5)Pt(C_6F_5)_3]^-$ [48].The latter is formed in the reaction of $[(C_6F_5)_4Pt](NBu_4)_2$ with $Hg(NO_3)_2$ in wet methanol, which involves the transfer of a pentafluorophenyl group from platinum to mercury and the hydrolysis of a Pt–C_6F_5 bond.

The third class of metalloligands (Scheme 11C) features two platinum(II) centers bridged by two ligands in an open-book geometry. The bridging ligands can be C_6F_5 [17, 49], Cl [50, 51], or OH [52]. A few years ago, Forniés and coworkers investigated the reactivity of phosphido-bridged dinuclear platinum(II) and palladium(II) complexes toward silver(I) sources. Surprisingly, the complex $[Pt_2(\mu\text{-}PPh_2)_2(C_6F_5)_4]^{2-}$ forms no Lewis acid–base complex with $AgClO_4$ but is instead oxidized to the platinum(III) dimer $[Pt_2(\mu\text{-}PPh_2)_2(C_6F_5)_4]$ (Scheme 12, top) [53]. In contrast, monoanionic complexes of type $[(C_6F_5)_2Pt(\mu\text{-}PPh_2)_2M\text{-}(acac\text{-}O,O')]$ (M = Pt, Pd) react with $Ph_3PAgClO_4$ to form the trimetallic complexes depicted in Scheme 12 (bottom) [54]. For M = Pd, the complex exhibits a short Pd–Ag contact (2.886 Å), which is remarkable given the low tendency of palladium to involve in donor–acceptor bonds [30].

Compounds of type D (Scheme 11D) consist of a six-membered Pt_3X_3 cycle acting as a tridentate metalloligand for the Lewis-acidic center. Three examples of this motif have been structurally characterized: $(NBu_4)\{[Pt(\mu\text{-}Cl)(C_6F_5)_2]_3M\}$ (M = Sn [55], Pb [56]), and $(NBu_4)_2\{[Pt(\mu\text{-}OH)(C_6F_5)_2]_3HgCl\}$ [57]. Unlike the Pt_2X_2 units in type C complexes, the Pt_3X_3 fragments have not been isolated in the absence of the central metal atom, indicating that the latter acts as a template.

Very recently, a new structural type has been found that involves an eight-membered $Pt_4(OH)_4$ cycle stabilized by coordination of each platinum(II) center to two silver(I) ions (Scheme 11E) [28]. The octanuclear complex $\{[Pt(C_6Cl_5)_2(\mu\text{-}OH)(\mu\text{-}Ag)]_4\}$ is formed by reacting the dinuclear complex $\{[Pt(C_6Cl_5)_2(\mu\text{-}OH)]_2\}^{2-}$

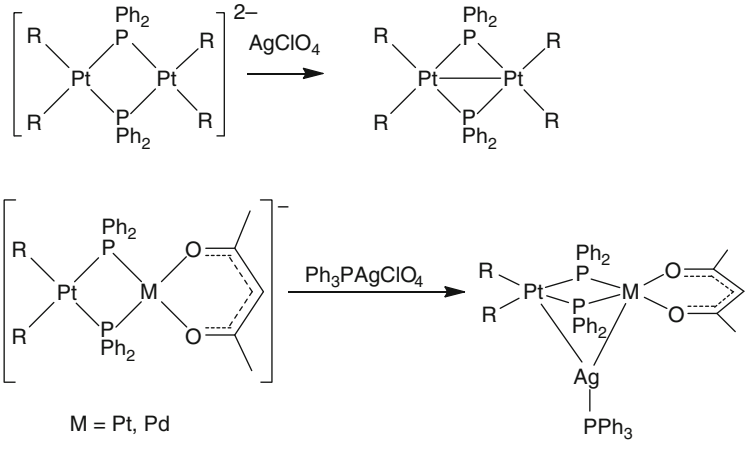

Scheme 12 Reactivity of phosphido-bridged dinuclear complexes toward silver(I) sources

with two equivalents of $AgClO_4$ in a 4:1 mixture of dichloromethane and benzene. Interestingly, the yellow solid exhibits a green-yellow luminescence which the authors assign to phosphorescence arising from the Pt–Ag interactions. The luminescence disappears reversibly when the solid is exposed to acetone vapor, possibly due to binding of acetone to the silver(I) centers in the crystal.

4.2.2 Extended Structures Incorporating Thallium(I)

In general, the reaction of perfluoroarylplatinum(II) complexes with d^{10} metals yields preferentially discrete compounds in which the platinum(II) center binds a metal on only one side of its coordination plane. However, recent work has demonstrated that thallium(I) tends to display a different behavior in that it forms extended structures [27, 46, 58, 59]. The growing interest in these compounds comes from the fact that many of them exhibit interesting luminescent properties.

A striking example [46] is that the salt $(NBu_4)_2[(C_6F_5)_4Pt]^{2-}$ reacts with $TlNO_3$ in a 1:1 ratio to form a solid made of one-dimensional polyanionic chains $\{[(C_6F_5)_4Pt]Tl\}_n^{n-}$ with tetrabutylammonium counterions (Scheme 13). Interestingly, when $TlPF_6$ is used instead of $TlNO_3$, a crystalline solid containing one equivalent of $(NBu_4)(PF_6)$ is formed in which the metal–metal-bonded chain is preserved. The polymeric structure is disrupted in solution, but luminescence studies in frozen dichloromethane solution indicate that aggregates of variable size are formed upon cooling. Recently, this work was extended to heteroleptic platinate anions such as *cis*- and *trans*-$[(C_6F_5)_2Pt(CN)_2]^{2-}$ [27] as well as mixed alkynyl-perfluoroarylplatinates [58, 59].

4.3 *Phenyl Complexes*

Given the ease of access and stability of simple phenylplatinum complexes, it is somewhat surprising that their reactivity as Lewis bases toward d^{10} metals was not studied until recently. In the absence of electron-withdrawing substituents, one expects the π-electron density of the aryl ring to play a significant role in the binding of soft Lewis acids. As a matter of fact, we have structurally characterized examples of type I, II, and III bonds with this class of compounds.

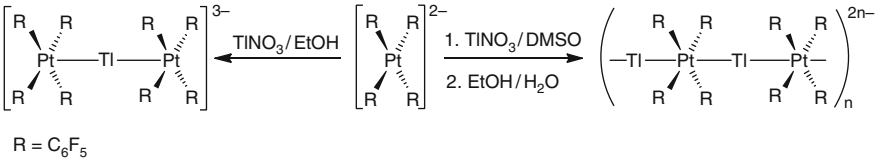

Scheme 13 Reactions of the tetrakis(pentafluorophenyl)platinate dianion with thallium(I) nitrate

We first observed the coordination of the diphenylplatinum(II) fragment to a copper(I) ion in tetranuclear complexes obtained from the reaction of the anionic complex $[(bmimp)PtPh_2]^-$ (bmimp = 3,5-bis(4-methoxyphenyl imino)acetyl-4-methylpyrazolate) with CuCl in acetonitrile followed by redissolution of the initially formed solvated dinuclear complex $\{[(bmimp)PtPh_2]Cu(NCMe)_{1\text{-}2}\}$ in benzene [60] (Scheme 14). One of the copper centers in this tetranuclear complex is held only by a cuprophilic interaction and a type II interaction with each platinum(II) center. Replacing the 4-methoxyphenyl moiety of the dinucleating ligand by the more bulky 2,6-dimethylphenyl results in the decoordination of a peripheral imine group without significant alteration of the tetranuclear arrangement, demonstrating its stability.

More systematic insight into the coordination of diphenylplatinum complexes to d^8 metals was obtained using the simple α-diimine ligand 2,3-bis(2,6-dichlorophenylimino)butane (NN). The complex $[(NN)PtPh_2]$ reacts with half an equivalent of MOTf (M = Cu, Ag) to form homoleptic 2:1 cationic complexes in which the coinage metal is bound to the diphenylplatinum unit in a type III fashion (Scheme 15, top). The X-ray crystal structure of the copper cation is presented in Figure 1.

UV–Vis and NMR spectroscopy revealed that in solution, complexes are formed of stoichiometries 1:1 and 2:2 with CuOTf and AgOTf, respectively. The aggregation state in solution was determined from the diffusion coefficients obtained by PFG NMR. None of these complexes was crystallized, but DFT calculations indicated two possible structures featuring a type III and a type II interaction, respectively. Interestingly, the first binding mode resembles that found in the 2:1 complexes $\{[(NN)PtPh_2]_2M\}^+$ (M = Cu, Ag), while the second one parallels that found in $\{[(bmimp)PtPh_2]_2Cu_2\}$.

Compounds with a higher coinage-metal content were also obtained in the presence of a large excess of CuOTf or AgOTf. With copper(I), a discrete complex of formula $\{[(NN)PtPh_2]_2Cu_6(OTf)_6\}$ was crystallized, in which each diphenylplatinum(II) unit is coordinated to one Cu(I) center *via* a type III interaction and to two additional ones by π-coordination of both phenyl groups. The parallel reaction with AgOTf yielded a coordination polymer in which each platinum(II) is involved in a type I and a type III interaction with two different silver(I) centers, showing that type I interactions are also accessible to diphenylplatinum complexes.

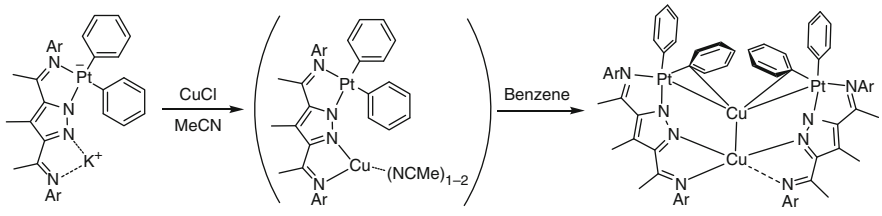

Ar = 4-$MeOC_6H_4$, 2,6-$Me_2C_6H_4$

Scheme 14 Preparation of the complexes $\{[(bmimp)PtPh_2]_2Cu_2\}$ and $\{[(bdmimp)PtPh_2]_2Cu_2\}$

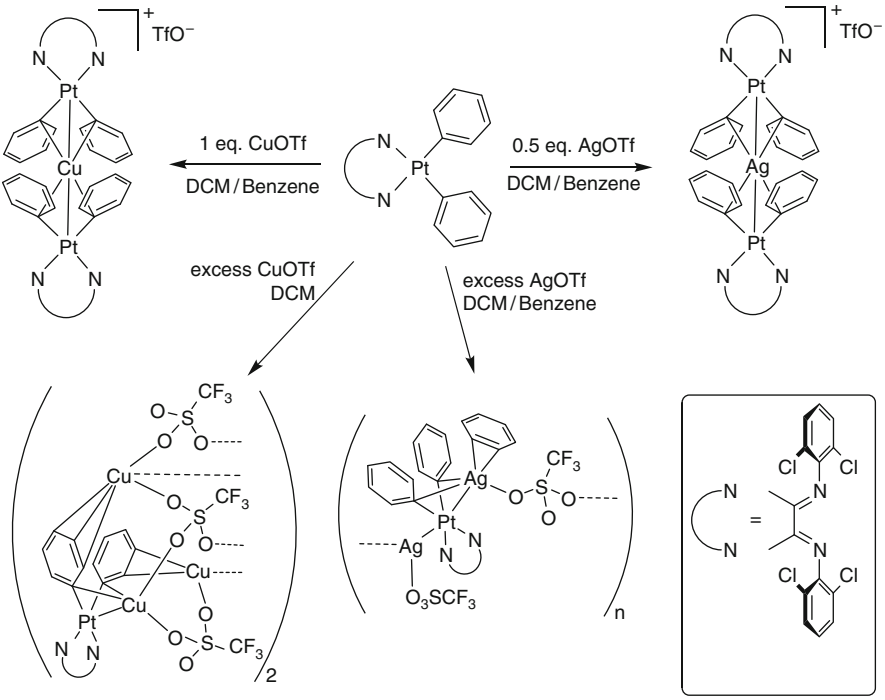

Scheme 15 Reactions of the complex [(NN)$PtPh_2$] with monovalent coinage metal triflates

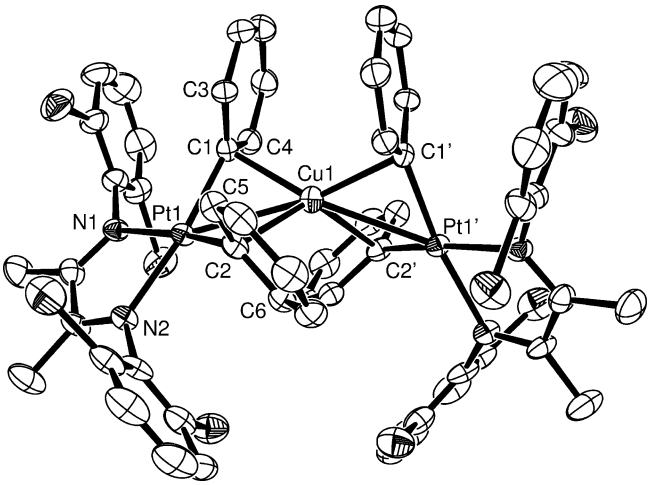

Fig. 1 ORTEP representation of the X-ray crystal structure of {[(NN)$PtPh_2$]$_2$Cu}(CF_3SO_3). Ellipsoids are drawn at 50% probability. Hydrogen atoms and the unbound $CF_3SO_3^-$ counterion are omitted for clarity. Selected distances [Å]: Cu1–Pt1 2.7254(3), Cu1–C1 2.138(5), Cu1–C2 2.336(5), Pt1–C1 2.033(5), and Pt1–C2 2.022(5). Reprinted with permission from ref [24]. Copyright 2009 American Chemical Society

5 Alkynyl Complexes

The proclivity of alkynyl ligands to form stable complexes with platinum(II) and their ability to bridge between metals made them ligands of choice to prepare a wide range of polynuclear heterometallic complexes, resulting from the reaction of an alkynylplatinum entity with Lewis-acidic metal centers. In most cases, the latter interacts mainly with the π-electron density of the triple bond, and only very weak metal–metal interactions, if any, are observed. This area has been recently covered in some excellent reviews [61–64] and is not discussed extensively here. Nevertheless, compounds are known in which the bond between an alkynylplatinum moiety and a d^{10} or s^2 center has a significant contribution of metal–metal interaction. Most of these fall into two categories: (1) complexes in which an electron-rich Pt^{II} center is basic enough to compete with the π density of the triple bond for the electrophilic center, and (2) complexes involving a bridging ligand that promotes the formation of type IV interactions. The first category is illustrated here by dianionic tetraalkynylplatinum(II) complexes, and the second one by recent work on dppm-bridged complexes (dppm = bis(diphenylphosphino)methane).

5.1 Tetraalkynylplatinates

The reaction of tetraalkynylplatinate dianions with coinage metal perchlorates (generated in situ for copper(I) and gold(I)) generally yields octanuclear structures in which four metal centers are sandwiched between two $[Pt(C{\equiv}CR)_4]^{2-}$ units (Scheme 16, bottom) [65–71]. Several structures have been crystallographically characterized, showing that the Pt–M distances (2.9–3.1 Å for M = Cu, 2.9–3.3 Å for M = Ag) are indicative of a very weak metal–metal interaction. These octanuclear units can assemble into oligomeric or polymeric structures *via* unsupported platinum–platinum bonds, and the resulting supramolecular assemblies have interesting optical properties such as long-lived luminescence and near-infrared emission [69].

The influence of electronic effects on the binding mode of tetraalkynylplatinate anions is apparent in the reactions of compounds of general formula $Li_2[Pt(C{\equiv}CR)_4]$ with thallium(I) nitrate [72]. For electron-rich alkynyl moieties (R = *p*-tolyl, 1-naphtyl), discrete hexanuclear structures are obtained (Scheme 16, top), in which each Tl^I center interacts with four C≡C triple bonds and not with the platinum atom. The introduction of a remote electron-withdrawing substituent on the alkynyl unit (R = *p*-$CF_3C_6H_4$) induces a dramatic change in the structure of the Lewis acid–base complex: each platinum atom now involves in donor–acceptor bonds with two thallium(I) ions (Pt–Tl: 2.9355(5) and 3.0272(5) Å), one on each face of its coordination plane. These Tl_2Pt units are interconnected by weak interactions of thallium with the π-electron density of the triple bonds.

As a last example, Berenguer et al. [73] recently reported that the reaction of $(NBu_4)_2[Pt(C{\equiv}CTol)_4]$ with $Pb(ClO_4)_2{\cdot}3H_2O$ yields a trinuclear complex of formula

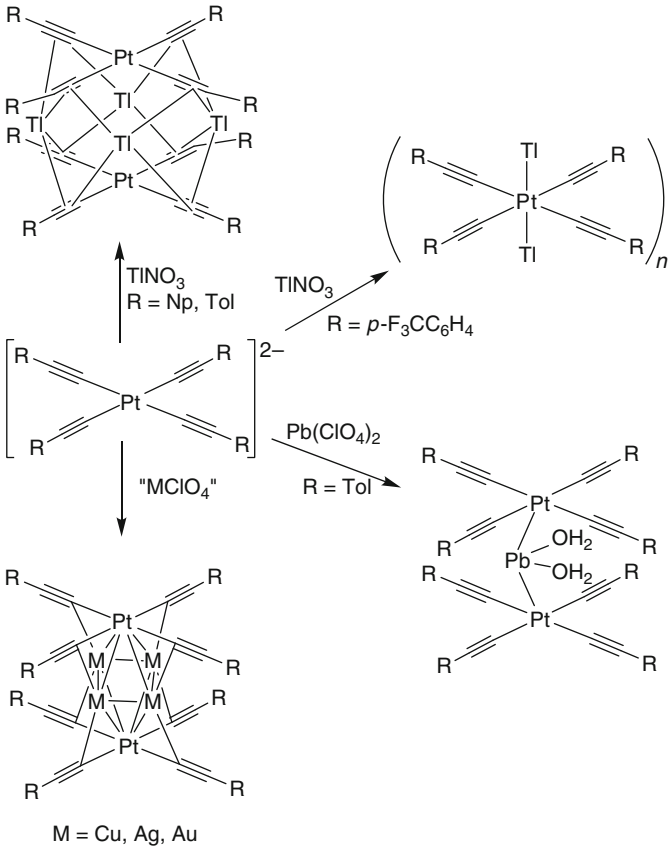

Scheme 16 Reactions of $[Pt(C{\equiv}CR)_4]^{2-}$ with salts of d^{10} and s^2 cations

$\{[Pt(C{\equiv}CTol)_4]\}_2Pb(OH_2)_2$. The lead(II) center is bound to both platinum(II) atoms and to two water molecules. Unlike the linear complex $\{[(C_6F_5)_4Pt]_2Pb\}^{2-}$, the lone pair on lead(II) in this complex is stereoactive, resulting in a geometry derived from a trigonal bipyramid.

5.2 Diphosphine-bridged Complexes

The second approach has been used only in complexes of general formula $[(RC{\equiv}C)_2Pt(\mu\text{-dppm})_2MX_n]$ (dppm = bis(diphenylphosphinomethane), MX_n = AgCl, AgI, CuCl, $HgCl_2$) as well as their cationic analogues $[(RC{\equiv}C)_2Pt(\mu\text{-dppm})_2M]^+$ (M = Cu, Ag, Au, Scheme 17), which were first prepared by Shaw and coworkers in the early 1980s [74, 75]. Since the two metals are held in close proximity by two dppm ligands, it is difficult to confirm with certainty the presence of a metal–metal bond. Initially,

Scheme 17 Dialkynylplatinum(II) complexes incorporating a donor–acceptor metal–metal bond supported by bis(diphenylphosphino) methane (dppm)

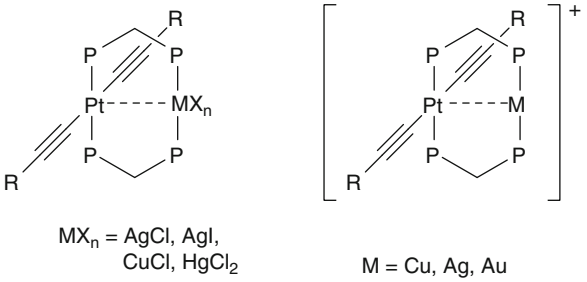

only the AgI complex was structurally characterized, and the long Pt–Ag distance of 3.146 Å did not indicate significant metal–metal bonding. In 1993, Yip et al. [76] obtained a crystal structure of the cationic gold complex $[(RC{\equiv}C)_2Pt(\mu\text{-dppm})_2Au]^+$ as its PF_6 salt and measured a gold–platinum distance of 2.910 Å. More recently, Yin et al. [77] presented a systematic study of the reactions of dianionic tetraalkynylplatinates with $[(\mu\text{-dppm})_2M_2(CNMe)_2]^+$ (M = Cu, Ag, Au), in which a series of analogous cationic copper(I), silver(I), and gold(I) complexes were structurally characterized. They reported a Pt–Ag distance of 2.981 Å (R = *t*-Bu), Pt–Cu distances between 2.727 (R = *o*-Tol) and 2.767 Å (R = *t*-Bu), and a Pt–Au distance of 2.927 Å (R = Ph). These distances may indicate some extent of metal–metal bonding, even though they are substantially longer than those found in unsupported Pt–Cu and Pt–Ag donor–acceptor bonds. In the case of copper and silver, an additional contact with the α carbon atom of one alkynyl ligand is observed.

6 Carbene Complexes

The strong σ-donating ability of N-stabilized carbenes should make their platinum(II) and palladium(II) complexes suitable donor metalloligands for Lewis-acidic d^{10} and s^2 centers. However, reports of such studies are scarce.

6.1 Platinum

For platinum(II), Balch and coworkers [78] have studied the reaction of a biscarbene platinum(II) dicyanide complex with thallium(I) in basic solution (Scheme 18). They obtained two polymorphs involving Pt^{II}–Tl^{I} contacts: a yellow dimeric structure and a red extended structure. Subsequent work by the same authors [79] showed that replacement of the CN ligands with dimethylglyoxime or maleonitrile dithiolate provides access to a range of extended structures based on Pt^{II}–Tl^{I} interactions.

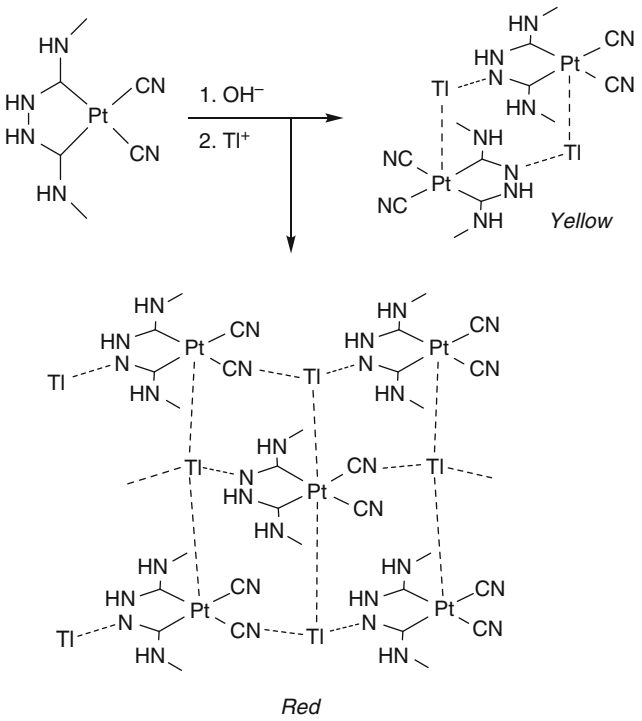

Scheme 18 Extended structures involving the interaction of thallium(I) with a dicyanoplatinum (II) dicarbene compound

6.2 Palladium

In recent years, there have been a few reports of NHC–palladium(II) (NHC = *N*-heterocyclic carbene) complexes engaged in donor–acceptor bonds with silver (I). These were generally obtained after halide abstraction using an excess of a silver salt (Scheme 19) [80–82]. The palladium(II) centers in these compounds are rendered very electron rich either by coordination of a methide group or by the use of two abnormal NHC ligands. Particularly striking is the complex reported by Heckenroth et al. [82] in which the dicationic fragment $[(CC)Pd(NCMe)_2]^{2+}$ (CC = bis (2-methyl-3-isopropylimidazol-5-yliden-1-yl)methane) acts as a Lewis base toward silver(I) to form the tricationic complex $[(CC)Pd(NCMe)_2]Ag(NCMe)_2]^{3+}$ (Scheme 19, bottom). The authors attribute this behavior to the exceptional σ-donor ability of this bidentate abnormal NHC ligand.

Reitsamer et al. [83] recently reported a palladium complex of a PCP pincer ligand that engages in a d^8–d^{10} with the AuCl fragment. The ligand, while involving a two-coordinate carbon atom, is not accurately described as a carbene but rather as a carbodiphosphorane. In this description, the central carbon(0) atom is coordinated

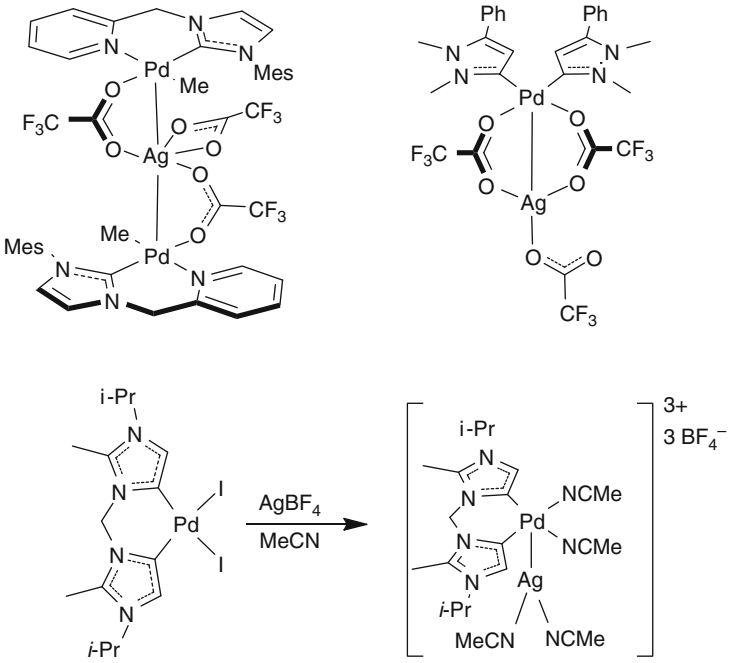

Scheme 19 *N*-Heterocyclic carbene complexes of palladium(II) involved in Pd(II)–Ag(I) bonds

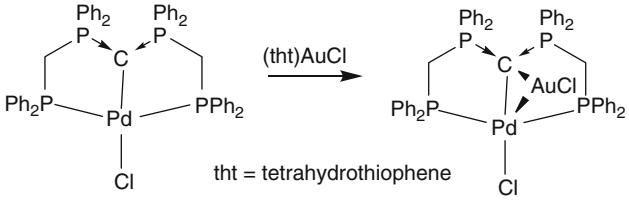

Scheme 20 Coordination of a (PCP)PdCl complex to gold(I) chloride

by two-donor phosphine ligand and formally has two lone pairs available for binding, which explains why a type II interaction is observed (Scheme 20).

7 Reactivity

Since copper(I), silver(I), and, to a lesser extent, thallium(I) are common components of palladium- and platinum-based catalytic systems, it appears likely that bimetallic species similar to those discussed in this chapter are involved in the corresponding catalytic cycles. Thus, while most of the studies on donor–acceptor bonds involving

palladium(II) or platinum(II) complexes focus on their structural – and sometimes optical – properties, the specific reactivity associated with these bonds is of high interest. In this section, we will summarize the results of recent investigations.

7.1 Electron Transfer Reactions

Oxidation of the platinum(II) center by silver(I) salts has occasionally been observed when attempting to prepare adducts containing platinum–silver bonds (for example, see Sect. 4.2.1). One can speculate that these oxidations could proceed *via* an inner-sphere process involving the transient formation of a Pt^{II}–Ag^{I} mixed species. Two examples have recently appeared in which the bimetallic species can be observed prior to oxidatively induced reactions of dimethylplatinum(II) and dimethylpalladium(II) species.

In the course of our study on the interaction of $[(NN)PtMe_2]$ (NN = 2,3-bis(2,6-dichlorophenylimino)butane) with copper(I) or silver(I) triflates in benzene [24], we observed a double aromatic C–H activation process yielding moderate yields of $[(NN)PtPh_2]$ (Scheme 21). We proposed the mechanism depicted in Scheme 22, which involves the initial one-electron oxidation of $[(NN)PtMe_2]$ by the coinage metal, on the basis of the following considerations:

- The platinum(IV) cation $[(NN)PtMe_3]^+$ was observed by ESI-MS.
- The disproportionation reaction (1) (Scheme 22) is known to occur upon one-electron oxidation of closely related complexes [84–86], and a very similar reaction has been reported that converts $[(bpy)PtMe_2]$ into [(bpy)PtMeCl] and $[(bpy)PtMe_3Cl]$ upon treatment with CuCl [20].
- Acid-catalyzed double C–H activation reactions of benzene have been reported [87–89], and they follow a mechanism similar to reaction (2).
- Exposure of $[(NN)PtMe_2]$ to a catalytic amount of the one-electron oxidant $[Cp_2Fe]^+OTf^-$ under the same conditions also results in the formation of $[(NN)PtPh_2]$. A small amount of $[(NN)PtMe_3]^+$ is observed as well, indicating that it is not involved in the cycle.

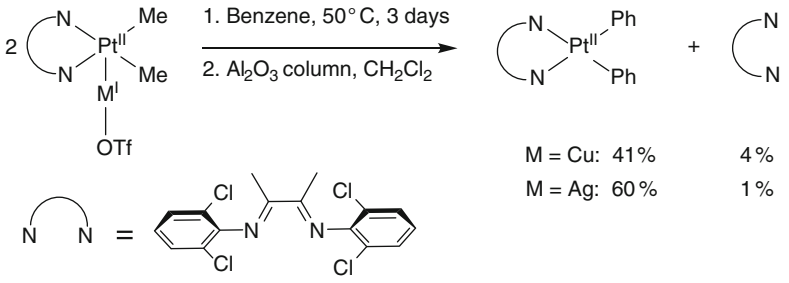

Scheme 21 Oxidatively induced C–H activation of benzene

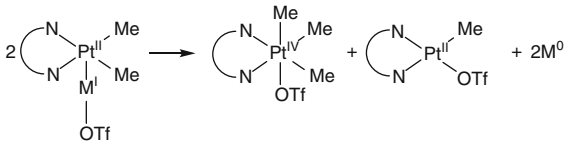

(1)

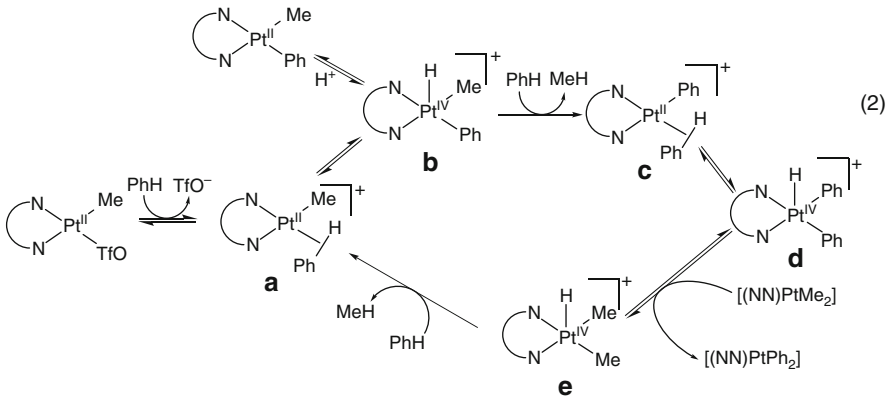

(2)

Scheme 22 Proposed mechanisms for the oxidatively induced C–H activation of benzene

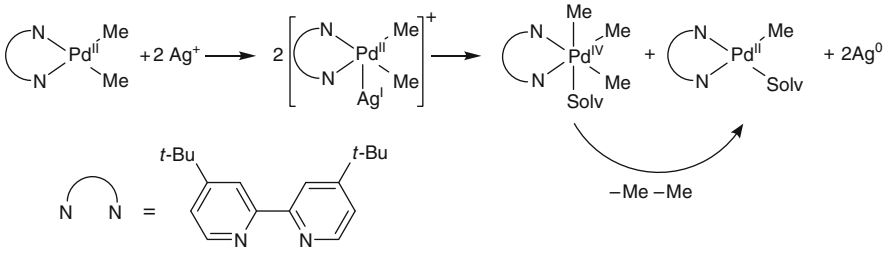

Scheme 23 Oxidatively induced reductive elimination of ethane from (t-Bu_2bpy)$PdMe_2$

Very recently, Lanci et al. [32] studied the reaction of [(t-Bu_2bpy)$PdMe_2$] with a range of oxidants, which generally resulted in an oxidatively induced reductive elimination process (Scheme 23). The proposed mechanism for this transformation parallels that of the initiation step for oxidatively induced C–H bond activation (Scheme 22 (1)), differing merely in that the formed trimethylpalladium(IV) complex is unstable and reductively eliminates ethane. With $AgPF_6$ as the oxidant, an intermediate was detected by ^{1}H NMR that was assigned to a metal–metal-bound species by comparison with the isolable thallium analogue (see Sect. 3.1.2).

7.2 *Ligand Migration Reactions*

7.2.1 Halide Migration

Efficient halide abstraction reactions using silver(I) and thallium(I) salts are among the most widely applied methods to generate cationic platinum(II) or palladium(II) species that are often active catalysts. There is increasing evidence for the involvement of metal–metal-bound, heterobimetallic intermediates in these salt metathesis reactions. Two isolable examples of such intermediates have been reported recently (Scheme 24).

First, Albano et al. presented a detailed study [90] of the mechanism of chloride abstraction from the complex [(NN)Pt(Me)(Cl)] (NN = 2,3-bis(2,6-diisopropylphenylimino)butane) by silver(I) salts, during which they isolated a trimetallic intermediate (Scheme 24, top) featuring a platinum–silver contact of 2.895 Å. This intermediate was stable in THF but released AgCl in chloroform, illustrating how subtle solvent effects may influence the course of such reactions.

Secondly, Oberbeckmann-Winter et al. [90, 91] observed the formation of a cationic bimetallic species instead of the expected chloride abstraction when the benzylplatinum(II) complex depicted in Scheme 24 (bottom) was treated with thallium(I) hexafluorophosphate in dichloromethane. The starting platinum complex acted as a chelating metalloligand, coordinating to thallium *via* both the platinum atom and the aromatic ring. Again, exposure of the bimetallic intermediate to the more polar solvent acetonitrile released TlCl.

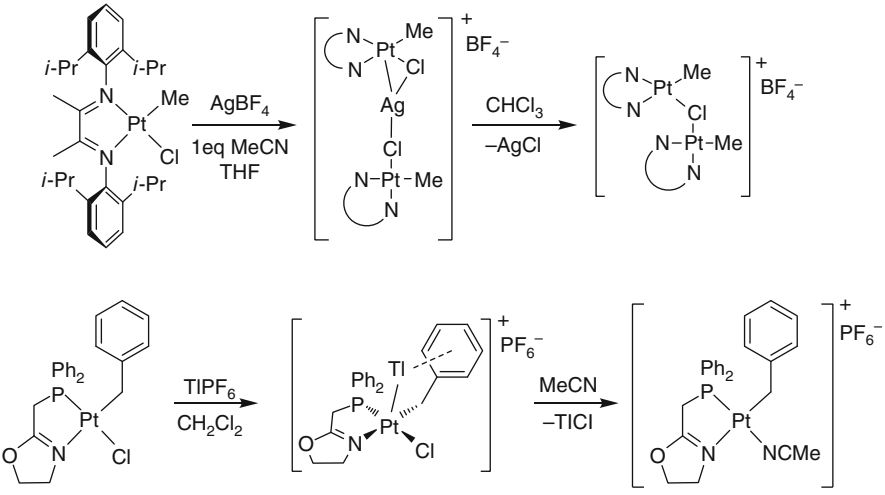

Scheme 24 Bimetallic intermediates in chloride abstraction reactions with Ag^{I} and Tl^{I} salts

7.2.2 Hydrocarbyl Migration

Compounds with relatively labile metal–metal bonds can be considered to be likely intermediates for hydrocarbyl transmetalation, which is a process of fundamental importance in many metal-catalyzed cross-coupling reactions. There are a few examples pointing at the possible involvement of d^8–d^{10} intermediates in transmetalation processes.

An early report from Puddephatt [20] indicated silver(I) tetrafluoroborate to catalyze scrambling of the deuterium labeling between $[(bpy)Pt(CH_3)_2]$ and $[(bpy)Pt(CD_3)_2]$ at temperatures above −40°C, which suggests reversible methyl group transfer from platinum(II) to silver(I) via the proposed trimetallic cation $\{[(bpy)Pt(C[H/D]_3)_2]_2Ag\}^+$. In addition, for the *cis–trans* isomerization of $[Pd(C_6Cl_2F_3)_2(tht)_2]$ (tht = tetrahydrothiophene) catalyzed by $[Au(C_6Cl_2F_3)(tht)]$, there is kinetic evidence for intermediates with a Pd–Au donor–acceptor bond, which, however, are too labile to be isolated [92]. Finally, a mass-spectrometric study [25] of the cation $\{[(dmpe)PtMe_2]Cu(PMe)_3\}^+$ revealed two distinct fragmentations involving platinum-to-copper methyl group transfer (Scheme 25) to eliminate either naked or phosphine-stabilized methylcopper(I). The activation energies of these processes were measured using threshold collision-induced dissociation (T-CID) and were found to be 30.5 and 53.0 kcal mol^{-1}, respectively. Considering that solvents would additionally stabilize the undercoordinated fragments, the low-energy process may be accessible in solution at relatively low temperatures, suggesting that similar transmetalation processes should be considered when discussing the mechanism of reactions catalyzed by palladium or platinum in the presence of copper or silver additives.

8 Perspectives

Metal–metal bonds involving platinum(II) or palladium(II) as a Lewis base have been known for several decades and are involved in a large variety of polymetallic assemblies, ranging from simple bimetallic compounds to high-nuclearity clusters

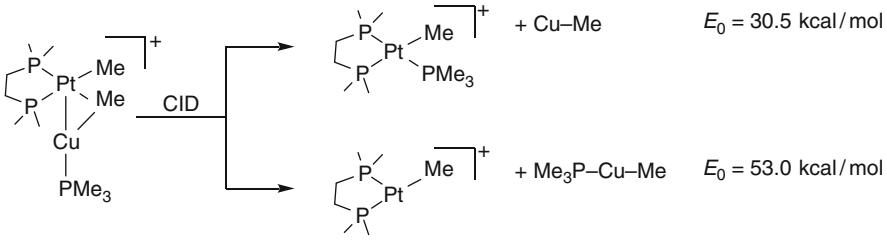

Scheme 25 Fragmentation reactions of the cation $\{[(dmpe)PtMe_2]Cu(PMe)_3\}^+$ observed by tandem mass spectrometry, with experimentally determined activation energies

and extended structures. Many of these compounds feature interesting optical properties such as long-lived, low-energy luminescence.

Recent investigations outline the involvement of this class of polymetallic compounds in reactions of fundamental importance to catalysis, such as inner-sphere oxidation or transmetalation. Given the widespread use of copper(I) and silver(I) salts – and, to a lesser extent, thallium(I) – as additives in palladium- and platinum-based catalytic systems, a systematic study of these reactions is warranted. Additionally, gathering further knowledge on the properties and reactivity of metal–metal-bound species is a critical step toward the rational design of truly bimetallic catalytic cycles.

Acknowledgements I am indebted to Prof. Dr. Peter Chen for his generous support and many stimulating discussions during the elaboration of this chapter. Financial support from the Swiss National Foundation is acknowledged.

References

1. Rendina LM, Puddephatt RJ (1997) Chem Rev 97:1735
2. Byers PK, Canty AJ, Skelton BW, White AH (1986) J Chem Soc, Chem Commun: 1722
3. Byers PK, Canty AJ, Crespo M, Puddephatt RJ, Scott JD (1988) Organometallics 7:1363
4. Wik BJ, Lersch M, Krivokapic A, Tilset M (2006) J Am Chem Soc 128:2682
5. Wik BJ, Ivanovic-Burmazovic I, Tilset M, van Eldik R (2006) Inorg Chem 45:3613
6. Ong CM, Jennings MC, Puddephatt RJ (2003) Can J Chem 81:1196
7. Lersch M, Tilset M (2005) Chem Rev 105:2471
8. Terheijden J, van Koten G, Mul WP, Stufkens DJ, Muller F, Stam CH (1986) Organometallics 5:519
9. Albrecht M, Gossage RA, Lutz M, Spek AL, van Koten G (2000) Chem Eur J 6:1431
10. Albrecht M, Lutz M, Spek AL, van Koten G (2000) Nature 406:970
11. Albrecht M, van Koten G (2001) Angew Chem Int Ed 40:3750
12. Yang DS, Bancroft GM, Dignardbailey L, Puddephatt RJ, Tse JS (1990) Inorg Chem 29:2487
13. Pyykkö P (1997) Chem Rev 97:597
14. van der Ploeg AFM, van Koten G, Vrieze K, Spek AL, Duisenberg AJM (1982) Organometallics 1:1066
15. van der Ploeg AFM, van Koten G, Brevard C (1982) Inorg Chem 21:2878
16. van der Ploeg AFM, van Koten G, Vrieze K (1982) Inorg Chem 21:2026
17. Usón R, Forniés J, Tomás M, Casas JM, Cotton FA, Falvello LR (1985) J Am Chem Soc 107:2556
18. Chen WZ, Liu FH, Nishioka T, Matsumoto K (2003) Eur J Inorg Chem: 4234
19. Navarro JAR, Freisinger E, Lippert B (2000) Eur J Inorg Chem: 147
20. Arsenault GJ, Anderson CM, Puddephatt RJ (1988) Organometallics 7:2094
21. Forniés J, Ibáñez S, Martín A, Sanz M, Berenguer JR, Lalinde E, Torroba J (2006) Organometallics 25:4331
22. Yamaguchi T, Yamazaki F, Ito T (1999) J Am Chem Soc 121:7405
23. Yamaguchi T, Yamazaki F, Ito T (2001) J Am Chem Soc 123:743
24. Moret M-E, Chen P (2009) J Am Chem Soc 131:5675
25. Moret M-E, Serra D, Bach A, Chen P (2010) Angew Chem Int Ed 49:2873
26. Forniès J, Martín A (1999) In: Braunstein P, Oro LA, Raithby RP (eds) Metal Clusters in Chemistry, vol 1. Wiley-VCH Verlag GmbH, D-69469 Weinheim, p. 417

27. Forniés J, García A, Lalinde E, Moreno MT (2008) Inorg Chem 47:3651
28. Falvello LR, Forniés J, Lalinde E, Menjón B, García-Monforte MA, Moreno MT, Tomás M (2007) Chem Commun: 3838
29. Song HB, Zhang ZZ, Hui Z, Che CM, Mak TCW (2002) Inorg Chem 41:3146
30. Forniés J, Martínez F, Navarro R, Urriolabeitia EP (1996) Organometallics 15:1813
31. Falvello LR, Forniés J, Martín A, Sicilia V, Villarroya P (2002) Organometallics 21:4604
32. Lanci MP, Remy MS, Kaminsky W, Mayer JM, Sanford MS (2009) J Am Chem Soc 131:15618
33. Forniés J, Martín A, Navarro R, Sicilia V, Villarroya P, Orpen AG (1998) J Chem Soc, Dalton Trans: 3721
34. Ara I, Falvello LR, Forniés J, Sicilia V, Villarroya P (2000) Organometallics 19:3091
35. Ara I, Forniés J, Sicilia V, Villarroya P (2003) Dalton Trans: 4238
36. Falvello LR, Forniés J, Martín A, Navarro R, Sicilia V, Villarroya P (1997) Inorg Chem 36:6166
37. Forniés J, Martín A, Sicilia V, Villarroya P (2000) Organometallics 19:1107
38. Janzen DE, Mehne LF, VanDerveer DG, Grant GJ (2005) Inorg Chem 44:8182
39. Jamali S, Mazloomi Z, Nabavizadeh SM, Milić D, Kia R, Rashidi M (2010) Inorg Chem 49:2721
40. Kickham JE, Loeb SJ (1995) Organometallics 14:3584
41. Braunstein P, Frison U, Oberbeckmann-Winter N, Morise X, Messaoudi A, Bénard M, Rohmer MM, Welter R (2004) Angew Chem Int Ed 43:6120
42. Usón R, Forniés J (1992) Inorg Chim Acta 198:165
43. Usón R, Forniés J, Tomás M, Ara I, Casas JM, Martín A (1991) J Chem Soc, Dalton Trans: 2253
44. Forniés J, Ibáñez S, Martín A, Gil B, Lalinde E, Moreno MT (2004) Organometallics 23:3963
45. Usón R, Forniés J, Falvello LR, Usón MA, Usón I (1992) Inorg Chem 31:3697
46. Falvello LR, Forniés J, Garde R, García A, Lalinde E, Moreno MT, Steiner A, Tomás M, Usón I (2006) Inorg Chem 45:2543
47. Casas JM, Forniés J, Martín A, Orera VM, Orpen AG, Rueda AJ (1995) Inorg Chem 34:6514
48. Usón R, Forniés J, Falvello LR, Ara I, Usón I (1993) Inorg Chim Acta 212:105
49. Casas JM, Forniés J, Martín A, Menjón B, Tomás M (1996) Polyhedron 15:3599
50. Usón R, Forniés J, Tomás M, Casas JM (1989) Angew Chem Int Ed 28:748
51. Usón R, Forniés J, Tomás M, Casas JM, Cotton FA, Falvello LR (1987) Inorg Chem 26:3482
52. Ara I, Forniés J, Gabilondo L, Usón MA (2003) Inorg Chim Acta 347:155
53. Alonso E, Casas JM, Cotton FA, Feng XJ, Forniés J, Fortuño C, Tomás M (1999) Inorg Chem 38:5034
54. Alonso E, Forniés J, Fortuño C, Martín A, Orpen AG (2003) Organometallics 22:5011
55. Usón R, Forniés J, Tomás M, Usón I (1990) Angew Chem Int Ed 29:1449
56. Ara I, Falvello LR, Forniés J, Gomez-Cordón J, Lalinde E, Merino RI, Usón I (2002) J Organomet Chem 663:284
57. Casas JM, Falvello LR, Forniés J, Gomez J, Rueda A (2000) J Organomet Chem 593:421
58. Ara I, Berenguer JR, Forniés J, Gómez J, Lalinde E, Merino RI (1997) Inorg Chem 36:6461
59. Charmant JPH, Forniés J, Gómez J, Lalinde E, Merino RI, Moreno MT, Orpen AG (2003) Organometallics 22:652
60. Moret M-E, Chen P (2008) Organometallics 27:4903
61. Lang H, del Villar A (2003) J Organomet Chem 670:45
62. Forniés J, Lalinde E (1996) J Chem Soc, Dalton Trans: 2587
63. Chen ZN, Zhao N, Fan Y, Ni J (2009) Coord Chem Rev 253:1
64. Berenguer JR, Lalinde E, Moreno MT (2010) Coord Chem Rev 254:832
65. Espinet P, Forniés J, Martínez F, Tomás M, Lalinde E, Moreno MT, Ruiz A, Welch AJ (1990) J Chem Soc, Dalton Trans: 791
66. Gil B, Forniés J, Gómez J, Lalinde E, Martín A, Moreno MT (2006) Inorg Chem 45:7788
67. Ara I, Forniés J, Gómez J, Lalinde E, Moreno MT (2000) Organometallics 19:3137

68. Ara I, Forniés J, Gómez J, Lalinde E, Merino RI, Moreno MT (1999) Inorg Chem Commun 2:62
69. Charmant JPH, Forniés J, Gómez J, Lalinde E, Merino RI, Moreno MT, Orpen AG (1999) Organometallics 18:3353
70. Yam VWW, Hui CK, Yu SY, Zhu NY (2004) Inorg Chem 43:812
71. Yam VWW, Yu KL, Cheung KK (1999) J Chem Soc, Dalton Trans: 2913
72. Berenguer JR, Forniés J, Gil B, Lalinde E (2006) Chem Eur J 12:785
73. Berenguer JR, Díez A, Fernández J, Forniés J, García A, Gil B, Lalinde E, Moreno MT (2008) Inorg Chem 47:7703
74. McDonald WS, Pringle PG, Shaw BL (1982) J Chem Soc, Chem Commun: 861
75. Cooper GR, Hutton AT, Langrick CR, McEwan DM, Pringle PG, Shaw BL (1984) J Chem Soc, Dalton Trans: 855
76. Yip HK, Lin HM, Wang Y, Che CM (1993) J Chem Soc, Dalton Trans: 2939
77. Yin GQ, Wei QH, Zhang LY, Chen ZN (2006) Organometallics 25:580
78. Stork JR, Olmstead MM, Balch AL (2005) J Am Chem Soc 127:6512
79. Stork JR, Olmstead MM, Fettinger JC, Balch AL (2006) Inorg Chem 45:849
80. Tulloch AAD, Winston S, Danopoulos AA, Eastham G, Hursthouse MB (2003) Dalton Trans: 699
81. Kessler F, Szesni N, Maass C, Hohberger C, Weibert B, Fischer H (2007) J Organomet Chem 692:3005
82. Heckenroth M, Kluser E, Neels A, Albrecht M (2007) Angew Chem Int Ed 46:6293
83. Reitsamer C, Schuh W, Kopacka H, Wurst K, Peringer P (2009) Organometallics 28:6617
84. Scollard JD, Day M, Labinger JA, Bercaw JE (2001) Helv Chim Acta 84:3247
85. Wik BJ, Tilset M (2007) J Organomet Chem 692:3223
86. Johansson L, Ryan OB, Rømming C, Tilset M (1998) Organometallics 17:3957
87. Thomas CM, Peters JC (2005) Organometallics 24:5858
88. Khaskin E, Zavalij PY, Vedernikov AN (2006) J Am Chem Soc 128:13054
89. Song DT, Jia WL, Wang SM (2004) Organometallics 23:1194
90. Albano VG, Di Serio M, Monari M, Orabona I, Panunzi A, Ruffo F (2002) Inorg Chem 41:2672
91. Oberbeckmann-Winter N, Braunstein P, Welter R (2004) Organometallics 23:6311
92. Casado AL, Espinet P (1998) Organometallics 17:3677

Index